TÜBİTAK

TÜRKİYE BİLİMSEL VE
TEKNİK ARAŞTIRMA KURUMU

THE SCIENTIFIC AND TECHNICAL
RESEARCH COUNCIL OF TURKEY

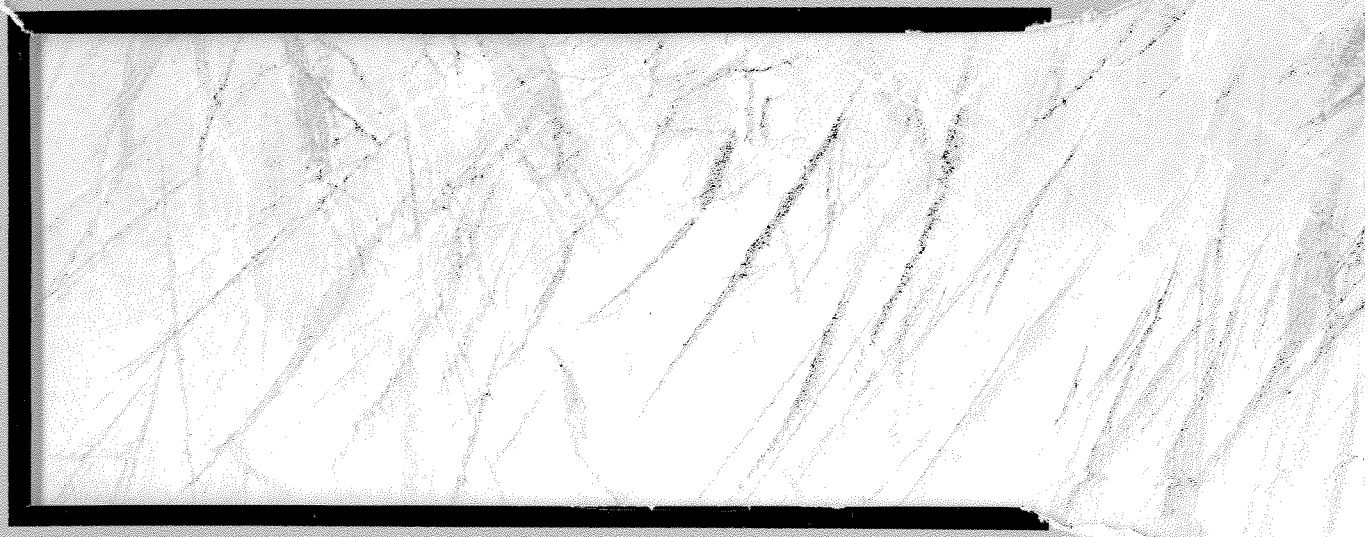

Elektrik, Elektronik ve Enformatik Araştırma Grubu

Electric, Electronics and Informatics Research Grant Committee

AYARLANABİLİR HIZLI RELÜKTANS MOTORU TAHRİK SİSTEMİ GELİŞTİRİLMESİ

PROJE NO : EEEAG - 16 / DPT

Dr.H.Bülent ERTAN
Dr.Kemal LEBLEBİCİOĞLU
Funda ŞAHİN
Saeid SAEIDI
Fariborz NIAKAN
Amir SAFAVI

NİSAN 1995
ANKARA

İÇİNDEKİLER

SEMBOL LİSTESİ iii

1. GİRİŞ 1

1.1 Gerçekleştirilen Çalışmalar 2

2. MOTOR TASARIMI 2

2.1 Analiz ve Tasarım Yazılımı 3

2.1.1 Analiz Bölümü 3

2.1.2 Analiz Programının Hassasiyeti 6

Moment - Konum Eğrisi 6

Endüktans Konum Eğrisi 9

Akım Dalga Şekilleri 10

Senkronizmadan Çıkma-Momenti-Hız Karakteristiği 10

2.1.3 Değerlendirme 13

2.2 Sayısal Alan Çözümü Moment ve Bağlanan Akı Konum Karakteristiğinin Kestirimi 14

Değerlendirme 18

3. MİKROİŞLEMCİ DENETİMLİ SÜRÜCÜ 19

3.1 Güç Devresinin Tasarımı 24

3.2 Konum Belirleyici 29

3.3 Mikro İşlemci Denetimli Sistemin Genel Yapısı 35

3.4. Mikro Denetleyici Yazılımları: 37

Ana Modül (Main Module): 37

Hazırlama Modülü (Initialization Module): 39

Veri Modulü (Data Module): 40

PCA Modülü (Programmable Counter Module): 41

Adım Komutu Modülü (Step Command Module): 42

4. HIZ KONTROLÜ 42

4.1. Hız Kontrol Stratejisi: 48

5. SİSTEMİN SINANMASI 54
5.1 Güç Katı Üzerinde Deneyler 54
5.2 Ön Uyartım Açısı Yazılımının Sınanması 57
5.3 Akım Sınırlayıcı Devre 58

6. SÜRÜCÜ SİSTEMİN SINANMASI 60
6.1 Deney Motorunun Yüklenmesi 60
6.2 Motor İmalat Problemleri 61
6.3 Sıcaklık Yükselmesi Deneyleri 62
6.4 Moment Hız Karakteristiğinin Ölçülmesi 64
6.5 Sabit Hızda Çalışma ve Çamaşır Makinası Üzerinde Deneyler 73
6.6 Akustik Gürültü Düzeyi 74

7. DEĞERLENDİRME 75

8. YAPILMASI GEREKEN ÇALIŞMALAR 77

9. YÜRÜTÜLMEKTE OLAN ÇALIŞMLAR 78

10. ÖNERİLER 79

KAYNAKLAR 81

SEMBOL LİSTESİ

A	.....	Amper
AR	.....	Anahtarlı Reluktans
AD	.....	Analog Sayısal
BJT	.....	Bipolar Transistor
C	.....	Kollektör
d/d	.....	devir/dakika
DA	.....	Doğru Akım
DAC	.....	Sayısal Analog Çevirici
E	.....	Emiter
e_k	.....	Akım Sensör Gerilimi
G	.....	Kapı (Gate)
I	.....	Akım
IGT	.....	İzole Kapılı Transistor
L	.....	Endüktans
Nm	.....	Newton - Metre
Pc	.....	Demir Kayıbı
PC	.....	Kişisel Bilgisayar
PH	.....	Faz
Po	.....	Bakır Kayıbı
PS	.....	Power Supply
Pt	.....	Transistor Kayıpları
R	.....	Direnç
s	.....	Transistor Sensör Ucu
SR	.....	Anahtarlı Reluktans (Switched Reluctance)
T_{av}	.....	Ortalama Moment
T_{MAX}	.....	Maksimum Moment
TR	.....	Transistor
T_{stmin}	.....	Kalkış Momenti Minimum
V	.....	Gerilim
w	.....	Açısal Hız Radyan Saniye
x_{ni}	.....	Faz Uyartım Konumu (normalize)
x_{nx}	.....	Faz Akımı Kesme Komutu (normalize)
λ	.....	Bağlayan Akı (flux linkage)
θ_i	.....	Ön Uyartım Açısı
θ_x	.....	Kapatma Açısı

DPT AG - 0016 PROJE RAPORU

1. GİRİŞ

Bu projede değişken hızlı anahtarlı relüktans motorlarının tasarımı sürücü elektroniği, ve bu tip motorların denetimi konusunda bir alt yapı oluşturmak, bir uygulama üzerinde geliştirilen öğeleri deneyerek bilgi düzeyini yükseltmek ve bir teknolojiye dönüşmeye ön hazırlık yapılması amaçlanmıştı. Uygulama olarak geniş bir hız aralığında denetim isteyen (1:40) ve bu nedenle özel zorluklar içeren bir çamaşır makinası uygulaması yapılması hedeflenmişti. Böylece, Türkiye'de üretim teknolojisi açısından bir hayli gelişmiş bulunan ve sınırlı da olsa ihracat yapabilen beyaz eşya sektörünün önemli bir ürününde tahrik sisteminden beklenenleri, bunların gerçekleştirilmesindeki zorluk ve araştırma alanlarını saptamak da projenin amaçlarından birini oluşturmaktaydı. Doğal olarak bu proje sırasında özellikle AR motorların bu tip uygulamalar için uygunluğu da araştırılarak mevcut universal veya seri DA motorlu tahrik sistemlerine bir alternatif oluşturup oluşturamayacağı konusunda bilgi kazanmak ta hedeflenmekteydi.

Takibeden bölümlerde bu araştırma projesi çerçevesinde yürütülen araştırmalar özetlenecek ve elde edilen sonuçlar

sunulacaktır. Araştırma sonuçları ve yöntemleri hakkında detaylı bilgi "ek" bölümlerde bulunabilir.

1.1 Gerçekleştirilen Çalışmalar

Bu çalşmada yapılan çalışmaları 4 grupta toplamak mümkündür. Bu gruplar ele alınış sırasıyla, motor tasarımı, sürücü geliştirilmesi, denetim ve deneyler olarak da ele alınmıştır. Bu grupların her birinde neler yapıldığı aşağıda değerlendirilmiştir.

2. MOTOR TASARIMI

Araştırmanın bu faaliyet dalında iki amaç güdülmüştür. Bunların biri tasarımı ve analizi özellikle zorluklar içeren SR motorlar için daha önce proje yöneticisince geliştirilen yöntemlerden yararlanarak bir PC üzerinde tasarım optimizasyonu ve performans analizi yapabilecek kullanıcı dostu bir yazılım geliştirmektir. Diğer amaç ise son yıllarda Elektrik Mühendisliği uygulamalarında da belli bir olgunluğa ulaşmış bulunan profesyonel alan çözümü programlarının tasarım amaçlı kullanımı konusunda deneyim kazandırmaktır.

2.1 Analiz ve Tasarım Yazılımı

Bu yazılımın bir demosu disket üzerinde çalışmamız, ekinde program kullanım klavuzuyla birlikte [Ek 1] sunulmuştur. Bilindiği gibi bir AR motorun performansı üzerinde sürücü devre çok belirleyici bir rol oynar. Bu çalışmada da gerilim kaynağından sürülen üzerinde akım sınırlamalı çalışma imkanı bulunan bir AR motorun tasarım ve performans analizi amaçlanmıştır. Yazılım iki ana bölümden oluşmuştur.

2.1.1 Analiz Bölümü

Bu bölüm menü ile sunulan bir yapıya sahiptir. İncelenecek motorun magnetik devresi, kullanılan malzeme ve sürücü devreye ilişkin bilgiler (akım limiti sınırı, kıyıcı hata bandı, anahtarlama açısı ve süresi vs.) kullanıcı tarafından girilir. Bu veriler bir dosya halinde saklanır ve gerektiğinde yeniden girmeye gerek kalmadan çağırılabilir.

Hazırlanan yazılım aşağıda belirtilen karakteristikleri 2 boyutlu alan çözümüne dayanarak oluşturulmuş boyutsuz verilerden hesaplayabilmektedir.

1- Statik moment - konum eğrisi

2- Endüktans - konum eğrisi

3- Kalkış momenti

4- Hız - konum eğrisi (özetle bu eğri motorun kararlı bir hızda çalışırken ürettiği momentin hıza bağımlı değişimini gösterir).

5- Motorun değişik hızlarda akım eğrisi

Ekranda "cursor" kullanılarak herhangi bir noktadaki sayısal değerlerin okunulması mümkündür. Program bu özellikleriyle kullanıcının değişik sürücü ve manyetik devreler için motor performansını hızla değerlendirmesine ve gerektiğinde analiz yoluyla tasarım yapmasına imkan vermektedir.

Yukarıda sözü edilen yöntemler 1 no'lu kaynakta detaylı olarak verilmiştir. Ek 3'te ise bu yöntemler özetlenmekte ve programın akış diagramları verilmektedir. Programın gerçekleştirilmesi Fariborz Niakan'ın "A Software For Predicting Quasi Stationary Characteristics of SR Motors" başlıklı tezinin konusunu oluşturmuş ve Eylül 1993 tarihinde bitmiştir.

Bu programda kullanılan yöntemlerin doğruluğunu kontrol etmek üzere değişik SR motorun deney sonuçları programdan belirlenen performans ile karşılaştırılmıştır.

Bu motorlardan biri 1500 d/d'de 1.1 kW güç vermek üzere daha önce tasarlanıp imal edilmiştir motorun (SR1) laminasyonu Şekil 1'de görülmektedir. (Ölçüler Ek 3'de Bulunabilir).

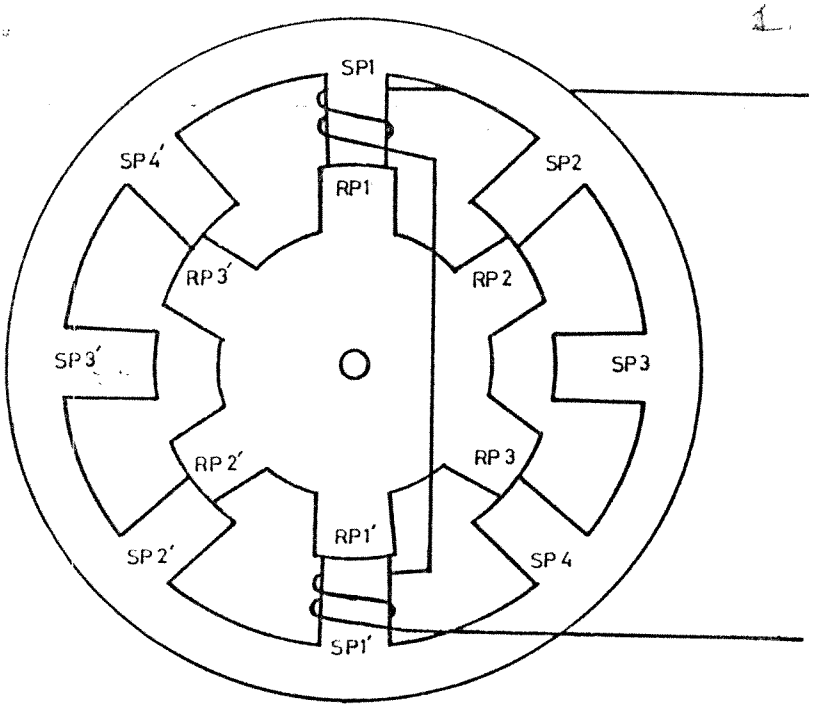

Şekil 1.

İkinci motor (SR2) bu araştırmada geliştirilen yazılım optimizasyon programı kullanılarak tasarlanıp geçekleştirilmiştir. Bu motorun gücü 10000 d/d'de 0.75 kW'tır. Optimizasyon proğramının bir çıktısı ve sembol listesi Ek. 2'de verilmiştir.

Burada kullanılan yöntemler optimizasyon programı içinde faydalanmak amacıyla geliştirildiğinden, kabul edilebilir bir kestirim hassasiyeti aranırken, hızlı sonuç vermeleri özellkle önemle ele alınmıştır. Ancak, bu şekilde optimizasyon sonucunun kabul edilebilir bir sürede alınması sağlanmıştır. (10-300 dak başlangıç noktasına bağlı olarak)

2.1.2 Analiz Programının Hassasiyeti

Geliştirilen tasarım programının hassasiyeti hakkında bir fikir vermek amacıyla bu altbölümde bazı sonuçlar verilecektir.

Moment - Konum Eğrisi

Şekil 2'de SR1 için ölçülmüş ve hesaplanmış moment eğrileri 3 değişik akım için verilmiştir. Bu sonuçların karşılaştırılması Tablo 1'de yapılmıştır. Şekil 3 ise 2A uyartımda SR2 için ölçülmüş ve hesaplanmış moment eğrilerini göstermektedir. Bu şekil doğrudan programın bilgisayar ekranında görünen biçimini yansıtmaktadır.

Elde edilen sonuçlar özellikle momentin tepe değerinin hesaplanmasında hataların meydana geldiğini, anma akımına yaklaşıldıkça hatanın azaldığını göstermektedir. Hata anma akımı civarında % 10 mertebesine düşmektedir. Buradaki amaçlar için bu yeterli bir hassasiyeti ifade etmektedir.

Hatanın kaynağı moment- konum eğrisinin, koenerji değişiminden hesaplanmasıdır. Bu yöntemde belli aralıklarla bu değişim hesaplandığından bir ortalama alma işlemi gerçekleşmekte bu ise özellikle değişimin hızlı olduğu koşullarda hataya yol açmaktadır. Bu eğrinin daha hassas hesaplanabilmesi için proje yöneticisinin geliştirdiği alan çözümü sonuçlarına dayalı bir analitik yöntem mevcuttur. Ayrıca alan çözümü yöntemleri de bu amaçla kullanılabilmektedir. (Bölüm 2.2'ye bakınız).

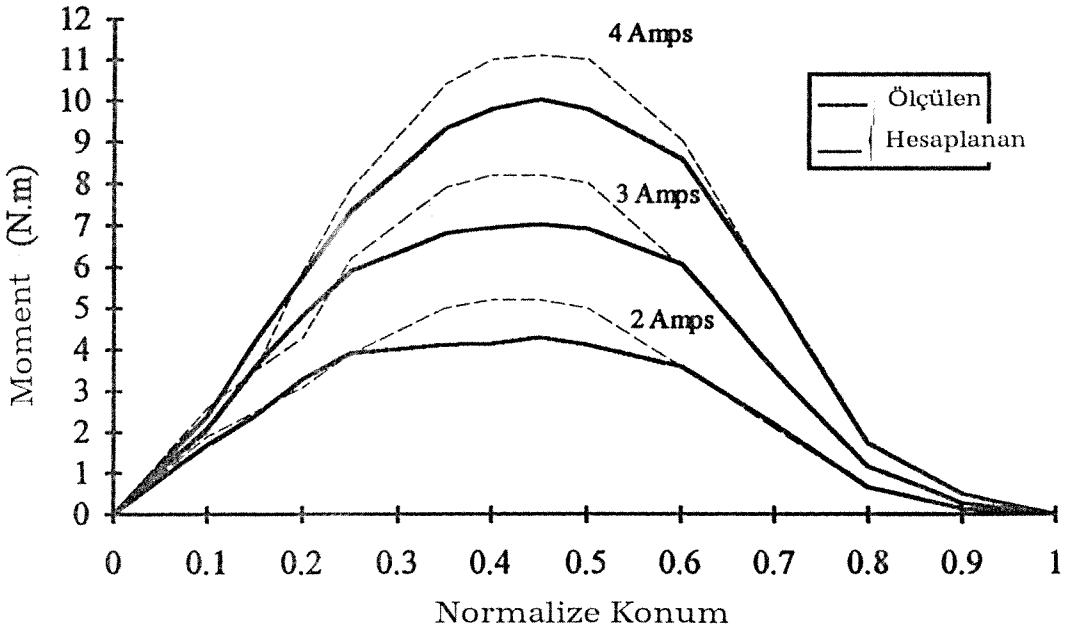

Şekil 2. SR1 için ölçülmüş ve hesaplanmış moment eğrileri

MOMENT (N.m)									
x_n	2 Amper			3 Amper			4 Amper		
	hesap.	ölçülen	hata	hesap.	ölçülen	hata	hesap.	ölçülen	hata
0.1	1.69	1.9	11	2.09	2	-4.3	2.39	2.6	8.7
0.2	3.3	3.1	-6	4.82	4.3	-10.7	5.8	5.9	1.7
0.3	4.05	4	-1.2	6.4	7.2	12.5	8.43	9.4	11.5
0.4	4.15	5.2	25	6.94	8.2	18.1	9.79	11	12.3
0.5	4.12	5	21.3	6.91	8	15.7	9.77	11	11
0.6	3.6	3.6	0	6.06	6	-1	8.57	9	5
0.7	2.2	2.1	-4.5	3.5	3.5	0	5.34	5.3	-0.7

Tablo 1. SR1 İçin Ölçülmüş ve Hesaplanmış Değerler ve Hata

Akım (A)	T_{stmin} (N.m)		hata
	hesaplanan	ölçülen	
2	2.86	2.35	-21.7
3	4.23	3.95	-7.08
4	5.68	5.6	-1.42

Tablo 2. SR1 için ölçülmüş ve hesaplanmış kalkış momenti

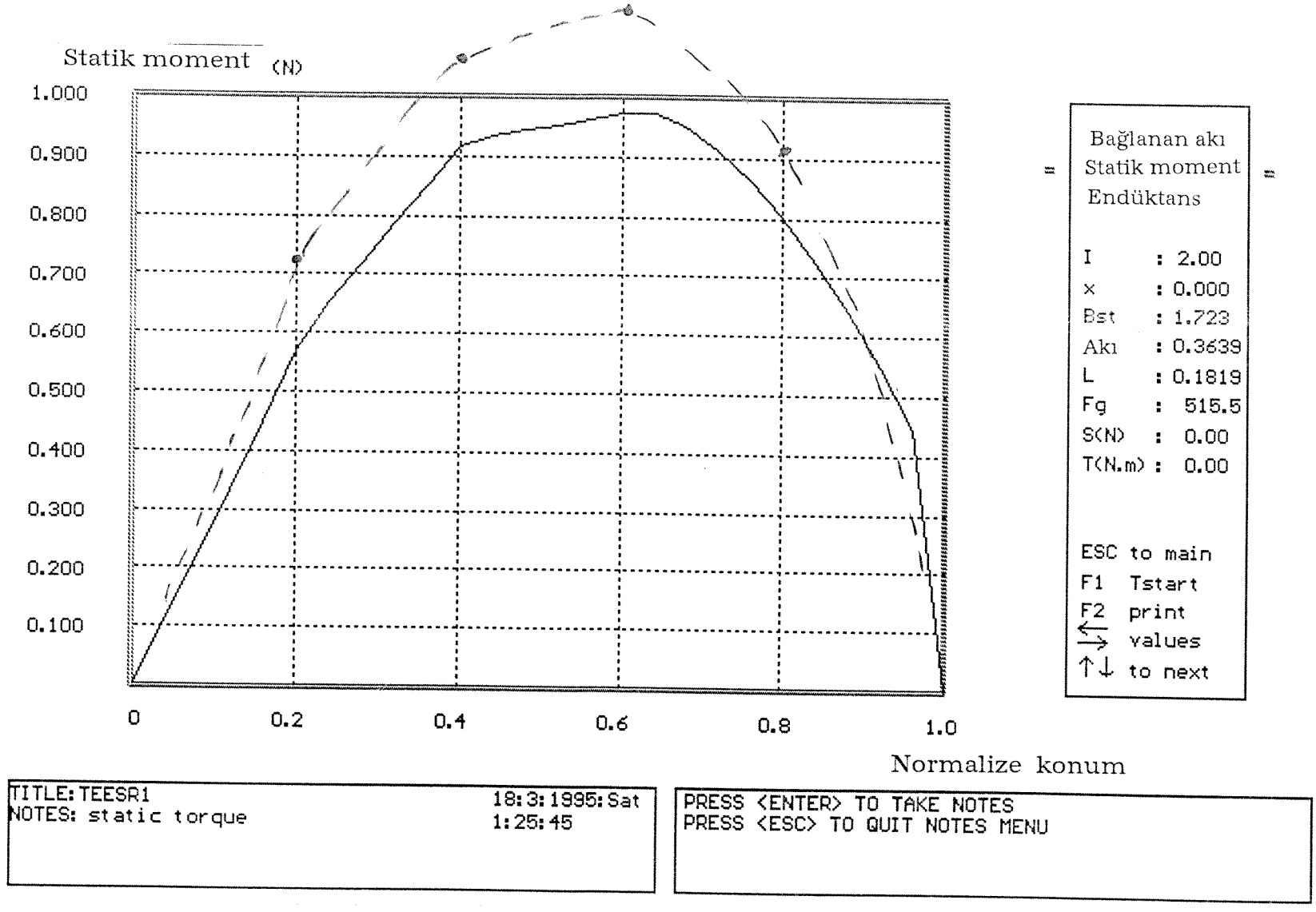

Şekil 3. SR2 için hesaplanmış ve ölçülmüş moment eğrileri

•·····•····ölçü ——hesap

Bilindiği gibi burada amaç daha ziyade verilen bir hızda motorun üretebildiği ortalama momentin belirlenmesidir. Yukarıda verilen şekiller değerlendirildiğinde, herhangi bir akım seviyesinde noktasal hataların büyük olabilmesine karşın ortalama momentte hatanın % -10 civarında kaldığı görülmektedir.

Endüktans Konum Eğrisi

Şekil 4'te SR1 için ölçülmüş ve programda kullanılan yöntemle hesaplanmış "bağlayan akı"[1]-konum karakteristiği verilmiştir. Genel olarak hesaplanan akı değişiminin ölçülenle uyumlu olduğu gözlenmektedir. Ancak burada bu eğriler (Ek 3)'de anlatıldığı gibi koenerji değişiminin hesabında kullanıldığından her bir konum eğrisinin altında kalan alanların farkı önemli olmaktadır. Bu farklar incelendiğinde hatanın en çok % -10 (ölçüme göre) civarında kaldığı izlenmektedir. bu sonuç daha önce statik konum eğrilerinden ortalama moment hesaplandığında bulunan sonuçla uyumludur.

[1] flux linkage

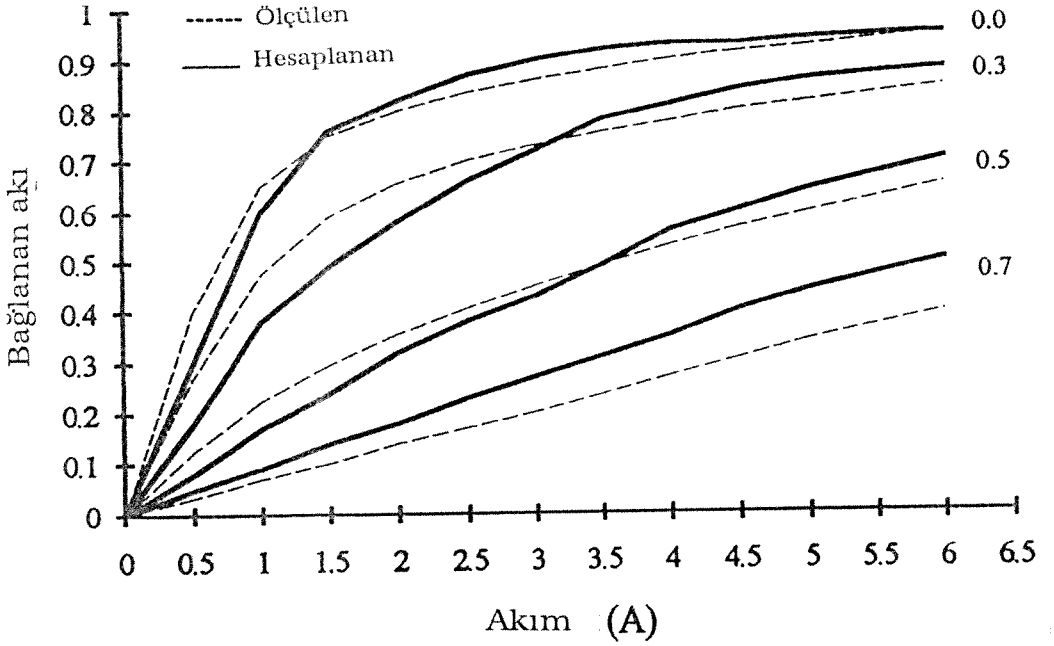

Şekil 4. SR1 için ölçülmüş ve hesaplanmış "bağlanan akı" konum eğrileri

Akım Dalga Şekilleri

Şekil 5'de SR1 için ölçülmüş ve programdan hesaplanmış akım dalga şekilleri verilmiştir. Görüldüğü gibi akım dalga şekilleri oldukça iyi kestirilebilmektedir.

Senkronizmadan Çıkma-Momenti-Hız Karakteristiği

Hazırlanan yazılımdan elde edilen senkronizmadan çıkma momenti-hız karakteristikleri, yazılımın hazırlandığı tarihlerde ancak SR1 mevcut olduğu için bu motor üzerinde yapılan ölçümlerle karşılaştırılabilmekteydi. Bu nedenle Fariborz Niakan çalışması sırasında SR1 için bir faz ve iki faz uyartımda ölçüm sonuçlarını hesaplama sonuçlarıyla karşılaştırılmıştır (Şekil 5 ve 6). Görüldüğü gibi ölçüm ve hesaplamalar sırasında büyük farklılıklar gözlenmektedir. Adı geçen öğrenciye tez jürisi bu hatalarını gidermesi için süre vermiştir. Ancak Ek3'de görüleceği gibi bay

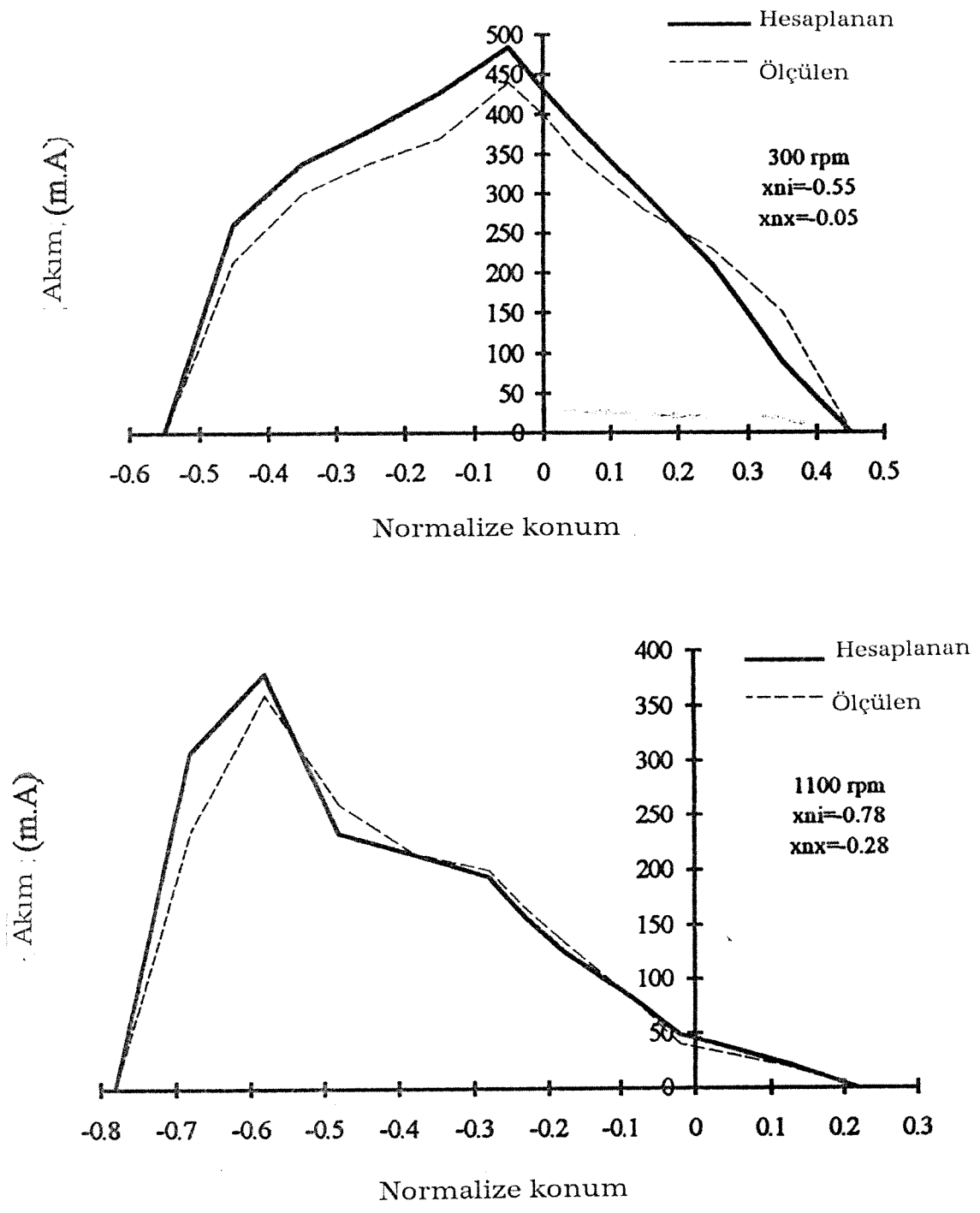

Şekil 5. SR1 için ölçülmüş ve hesaplanmış akım dalga şekilleri

Niakan bu çalışmayı tamamlamadan bu süreyi doldurmuş, süre bitiminde çalışmasını tamamlayacağını bildirmesine karşın aniden İran'a dönerek çalışmayı yarıda bırakmıştır. 1993 yılı sonunda meydana gelen bu olaydan sonra bu konuda çalışacak bir öğrenci bulunması için çalışılmış ve proje raporu motor imalatı sorunları nedeniyle de geciktirilmiştir. Ancak Haziran 1994'te Y. Lisans programına giren öğrenciler henüz ders almakta olduğundan ve başka bir insan kaynağı bulunamadığından çalışmanın bu bölümü tamamlanamamıştır. Raporun sonuç bölümünde bu konuda daha detaylı bir değerlendirme yapılmıştır.

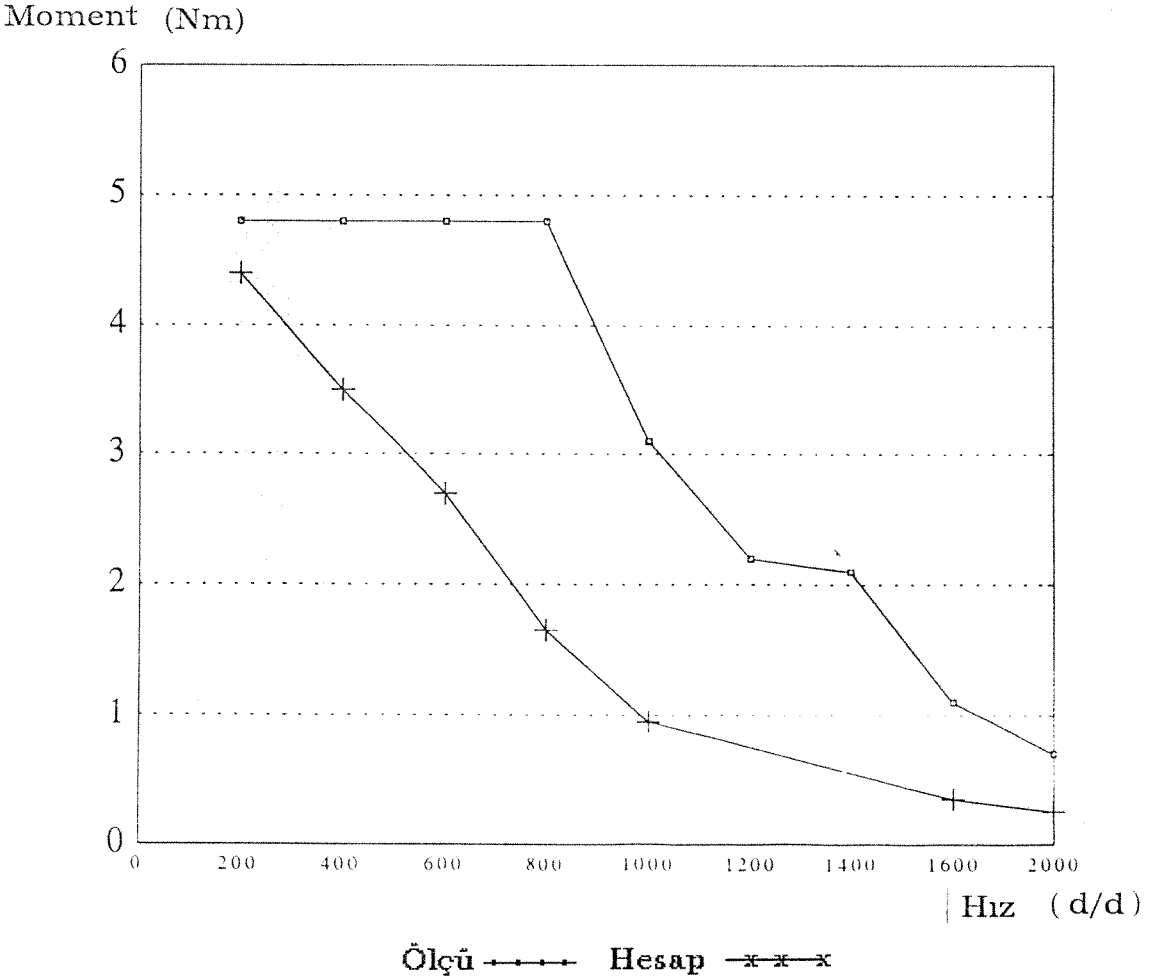

Şekil 6. SR1 için 1 faz uyartımda ölçülmüş ve hesaplanmış moment hız karakteristiği
θ_i Ön Uyartım açısı = -0.5 I= 4 ± 0.5 A θ_x Kapatma açısı =0°

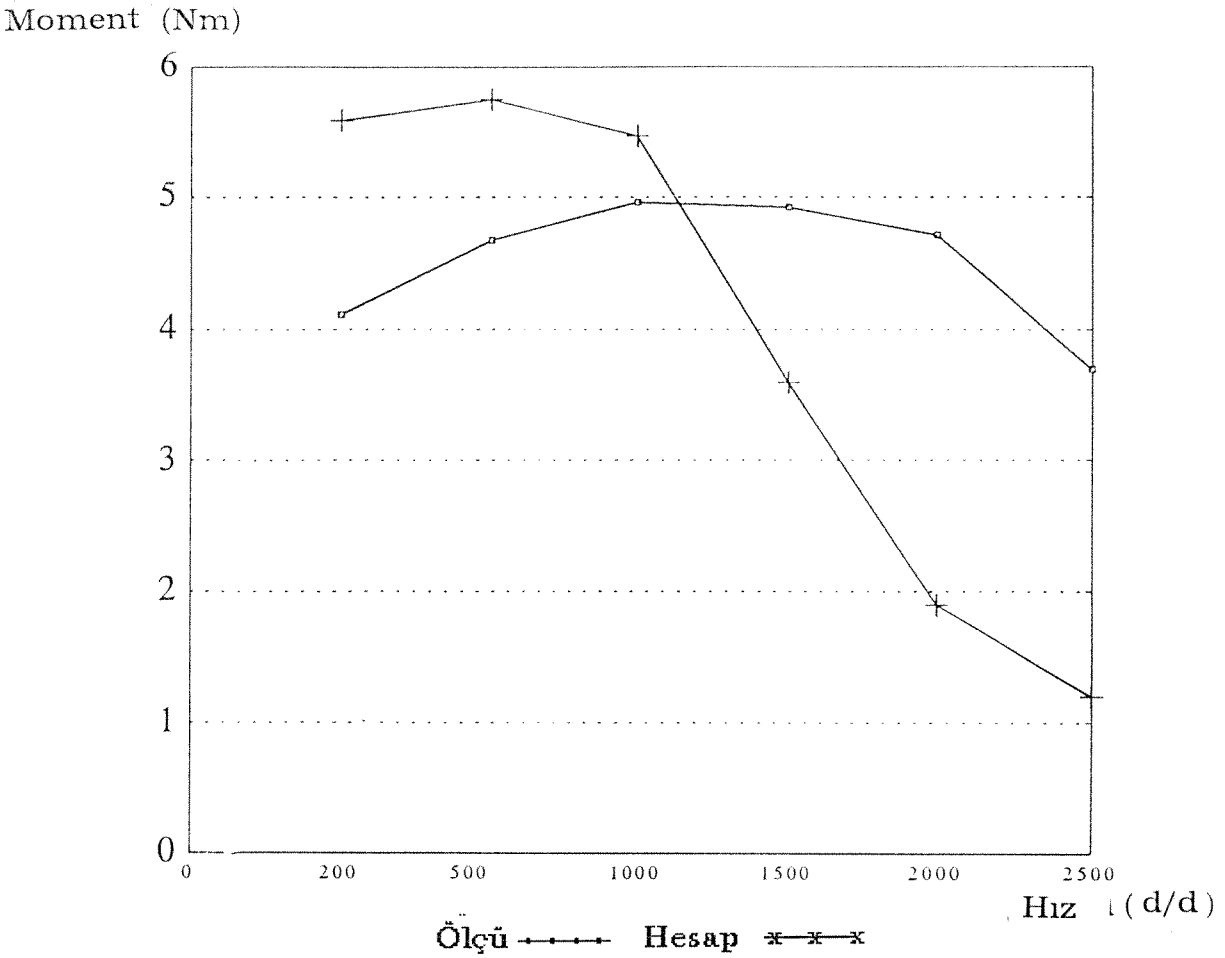

Şekil 7. SR1 için 2 faz uyartımda ölçülmüş ve hesaplanmış moment hız karakteristiği
$\theta_i = -0.9$, $\theta_x = 0.1$, $I = 4 \pm 0.5$ A

2.1.3 Değerlendirme

Çalışmanın bu bölümünde yapılması öngörülen çalışma kısmen gerçekleştirilebilmiştir.

Bu sorun Proje Araştırmacılarından Fariborz Niakan'ın sorumsuz ve ahlaksızca davranmasından kaynaklanmıştır. (Altbölüm 2.2'ye bakınız).

Mevcut program statik bağlayan- akı ve moment karakteristiklerini doğru olarak verir görünmektedir. Ancak, moment- hız karakteristikleri kestiriminde büyük hatalarla karşılaşılmıştır.

Proje yöneticisinin ve Dr. Müjdat Tohumcu'nun gerçekleştirdiği çalışmaların doğruluğu daha önce denenmiştir. Bu bakımdan kestirimde gözlenen sorun tümüyle öğrencinin programlama hatalarından kaynaklanmaktadır. Ancak, önceki bölümlerde belirtildiği gibi projenin uzun bir süre gecikmesine karşın bu konuda çalışacak bir öğrenci bulunamamıştır. (Bu öğrenci 1993 sonunda ayrılmıştır) 1994 Haziran döneminde Y. Lisans programına giren öğrenciler ise henüz derslerini tamamlamaktadır.

Maalesef TÜBİTAK'ın o tarihte (ve sanırım halen de) uyguladığı araştırıcılara ücret ödeme politikası, bu tip projelere insan kaynağı bulunmasına imkan vermemektedir ve sorunun temel öğelerinden birini oluşturmaktadır. (sonuç bölümüne bakınız.)

2.2 Sayısal Alan Çözümü Moment ve Bağlanan Akı Konum Karakteristiğinin Kestirimi

Bu çerçevede yapılan çalışmalar iki amaçlı olarak yürütülmüştür. Bunlardan birisi çağdaş bir tasarım aracı olarak elektrik endüstrisinde kullanımı yaygınlaşmakta olan profesyonel manyetik alan çözümü yöntemlerine hakim olmak ve hangi koşullarda ne hassasiyetle sonuç verdiklerini incelemektir. Diğeri ise, analiz programıyla tasarlanmış test motorlarının üretim öncesi performansını doğrulamak için alan çözümü yöntemlerini kullanmaktır. Bu çerçevede yapılan çalışmalar Ek 4'de detaylı olarak anlatılmıştır. Bu bölümde bu çalışmalar özetlenecektir.

Alan çözümü çalışmaları, laboratuarlarımızda daha önceki araştırmalarımızda tasarlanmış ve gerçekleştirilmiş bir AR motor üzerinde (SR1) başlatılmıştır. Bu araştırmanın amacı motor momentinin ve sarımları bağlayan akının, hassas olarak hesaplanması için göz dağılımının ve eleman sayısının optimize edilmesidir. Bu amaçla değişik sayıda ve dağılımda sınırlı elemanlar kullanılarak alan çözümleri elde edilmiştir. Sonuç olarak yapılan motor karakteristiklerinin doğru olarak belirlenmesi hedeflendiğinden, belli bir koşulda üretilen momentin ve bir fazı bağlayan akının alan çözümlerinden belirlenmesi gerekmektedir. Bu amaçla iki adet "makro" geliştirilmiş ve bu "makro"lardan hesaplanan moment ve akı değerleri ölçümlerle karşılaştırılmıştır.

Bu araştırma sonucu istenilen değişkenleri hassas olarak elde edebilmek için göz sayısı ve dağılımını belirleyecek ana kurallar ortaya konmuştur.

Bu konudaki çalışmamız çamaşır makinası uygulaması için tasarlanmış ikinci anahtarlı reluktans motoru (SR2) üzerinde sürdürülmüştür (8/6 kutuplu 4 fazlı). SR1 üzerinde yapılan çalışmadan yararlanılarak oluşturulan modelden çeşitli akım seviyelerinde moment ve sarımları bağlayan akı karakteristikleri elde edilmiştir. (Şekil 8 ve 9).

Elde edilen sonuçların doğruluğunu sınamak için SR2 imal edildikten sonra ölçümler yapılması gerekmiştir. Bu amaçla,

konum ve moment ölçücü bir düzen oluşturulmuştur. Akı ölçümü için de bir devre gerçekleştirilerek ölçümler yapılmıştır. Ölçülen ve alan çözümünden elde edilen moment karakteristikleri Şekil 8'de, ölçülen ve hesaplanan kutbu bağlayan akı, 2A ve 3A faz akımında, Şekil 9'da gösterilmiştir.

Bu sonuçlar incelendiğinde moment karakteristiğinin 2A ve 3A faz akımlarında çok hassas olarak belirlenebildiği gözlenmektedir. 1A seviyesindeki hata moment duyargasının hassasiyetinin bu düşük seviyeleri ölçmek için yeterli olmamasından kaynaklanmaktadır.

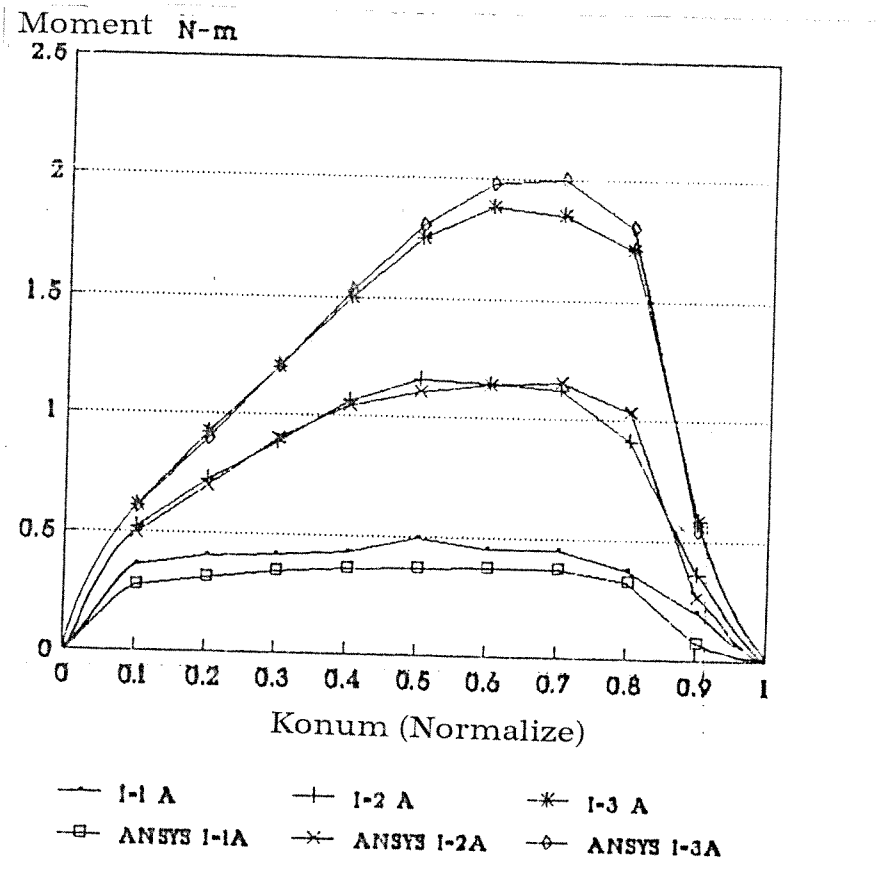

Şekil 8. SR2 için ölçülmüş ve hesaplanmış moment konum karakteristiği (alan çözümü)

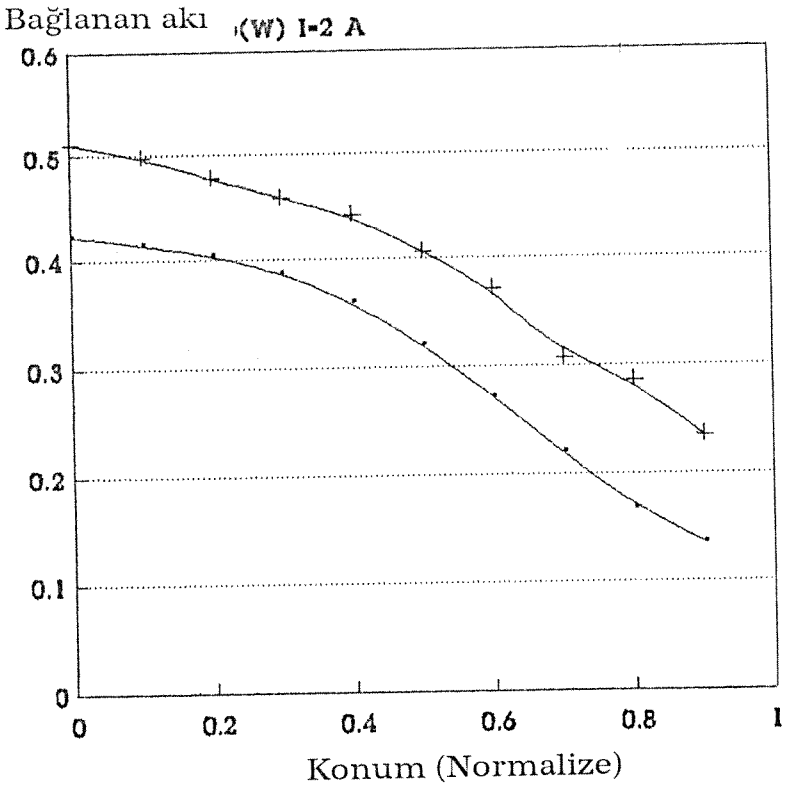

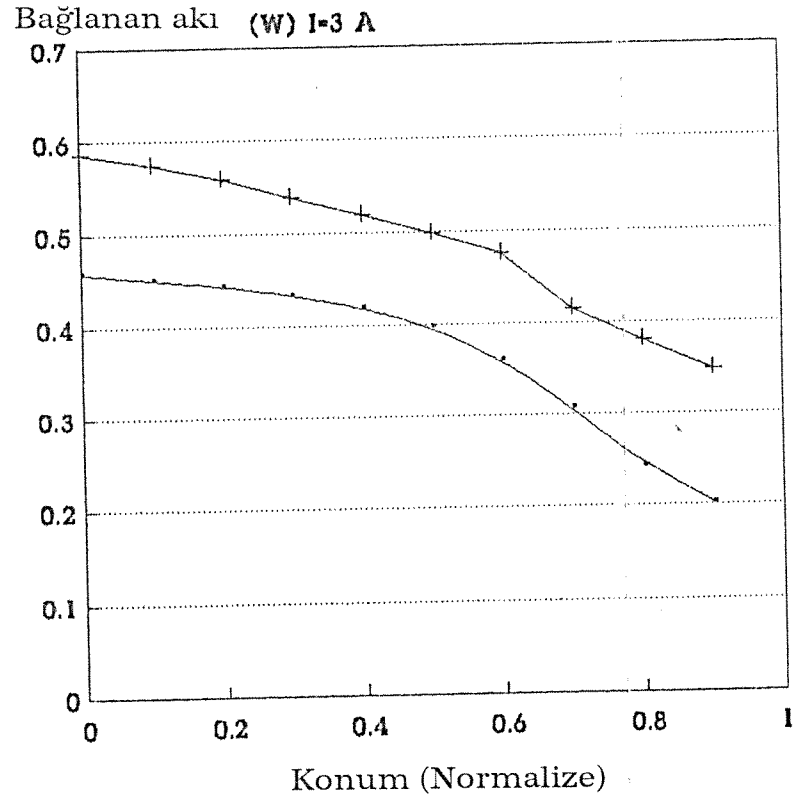

Şekil 9. SR2 için değişik akım seviyesinde kutbu bağlayanakı konum karakteristiği (alan çözümü)

Kutup akısının ölçümünde ise değişimin şeklinin iyi belirlenmekle birlikte ölçüm ve hesaplama arasında (belli bir akımda) sabit bir fark olduğu gözlenmektedir. Bu fark 2 boyutlu çözümde dikkate alınamayan sargı başlarını bağlayan akıdan kaynaklanmaktadır. Bu akının hesaplanması için analitik yöntemler [2]'de önerilmiş olmakla birlikte, sayısal alan çözümünün bu amaçla kullanılmasının bir araştırma konusu olarak ele alınması düşünülebilir.

Değerlendirme

Bu bölümde yapılan çalışmanın her bakımdan amaca ulaştığı söylenebilir. Çalışma süresinde alan çözümünü etkin olarak kullanabilen personel yetiştirilmiş bu çözümlerden istenen karakteristiklerin hassas olarak elde edilebilmesi için usul ve yöntemler geliştirilmiş ve sınanmıştır.

Bu çalışmalar sonucunda SR motorlarda önemli bir sorun olan moment dalgalanması konusunu inceleyen ve en aza indirilmesi için koşulların belirlenmesini gerektiren bir çalışma ileri bir safhaya getirilmiştir. İlk bulgular Eylül'95 ayında yapılacak uluslararası bir toplantıda sunulacaktır. Daha sonra bir hakemli dergi makalesi üretilmesi öngörülmektedir.

Burada şu noktanın vurgulanması gereklidir. Alan çözümleri doğrudan sadece motor statik moment ve akı karakteristiğini

vermektedir. Ancak bu karakteristikler motorun belli bir sürücü ile dinamik performansını belirlemekte kullanılabildiği işaret edilmesi gereken bir noktadır. Böyle bir simulasyon yazılımı halen geliştirilmektedir. Kuşkusuz böyle bir model yardımıyla, rotor konumunu izleyen bir gözleyici (oberver) yapılması çeşitli kontrol önerilerinin değerlendirilmeside mümkün olacaktır.

3. MİKROİŞLEMCİ DENETİMLİ SÜRÜCÜ

Bu çalışmadaki amaçlardan biri de Anahtarlı Reluktans (AR) motorlarını geniş bir hız aralığında sürebilecek (400-10000 rpm) bir sürücü geliştirilmesidir. AR motorun yüksek hızlarda sürülmesi motorun ufalmasını sağlamakta buna karşın sürücüden beklenen performansın sıra dışı olması sonucunu ve zorluklarını da beraber getirmektedir. Burada uygulamanın bir çamaşır makinası olması sürücü üzerine ek kısıtlar ortaya çıkartmaktadır. Bunlar arasında sürücünün kapladığı yer ve özellikle maliyeti en önemli öğelerdir.

Bu çalışmada sürücü gerçekleştirilirken bazı ek kısıtlar da tasarımcı tarafından getirilmiştir.

Bu kısıtlar şöylece özetlenebilir.

a) Geliştirilecek sürücü dört fazlı bir motoru bir faz açık, iki faz açık ve yarım adım uyartım biçimlerinde sürebilmelidir. Burada amaçlanan motor performansının

değişik koşullarda incelenmesine imkan vermektir. Gerektiğinde sürücünün bu özelliklerinden daha üstün bir performans elde etmek için kullanılabileceği düşünülmüştür.

b) Sürücü en az donanım (hardware) ile gerçekleştirilmeli çeşitli denetim ve duyargasız konum sezme yöntemlerinin sınanmasına imkan vermelidir.

Bu değerlendirmeler sonucunda donanım açısından sürücünün aşağıdaki özelliklere sahip olması düşünülmüştür.

1- Maliyeti belirleyici unsur olarak güç elemanları önemli bir öğedir. Bu açıdan gerçekleştirilecek sürücü faz başına en az sayıda güç elemanı kullanmalıdır.

2- Sistemin mikro işlemci ile desteklenmesi arzu edilen esneklik ve denetim sistemi sınamasına imkan verecektir. Ancak, bu mikroişlemcinin pahalı olmaması hedeflenmelidir. (Sürücü maliyeti 50 ` US $ civarında tutulmalıdır). Bu nedenle 8 bitlik bir mikro denetleyicinin amaca uygun olacağı düşünülmüştür. Laboratuarımızda bir emülatör ve yazılımları da bulunduğundan Intel 8051 mikro denetleyicinin kullanımı yeğlenmiştir.

3- Faz akımı denetiminin doğrudan mikro işlemci ile yapılması AD dönüşüm gerektireceğinden ve çok hızlı bir

denetleyici ihtiyacı doğuracağından benimsenmemiştir. Faz akımı denetimi için analog bir devre gerçekleştirilip referans değerinin mikro işlemci tarafından üretilmesi yeğlenmiştir.

4- Denetim amaçlı kullanılabilecek, faz akımı seviyesi (kıyıcı için), iletimde kalma süresi ve ön uyartım açısı mikro işlemci tarafından denetlenebilmelidir. Bu durumda, mikro denetleyicinin rotor konum bilgisine sahip olması (dolayısıyla dönme hızı) yapılacak denetim için yeterli olacaktır.

Yukarıda belirtilen amaçları gerçekleştirebilmek amacıyla ilk olarak bilinen sürücü devre şemaları gözden geçirilerek çeşitli açılardan değerlendirilmişlerdir. Bu değerlendirme sonucu Tablo 3, 4 ve 5'de verilmiştir. Ek 5'de bu tablonun hazırlanmasında göz önüne alınan unsurlar ve varsayımlar detaylı olarak verilmiştir.

Bu araştırma sonucunda 3 no'lu kaynakta 1990 yılında önerilen devre güç elemanı sayısını en aza indirmesi ve bir çok konuda avantajlı olması nedeniyle seçilmiştir. Bu devre avantajlarına karşın kapatılan fazdaki akımın boşaltılmasını hızla yapamadığı için önemli bir dezavantaj da içermektedir. Ancak, literatürde elde edilecek performans konusunda bir bilgi bulunmadığından bu devrenin sınanması kararlaştırılmıştır.

	3 telli güç kaynağı	"Bifilar" sargı	Asimetrik yarım köprü	Ayrık DA Güç Kaynağı	Yeni
# Dört Fazdaki transistör sayısı	4	4	8	4	4
# Dört fazdaki diyot sayısı	4	4	8	4	8
Yarı iletkenlerin anma gerilimi	2Vs	2Vs	Vs	2Vs	Vs
Yarı iletkenlerin anma akımı	I	I	I	I	2I
Sürücü kıyma modu (Chopping mode)'da kullanılabilir	Evet	Evet	Evet	Evet	Evet
Verilen bir kaynak için verim	Yüksek	Yüksek	Orta	Orta	Yüksek
# Faz başına gerekli gerilim kaynağı sayısı	2	1	1	2	1
Bakırın verimli kullanımı	Evet	Evet	Evet	Evet	Evet
Faz sayısında sınırlama	Hayır	Hayır	Hayır	Evet	Hayır
Motor sargılarına uygulanan gerilim	Vs	Vs	Vs	Vs/2	Vs
Faz anahtarı kapatıldığında kaynağa geri dönen enerji	Evet	Evet	Evet	Evet	Evet
Kıyma esnasında geri dönen enerji	Evet	Evet	Hayır(*)	Evet	Hayır(*)
Bakır kayıpları	Aynı	Aynı	Aynı	Aynı	Aynı
Demir kayıpları	Aynı	Aynı(**)	Aynı	Aynı	Aynı
Dinamik tepki motor anahtar gerilim oranı	Orta	Orta	Orta	Orta	Yüksek
Akım "duty cycle"	Orta	Orta	Yüksek	Orta	Yüksek

(*) : Ne alındı ne de geri döndü.

(**) : Tek ve çift yönlü sargılı herhangi bir AR motoru için akı dalga şekilleri aynı olduğundan demir kayıpları da aynı [11].

Tablo 3. Çeşitli sürücü devrelerin karşılaştırılması

	3 telli güç kaynağı	"Bifilar" sargı	Asimetrik yarım köprü	Ayrık DA Güç Kaynağı	Yeni
Herbirim faz akımı	1	1	1	1/2	1
Her birim faz gerilimi	1	1	1	1/2	1

Tablo 4. Değişik sürücüler ıçin gerilim ve akım (Herbirim)

	3 telli güç kaynağı	"Bifilar" sargı	Asimetrik yarım köprü	Ayrık DA Güç Kaynağı	Yeni
Transistör anahtarlama kayıpları	Pt1	Pt1	2Pt1	Pt1	Pt1
Bakır kayıpları	Po	Po	Po	Po(*)	Po
Demir kayıpları	Pc	Pc (***)	Pc	Pc	Pc
Faz gerilimi	Vs	Vs	Vs	Vs/2	Vs
Faz akımı	I	I	I	2I (**)	I
Toplam kayıplar	Düşük	Düşük	Orta	Orta	Düşük
Verim	Yüksek	Yüksek	Orta	Orta	Yüksek

(*) : Burada çevirici akımın 2I olması bakır kayıplarının 4xPo olacağını düşündürebilir, fakat kablo kesiti ve sarım sayısı değiştiğinden kayıplar diğer çeviricilerinki ile aynı (Po) kalacaktır.

(**) : Akım değerinin 2I olnması, daima aynı güç çıkışına sahip olacağımız hipotezinden kaynaklanmaktadır. Ayrık DA çevirici gerilimi Vs/2 olduğundan kayıpsız bir makina da aynı güç çıkışını elde etmek için faz akımının 2I olması gerekmektedir..

(***) : Daha önce açıklandığı gibi, akı dalga şekillerini tek ve çift yönlü sargılarda aynı olduğu için, demir kayıpları da aynı olacaktır.

Toblo 5. Değişik sürücülerin kayıp ve verimleri

	3 telli güç kaynağı	"Bifilar" sargı	Asimetrik yarım köprü	Ayrık DA Güç Kaynağı	Yeni
Herbirim faz akımı	1	1	1	1/2	1
Her birim faz gerilimi	1	1	1	1/2	1

Tablo 4. Değişik sürücüler ıçin gerilim ve akım (Herbirim)

	3 telli güç kaynağı	"Bifilar" sargı	Asimetrik yarım köprü	Ayrık DA Güç Kaynağı	Yeni
Transistör anahtarlama kayıpları	Pt1	Pt1	2Pt1	Pt1	Pt1
Bakır kayıpları	Po	Po	Po	Po(*)	Po
Demir kayıpları	Pc	Pc (***)	Pc	Pc	Pc
Faz gerilimi	Vs	Vs	Vs	Vs/2	Vs
Faz akımı	I	I	I	2I (**)	I
Toplam kayıplar	Düşük	Düşük	Orta	Orta	Düşük
Verim	Yüksek	Yüksek	Orta	Orta	Yüksek

(*) : Burada çevirici akımın 2I olması bakır kayıplarının 4xPo olacağını düşündürebilir, fakat kablo kesiti ve sarım sayısı değiştiğinden kayıplar diğer çeviricilerinki ile aynı (Po) kalacaktır.

(**) : Akım değerinin 2I olnması, daima aynı güç çıkışına sahip olacağımız hipotezinden kaynaklanmaktadır. Ayrık DA çevirici gerilimi Vs/2 olduğundan kayıpsız bir makina da aynı güç çıkışını elde etmek için faz akımının 2I olması gerekmektedir..

(***) : Daha önce açıklandığı gibi, akı dalga şekillerini tek ve çift yönlü sargılarda aynı olduğu için, demir kayıpları da aynı olacaktır.

Toblo 5. Değişik sürücülerin kayıp ve verimleri

Şekil 10'da kullanılması öngörülen devrenin şeması verilmiştir. Devrenin çalışması şöylece özetlenebilir. 1. fazı (PH1) uyartabilmek için TR2 ve TR1 anahtarları kapatılır akım faz üzerinden geçmeye başlar. Akım kıyıcının sınırlayacağı seviyeye geldiğinde örneğin TR2 anahtarı açılarak akımın PH1, diyod ve TR1 üzerinden düşmesi sağlanır. Akım alt sınıra ulaştığında TR2 tekrar iletime girer. Faz tamamen kapatılmak istendiğinde TR1 ve TR2 birlikte açılırsa PH1 akımı diodlar (D1, D2, D3) üzerinden kaynağa geri döner. Ancak TR2 anahtarı PH2'ninde uyartımında kullanılmaktadır. TR2 kapatılır kapatılmaz akım kaynak üzerinden yolunu tamamlamak yerine D_1, TR2 ve PH_1 üzerinden yolunu tamamlar. Bu durumda PH_1 akımının sıfıra düşme süresi uzayacak, bu nedenlede bu fazdan kaynaklanan negatif momentler üretilecek ve motorun genel performansında bir düşme söz konusu olabilecektir.

3.1 Güç Devresinin Tasarımı

Bir önceki bölümde üzerinde çalışılması kararlaştırılan güç devresinin tasarımı detaylı olarak 3 no'lu kaynakta verilmiştir. Bu bölümde kullanılan yaklaşım ve gerçekleştirilen devre özetlenecektir. Bu devrenin geliştirme safhasındaki durumu Fotograf 1'de gözlenmektedir.

Öngörülen devrenin tasarımında ilk aşama güç yarı iletkenlerinin seçimidir. Basit bir hesaplamayla 4 fazlı 6/8

yapısındaki bu motorun 12000 d/d'de dönebilmesi için her anahtarın saniyede 2400 defa açılıp kapanması gerektiği kolayca belirlenebilir. Bu anahtarlama hızına BJT, Mosfet ve IGT (Insulated Gate Transistor) transistörler ile ulaşmak mümkündür.

BJT baz akımının yüksek olması sonucunu doğurduğu bunun da sürücü devrede eleman sayısının artmasına yol açacağı gerekçesiyle dikkate alınmamıştır. Diğer iki transistörde bu uygulama için uygundur. Ancak Mosfet transistörlerin kayıpları IGT'lere göre bir kaç kat fazladır. Daha öncede belirtildiği gibi fiat bu uygulamada önemli bir unsurdur. Maliyette önemli bir öğe olan güç anahtarlarının bu önemli kriteri dikkate alarak seçilmesi gereklidir. Bu ise piyasa koşullarına ve satın alınan sayıya bağlı bir unsurdur ve bir prototip çalışması sırasında gerçekçi olarak fiat belirlenmesi hemen hemen imkansızdır. Ancak gerek IGT gerek Mosfet transistor sürücüleri aynı nitelikleri taşıyacağından tasarlanan devrelerin anahtar seçiminden etkilenmesi söz konusu değildir.

Bu uygulamada IGT'ler yeğlenmiştir. Harris firmasının üretiği 25A, 500V, üzerinde akım ölçülmesine imkan veren bir bacağı bulunan bir transistör anahtar olarak kullanılmıştır.

Güç devresi Şekil 10'da gösterilmiştir. Bu şekilden izlenebileceği gibi bloklar halinde gösterilen;

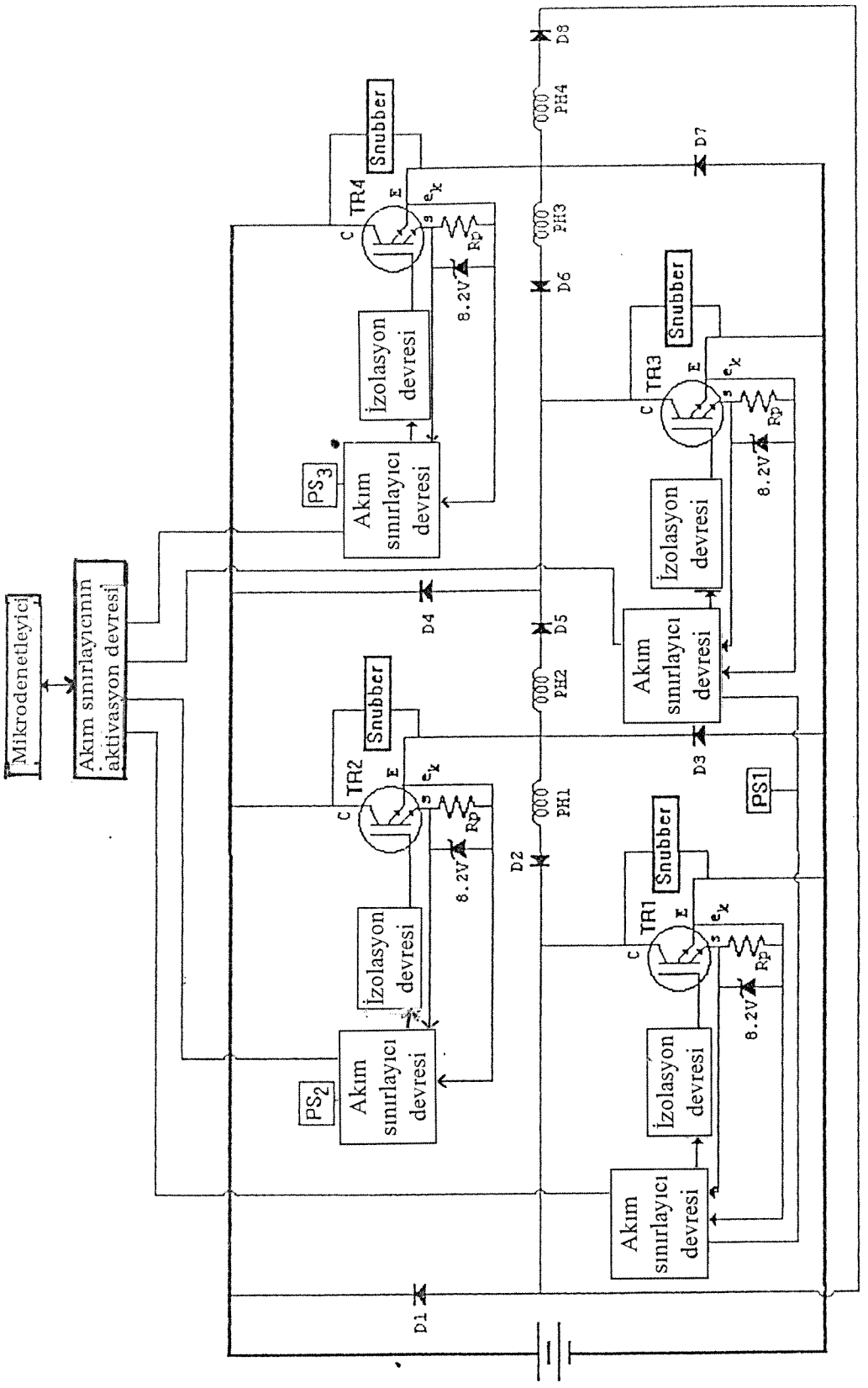

Şekil 10. 4 Fazlı 4 anahtarlı sürücü

a) Snubber

b) İzolasyon devreleri (isolation circuit)

c) Akım sınırlayıcı (current limiter)

d) Akım sınırlayıcı aktivasyon

devrelerinin tasarım ve gerçekleştirilmesi gerekmektedir. Güç katının beslenmesinde 3 ayrı güç kaynağına ihtiyaç duyulacağıda yine Şekil 10'dan izlenebilmektedir. Bu devreler bu bölümde kısaca gözden geçirilecektir.

a) Snubber Devresi : Kimi IGT uygulamaları için snubber ihtiyacı doğmayacağı bilinmektedir. Ancak burada çalışma hızının yüksek olmaması nedeniyle ve emniyet amaçlı olarak bir snubber devresi kullanılmıştır. (Şekil 3.3)

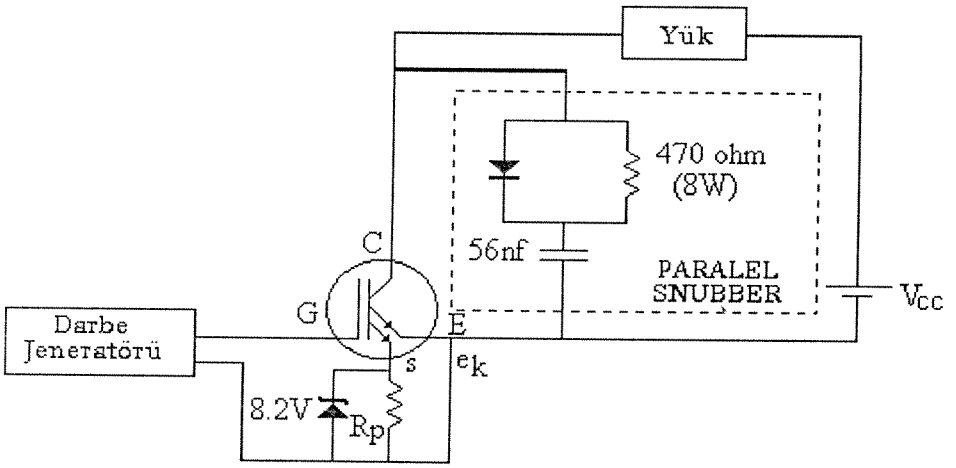

Şekil 11. Snubber devresi

b) İzolasyon Devresi : Güç katının mikroişlemciden izole edilmesi mutlak bir gereksinimdir. Burada bu amaçla hızlı

optoizolatörler kullanılmıştır. Tasarlanan devre Şekil 12'de görülmektedir.

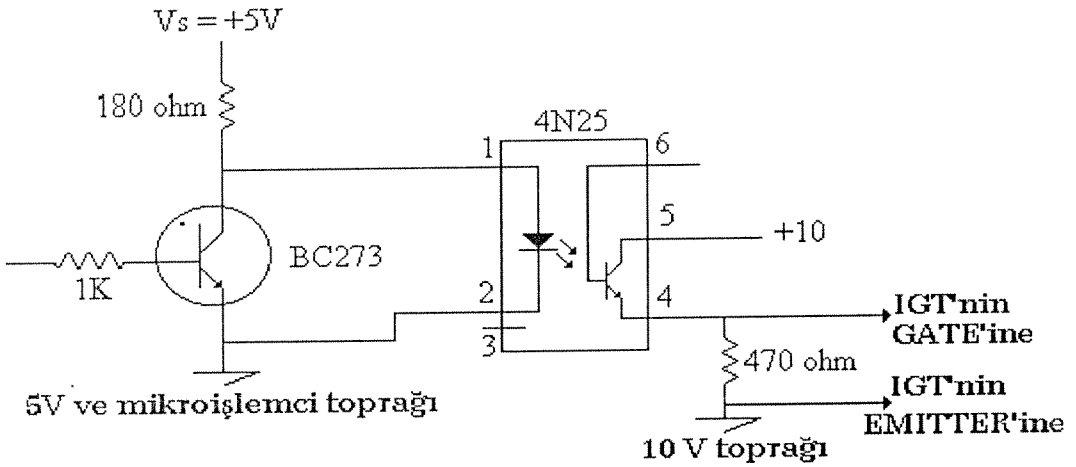

Şekil 12. IGT ve Kontrol bölümleri İzolasyon ve İnversiyon Devreleri

c) Akım Sınırlayıcı : Yüksek hızlarda motordan yeterli moment elde edilebilmesi amacıyla motor 280 V gerilimde beslenmektedir. Bu nedenle düşük hızlarda bir Schmitt Trigger aracılığıyla akım belli sınırlar arasında tutulmalıdır. Burada kullanılan akım sınırlayıcı devrenin akım sınırlama seviyesi, mikroişlemci- D-A konverter aracılığıyla veya doğrudan bir analog sinyal verilerek ayarlanabilmektedir. Hangi yöntemin seçileceği kullanıcının devredeki anahtarı aldığı konuma bağlıdır. (Şekil 13) Bu özelliğiyle devre, kontrol sisteminin mikro işlemcide hesaplama yoluyla belirleyeceği bir akım seviyesinde motorun çalışmasını sağlayabilir.

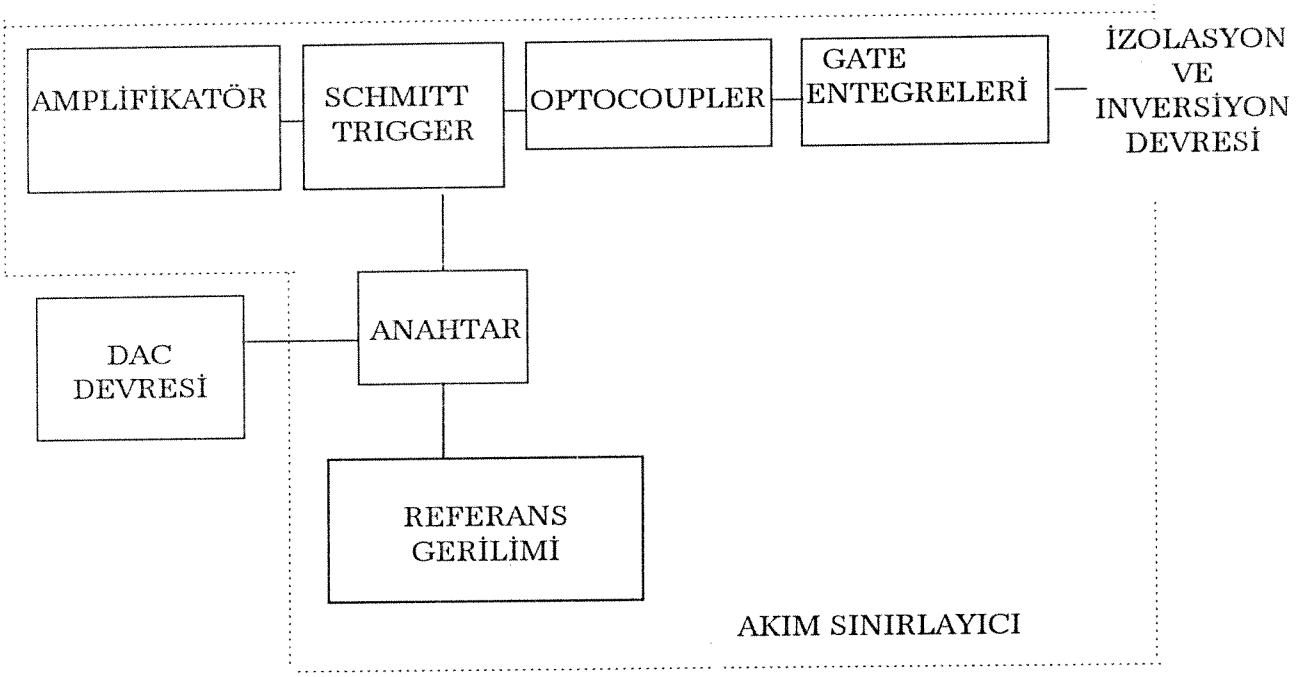

Şekil 13. Akım Sınırlayıcı Devrenin Genel Şeması

d) Akım Sınırlayıcı Aktivasyon Devresi: Devrenin blok şeması Şekil 11'de verilmiştir. Bu devre değişik çalışma koşullarında (Tek fazlı, iki faz ve yarım adım uyartım) hangi transistörün Akım Sınırlayıcı Devresinin, akımın istenilen seviyede tutmak için kıyıcı olarak kullanılacağını belirler. Bu devre Şekil 14'ün sağ alt köşesindeki blokta verilmiştir. İzlenebileceği gibi aktivasyon için işlemciden gelen işaretler kullanılmaktadır. Böylece yazılım yoluyla tek faz enerjili, yarım adım veya iki faz enerjili çalışma koşulları kolayca seçilebilir.

3.2 Konum Belirleyici

Güç devresini denetleyecek olan denetleyiciye konum bilgisinin ulaştırılması motor performansının yüksek olabilmesi için mutlaka gereklidir [6]. Bu amaçla iki yol izlenebilir. Bunlar;

a) Konum belirleyici

b) Dalga şeklinden konum kestirilmesi

teknikleridir. Dalga şeklinden konum belirleyici bir sistem için, seçilenden daha hızlı bir mikro işlemci gerekecektir. Bu aşamada bu yeni ve az sınanmış yöntemin yaratacağı problemlerin AR motorun bu uygulama için uygun olmadığı değerlendirmesinin sağlıklı bir biçimde yapılmasını engelleyebileceği düşüncesiyle bu tekniğin uygulanmasından vazgeçilmiştir. (Ara Rapor 2).

Burada kullanılacak konum belirleyicinin maliyetinin, sistem maliyetinin ufak bir kesri olması gereği ortadadır. Bu bakımdan basit hızdan etkilenmeyen bir özel konum belirleyici geliştirilmiştir. (Şekil 14 ve Fotograf 2)

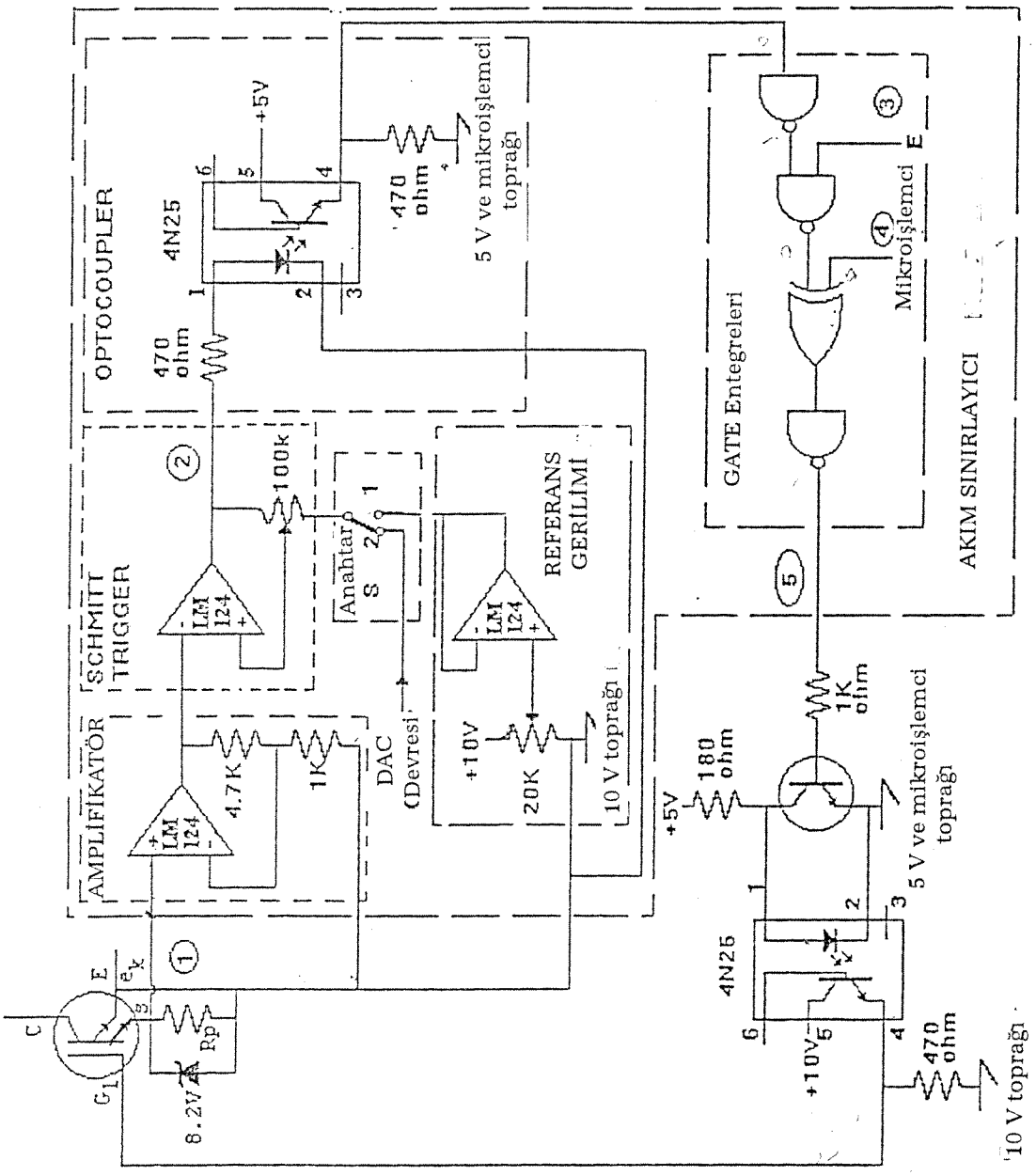

Şekil 14. Akım sınırlayıcının detaylı devresi

Konum belirleyici Şekil 15'de görüldüğü gibi "Hall Efect" sensörlerin (her faz için bir adet) bulunduğu konumu ayarlanabilen duran bir çember ve bunun içinde rotorla birlikte dönen ve rotor dişi konumunda sayısında şerit mıknatıslardan oluşmaktadır.

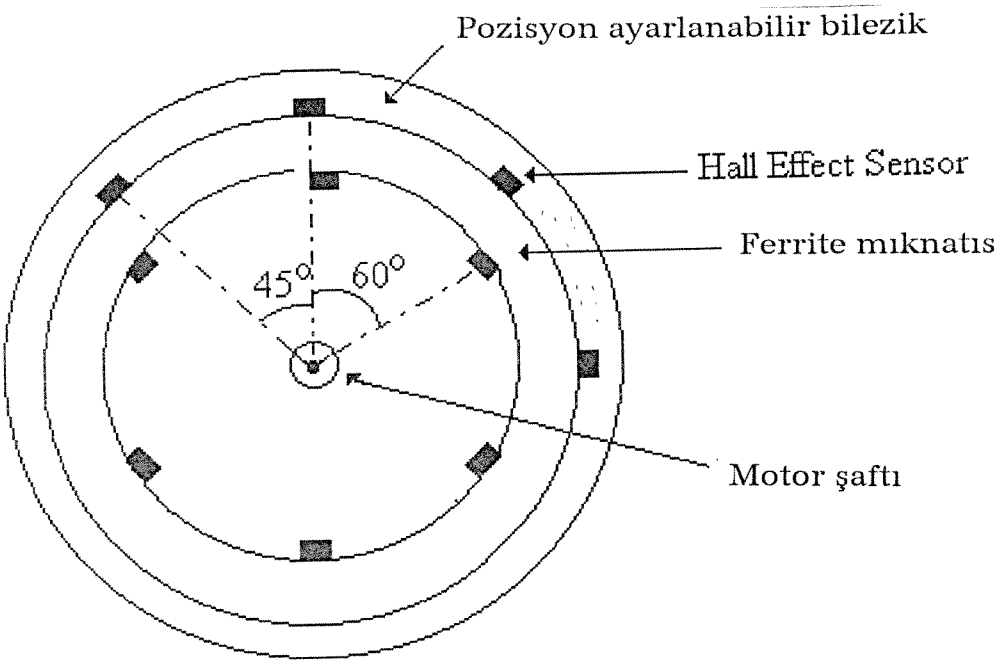

Şekil 15. Kullanılan enkoderin kesiti

Bu kodlayıcının;

a) Rotor konumuna ilişkin ürettiği darbenin yeri mekanik olarak seçilebilmektedir.

b) veya rotor konumunda önceden bilinen bir yerde işaret alınarak, mikro işlemciye bilgi aktarılmakta fazlar bu bilgiden yararlanılarak istenilen ön uyartım açısında fazların uyartılması aracılığıyla da gerçekleştirilebilmektedir.

Şekil 16'da konum kodlayıcıdan gelen işaretleri değerlendirmek ve mikro işlemciye iletmek için kullanılan devre gösterilmiştir. Şekil 17 ve 18'de 500 d/d ve 3550 d/d'da konum belirleyicinin çıkış sinyali (sinyal işleyici devre çıkışında) görülmektedir. Bu şekillerden sinyal seviyesinin hızdan etkilenmediği gözlenmektedir. Ancak laboratuarımızdaki imkanlar 6000 d/d üstünde kodlayıcı çevirmeye imkan vermediğinden kayıt alınamamıştır.

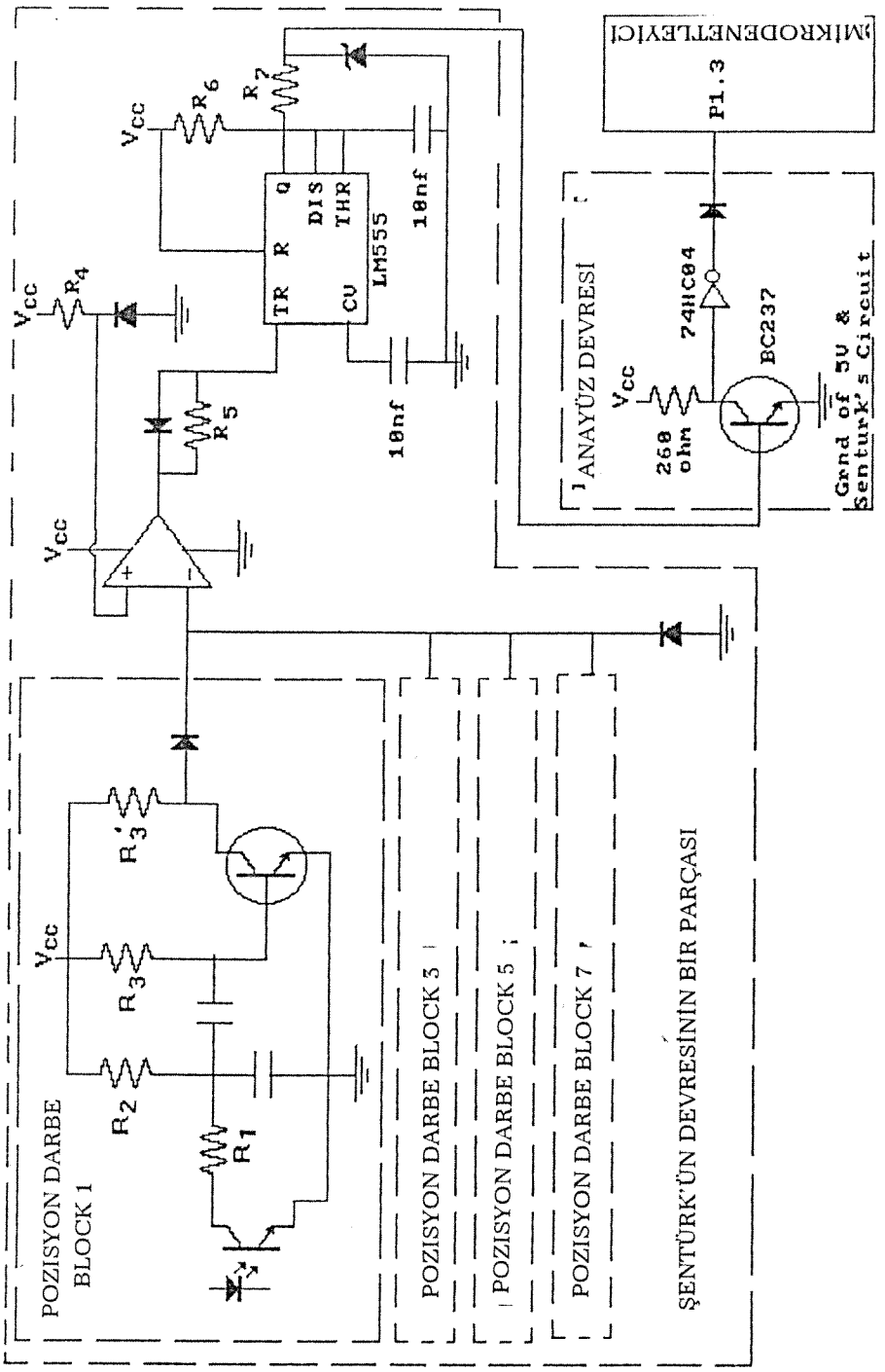

Şekil 16. Enkoder işaretlerinin işleme devresi

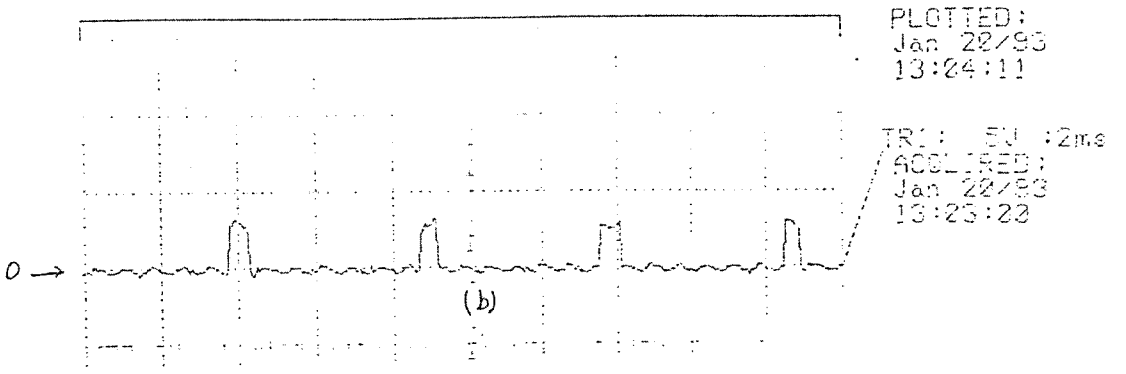

Şekil 17. Konum kodlayıcıdan gelen işaretler (n=500 d/dk)

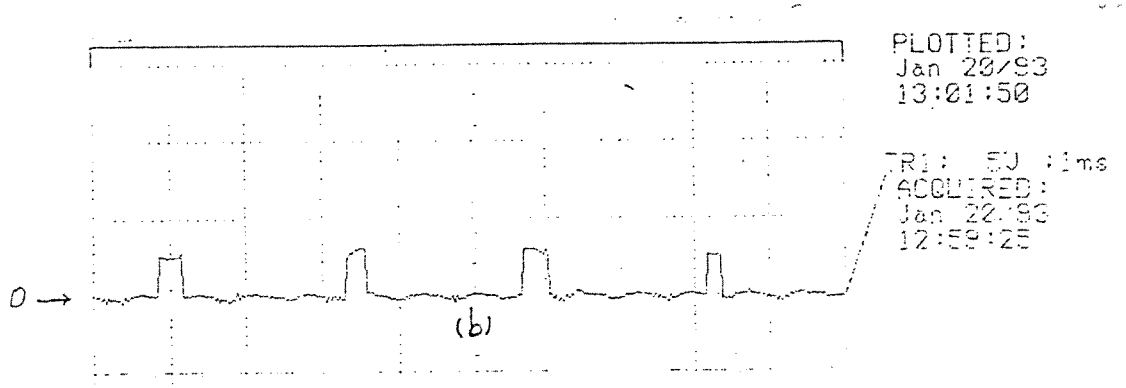

Şekil 18. Konum kodlayıcıdan gelen işaretler (n=3550 d/d)

3.3 Mikro İşlemci Denetimli Sistemin Genel Yapısı

Şekil 19'da denetleyici sistemin genel yapısını ve motor sürücü devresinin ve konum belirleyicinin sistem içindeki yerlerini göstermektedir.

Bu sistemin geliştirilmesi sırasında sağladığı kolaylıklar nedeniyle 8051 mikro işlemcisi için hazırlanmış bir "geliştirme kartı" kullanılmıştır. Bu karta ilişkin bilgiler kaynak 3'de verilmiştir. Burada tekrarlanmayacaktır. [Şekil 20]

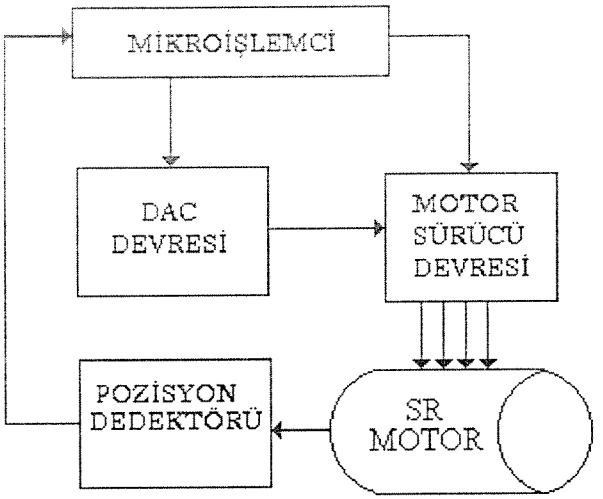

Şekil 19. Mikro işlemci denetimli kapalı döngü denetim sisteminin genel blok şeması

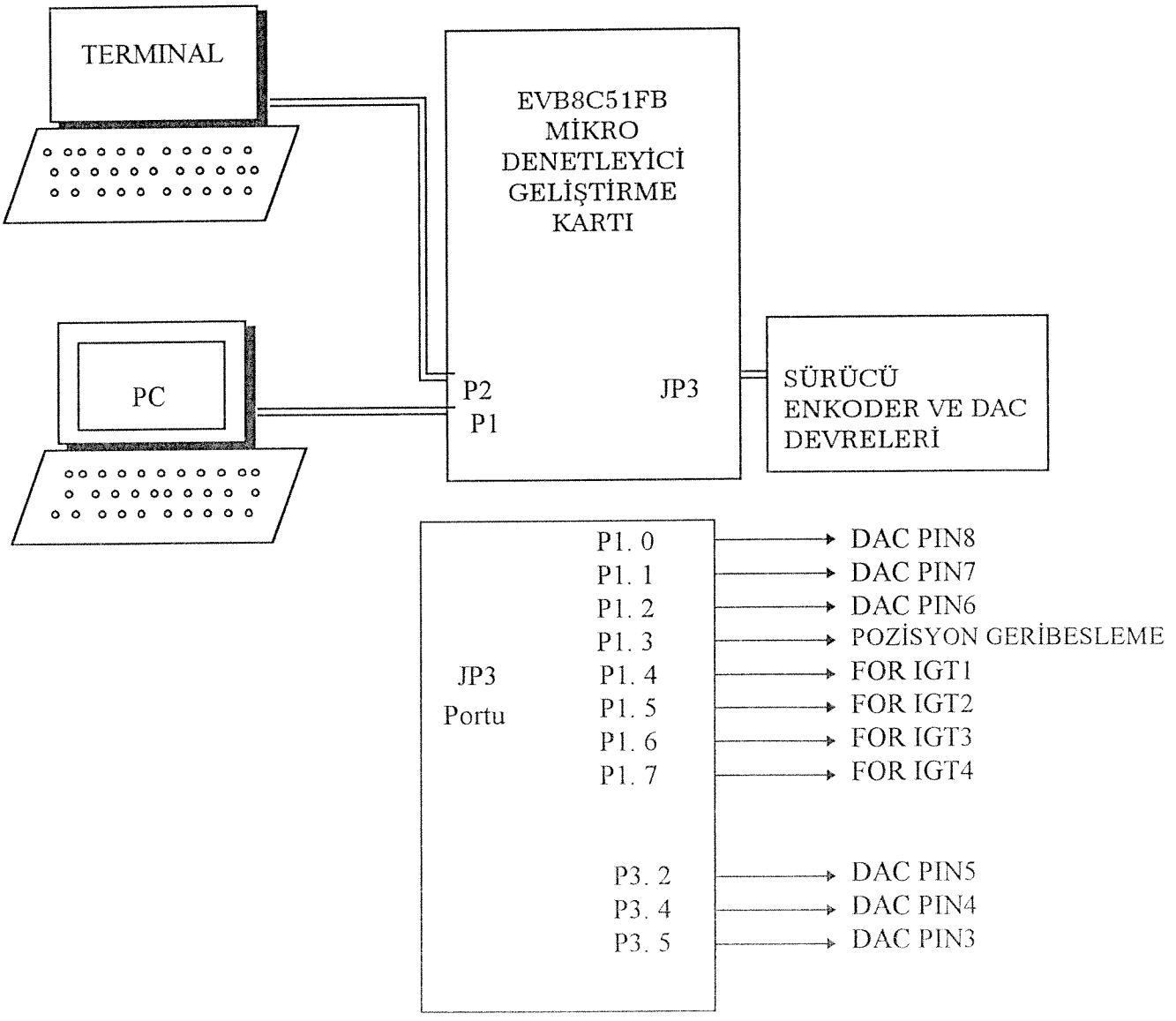

Şekil 20. 8051 kartı, bilgisayar, komuta terminali ve güç devresi

Blok şemada şimdiye kadar üzerinde durulmamış tek blok DAC bloğudur (Digital to Analog Converter). Bu devrenin fonksiyonu mikro işlemcinin denetim yazılımının belirleyeceği akım seviyesinde sürücünün kıyma işlevini yapabilmesi için gerekli referans gerilimini analog bir işaret olarak sürücü devreye iletmektir.

Bu amaçla geliştirilen devre Şekil 21'de verilmiştir. Bu devre mikro işlemciden aldığı 6 bit sayısal işareti Motor akımını 1-5A arasında 62.5mA adımlarla denetlenebilen 3-4.7V arasında bir gerilime çevirmektedir.

3.4. Mikro Denetleyici Yazılımları:

Mikro denetleyici yazılımın ana yapısı Şekil 22'de gösterildiği gibidir. Hemen farkedileceği gibi bu yapının modüler olması hedeflenmiştir. Böylece modüllerin bağımsız olarak değiştirilmesi ve geliştirilmesi mümkün olacaktır. Programın bir diğer özelliği de sürücünün çalışma modu'nun kullanıcı tarafından kolayca programlanabilecek şekilde hazırlanmış olmasıdır. Modüllerin görevi aşağıda kısaca özetlenmiştir. Detaylı bilgi ve akış diagramları 3 no'lu kaynakta verilmiştir.

Ana Modül (Main Module): Ana modül yardımcı modüllerden gerekeni çağırmakla yükümlüdür. İlk işlem hazırlama Şekil

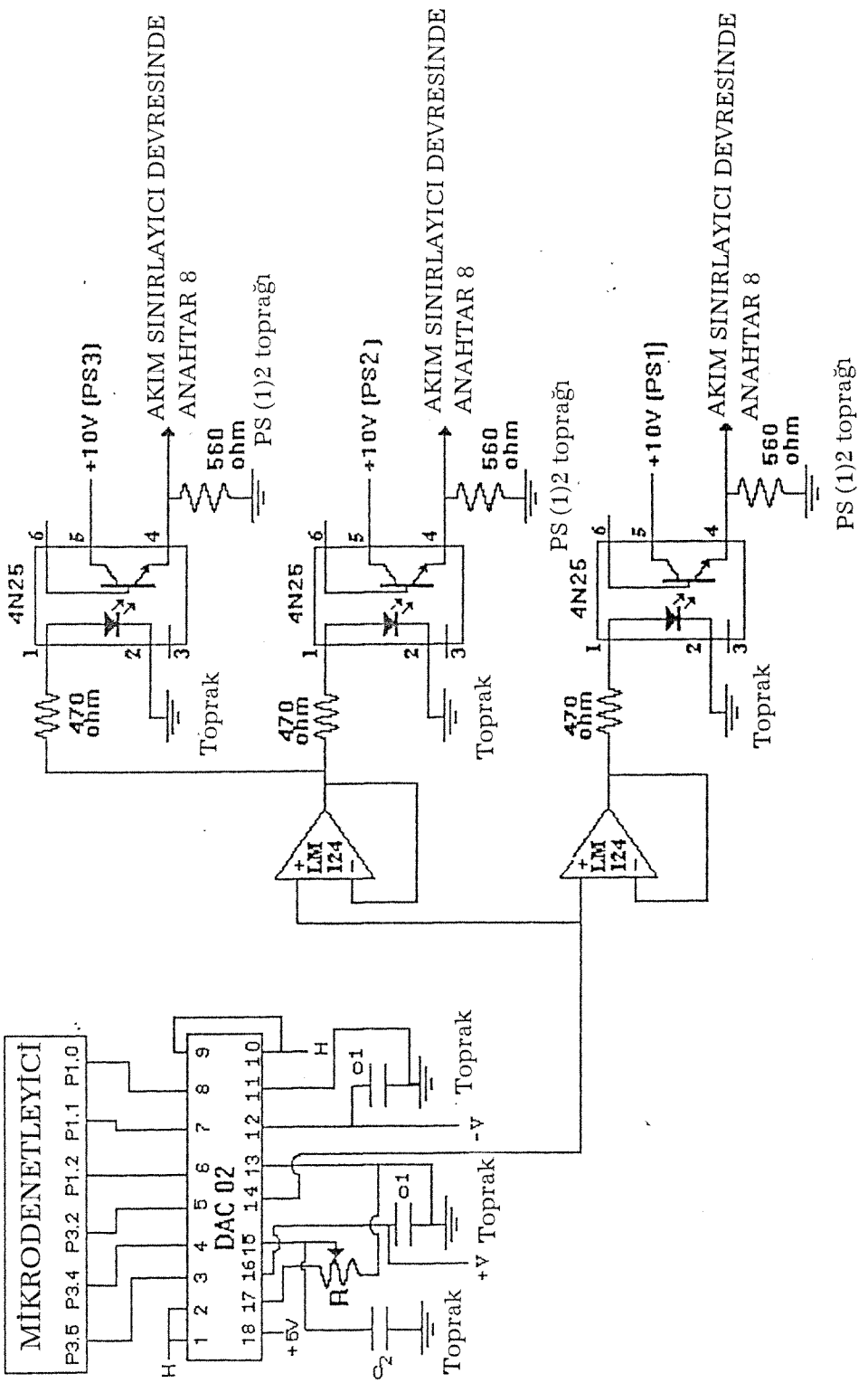

Şekil 21. DAC devresi

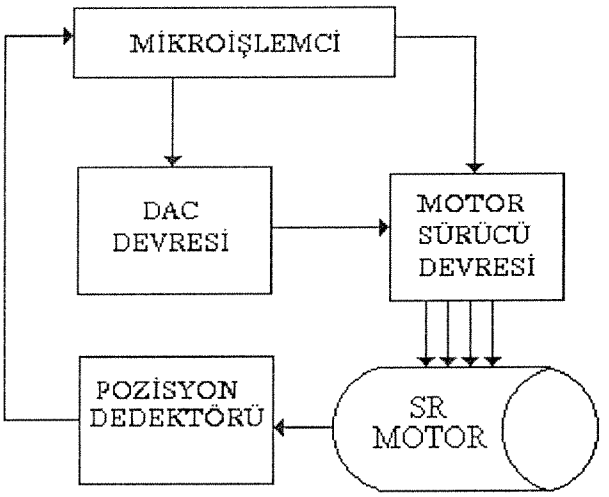

Şekil 19. Mikro işlemci denetimli kapalı döngü denetim sisteminin genel blok şeması

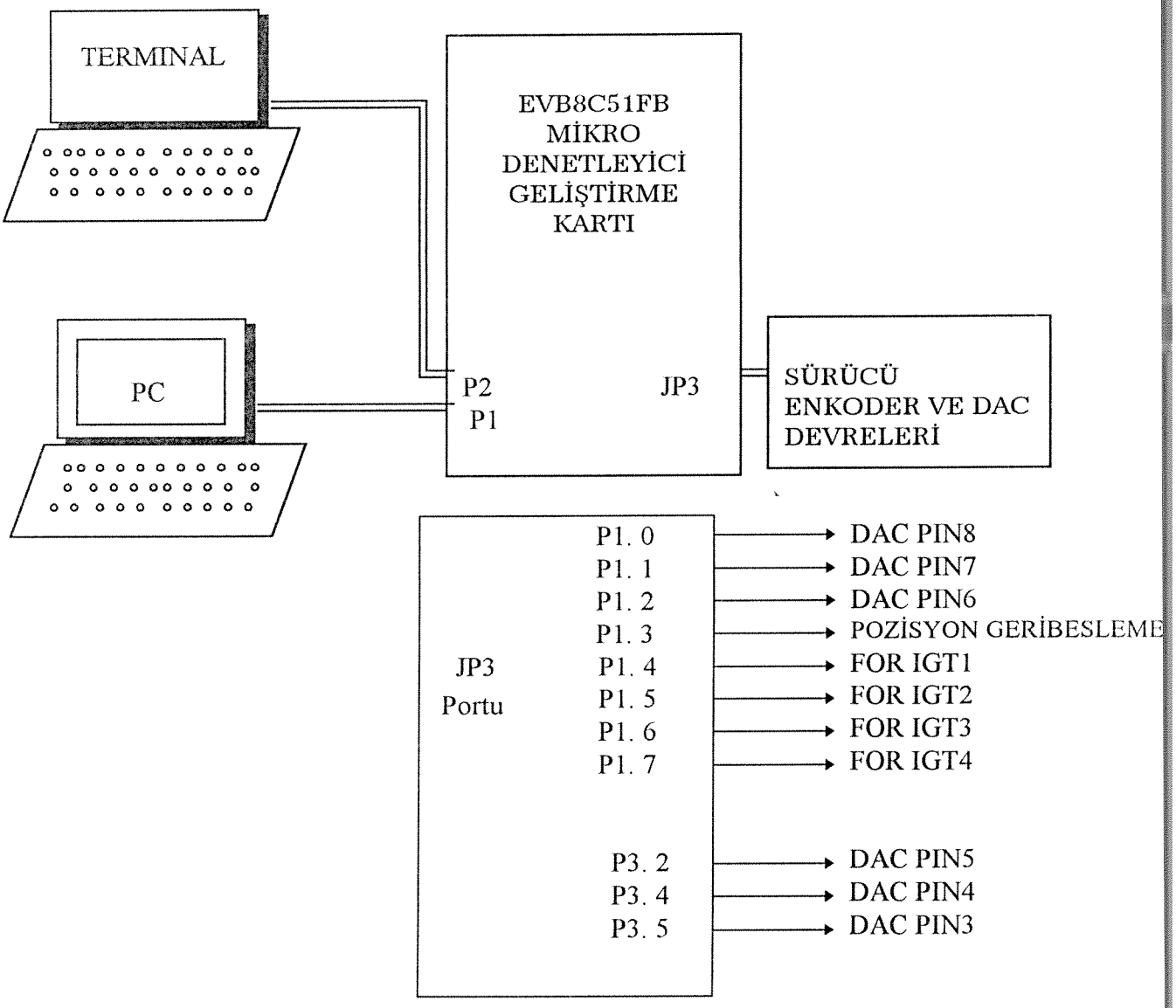

Şekil 20. 8051 kartı, bilgisayar, komuta terminali ve güç devresi

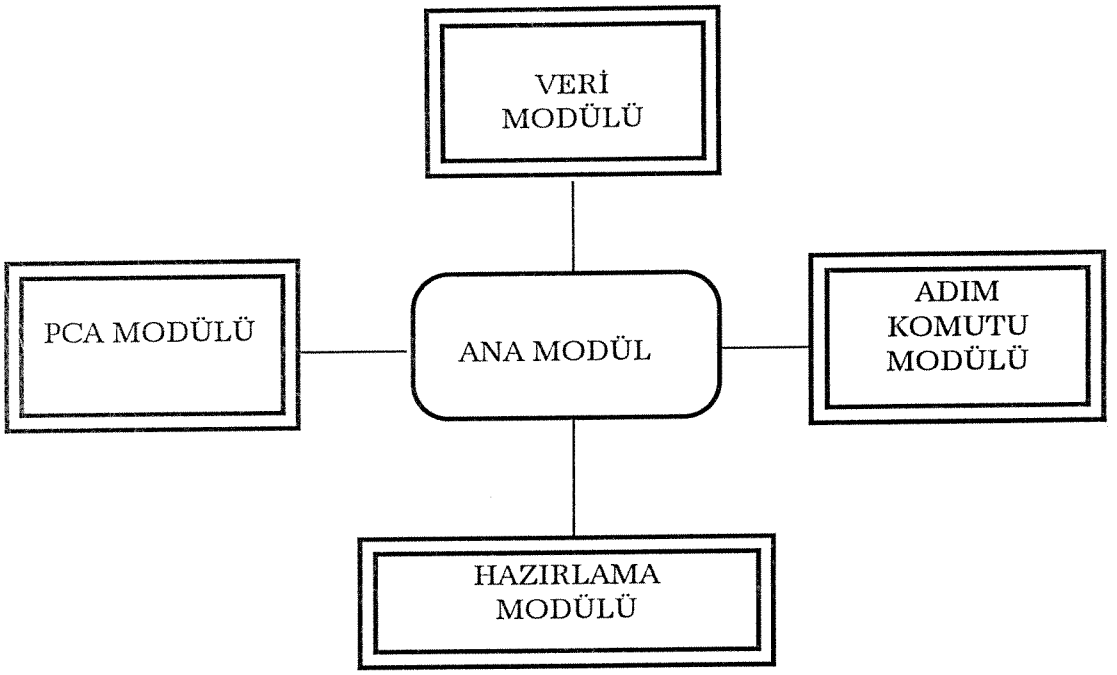

Şekil 22. Yazılımın Genel Yapısı

modülünün (Initialization module) çağırılmasıdır. Bu işlem tamamlandığında "veri modülü" (Data modüle) çağırılır. Bu modülün görevi kullanıcıdan bilgi almaktır. Bundan sonraki işlem gerektiğinde değiştirilebilen bir frekansta 3 faz uyartım işaretinin gönderilmesidir. Bunun amacı motorun bilinen bir fazının öncelikle kararlı hale getirilerek motorun istenilen yönde dönüşünden emin olmaktır. Diğer bir amaç ise durma-kalkma bölgesinde seçilmiş olan bir hızda motoru istenen yönde döndürerek, geri besleme işaretlerinin konum belirleyiciden alınmasını sağlamaktır.

Hazırlama Modülü (Initialization Module): Bu modül mikroişlemciyi bilinen şekilde çalışmaya hazırlar.

Veri Modulü (Data Module): Bu modül kullanıcının motorun çalışmasına ilişkin isteklerini sürücüye aktarır. Daha sonraki aşamalarda bu işlem hafızaya yazılmış bir çalışma programının okunması şeklinde yapılacaktır.

Veri modülü aşağıdaki sırada soruları kullanıcı terminali yansıtır.

Do you want to enter control parameter values (Y/N) Eğer cevap evet (Y) ise aşağıdaki sorular ekranda belirir.

Enter advance angle (0, $^1/_2$, $^1/_4$, $^1/_8$, $^1/_{16}$, $^1/_{32}$)*

Enter phase current (1.0, 1.5, 2.0.....5.0)

Enter mode of operation (O, T, H)

O- Bir fazlı uyartım

T- İki faz birden uyartım

H- Yarım adım modunda uyartım

Do your want rotation be CW ? (Y/N)

Dönüş yönünün belirlenmesini sağlar.

Programın bu hali kullanıcı tarafından belirlenen ön uyartım açısında ve iletim açısını 0.5 birim (rotor adım açısının faz sayısına bölünmesine karşı gelen sayı) çalıştırmaktadır. Kontrol sistemi son

* Bölme işlemi çok uzun bir süre aldığından bu açılar kaydırma işleminin müsade ettigi açılar olarak alınmıştır (EK 5'e bakınız)

haline geliştirildiğinde bu bilgi yanında, motor akım seviyesi ve iletim açısı, kontrol modülünce belirlenecektir.

3.5. Bölümde verilen hız kontrolü modulüyle kullanıldığında, soru listesine

operating speed ?

sorusu da eklenecektir.

PCA Modülü (Programmable Counter Module): Bu modül mikro işlemci saat darbeleri cinsinden konum belirleyicinin iki işareti arasındaki süreyi ölçer. Diğer bir görevi ise motor hızının bir sonraki adımda değişmeyeceği varsayımıyla istenilen ön uyartım açısına karşı gelen mikro işlemci saat darbe sayısının hesaplanması belirlenecek bir 16 bit "timer"a yüklenmesi ve iletim süresi tamamlandığında uyartılmış olan fazın kapatılmasıdır.

Burada ilk aşamada programlama kolaylığı nedeniyle iki konum belirleyici darbesi arasındaki sürenin $^1/_4$, $^1/_8$, $^1/_{16}$, ve $^1/_{32}$'sinin ön uyartım için kullanılması benimsenmiştir. Hazırlanan yazılımın akış diagramı Şekil 22'de verilmiştir.

Bu noktada konum bilgisini veren darbenin geldiği andaki rotor konumunun mekanik olarak seçilebildiğinin hatırlanmasında yarar vardır. Böylece istendiğinde motorun ön uyartım açısı ara değerlere ayarlanabilir.

Adım Komutu Modülü (Step Command Module): Bu modül iki görevi birden üstlenmektedir. Bunlardan bir kullanıcı tarafından belirlenen veya hız kontrol modülünün talep ettiği akım sınırlayıcı devreye DAC aracılığıyla iletilmesidir. Diğer işlev ise seçilen dönüş yönüne göre uyartılacak fazın seçilmesidir.

4. HIZ KONTROLÜ

Önceki bölümlerde bir SR motoru senkronizmadan çıkma egrisi üzerinde çalıştırabilmek amacıyla (bu yöntemde motor üzerindeki konum belirleyiciden gelen işaretlere kitlenmiştir. ("self synchonized") hazırlanan devreler ve microdenetleyici yazılımları tanıtılmıştı. Şekil 23'de tipik bir SR motorunun senkronizmadan çıkma eğrisi gösterilmiştir. Bu eğri kıyıcının devrede olduğu ve faz akımının sabit kaldığı varsayılan sabit moment bölgesi ve momentin hızın yaklaşık olarak tersi oranında düştüğü iki bölgeden oluşmaktadır. Bu eğriyi kontrol eden belli başlı 3 parametre vardır. Bu parametreler.

a) Kıyıcı ile denetlenen bölgede akım seviyesi
b) Ön uyartım açısı (advance angle, ignition angle)
c) İletimde kalma süresi (Conduction period)

Şekil 24'de her bir parametrenin moment-hız eğrisini nasıl etkileyeceği gösterilmiştir. Detaylı olarak (1 no'lu) kaynakta verilen ve motorun doğrusal davrandığı varsayımına dayanan bu sonuçlardan iki gözlemde bulunmak mümkündür. Bunlardan ilki moment hız karakteristiğinin sınır (maksimum) değerini iletim süresinin en yüksek (yaklaşık rotor diş adımının yarısı) olduğu konumda, ön uyartım açısının ise hıza bağımlı olarak ayarlandığı koşullarda verdiğidir.

Bir diğer gözlem ise denetim parametreleri sabit tutulduğu sürece belli bir yük için tanımlı bir çalışma hızı elde edilebileceğidir. (Şekil 23)

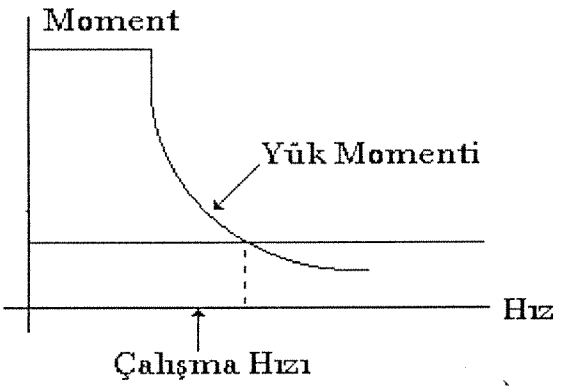

Şekil 23.

Bu değerlendirmeler motorun istenilen momenti istenilen hızda verebilmesi için bir denetim yöntemi ortaya konulması ve denetim parametrelerinin kullanılması yönteminin belirlenmesi gereklidir. Doğal olarak böyle bir çalışma bir dinamik motor modeli üzerinde araştırmalar yapılmasını gerektirmektedir. Ancak,

bu çalışmanın amaçları arasında böyle bir model geliştirilmesi bulunmadığından daha empirik bir yaklaşım benimsenmesi gereği doğmuştur. Ancak, bu önemli konuda da bir araştırma başlatılmış fakat henüz sonuçlanmamıştır.

Buradaki uygulamada SR motorun 400 d/d'de 1 Nm üretirken belli zaman aralıklarında he iki yönde de dönmesi, zaman zaman da 10000 d/d civarına kadar hızlanması (Sıkma) daha sonra tekrar düşük devirlerdeki çalışmaya dönmesi gerekmektedir. Hızlanma işlemi sırasında makinada aşırı titreşim olduğu takdirde yükü dengeleyecek bir yöntemin kullanılması gereklidir. Bütün bu işlemler sırasında yükün yığılmalar veya başka bir nedenle kısa süreli değişmesi kontrolun kaybına sebep olmamalıdır.

Diğer dikkat edilmesi gereken bir unsur ise istenilen momentin denetim parametrelerinin değişik kombinasyonları için elde edilebileceğidir. Örneğin düşük hızda çalışmada yüksek bir sabit akım değeri ve büyükçe bir ön uyartım açısı seçilebilir. Alternatif olarak düşük bir faz akımı küçük bir ön uyartım açısında aynı talebin karşılaması mümkündür.

Akım değerinin yüksek tutulduğu denetimde motor sıcaklık sınırlarına yakın çalışacak verimliliği düşük olacaktır. Ancak, denetimden çıkmaması için bir sonraki akımda ön uyartım açısı kolaylıkla değiştirilerek (ufaltılarak) mevcut yüksek ortalama moment potansiyelinden yararlanılabilir. Faz akımının küçük

olduğu durumda ise motor daha verimli ve soğuk çalışacaktır. Ancak, üretilebilecek ortalama momentin alabileceği en yüksek değer (ön uyartım açısıyla denetlenebilen) bu halde daha ufaktır. Daha büyük bir moment elde edilebilmesi için akımın arttırılması gerekecektir. Bu iki yaklaşımdan hangisinin daha "robust" bir denetim vereceği de bir araştırma konusudur.

SR motorun diğer bir özelligi de "self synchronized" mod'da çalıştırılmadığında rotor konumunun (ön uyartım açısının) kendiliğinden momenti dengeleyecek bir noktada çalışabilir olmasıdır. Bu bakımdan, eldeki imkanların daha detaylı bir çalışmaya elvermemesi nedeniyle, düşük verimli olmasına karşın daha yüksek akımdan çalışılması ve motor istenilen hıza getirildikten sonra açık döngü çalışıyormuş gibi serbest bırakılarak, doğal "robust"luğundan yararlanılması yöntemi benimsenmiştir.

Takibeden bölümde bu araştırmanın başında geliştirilen ve motorun konum belirleyiciden gelen darbelere kitlenerek çalışabilmesi için hazırlanan yazılım tanıtılmaktadır. Altbölüm 4.1.'de ise daha sonra geliştirilerek mevcut yazılıma eklenen motorun hızlanmasını, sabit hızda çalışmasını ve yavaşlatılmasını sağlayan algoritmalar özetlenmiştir.

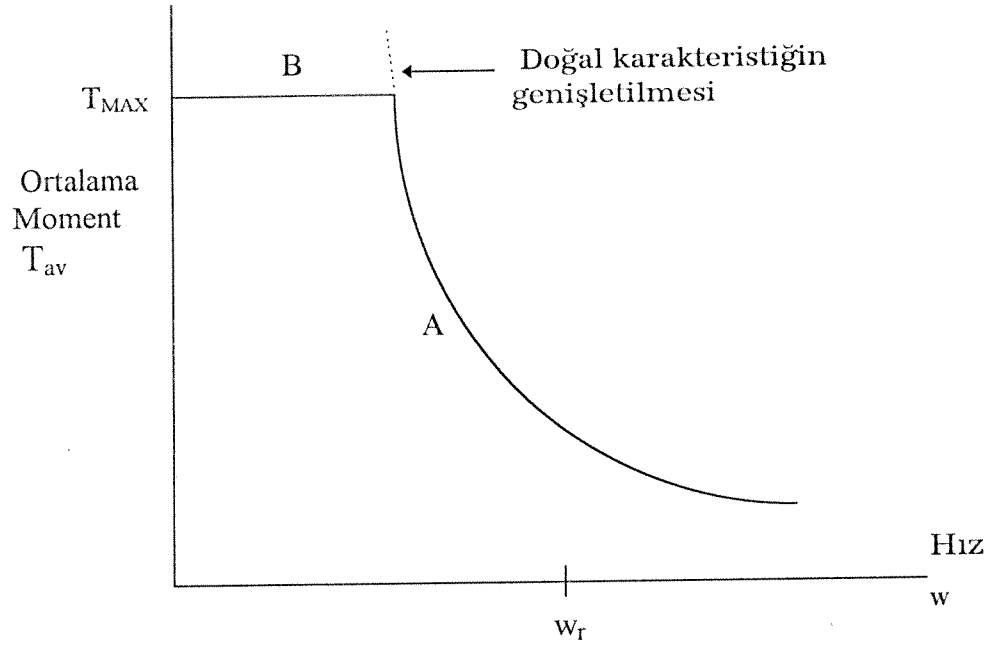

a) SR motor için tipik senkronizmadan çıkma eğrisi

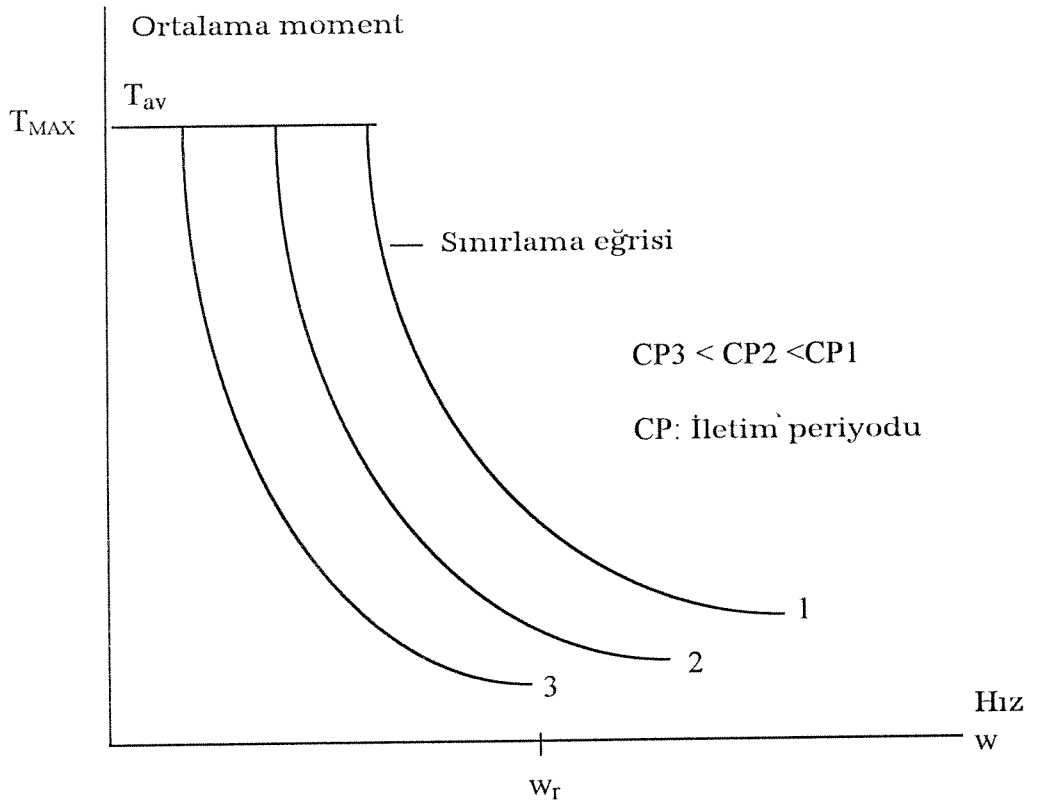

b) SR motorun sabit gerilim kaynağı, değişik iletim açılarında karakteristiği

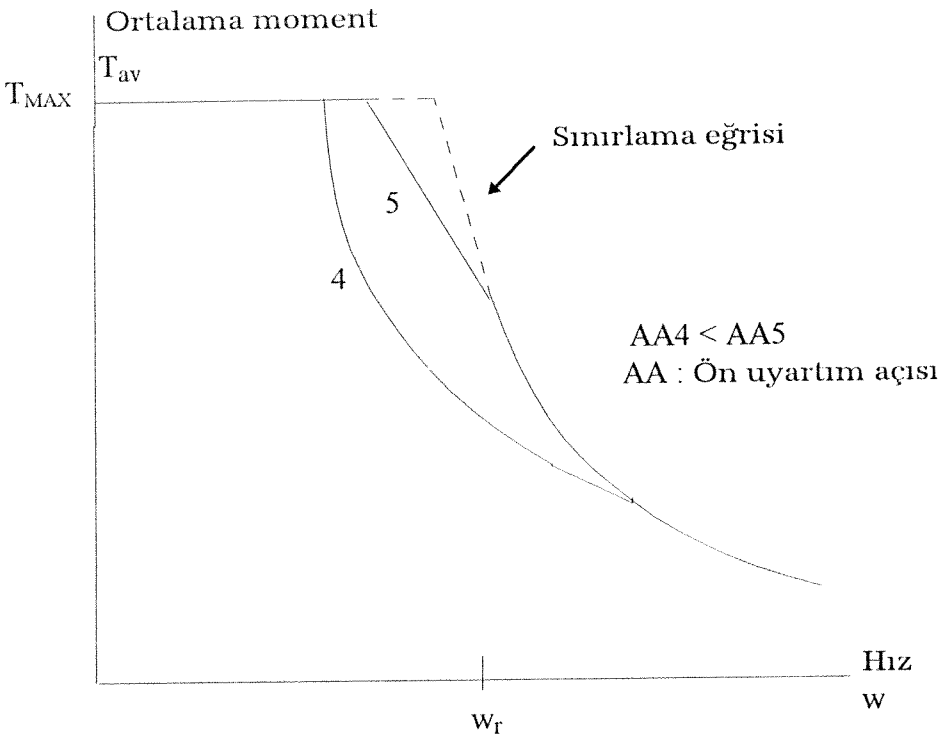

c) Ön uyartım açısının senkronizmadan çıkma eğrisine etkisi

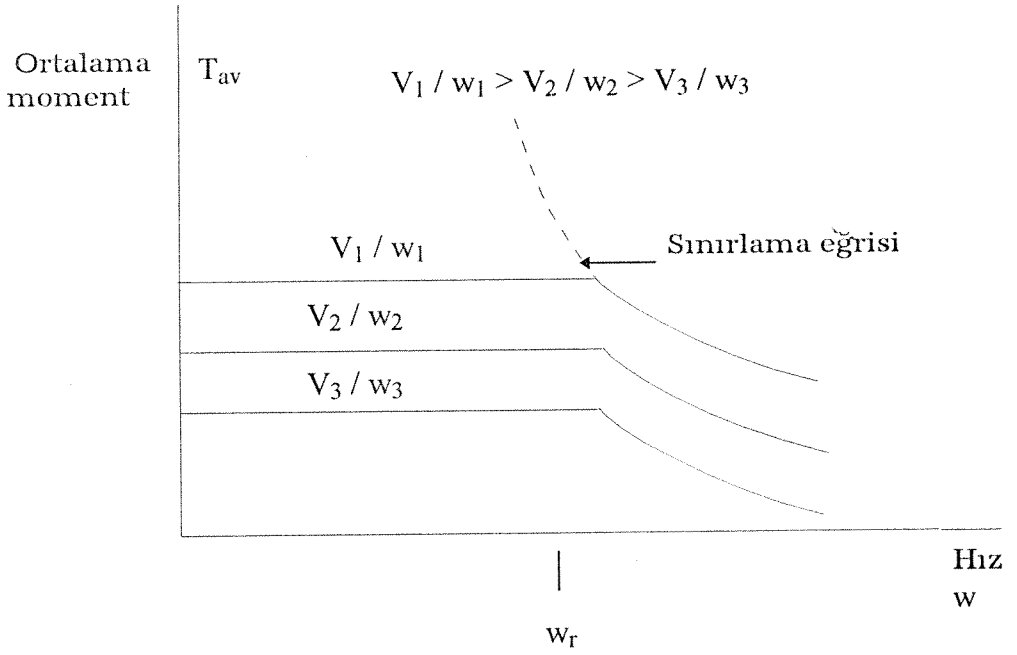

d) SR motorun sabit ön uyartım ve iletim açısında değişken genlikli kaynaktan sürüldüğünde karakteristiği

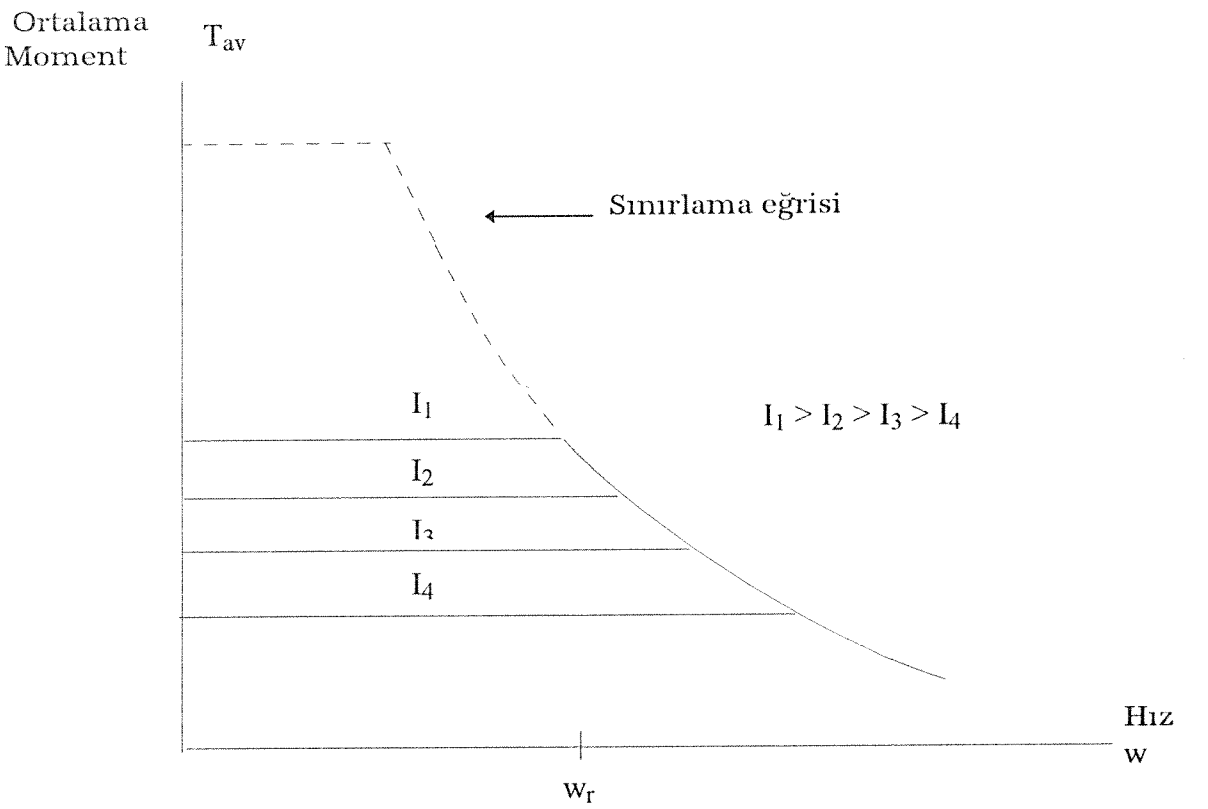

e) SR motorun faz akımı ayarlanabilen bir kaynaktan, sabit ön uyartım ve iletim açısından sürülmesi

Şekil 24. a, b, c, d, e Kontrol parametrelerinin SR motor karakteristiği etkisi

4.1. Hız Kontrol Stratejisi:

Daha önce Veri Modulü (Bölüm 3.4) bölümünde tarif edildiği gibi motor hız kontrolü modunda çalıştırılacağı zaman veri modülü diğer sorulara ilaveten motorun çalışmasının istendiği hız ve ne kadar süreyle bu modda çalışacağı da sorulmaktadır.

Hız 50-9990 d/d (n) arasında 10 d/d aralıklarla girebilmektedir. Bu durumda μc bir adıma karşı gelen darbe periodunu hesaplar

$$\text{Saniyede devir} = \frac{n}{60}\ \text{dd/sn}$$

$$f = \text{Darbe/sn} = \frac{n}{60} \times 24 = \frac{n.2}{5} \qquad T = \frac{1}{f} = \frac{5}{2n}$$

Motorun istenen hızda çalışma süresi ise 50 ms katları olmak üzere 1-9999'a kadar bir sayı olarak girilebilir. Böylece en çok 500 dakikalık bir çalıştırma süresi söz konusudur.

Hız kontrolü sistemi, kalkma-durma bölgesindeki bir hıza karşı gelen frekansta (20 adım/sn) 3 darbe gönderilerek başlatılır. 1.darbe ile rotor bilinen bir fazın altında kararlı duruma getirildikten sonra, takip eden 2 darbede konum belirleyiciden gelen darbelerden hız ölçme işlemi (PCA modulü) başlar.

Hızlanma:

3 darbeden sonra motor hızlanma algoritmasına girmiştir. Motor hızı sürekli olarak ölçülür ve hedef hızla karşılaştırılır. Motor anma hızının -5.25 %'sine ulaşana kadar kullanıcının girdiği ön uyartım açısında konum belirleyici darbelere kitlenerek hızlanır. Bu yöntemde hızlanma mümkün olan en yüksek hızda gerçekleştirilir. Motor hızı belirlenen bandın içine girdiğinde (anma hızının%-5.25, + % 6.25 arası), anma hızına karşı gelen

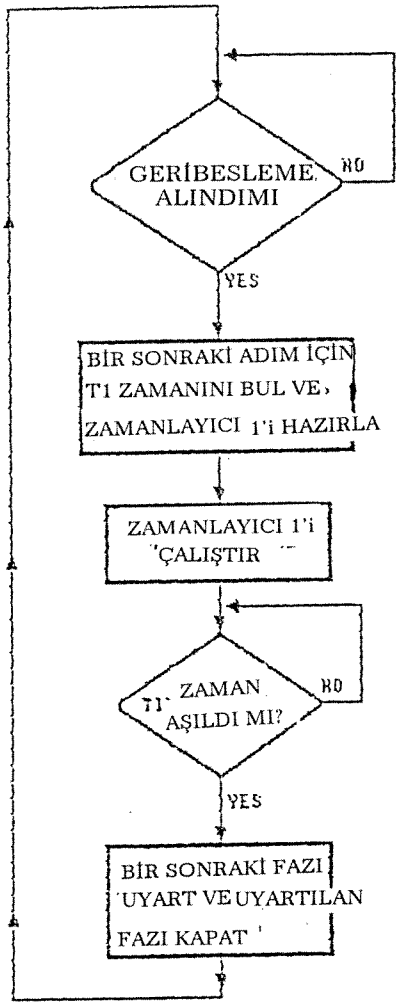

(a)

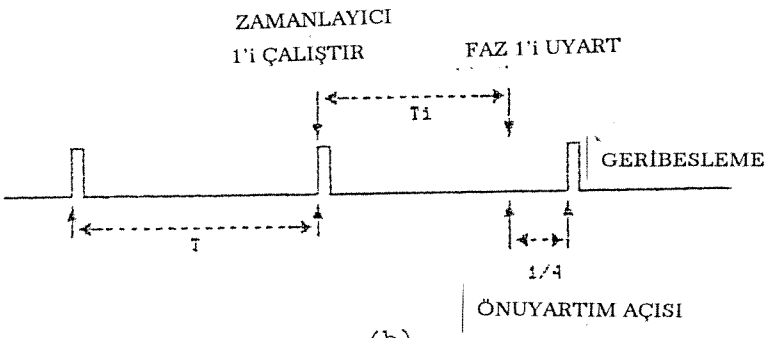

(b)

Şekil 25. Ön uyartım açısının mikro işlemci tarafından belirlenmesi

a) Yazılımın akış diagramı

b) 1/4 ön uyartım açısı için darbelerin yeri

frekansta darbeler gönderilir. Bu çalışma biçimi "robust" bir kontrol yöntemidir. Yük değişmeleri, aynı bir senkron motorda olduğu gibi, rotor konumunun uyartım noktasına göre geri kayışına bağlı olarak dengelenir ve motor o hızda yükü karşılayacak momenti üretebiliyorsa motor senkronizmadan çıkmaz. Ancak, bu süre içerisinde PCA modeli hız ölçümüne (period ölçümüne) devam eder ve motorun belirlenen sınırlar içinde kalıp kalmadığını gözetler. Eğer motor hızı bu sınırlar dışına çıkarsa motor tekrar konum belirleyici darbelerine kitlenir ve yükün müsade ettiği bir hızda senkronizmayı kaybetmeden çalışır.

Yukarıda verilen algoritmanın akış diagramı Şekil 26'da gösterilmiştir.

Yavaşlama:

Hazırlanan yazılım, istenilen hızda çalışma süresi tamamlandığında motorun yavaşlama moduna geçmesini sağlamaktadır. Bu amaçla faz sırası tersine çevrilmekte ve konum belirleyicinin darbelerine kitlenilmektedir. Bu modda çaışma hızı durma kalkma bölgesine düştüğünde bir faz açık olarak bırakılmakta ve sistem durmaktadır.

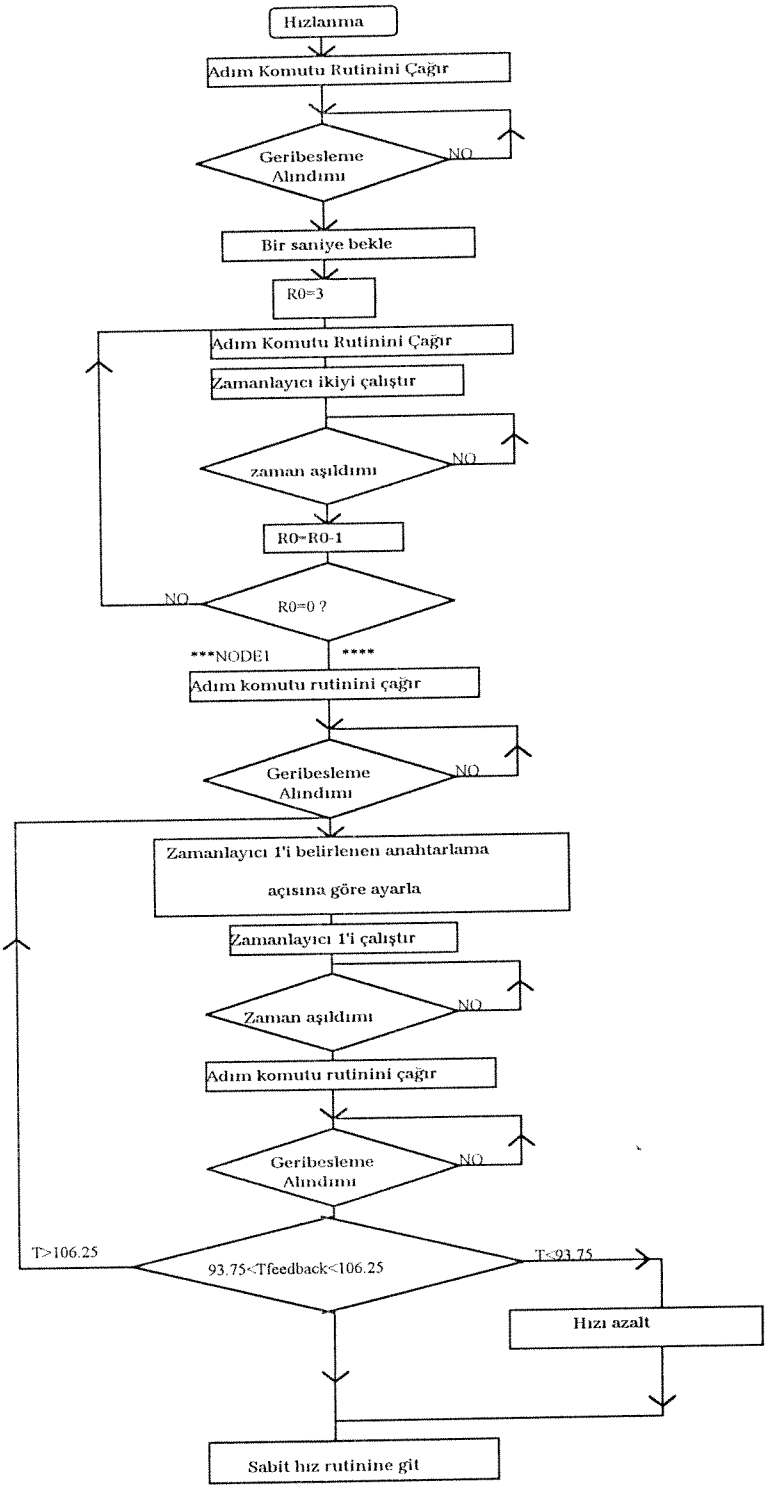
Hızlanma
Adım Komutu Rutinini Çağır
Geribesleme Alındımı
NO
Bir saniye bekle
R0=3
Adım Komutu Rutinini Çağır
Zamanlayıcı ikiyi çalıştır
zaman aşıldımı
NO
R0=R0-1
NO
R0=0 ?
***NODE1
****
Adım komutu rutinini çağır
Geribesleme Alındımı
NO
Zamanlayıcı 1'i belirlenen anahtarlama açısına göre ayarla
Zamanlayıcı 1'i çalıştır
Zaman aşıldımı
NO
Adım komutu rutinini çağır
Geribesleme Alındımı
NO
T>106.25
93.75<Tfeedback<106.25
T<93.75
Hızı azalt
Sabit hız rutinine git

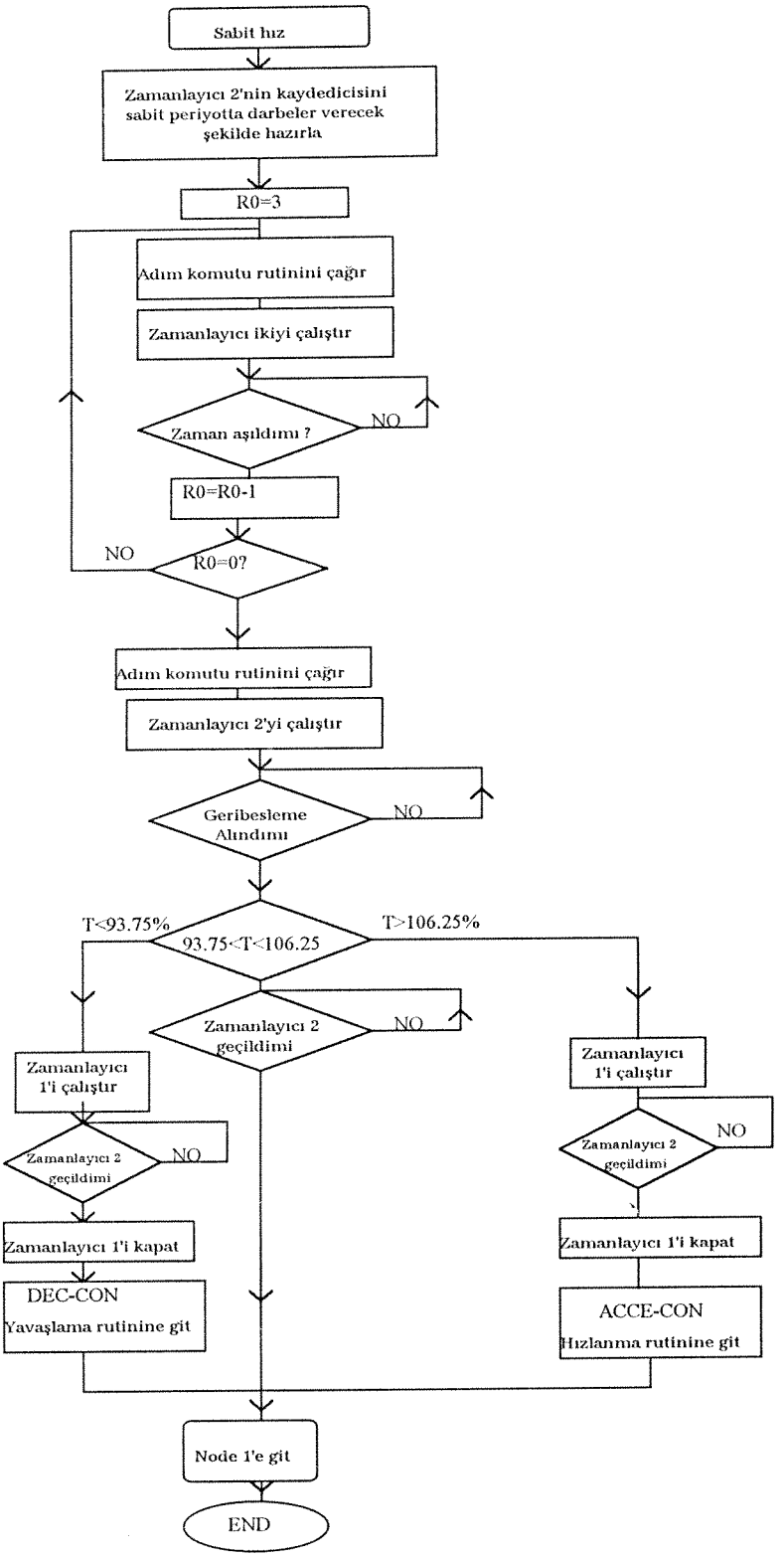

Şekil 26. Hızlanma ve sabit hız yazılımı akış diagramı

5. SİSTEMİN SINANMASI

Geliştirilen donanım ve yazılımın sınanması için bir dizi deney yapılmıştır. Bu deneyler detaylı olarak kaynak 4'te verilmiştir. Sonuçlar bu bölümde kısaca özetlenecektir.

5.1 Güç Katı Üzerinde Deneyler

İlk deneyler güç katı transistörleri üzerinde yapılmıştır. IGBT transistörlerin yaklaşık 0.7μs'de iletime geçtiği 5μs'de ise kapatılabildiği gözlenmiştir. (Şekil 27 ve 28) Şekil 28'den izlenebileceği gibi snubber devresinin transistör, kollektör, emiter uçları arasında aşırı gerilim oluşmasının engellenebildiği gözlenmektedir.

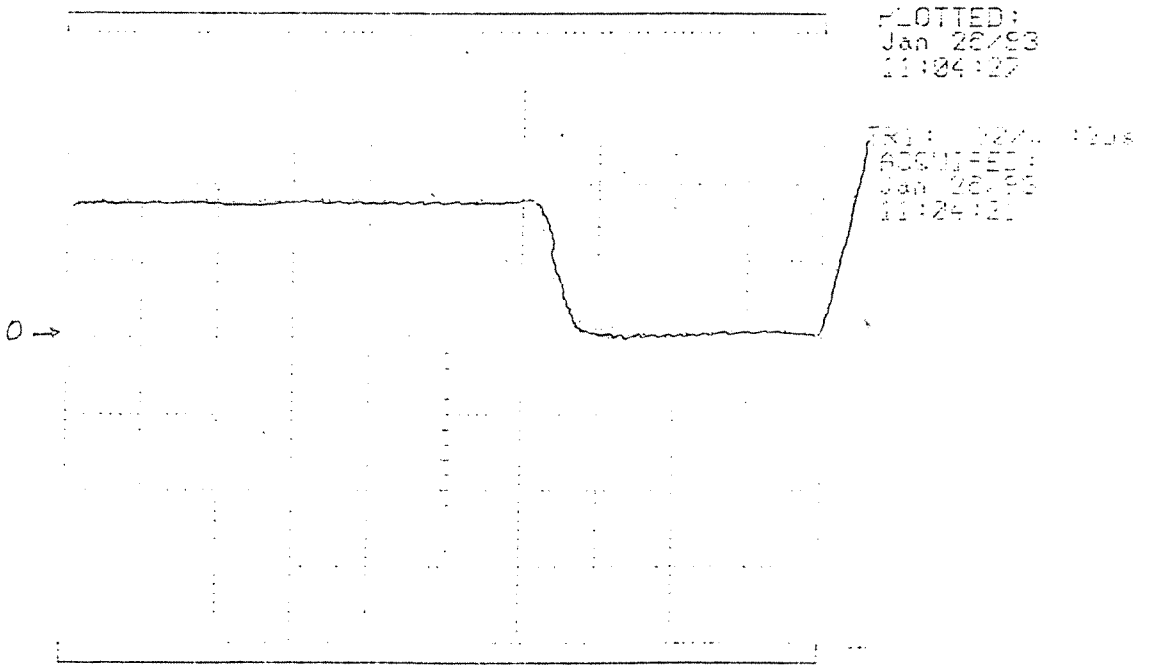

Şekil 27. Bir IGT'nin iletime girmesi sırasında kollektör emitör voltajı

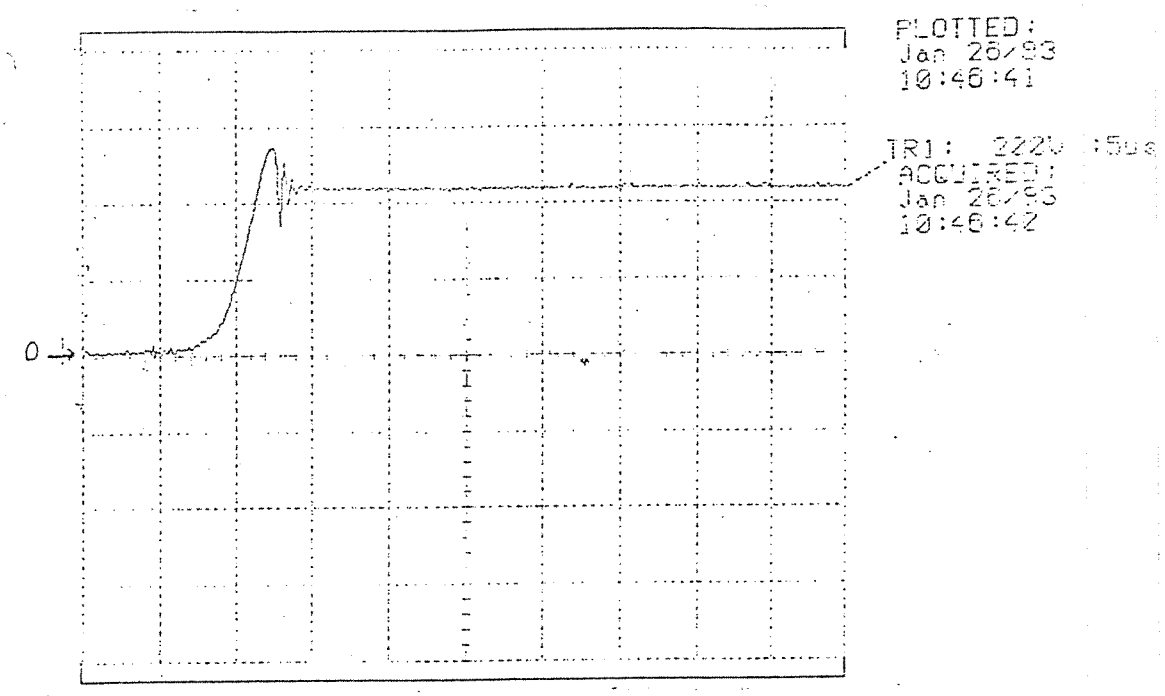

Şekil 28. Kapanma sırasında bir IGT'nin kollektör emiter voltajı

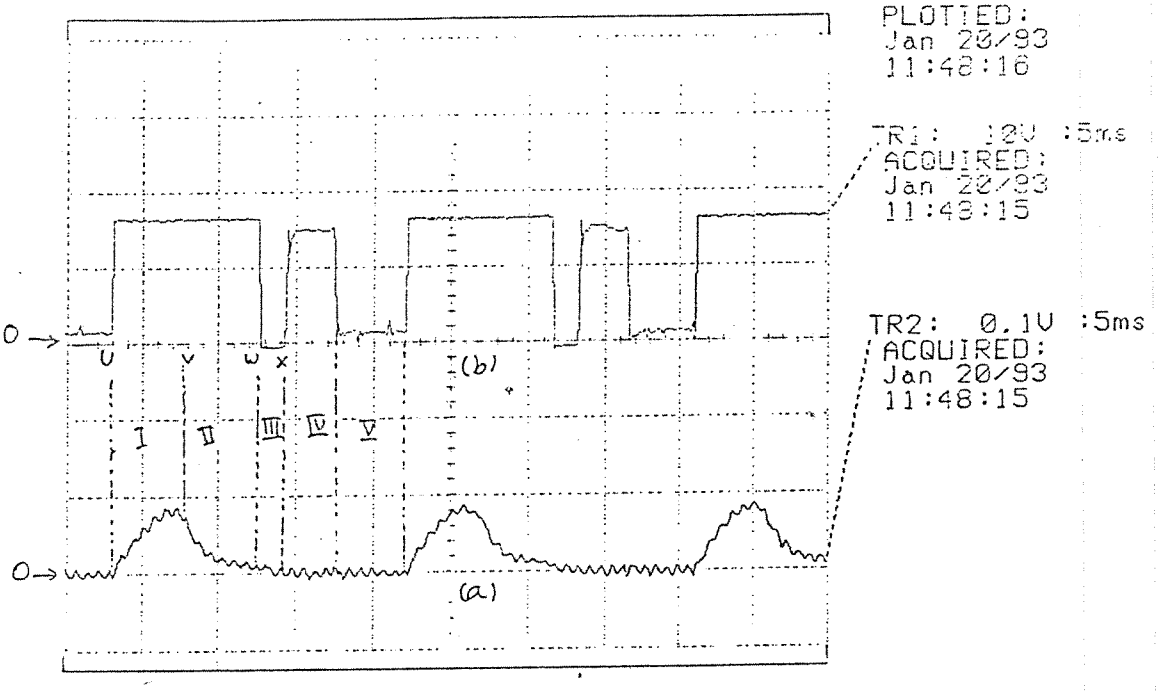

Şekil 29.

a) Faz akım dalga şekli

b) Vce dalga şekli (n=500d/d, θ_i=0)

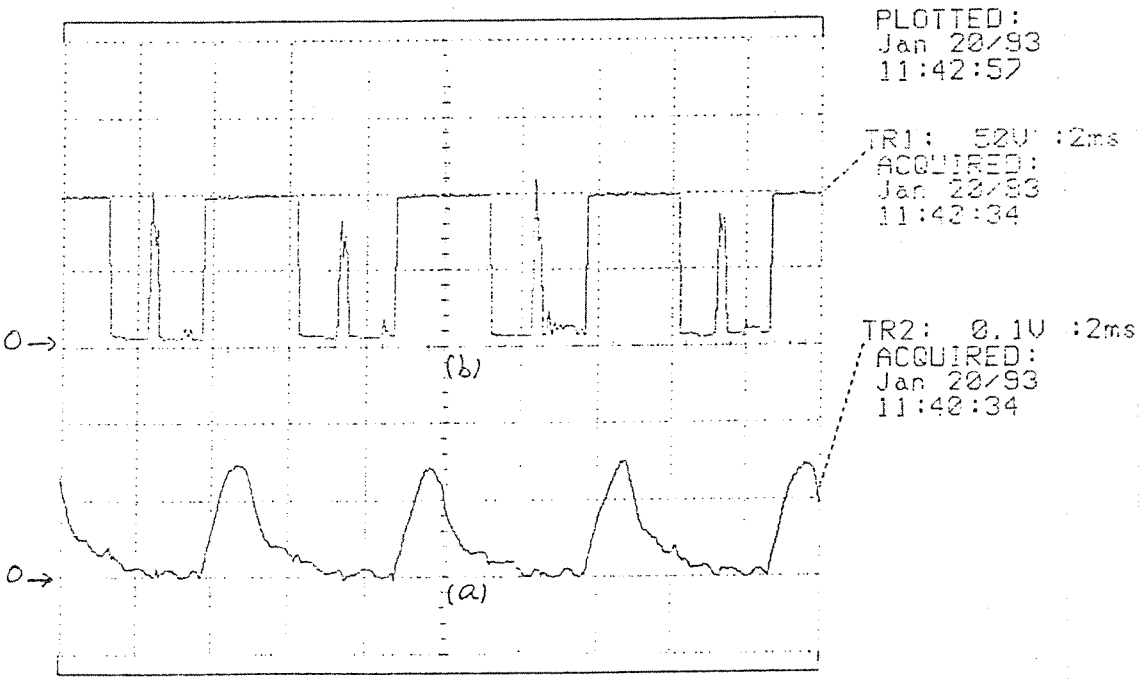

Şekil 30.

a) Faz akımı dalga şekli

b) Vce dalga şekli (n=2000 , θ_i =0)

Şekil 20 ve 30 de ise 2 değişik hızda, ön uyartım açısı "0" iken ölçülen kollektör emiter gerilimleri ve faz akımları gözlenmektedir.

5.2 Ön Uyartım Açısı Yazılımının Sınanması

Şekil 31 ve 32'da konum belirleyiciden gelen darbeler ve ilgili transistörün kapısında gözlenen işaretler $^1/_4$ (3.75°) ve $^1/_2$ (7.5°)ön uyartım için verilmiştir. Şekillerden izlenebileceği gibi yazılım verilen komutlara uygun olarak istenen gecikmelerle transistörleri açabilmektedir.

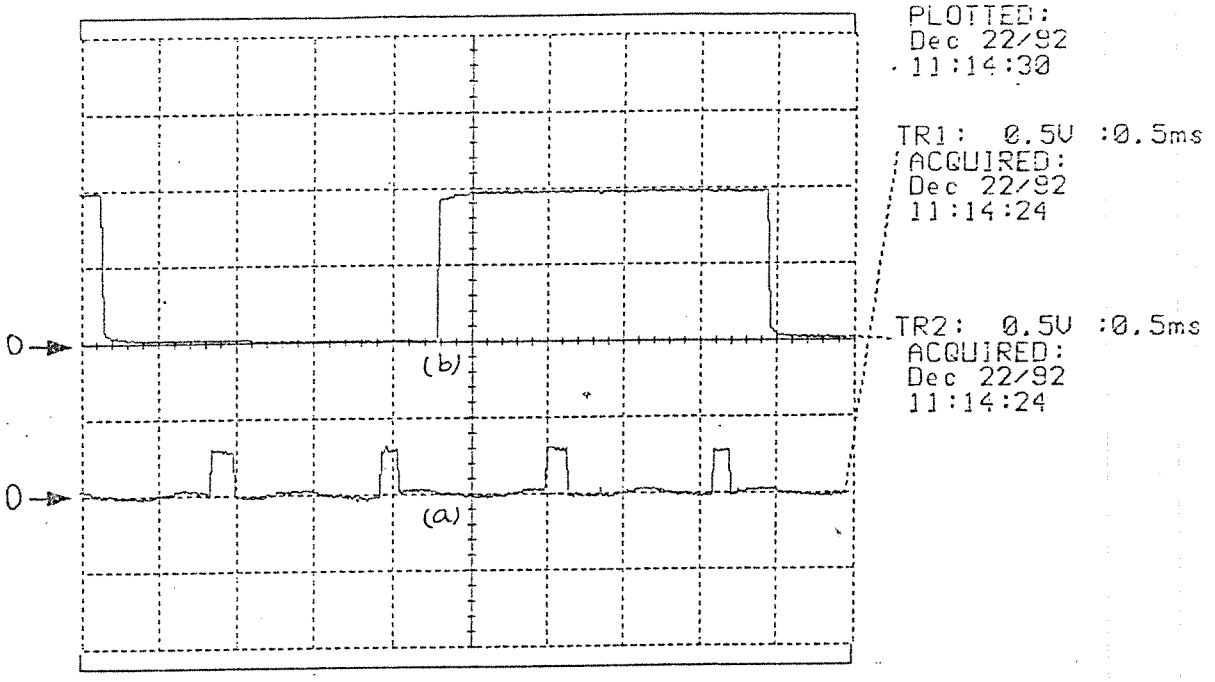

Şekil 31.

a) Enkoder işaretleri

b) Transistör baz gerilimleri (θ_i =3.75º)

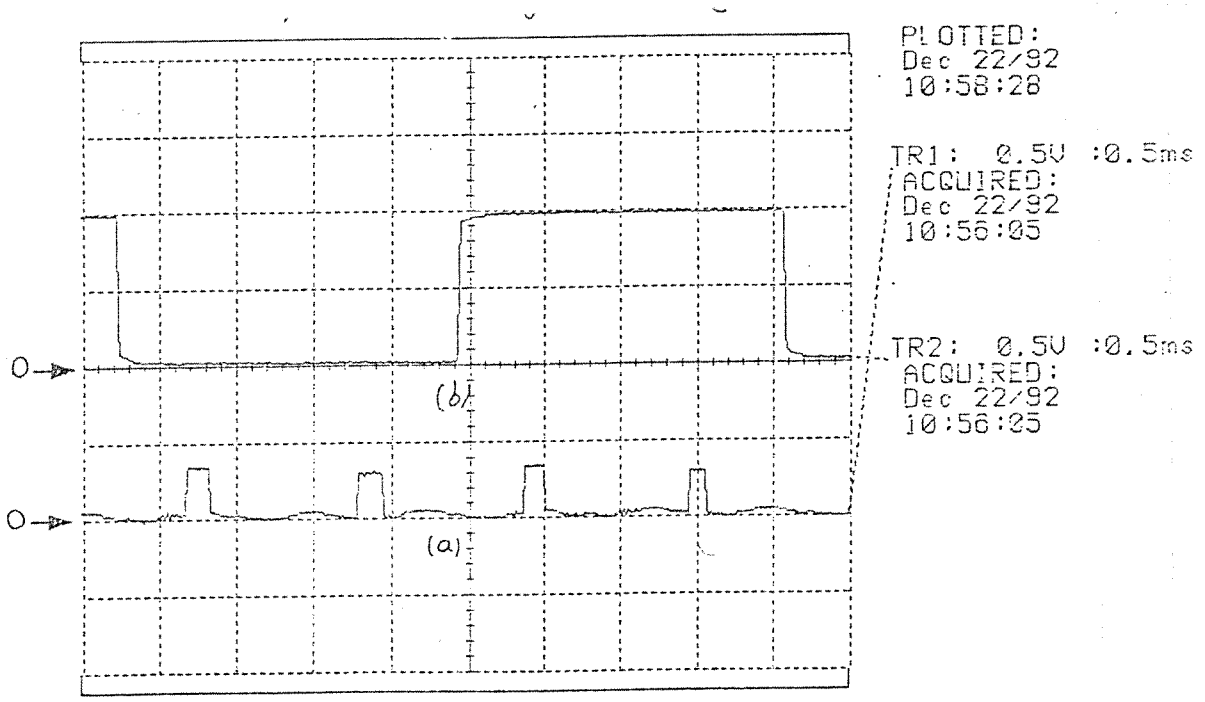

Şekil 32.

a) Enkoder işaretleri

b) Transistör baz gerilimleri (θ_i =7.5º)

5.3 Akım Sınırlayıcı Devre

Bu devrenin sınanması için faz gerilim seviyesi ayarlanarak önce devrenin çalışmadığı koşullarda (Şekil 33) ve daha sonra faz akımı referansı düşürülerek devrenin akımı sınırladığı koşullarda (Şekil 34), referans gerilimi ve transistör kapısındaki işaretler kaydedilmiştir.

Şekillerden izlenebileceği gibi akım sınırlayıcı devre akım referansı değişikliklerini takip etmektedir.

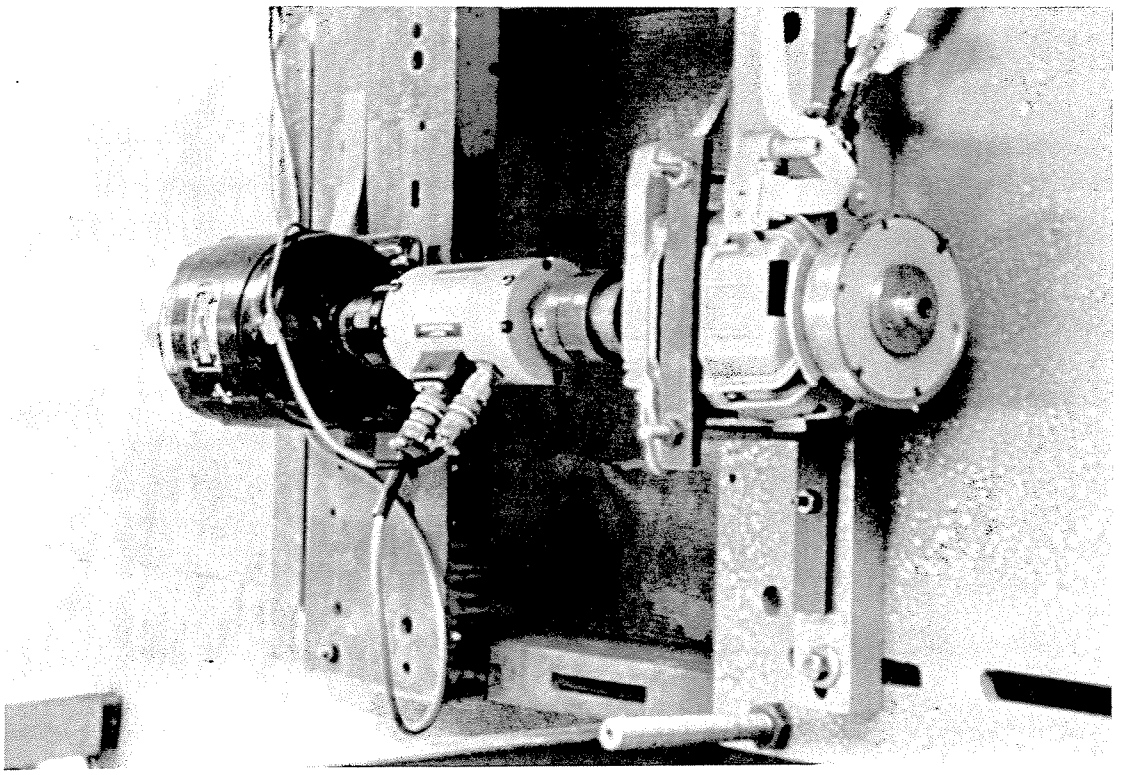

Fotograf 1 Motor yükleme düzeneği (DA generatör ile)

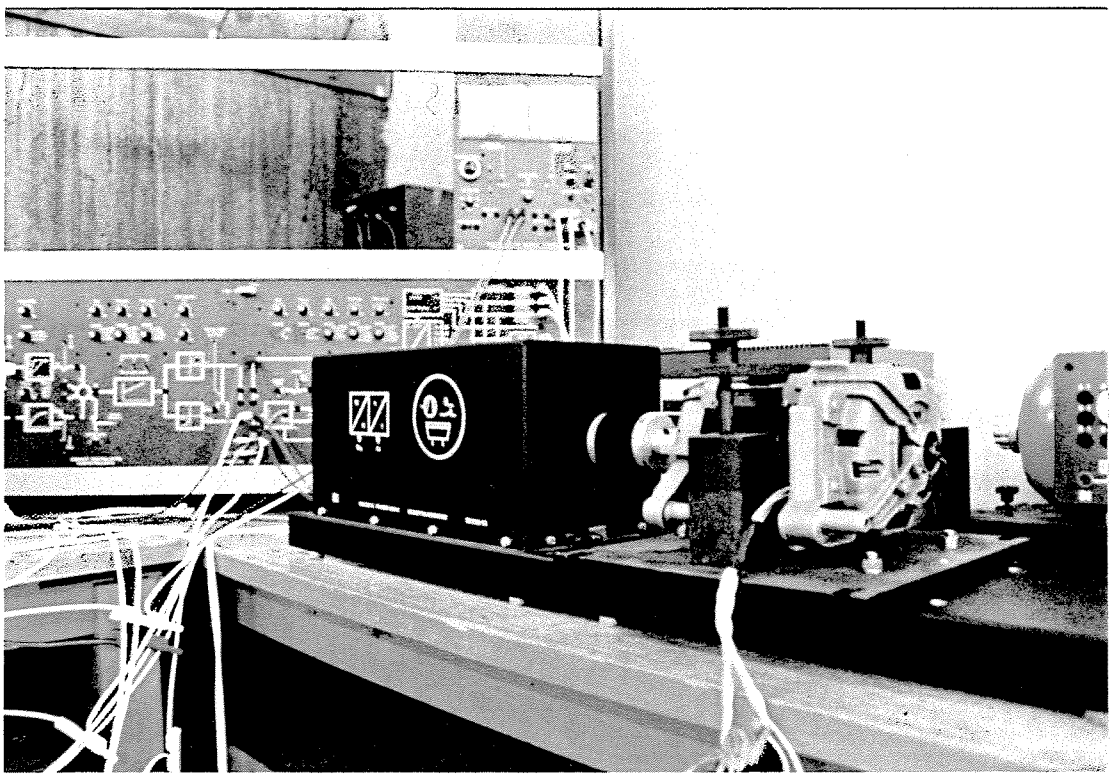

Fotograf 2. Motor yükleme düzeneği ("Powder Brake" ile)

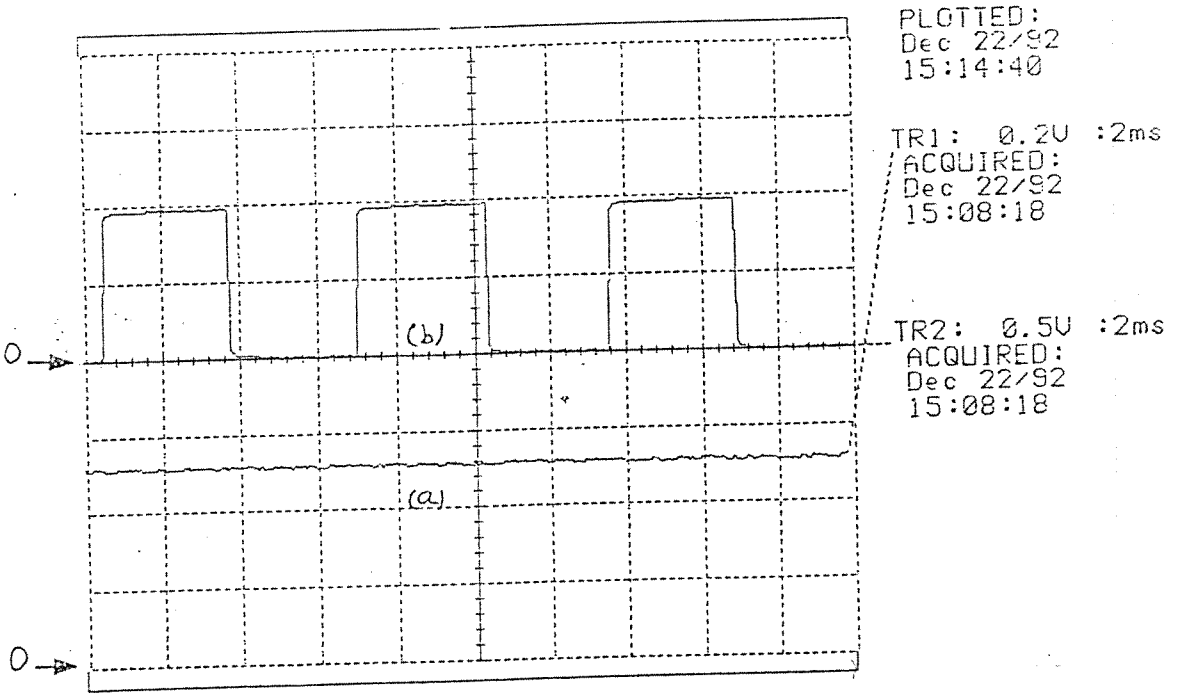

Şekil 33.

a) Akım sınırlayıcı referans voltajı
b) Akım seviyesi 5A'da iken transistör kapı darbeleri

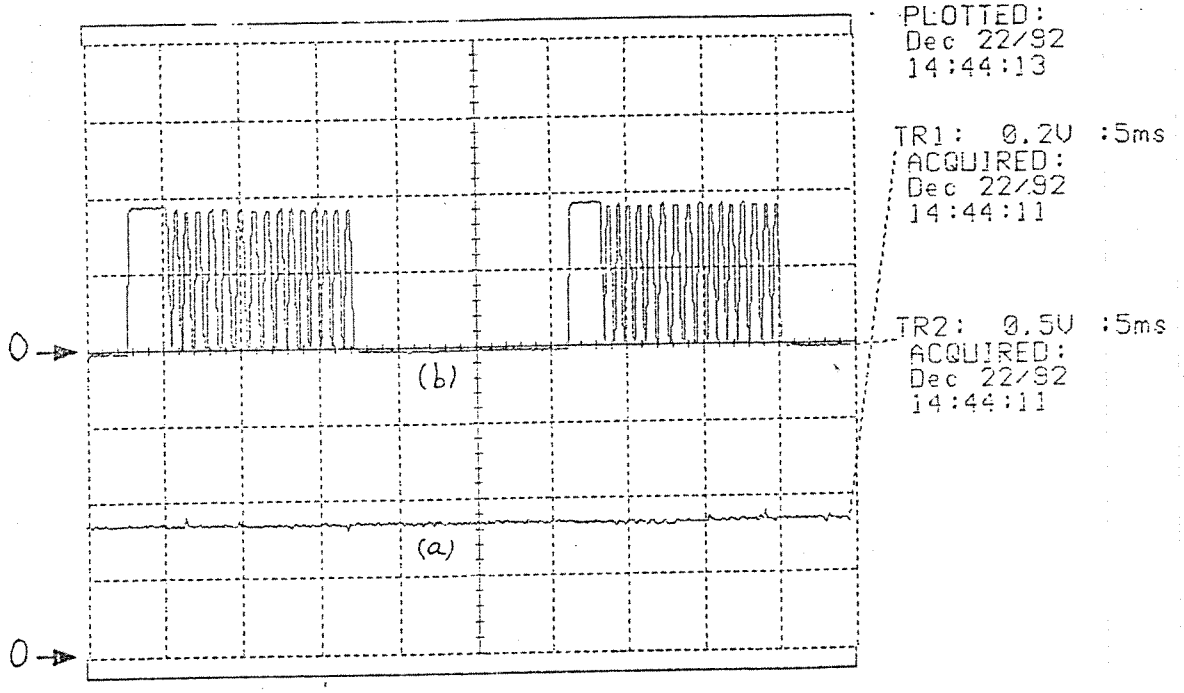

Şekil 34.

a) Akım sınırlayıcı referans voltajı
b) Akım seviyesi 1A'da iken transistör kapı darbeleri

6. SÜRÜCÜ SİSTEMİN SINANMASI

Bu projede bir SR motorun çamaşır makinası tahrik sisteminde kullanılabilirliğinin araştırılması ve araştırma ve geliştirme konularının ve problemlerin belirlenmesi amaçlanmıştı.

2. ara raporda belirtildiği gibi çamaşır makinası üzerinde yapılan ölçümler tahrik sisteminin, motor şaftında

400 d/d'da 40 Watt 0.95 Nm

10-12000 d/d da 750 Watt en çok 0.6 Nm, genellikle 0.3 Nm civarında momente ihtiyacı olacağını göstermiştir.

Bu bölümde geliştirilen sistem üzerinde yapılan ölçüm sonuçları verilecektir.

6.1 Deney Motorunun Yüklenmesi

Bu amaçla iki değişik deney düzeni kullanılmıştır. Bunlardan birinde yükleme amacıyla bir DA generatör (Fotograf 1) kullanılırken, diğerinde bir "powder brake" kullanılmıştır (Fotograf 2). Her iki düzende de moment ölçer deney motoru ve yük arasında yerleştirilmiş bulunmaktadır. Ancak, her iki sistem de en çok 6000 d/d'ya kadar hızlarda çalıştırılabilmektedir. "Powder brake" kullanan sistem otomatik ölçüm imkanı

verdiğinden çoğu kez tercih edilmiştir. Burada verilen sonuçlar bu düzenekte yapılan ölçümlerin sonucudur.

6.2 Motor İmalat Problemleri

Bu çalışmada SR2 adıyla anılan motor imal edildikten sonra ilk denemeler motor boşta çalıştırılarak yapılmıştır. Motordan 6000 - 7000 d/d civarında sürtünme sesleri geldiği gözlenmiştir.

Motor sökülerek incelendiğinde statorun değişik kutuplarında uzunluğun farklı olduğu anlaşılmıştır. Netice olarak hava aralığının değişken olduğu (0.2 - 0.25 mm arası ve benzer bir durumun rotorda da olduğu belirlenmiştir. Bunun sonucu ortaya çıkan dengesizlik yüksek devirlerde sürtünme problemini doğurmaktadır. Hava aralığı rotor tornalanarak 0.30 mm'ye çıkartıldığında yüksek hızda sürtmenin sürmesi mekanik balanssızlığın ve hava aralığı düzensizliğinin yarattığı dengesiz kuvvetlerin etkili olduğu kuşkusunu arttırmıştır.

Bunun üzerine ikinci bir motor imalatının gerektiği kanısına varılmış, endüstriden sağlanan destek ile ikinci bir motor üretimi yoluna gidilmiştir. Bu motorda hava aralığı ancak 0.3 mm olarak gerçekleştirilebilmiştir. Hesaplanan hava aralığına göre (0.225 mm) %35'lik bu sapma doğal olarak motor performansını etkilemektedir.

2. prototipte sürtünme sorunları gözlenmemiştir. Motor hızının boşta 10000 d/d'ye kadar yükseltilebildiği izlenmiştir. Bunun üzerine ölçümlere geçilmiştir.

6.3 Sıcaklık Yükselmesi Deneyleri

İlk olarak motorun hangi akım seviyesinde sıcaklık yükselmesi sınırlarında kalarak hangi gücü üretebileceği araştırılmıştır. Bu amaçla 1 fazlı uyartımda 2 akım seviyesinde sıcaklık yükselmesi deneyleri yapılmıştır. bu testler motorun özellikle 400 d/d yıkama yaparken uzun sürelerle çalışacağı bu hızlarda soğutma etkisi olmadığı dikkate alınarak bu hız civarında yapılmıştır. Deney, motor kararlı bir sıcaklığa gelene kadar yüklenmiştir.

Deney motoru F sınıfı izolasyona sahiptir. Sıcaklık yükselmesi üst sınırı 100 C 'tir (40 C ortam sıcaklığında direnç yöntemi için).

Tablo 1'de kıyıcı akımı 3A'da sınırlandığında 500 d/d'da yapılan deney sonucu izlenmektedir. Görüldüğü gibi motor 1 faz uyartımda istenilen momenti (yıkamada 1.2 Nm) sağlamakta ve sıcaklık yükselmesi 73.5°C de kalmaktadır. Sıcaklık yükselmesi direnç yöntemi ile ölçülmüştür.

Akım sınırlamasının arttırılmasının moment ve sıcaklık yükselmesi üzerindeki etkisini incelemek üzere, kıyıcı akımı 3.75A çıkartılmış deney tekrarlanmıştır. Tablo 2 bu deneyin sonucunu vermektedir. İzlenebileceği gibi sıcaklık yükselmesi yine

sınırın altında 91°C'de kalmaktadır. Motor bu koşulda talep edilen 1.2 Nm'den fazla, 1.5 Nm moment üretebilmektedir.

Böylece motorun yıkama işlevini yerine getirebileceği ve sürekli çalışmaya uygun olduğu anlaşılmaktadır. Bilindiği gibi çamaşır makinalarında motor kesintili olarak çalışmaktadır. Bu nedenle daha ufak bir motorunda istenilen sonucu verebileceği sonucuna varmak mümkündür.

R_2 (ohm)	T_2 (C°) Sıcaklık Yük	T_1 (C°) Ortam	$T_{yük}$ (Nm)	n (d/d)	Kıyma (A)	Zaman hr:min
5.0		18	1.25	500	3	0:0
5.6	48.3	18	1.325	400		0:30
5.8	58.4	19	1.3	550		0:55
5.9	63.45	19	1.3	550		1:15
5.9	63.45	19	1.3	500		1:35
6.1	73.55	19	1.3	525		1:55
6.1	73.55	18	1.3	500		2:15
6.1	73.55	18	1.3	500		2:35

Tablo 1. 3A kıyıcı akım sınırlamasında sıcaklık yükselmesi

R_2 (ohm)	T_2 (C°) Sıcaklık Yük	T_1 (C°) Ortam	$T_{yük}$ (Nm)	n (d/d)	Kıyma (A)	Zaman hr:min
4.9		15	1.45	400	3.75	0:0
5.8	60.8	15	1.5	400		0:31
6.2	81.2	15	1.5	400		1:15
6.4	91.37	15	1.5	400		1:55
6.4	91.37	15	1.5	400		2:10
6.4	91.37	15	1.5	400		2:32

Tablo 2. 3.75 A kıyıcı akım sınırlamasında sıcaklık yükselmesi

6.4 Moment Hız Karakteristiğinin Ölçülmesi

Bölüm 6.1'de belirtilen şekilde yüklenen motor üzerinde iki akım seviyesinde ölçüm yapılmıştır.

3A akım seviyesinde yapılan ölçümlerden, ön uyartım açısı 0, ve 4° olduğunda elde edilen sonuçlar Şekil 35, ve Şekil 36'da verilmiştir. Bu şekillerden, beklendiği gibi, ön uyartım açısı arttıkça düşük hızalarda moment düşerken motorun 0.6 Nm üretirken çalışabileceği hızın yükseldiği gözlenmektedir. Bu şekillerde verilen sonuçlar 15° iletim açısında (0.5 her birim) elde edilmiştir.

Bu deneyler deney düzeninin 0.6 Nm civarında bir yük momentinin altına inmeye müsade etmediğini göstermiştir. Ayrıca yüksek hızlarda ölçülen moment değeri beklenenin altında bulunmuştur. Bu sonuçlar, hesaplanandan büyük hava aralığı yanında, tarak şeklindeki rotorun rüzgar kayıplarının da devirin yaklaşık karesiyle artmasından da kaynaklanmaktadır. Bu safhada rüzgar kayıplarını ayırma imkanı bulunamadığından motorun ürettiği gerçek momentide hesaplamak mümkün olmamaktadır.

Motor moment eğrisi akım seviyesi yükseltilerek çeşitli ön uyartım açılarında ölçülmüştür. (Şekil 37, 38, 39). Bu deneyler sırasında da iletim açısı 15° tutulmuştur. İzlenebileceği gibi ufak ön iletim açılarında düşük hızlarda moment artmaktadır.

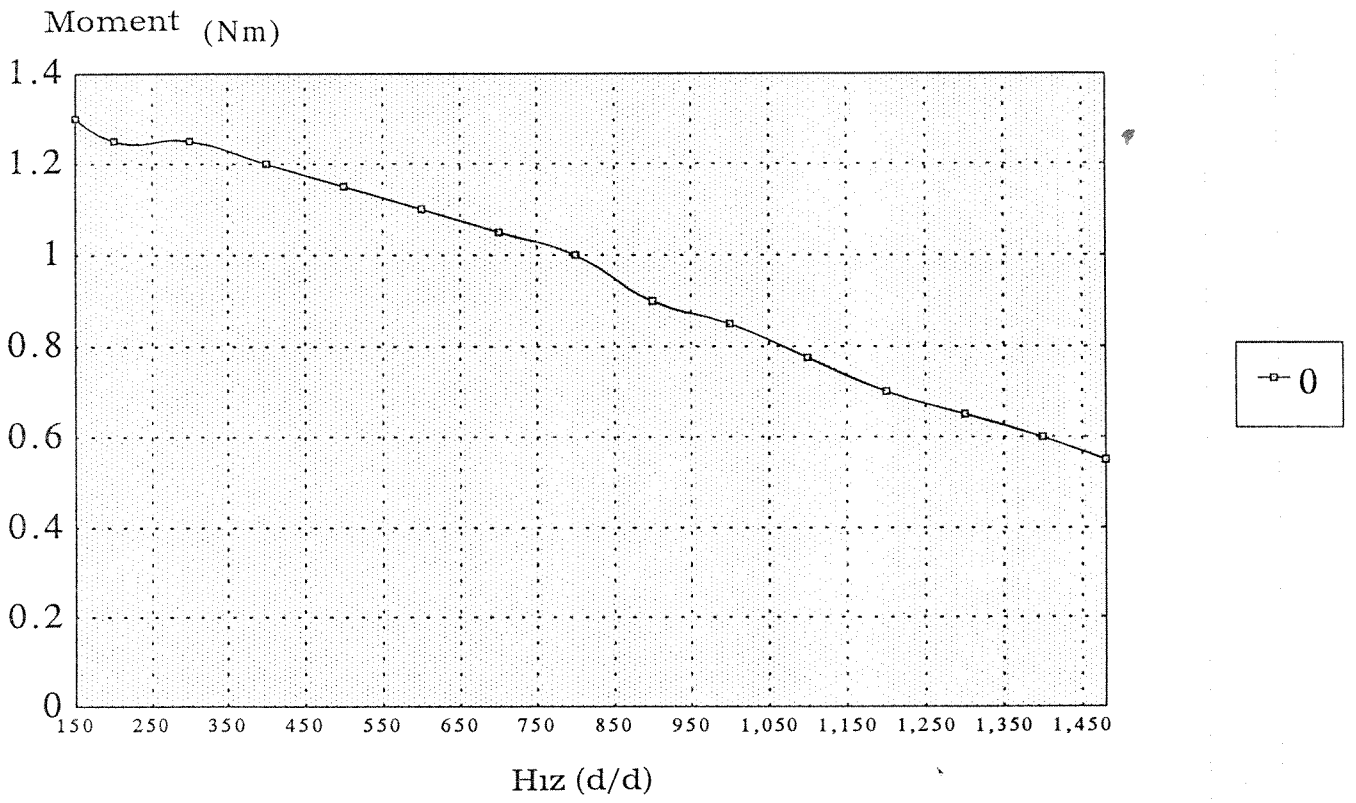

Şekil 35. 3A akım sınırlamada moment - konum eğrisi
ön uyartım açısı O^{o}, iletim süresi 15^{o}

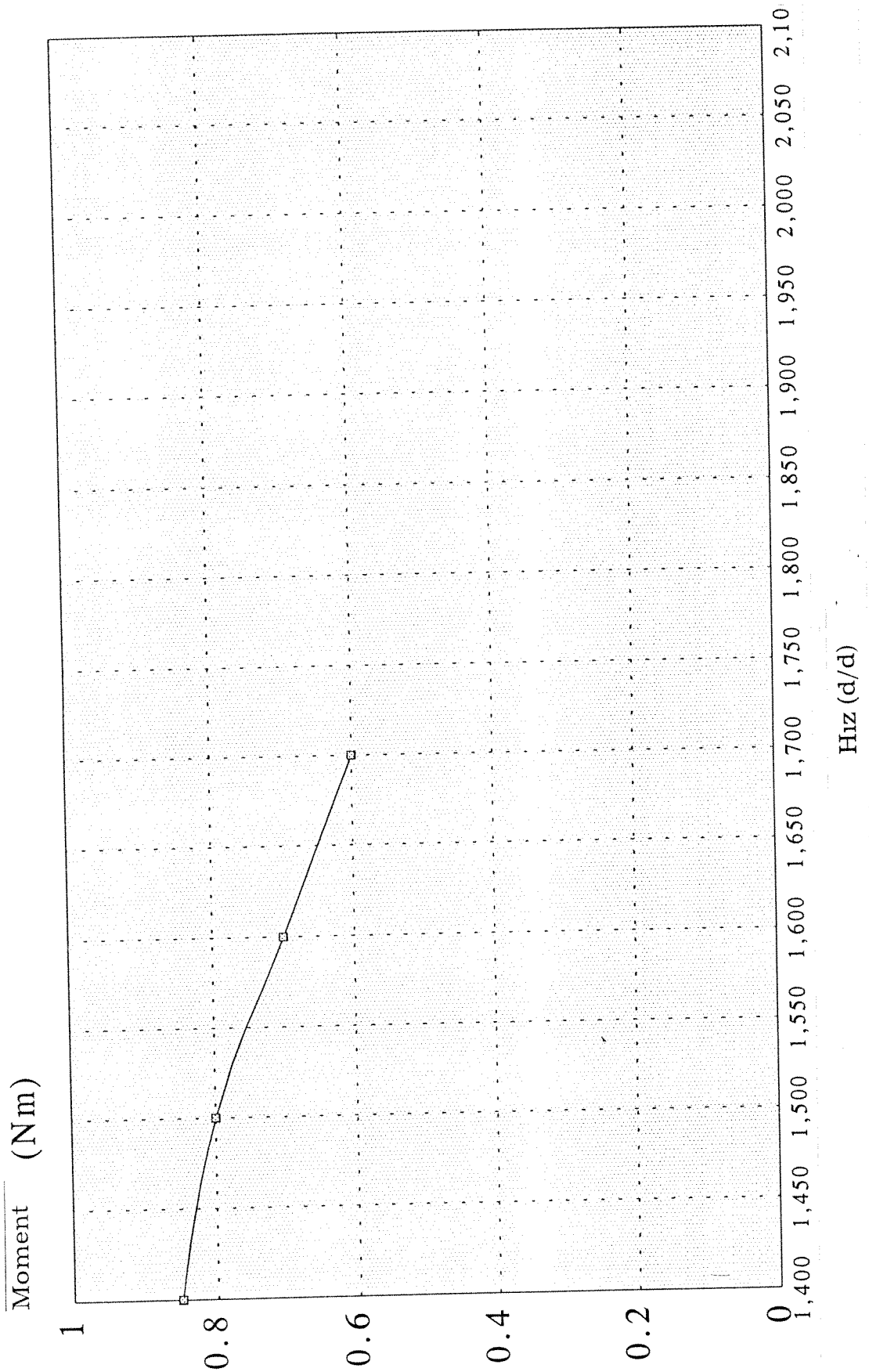

Şekil 36. 3A akım sınırlamada moment - konum eğrisi.

Ön uyartım açısı 4°, iletim süresi 15°

Büyük uyartım hızlarında ise, motorun belli bir momentte daha yüksek hızlara çıkılabildiği gözlenmektedir.

Bölüm 2.1.2'de belirtildiği gibi simulasyon programının moment-hız karakteristiğini hesaplayan bölümünde hata bulunduğundan deney ve ölçüm sonuçlarının karşılaştırılması yoluna gidilmemiştir.

Ölçümler iletim açısının etkisini gözlemek için tekrarlanmıştır. Bu kez motorun en yüksek moment üreteceği bilinen [1] 30° ($\lambda/2$'ye karşı gelmektedir) iletim açısında deneyler tekrarlanmış ve motorun 6000 d/d'ye kadar 0.6 Nm üretebildiği gözlenmiştir. Ancak, yine rüzgar kayıplarının etkisi ölçülemediğinden bu etki giderildiğinde (rotor kutuplarının arası doldurularak rüzgar kaybı önemli ölçüde azaltılabilir) ne kadar moment üretilebileceği kestirilememektedir.

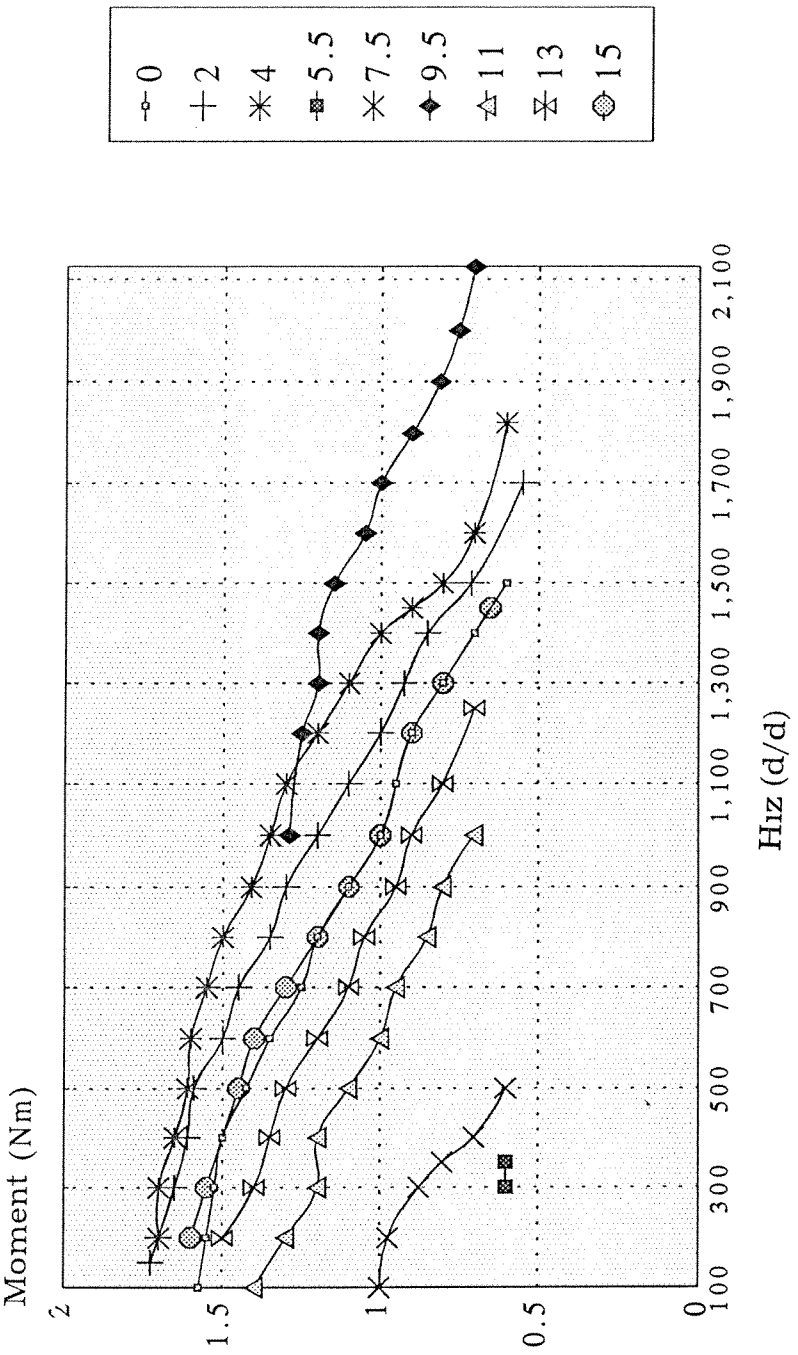

Şekil 37. SR2 için moment - hız eğrileri
Akım sınırlama: 3.75A, İletim açısı 15°

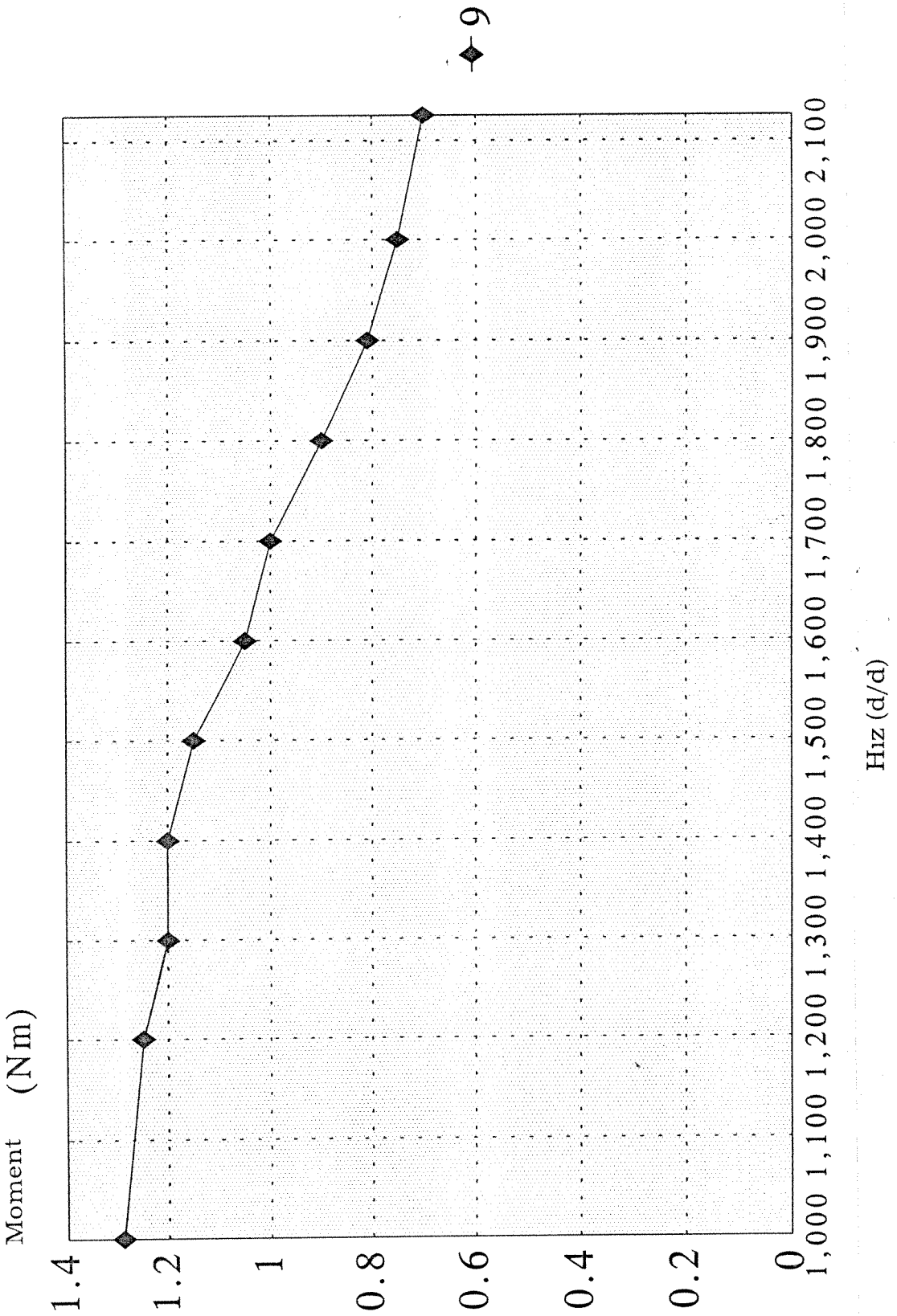

Şekil 38. SR2 için moment - hız eğrileri
ön uyartım açısı 9.5°, iletim açısı 15°

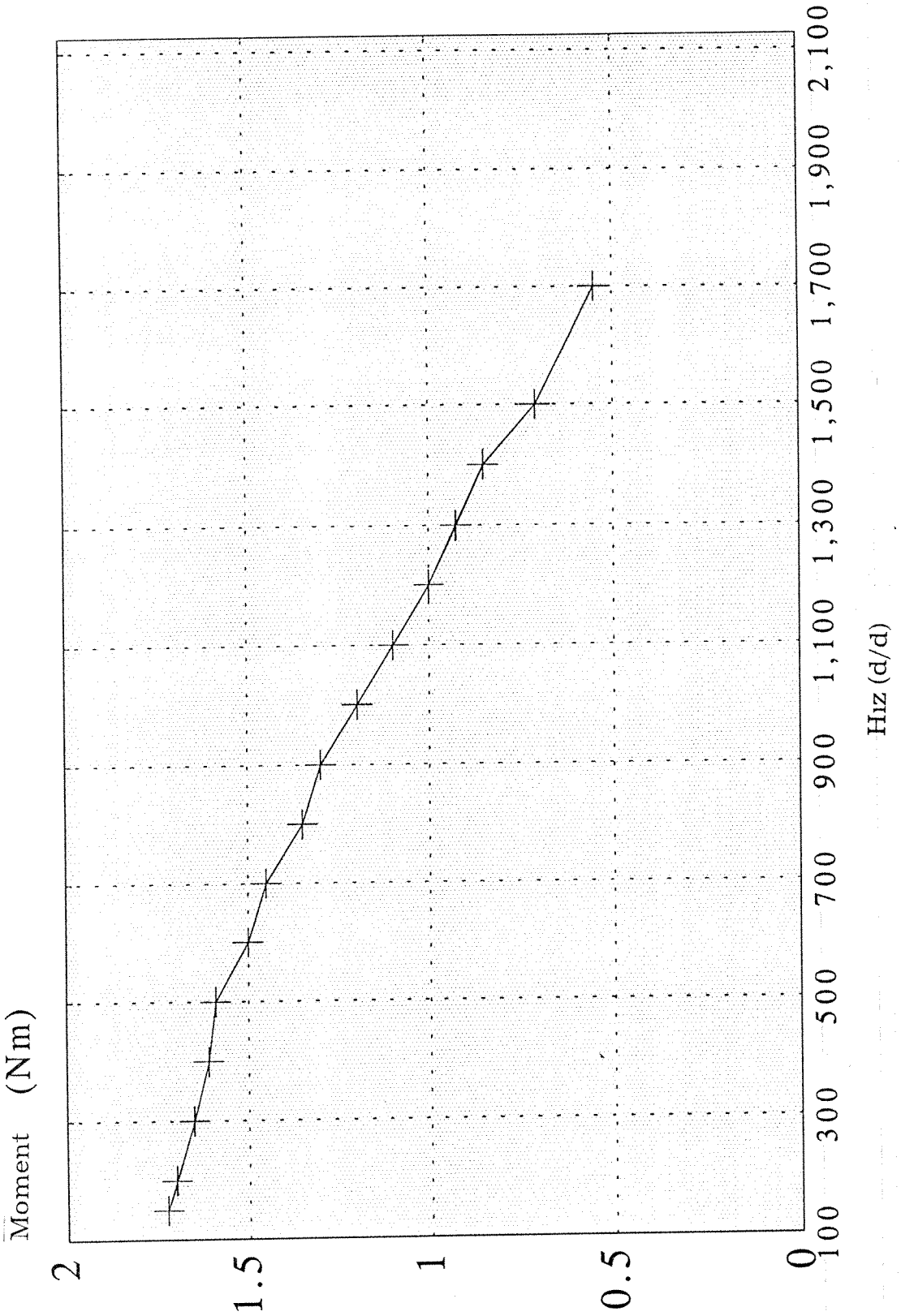

Şekil 39. SR2 için moment - hız eğrisi
ön uyartım açısı 2°, iletim açısı 15°

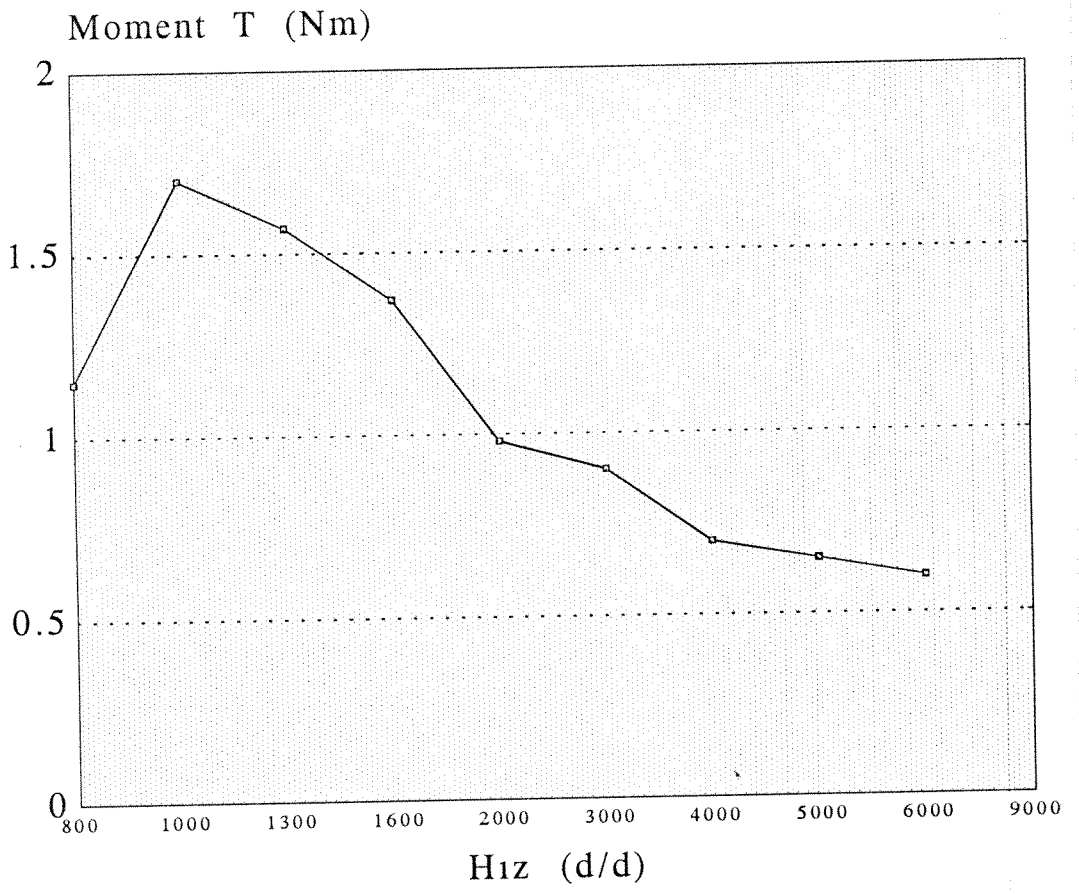

Şekil 40. SR2 moment -hız karakteristiği

İletim açısı 30°, Akım sınırlama 3.75A ön uyartım açısı 9.5°

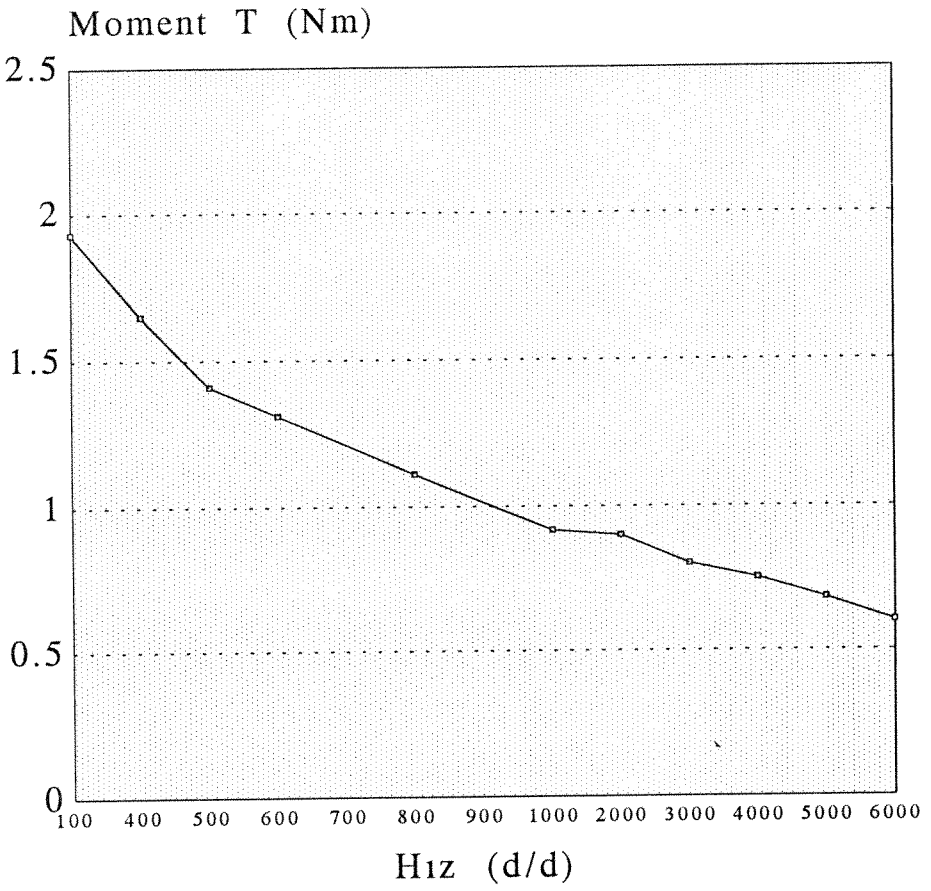

Şekil 41. SR2 moment - hız karakteristiği

İletim açısı 30°, Akım sınırlama 3.75A ön uyartım açısı 11°

6.5 Sabit Hızda Çalışma ve Çamaşır Makinası Üzerinde Deneyler

Motor yazılımın sabit hız bölümüyle de çalıştırılmış ve moment değişirken hızın sabit kalabildiği gözlenmiştir.

Ancak moment - hız karakteristiği kayıtları incelendiğinde, bu karakteristiğin, iletim açısına akım seviyesine ve ön uyartım açısına duyarlılığı açıkça gözlenmektedir.

Mevcut hız kontrol sistemi sabit bir ön uyartım açısında motoru hızlandırmaktadır. Geniş bir aralıkta hız denetimi yapılacaksa ve yüksek hızlara çıkılacaksa ön uyartım açısının denetlenmesi gereği açıktır.

Motor momentinin belli bir ön uyartım açısında konrolü için iletim açısı veya akım denetlenebilir. Bunun etkisi o çalışma koşullarında motor verimini değiştirmek şeklinde gözlenecektir. Ancak buradaki uygulamada verim çok önemli olmadığından üzerinde durulmayabilir.

Özetle daha sofistike bir denetim yaklaşımı ihtiyacı gözlenmektedir. Doğal olarak böyle kapsamlı bir araştırmanın bütününün tek bir projede gerçekleştirilmesi mümkün değildir. Ancak, araştırmalar sürdürülmektedir.

Çamaşır makinasına monte edilen motor üzerinde de kısıtlı boyutlarda deney yapılmıştır. Bu düzen içinde ölçüm imkanı (moment veya hız) olmadığından detaylı deneylere gerek görülmemiştir. Kaldıki çamaşır yıkanmasının sınanabilmesi için yeni yazılımlara ihtiyaç vardır.

6.6 Akustik Gürültü Düzeyi

Laboratuarlarımızda akustik gürültü düzeyini ölçebilen bir düzenek olmadığından gürültü düzeyi sadece kulakla dinlenerek belirlenebilmektedir. İleride bu deneyler İstanbul'da mevcut imkanlar kullanılarak yapılmaya çalışılacaktır. Bu deneyler gürültünün kaynağı ve giderilme yolları hakkında bilgi sağlayacaktır.

SR1 ve SR2 gürültü düzeyi açısından karşılaştırıldığında, SR1'in çok daha sessiz olduğu (hemen hemen evirgeçle sürülen asenkron motor gürültüsü düzeyi), ancak SR2'de sesin yüksek olduğu belirlenmiştir. Bu büyük ihtimalle motor gövde yapısının, mevcut eski motorla aynı olma zorunluluğu nedeniyle zayıf ve titreşime yatkın olmasından kaynaklanmaktadır. Ancak, bu konuda kesin bir yargıya varmak için detaylı araştırmalar gerekmektedir.

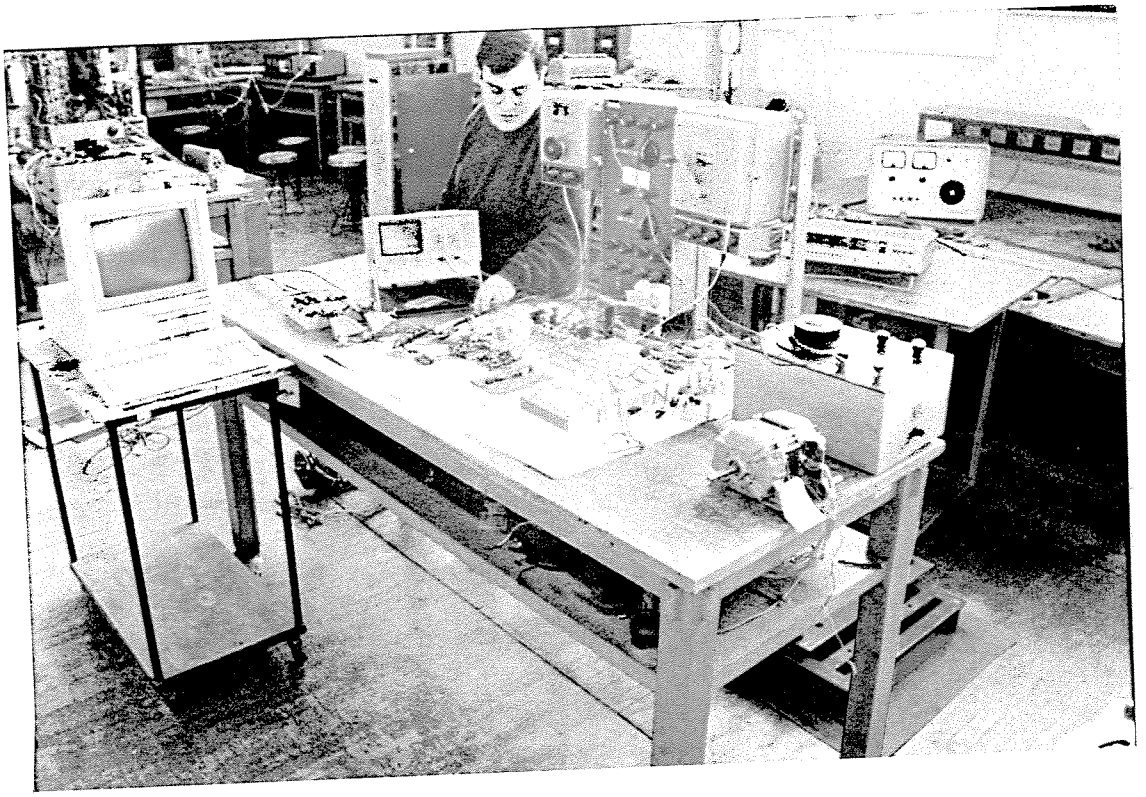

Fotograf 3 Geliştirme safhasında sürücü devre

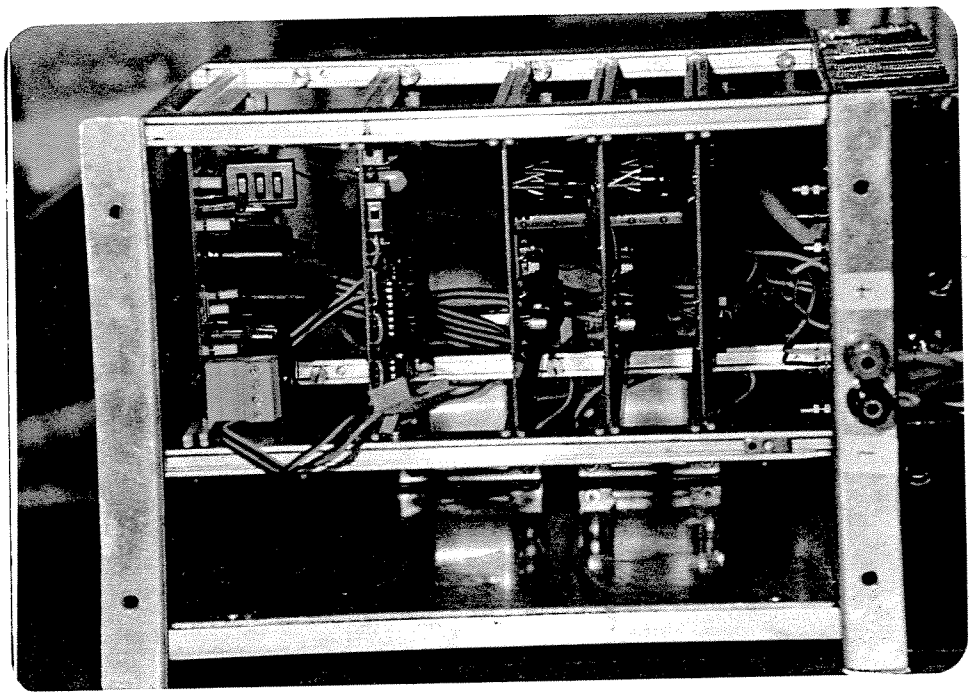

Fotograf 4 Sürücü devrenin son hali

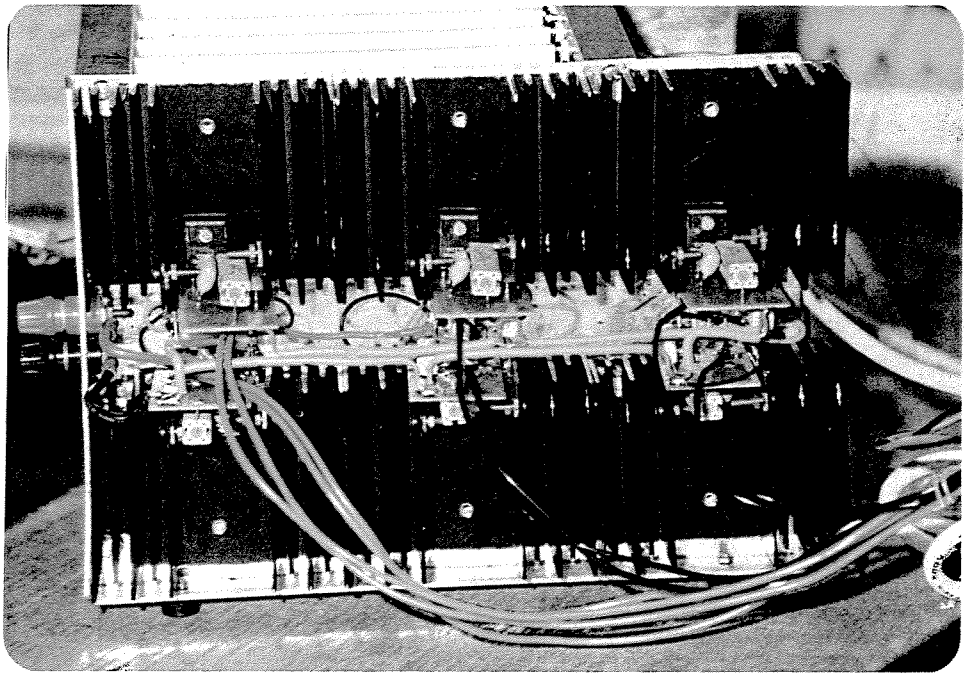

Fotograf 5 Sürücü devre çıkış katı

7. DEĞERLENDİRME

Bu bölümde proje teklifinde öngörülen çalışmaların ne ölçüde gerçekleştiği açısından bir değerlendirme yapılacaktır.

Proje önerisinde;

a) Kullanıcı dostu bir tasarım yazılımı gerçekleştirilmesi öngörülmüştü. Bu amaçla proje yöneticisince geliştirilen yöntemlerin kullanılması amaçlanmıştı. Bu yazılım gerçekleştirilmiştir. Ancak analiz bölümünde motor statik karakteristiğini hesaplayan bölümlerden olumlu sonuçlar alınırken, moment-hız karakteristiği bölümünde hataların varlığı belirlenmiştir. Bu yazılımı gerçekleştiren öğrencinin çalışmalarını tamamlamadan ayrılması amaca tam olarak ulaşılmasını engellemiştir. Bu konuda çalışacak bir öğrenci henüz Y. Lisans derslerini tamamlamaktadır. Programın optimizasyon bölümü analiz bölümünden bağımsızdır ve sonuç vermektedir.

- Yazılım Güvenilirliği: Bu konuda yazılımın bütününü test edici ilave çalışmalar yerinde olacaktır. Ancak bundan sonra, yazılım güvenilir bir tasarım aracı olarak kullanılabilecektir.

b) Alan Çözümü: Bu konuda profesyonel alan çözümü programlarının kullanımında önemli bir deneyim elde edilmiştir. Programlar ve kullanılan "grid" oluşumu, moment ve endüktans hesaplama yöntemlerinin geçerliliği deneylerle karşılaştırılarak doğrulanmıştır.

c) Güç Yarı İletkeni Kullanım Deneyimi: IGBT'lerin sürülmesi ve korunması konusunda önemli bir deneyim elde edilmiştir.

d) Sürücü Devre: Bir sürücü devre geliştirilmiş ve motor başarıyla sürülmüştür. Bu çalışmalar daha sonra yeni bir sürücü konfigürasyonu elde edilmesine yol açmıştır. Bu konuda bir yayın hazırlama çalışması sürmektedir. Sürücü devrenin geliştirme safhasındaki hali (Foto 3) ve bitmiş hali (Foto 4) 'te görülmektedir.

e) Çamaşır makinası sürebilen bir düzenek gerçekleştirilmiştir. Bu çerçevede bir imalat prototipi gerçekleştirilebilmesi ve performansın iyileştirilmesi için ne gibi araştırmalar yapılması gerektiği belirlenmiştir. (bölüm 8'e bakınız).

f) AR motorun çamaşır makinası için en iyi seçeneği oluşturup oluşturmadığı henüz belirsizliğini korumaktadır. Bu konu ancak Bölüm 8'deki çalışmaların sürdürülmesi ile açıklığa kavuşacaktır. Laboratuarlarımızda alternatif sistemler üzerinde yürütülen çalışmalar da bu konuda yardımcı olacaktır.

g) Yapılan çalışmalar bir prototip geliştirilmesi için gereken insan niteliği, adam ay, organizasyon ve araştırma konularını belirleyerek çok önemli bir katkıda bulunmuştur. Ayrıca bir takım altyapı eksiklikleri giderilmiştir.

Bu proje'de çalışan Fariborz Niakan, Amir Safavi Y. Lisans tezlerini almışlardır. Funda Şahin çok başarılı bir Y. Lisans çalışmasını tamamlamak üzeredir. Balkan Şimşir bu çerçeve'ye ilişkin başladığı çalışmalarını alternatif bir sistem üzerine

kaydırarak, Mustafa Parlar Ödülüne layık bulunan bir Y. Lisans tezi tamamlamıştır.

Said Saeidi ve Fatih Erdem ise araştırmalarını yarıda bırakmışlardır, endüstride çalışmalarını sürdürmektedirler.

İşaret edilmesi gereken bir diğer nokta da yüksek devirde (6000 d/d'nin üstü) çalışan sürücüleri sınayabilecek bir düzeneğin kurulması ihtiyacıdır.

8. YAPILMASI GEREKEN ÇALIŞMALAR

Yürütülen bu araştırma projesi çerçevesinde elde edilen deneyim, bir çok yeni araştırmanın sürdürülmesinin gerekli olduğuna işaret etmektedir. Bunlar şöylece özetlenebilir.

a) Motor tasarımı yazılımının geliştirilmesi ve güvenilirliğinin pekiştirilmesi, ekran görünümlerinin iyileştirilmesi. Buna dayanarak motorun yüksek hızda, yüksek performansla çalışmasını en iyileştirecek koşulların araştırılması.
b) Gürültü ve titreşim kaynaklarının tanımlanması giderilmesi için manyetik devre ve sürücü ve gövde yapısı açısından önemli unsurların tanımlanması.
c) Sürücü için geliştirilen yeni konfigürasyonun incelenmesi ve performansının daha da yükseltilmesi.

d) Dinamik koşullarda motor ve sürücü simülasyonu sağlayan bir yazılım geliştirilmesi.
e) (d)'deki yazılıma dayanan bir kontrol yöntemi geliştirilmesi
f) Rotor konumunun sensörsüz belirlenebilmesi için (d)'deki yazılıma dayanan çalışmalar.

Burada sıralanan çalışmaların bir kısmı başlatılmış bulunmaktadır. Bunlar Bölüm 9'da kısaca tanımlanmıştır.

9. YÜRÜTÜLMEKTE OLAN ÇALIŞMLAR

Halen bir kısmı oldukça ileri safhada bir dizi anahtarlı relüktans motoru araştırması sürdürülmektedir. Özetle;

a) Düşük ve yüksek hızlarda moment dalgalanmasını manyetik devre düzenlemesiyle en aza indirerek akustik gürültünün azaltılması.

Bu çalışmayı Funda Şahin yürütmektedir.

Modelleme için neural net yaklaşımının kullanıldığı ve yeni optimizasyon tekniklerinin denendiği bu çalışmamıza ilişkin bir bildirimiz uluslararası bir toplantıda sunulmak üzere kabul edilmiştir.

b) Motor dinamik performansını simule edebilen bir yazılım geliştirilmesi ve gözlemci (observer) tasarımı.

Bu çalışma Bülent Özhorasan tarafından yürütülmektedir.

c) Motor tasarım yazılımı güvenilirliğini oluşturan sürücü sistemle sınanarak açıklığa kavuşturulması, yazılımların iyileştirilmesi, sürücü denetimyazılımlarının iyileştirilmesi.

Bu çalışma Burak Daşdemir tarafından yürütülecektir. Öğrenci Y. Lisans derslerini tamamlamaktadır.

10. ÖNERİLER

Bu proje çalışmasından elde edilen deneyimden daha sonraki desteklenecek araştırmalarda başarı düzeyinin yükseltilmesi açısından önemli gördüğümüz bazı konuları dikkate sunmakta yarar görüyorum.

Ciddi bir araştırma çalışmasının en önemli öğeleri donanım ve iyi yetişmiş insan gücüdür. Bu öğelerden biri yetersiz kaldığında başarılı ve teknolojiye katkıda bulunabilecek bir sonuç elde etmek düş kurmaktan öteye gitmeyecektir.

Tübitak'ın projenin başlatıldığı tarihteki politikası bu öğelerden araştırıcı gücünü tamamen göz ardı eden bir yaklaşımı

yansıtmaktadır. Ciddi araştırmaların araştırma görevlileriyle yürütülmesi, bu kişilerin ders ve laboratuar yükleri ve araştırma çalışmalarını başlatabildikleri tarihlerin proje ile çakışmaması nedeniyle başarılı olmamakta, çalışmalar çok yavaş yürümektedir.

Araştırıcılar için verilen telif ücretleri ise Türkiye'de yaşam koşullarıyla hiç uyuşmayan bir niteliktedir. Bu nedenle bir işte çalışmayan araştırmacı veya tez öğrencisi bulunamamaktadır. Nitekim bu projede de, öğretim üyeleri telif ücretlerini tümüyle bir işte çalışmayan araştırıcılara ödemelerine rağmen (Amir Safavi, Fariborz Niakan, Saeid Saeidi) istenilen kalitede araştırıcı bulamamışlardır.

Projenin yürütülmesi sırasında mali imkanların yetersizliği nedeniyle Fariborz Niakan, Saeid Saeidi, Fatih Erdem çalışmalarını tamamlamadan ayrılmışlardır.

Projenin ciddi bir düzeyde yürütülmesi için hiç bir işte çalışmayan araştırmacının önemi yadsınmamalı ve ödeme düzeyi en az araştırma görevlisi seviyesinde olmalıdır.

Projenin yürütülmesinde pek çok irili ufaklı sorunla karşılaşılmıştır. Ancak, yukarıda belirtilen tam zamanlı araştırmacı en önemli öğedir ve gözden kaçırılmaması için diğer sorunlara değinilmeyecektir.

Ek 1

Analiz ve Optimizasyon Yazılımı Kullanım Kılavuzu

CHAPTER V

HOW TO USE SR

5.1 Introduction

SR is a user friendly program that anyone can use it without knowing much about the software. It is sufficient to follow the commands which appear on the screen during execution. To run SR, change directory to C:\SR. By typing "SR" and pressing enter the main menu will appear on the screen.

5.2 Main Menu

The main menu of SR controls the main flow of program according to the user choice. In order to choose an option from the main menu bring the highlighted bar on it and press enter.

In the following sections detailed explanation of the choices in the main menu are discussed.

5.3 Data

This option should be chosen by the user before proceeding any further. The sub menu for this option includes:

5.3.1. Load

The user can load one of already available motor parameters. The motor parameters are stored in three arrays, ai, ar, and ad. The list of parameters in each array are given in Tables 5.1, 2, and 3.

Table 5.1 ai array parameters

array number	name used in thesis if any	description
1	N_s	# of stator poles
2	N_r	# of rotor poles
3	NTSP	# of teeth per stator tooth
4	NTRP	# of teeth per rotor tooth
5	NOS	# of stacks

Table 5.2 ar array parameters

array number	name used in thesis if any	description
1	Do	stator outer diameter
2	d_i	rotor outer diameter
3	d_u	rotor inner diameter
4	L_c	core length
5	Y_b	backcore width
6	g	airgap
7	t_s	stator tooth width
8	t_r	rotor tooth width
9	I	current
10	N_t	# of turns per pole
11	V_s	applied voltage
12	V	voltage at chopping
13	n	speed (rpm)
14	x_{ni}	switch on
15	x_{nx}	switch off
16	chophigh	max current at chopping
17	choplow	min current at chopping
18	R_1	primary resistance
19	R_2	auxilary resistance
20	max av. speed	max x-axis scale in t_{av}
21	-----	stacking factor
22	empty	empty

23	-----	Cu resistivity (Ω/meter)
24	-----	Fe density (gr/mm^3)
25	-----	Cu density (gr/mm^3)
26	-----	Fe price (TL./gr)
27	-----	Cu price (TL./gr)
28	-----	Cu primary diameter (mm)
29	-----	Cu second. diameter (mm)
30	empty	empty
31	empty	empty
32	vs	refer to Figure 3.5
33	ws	"
34	tz	"
35	ty	"
36	h3	"
37	h2	"
38	h1	"
39	a	distance from tip of pole
40	empty	empty
41	empty	empty
42	empty	empty
43	empty	empty
44	empty	empty
45	empty	empty

Table 5.1 ad array parameters

array number	name used in thesis if any	description
1	lambda_a	stator pole pitch
2	lambda_b	rotor pole pitch
3	t_{sn}	normalized stator width
4	t_{rn}	normalized rotor width
5	h_r	stator tooth height
6	h_s	rotor tooth height

5.3.2 New

Allows the creation of a new motor file. The user is asked to give a name to the new motor. The name should be different than the ones already available (a list of available motors is given). The name should be a string of 3 characters. The first two characters (small characters) describe the motor type, and the third character is a number representing how many of this type of motors available. The types are distinguished as follows:

- sr one tooth per pole, single stack
- mt multi teeth per pole, single stack
- ms multi stack

As an example mt5 means the fifth of mt type motors. Pressing enter will create a new motor file if a name is given otherwise will cancel the operation.

5.3.3 Delete

Deletes one of available motors. Use the arrow keys to select the motor to be deleted and press enter. Pressing Esc will cancel the operation.

5.3.4 Change

Allows the user to change the BH curve and flux linkage data assigned to a motor. Select the motor with arrow keys and press enter. The user will be asked for a new BH curve name. This curve could be one of available BH curves or it could be a new one. Pressing enter will change the name if a new name is given otherwise it will ask for a new flux linkage file name. In case the files are new it is the users responsibility to provide them by using option 8 (Make).

5.4 Motor Parameters

Loaded motor parameters (section 5.3.1) can be observed and changed if necessary by using this option. The parameters which are related are gathered and shown in a sub menu as explained next.

5.4.1 Motor Independent Parameters

These are the first 8 shown in Table 5.2. Any variable can be chosen (if its value is to be changed) by arrow keys and selected by pressing enter.

5.4.2 Motor Dependent Parameters

These variables are shown in Table 5.3. The reason for calling these variables "dependent" is that they can be obtained from the independent ones. Note that these parameters are not allowed to be changed.

5.4.3 Motor Type

The first part of these variables which represent the motor type is given in Table 5.1 and the second part representing dimensions of a pole are given in Table 5.2 (variables 32 through 39). In case the motor is of type sr then the second part of these variables should be entered as zero.

5.4.4 Operating Conditions

These are the variables in Table 5.2 numbered from 9 to 21. Any of these can be changed as explained in section 5.4.1.

5.4.5 Miscellaneous

These variables are in Table 5.2 from 23 through 29.

5.5 Starting Performance

Flux linkage, static torque, and inductance against position curves can be seen using this option for either one phase on or two phase on operations. The user can select one at a time by bringing the highlighted bar on the desired option and pressing enter.

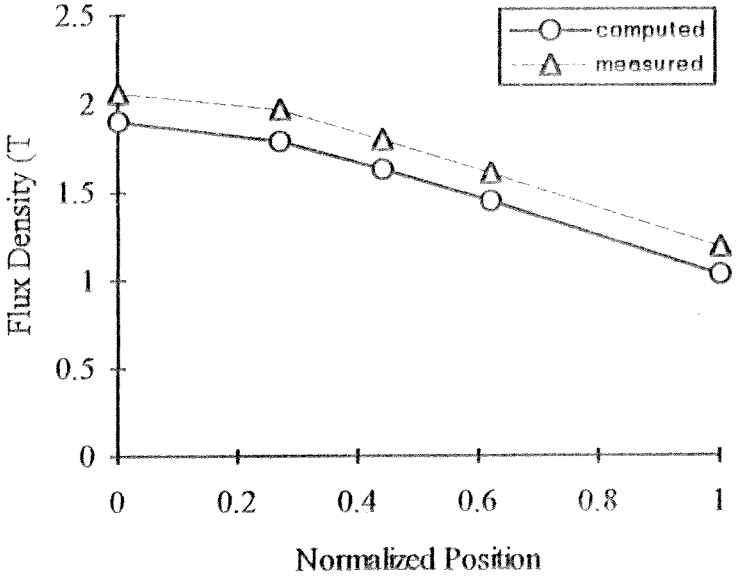

Figure 4.7 Comparison of Flux Density for Test Motor 2

The current waveforms were recorded by the help of a x-t recorder [4]. The motor adjusted its switching position according to its torque demand. Ideally at zero torque the effect of positive torques is overcome by negative torque which means switch ON ideally occurs at x_{ni}=-0.5. However the motor at no load requires some torque to overcome the bearing friction.

4.6 Conclusion

In this chapter measured results were taken from references 1,2, and 4. The measured data for the test motor consist of flux linkage and static torque curves (both as a function of current and rotor position). When compared with computed curves it is observed that the consistency between measured and computed static torque data is satisfactory for test motors 2 and 3, and a bit short of the peak value for test motor 1 (the i/λ value was not in the range were the data is available). For flux linkage data however a certain amount of discrepency is observed for positions close to OUT position.

The current waveform was obtained from flux linkage data. In general it can be concluded that the computed results supported the measured ones.

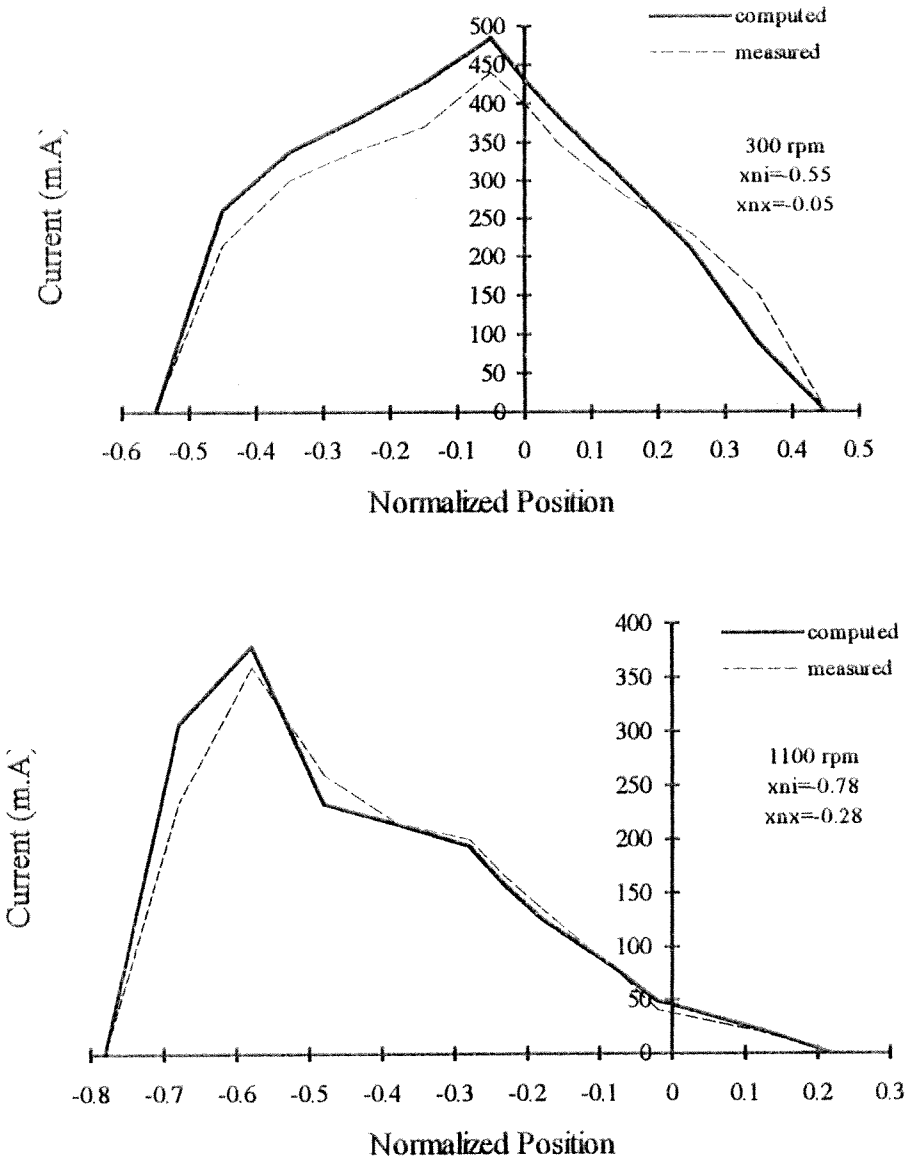

Figure 4.8 Current Waveform

CHAPTER V

CONCLUSION

The aim of this thesis was to develop a computer program to analyze performance of a 4 phase switched reluctance motor. This gives the designer the opportunity to design a motor with characteristics according to his demands.

Throughout calculation of the performances the force vs. mmf and flux density vs mmf data for a symmetrical doubly salient geometry with a core length and rotor tooth pitch of 1 meter (udss) is used. A conversion is made to transfer the data from udss to real geometry at which the performance is required.

The following performances can be predicted at the design stage:

- static torque vs. position
- flux linkage and inductance vs. position for a specific applied current
- current waveform as a function of switching positions, voltage and speed
- average torque vs. speed

It is found that the methods used predict the static torque curves very accurately in shape but smaller peak values (around 7-10 %) are predicted for test motor 1 as compared with the measurements, and very accurate for other test motors. The starting torque is in good agreement with the measured ones even for test motor 1 since it is the torque at the intersection of two successive curves and independent of the peak region of the torque. The flux linkage vs. position as a function of current are computed using B_t vs. F data. In deriving the computed flux linkage data, back iron mmf is also taken into account. The discrepancy between measured and computed flux linkages increases as the rotor moves toward the out position. The computed curves over estimate the measured ones. Sources of errors were discussed in chapter 4. Current waveshapes were computed by solving the terminal equation with numerical integration method. In solving the differential equation the flux linkage data (in tabular form) of the motor was used in computation. As discussed the computed curves matched the measured curves very accurately. Average torque

is computed using the energy factor concept. In this the area under the current vs flux linkage (mmf vs flux density) loops is computed. Dealing with area causes the percentage error reflected to average torque to be less than the error computed for flux linkage curves alone (both increasing and decreasing named curves in figure 3.16 will over or under estimate the actual ones and as a result the area stays almost constant). The calculated inductance is a bit lower as to what it should be since there is some leakage flux at the tip of the coil which is not taken into account.

Remembering that the test motor 1 has a t/λ ratio out of the t/λ ratios available in the data, which certainly produces significant amount of error due to extrapolation, it can be concluded that the results presented indicate that using the methods discussed, the performance of SR type motors can be predicted within acceptable limits of errors for practical purposes.

REFERENCES

[1] H. B. Ertan, "Prediction of Static Torque of Step Motors", Ph.D thesis in Electrical Engineering, The University of Leeds, (1977).

[2] H. B. Ertan, " Asimetrik Çikik Kutuplu Magnetik Yapilarda Kuvvetin Hesabi", Elektrik Mühendesliginde Doçentlik Tezi, (1982).

[3] J. M. Stephenson, J. Corda, " Computation of Torque and Current in Doubly Salient Reluctance Motors from Nonlinear Magnetization Data", Proc. IEE 126 (5), pp.393, (1979).

[4] M. Tohumcu, "Optimum Design of Switching Reluctance Motors", Ph.D thesis in Electrical and Electronics Engineering, METU, (1985).

[5] O. F. Yagan, " A New Approach to the Design Optimization of Switching Reluctance Motors", M.S. Thesis in Electrical and Electronics Engineering, METU, (1990).

APPENDIX A

THE DATA

It was stated that due to heavy saturation in doubly salient type motors, either numerically computed or experimentally measured data which contains information about the nonlinear nature of the problem should be used. In this section the data used throughout the computation of performance of a switching reluctance motor is given. Ertan [1] computed normalized permeance and force and force per unit length for a doubly salient geometry with equal and identical stator and rotor teeth as being a function of the following parameters for the given values:

λ/g - 40, 55, 70

t/λ - 0.3, 0.4, 0.5

B_t - 0, 0.1, 0.2, 0.3, ... , 2.1

x_n - 0, 0.2, 0.4, 0.6, 0.8, 1

The geometry for which data have been computed has a tooth pitch equal to 0.0172 meter. Later this data was extrapolated for higher λ/g values and tabulated by Yagan [4] as a function of:

λ/g - 40, 70, 100, 150, 200, 250

t/λ - 0.3, 0.4, 0.5

mmf - 10, 20, 30, 40, 50, 60, 70

x_n - 0, 0.2, 0.4, 0.6, 0.8, 1

These data are flux density vs. mmf and force vs. mmf for a udss. The B-H curve of the material used to construct test motor 1 is also given. Note that the B-H curve may change for different motors.

Table A.1 Data for B(T) vs mmf(*1000 A) Curves for a Unity Length

Unity Rotor Pitch Configuration

		0.3						0.4						0.5					
x	l/g mmf	40	70	100	150	200	250	40	70	100	150	200	250	40	70	100	150	200	250
0.0	0	0.00	0.00	0.00	0.00	0.00	0.00	0.00	0.00	0.00	0.00	0.00	0.00	0.00	0.00	0.00	0.00	0.00	0.00
	10	0.62	1.00	1.36	1.62	1.76	1.86	0.58	0.98	1.30	1.60	1.74	1.83	0.56	0.84	1.30	1.58	1.72	1.80
	20	1.26	1.64	1.76	1.94	2.05	2.14	1.17	1.58	1.74	1.90	2.00	2.08	1.14	1.48	1.72	1.84	1.97	2.04
	30	1.60	1.80	1.94	2.08	2.18	2.26	1.60	1.76	1.90	2.02	2.10	2.18	1.52	1.74	1.88	2.00	2.06	2.12
	40	1.73	1.92	2.04	2.14	2.22	2.30	1.70	1.87	1.99	2.10	2.14	2.20	1.66	1.84	1.98	2.06	2.14	2.20
	50	1.80	1.98	2.12	2.20	2.28	2.36	1.78	1.94	2.04	2.18	2.22	2.26	1.73	1.92	2.04	2.14	2.20	2.27
	60	1.84	2.04	2.18	2.26	2.34	2.38	1.84	2.00	2.10	2.24	2.28	2.32	1.78	1.96	2.08	2.20	2.24	2.30
	70	1.86	2.06	2.20	2.28	2.36	2.40	1.88	2.06	2.16	2.26	2.32	2.35	1.84	2.01	2.12	2.23	2.26	2.31
0.2	0	0.00	0.00	0.00	0.00	0.00	0.00	0.00	0.00	0.00	0.00	0.00	0.00	0.00	0.00	0.00	0.00	0.00	0.00
	10	0.40	0.82	1.06	1.38	1.46	1.52	0.52	0.82	1.14	1.42	1.53	1.58	0.52	0.82	1.14	1.44	1.56	1.62
	20	0.78	1.44	1.60	1.72	1.76	1.82	1.06	1.40	1.62	1.74	1.78	1.82	1.04	1.48	1.66	1.76	1.79	1.84
	30	1.12	1.72	1.79	1.90	1.97	2.02	1.46	1.72	1.80	1.88	1.93	1.98	1.46	1.70	1.79	1.88	1.92	1.96
	40	1.25	1.84	1.92	2.03	2.10	2.17	1.62	1.83	1.92	1.98	2.00	2.04	1.62	1.80	1.88	1.96	2.00	2.04
	50	1.32	1.90	2.00	2.11	2.19	2.24	1.74	1.88	1.94	2.00	2.05	2.10	1.73	1.86	1.93	2.00	2.06	2.08
	60	1.36	1.94	2.06	2.18	2.26	2.30	1.86	1.92	1.98	2.05	2.10	2.14	1.80	1.88	1.96	2.04	2.08	2.14
	70	1.40	1.98	2.12	2.25	2.30	2.32	1.92	2.02	2.07	2.10	2.15	2.19	1.87	1.90	2.00	2.08	2.10	2.16
0.4	0	0.00	0.00	0.00	0.00	0.00	0.00	0.00	0.00	0.00	0.00	0.00	0.00	0.00	0.00	0.00	0.00	0.00	0.00
	10	0.42	0.58	0.70	0.76	0.82	0.86	0.42	0.64	0.84	1.04	1.12	1.16	0.44	0.68	0.93	1.14	1.23	1.29
	20	0.82	1.06	1.10	1.14	1.20	1.24	0.84	1.16	1.27	1.34	1.38	1.41	0.86	1.24	1.38	1.44	1.47	1.50
	30	1.22	1.36	1.38	1.42	1.48	1.52	1.22	1.42	1.46	1.51	1.56	1.60	1.26	1.50	1.54	1.58	1.61	1.64
	40	1.46	1.54	1.56	1.60	1.66	1.70	1.44	1.54	1.58	1.63	1.68	1.72	1.48	1.61	1.66	1.69	1.71	1.72
	50	1.64	1.70	1.72	1.76	1.82	1.85	1.58	1.64	1.66	1.71	1.76	1.80	1.62	1.70	1.74	1.78	1.80	1.82
	60	1.77	1.82	1.84	1.89	1.94	1.98	1.66	1.70	1.73	1.78	1.82	1.84	1.72	1.76	1.80	1.83	1.86	1.88
	70	1.84	1.90	1.96	2.02	2.06	2.08	1.74	1.76	1.80	1.81	1.83	1.85	1.82	1.86	1.90	1.93	1.96	1.98

Table A.1 Cont'd

		0.3						0.4						0.5					
x	l/g mm f	40	70	100	150	200	250	40	70	100	150	200	250	40	70	100	150	200	250
0.6	0	0.00	0.00	0.00	0.00	0.00	0.00	0.00	0.00	0.00	0.00	0.00	0.00	0.00	0.00	0.00	0.00	0.00	0.00
	10	0.26	0.29	0.30	0.36	0.39	0.42	0.32	0.44	0.55	0.65	0.70	0.74	0.36	0.52	0.68	0.85	0.90	0.95
	20	0.50	0.56	0.60	0.66	0.72	0.76	0.64	0.80	0.86	0.90	0.96	0.99	0.70	0.98	1.06	1.10	1.12	1.16
	30	0.74	0.82	0.84	0.90	1.03	1.07	0.91	1.03	1.06	1.11	1.16	1.20	1.02	1.20	1.22	1.24	1.28	1.32
	40	0.96	1.08	1.14	1.16	1.26	1.35	1.14	1.22	1.24	1.28	1.34	1.38	1.26	1.34	1.38	1.41	1.44	1.50
	50	1.20	1.32	1.37	1.42	1.50	1.58	1.30	1.36	1.38	1.42	1.46	1.52	1.41	1.44	1.49	1.52	1.55	1.60
	60	1.42	1.56	1.63	1.67	1.74	1.80	1.44	1.50	1.52	1.55	1.60	1.64	1.50	1.56	1.60	1.63	1.66	1.70
	70	1.64	1.78	1.85	1.89	1.93	1.95	1.58	1.64	1.66	1.69	1.74	1.76	1.60	1.66	1.70	1.73	1.75	1.76
0.8	0	0.00	0.00	0.00	0.00	0.00	0.00	0.00	0.00	0.00	0.00	0.00	0.00	0.00	0.00	0.00	0.00	0.00	0.00
	10	0.16	0.17	0.18	0.20	0.24	0.28	0.21	0.23	0.25	0.28	0.30	0.34	0.28	0.38	0.46	0.55	0.59	0.63
	20	0.33	0.35	0.37	0.42	0.48	0.54	0.42	0.46	0.50	0.52	0.55	0.62	0.55	0.70	0.73	0.78	0.82	0.86
	30	0.51	0.53	0.55	0.62	0.71	0.82	0.64	0.68	0.70	0.74	0.78	0.88	0.80	0.88	0.90	0.93	1.02	1.06
	40	0.78	0.82	0.85	0.92	0.94	1.05	0.83	0.87	0.90	0.95	0.96	1.11	1.02	1.08	1.12	1.17	1.22	1.25
	50	1.02	1.07	1.11	1.14	1.16	1.28	1.02	1.08	1.10	1.14	1.19	1.25	1.20	1.24	1.28	1.32	1.36	1.40
	60	1.24	1.26	1.28	1.34	1.38	1.50	1.32	1.37	1.40	1.44	1.46	1.47	1.36	1.40	1.42	1.44	1.45	1.46
	70	1.40	1.46	1.49	1.52	1.54	1.55	1.52	1.55	1.57	1.58	1.59	1.60	1.50	1.54	1.56	1.57	1.58	1.59
1.0	0	0.00	0.00	0.00	0.00	0.00	0.00	0.00	0.00	0.00	0.00	0.00	0.00	0.00	0.00	0.00	0.00	0.00	0.00
	10	0.14	0.16	0.18	0.20	0.23	0.26	0.09	0.12	0.16	0.18	0.20	0.24	0.22	0.26	0.30	0.32	0.36	0.38
	20	0.33	0.37	0.39	0.42	0.45	0.52	0.29	0.32	0.34	0.37	0.42	0.46	0.48	0.52	0.56	0.59	0.62	0.66
	30	0.53	0.57	0.60	0.63	0.66	0.70	0.47	0.49	0.51	0.55	0.62	0.69	0.72	0.75	0.78	0.81	0.86	0.90
	40	0.74	0.81	0.85	0.88	0.91	1.03	0.75	0.80	0.85	0.90	0.95	0.98	0.95	1.00	1.02	1.05	1.09	1.13
	50	1.00	1.04	1.10	1.12	1.14	1.20	1.02	1.05	1.08	1.11	1.15	1.18	1.18	1.22	1.25	1.29	1.32	1.35
	60	1.18	1.22	1.25	1.30	1.31	1.31	1.20	1.23	1.27	1.29	1.31	1.34	1.39	1.44	1.49	1.50	1.50	1.50
	70	1.33	1.34	1.37	1.40	1.42	1.47	1.34	1.36	1.38	1.40	1.44	1.50	1.50	1.51	1.53	1.54	1.55	1.56

Table A.2 Data for S(k.Nt) vs mmf(*1000 A) Curves for a Unity Length

Unity Rotor Pitch Configuration

x	l/g	t/l=0.3						t/l=0.4						t/l=0.5					
	mmf	40	70	100	150	200	250	40	70	100	150	200	250	40	70	100	150	200	250
0.2	0	00.00	00.00	00.00	00.00	00.00	00.00	0.00	0.00	0.00	0.00	0.00	0.00	0.00	0.00	0.00	0.00	0.00	0.00
	10	03.41	05.23	07.95	09.81	11.13	11.82	3.44	5.10	7.29	9.51	10.76	11.57	3.19	6.53	7.76	9.49	10.69	11.51
	20	08.35	12.57	18.05	21.12	13.15	24.14	8.35	12.24	16.44	20.28	22.23	23.42	7.93	13.31	17.13	19.98	21.80	23.02
	30	13.90	20.05	27.40	31.16	33.53	34.68	13.90	19.64	25.17	29.87	32.15	33.53	13.39	19.85	25.52	29.05	31.19	32.60
	40	19.37	26.93	35.38	39.46	41.93	43.13	19.50	26.63	32.92	37.95	40.33	41.76	18.93	25.81	32.65	36.51	38.75	40.22
	50	24.08	32.47	41.38	45.54	47.98	49.20	24.56	32.53	39.12	44.18	46.53	47.95	23.92	30.84	38.20	42.15	44.38	45.85
	60	27.35	35.93	44.79	48.91	51.35	52.58	28.49	36.66	43.22	48.20	50.53	51.95	27.74	34.59	41.88	45.78	47.99	49.44
	70	28.50	36.55	44.98	49.10	51.67	52.96	30.70	38.35	44.66	49.69	52.13	53.61	29.74	36.71	43.38	47.19	49.47	50.98
0.4	0	0.00	0.00	0.00	0.00	0.00	0.00	0.00	0.00	0.00	0.00	0.00	0.00	0.00	0.00	0.00	0.00	0.00	0.00
	10	1.00	4.88	7.50	9.63	10.96	11.78	1.91	5.34	7.95	9.95	11.00	11.70	1.76	5.14	7.86	9.91	10.84	11.53
	20	8.08	15.87	20.68	24.12	26.16	27.39	8.26	15.91	20.90	24.07	25.58	26.57	7.94	15.13	20.37	23.69	25.01	25.98
	30	19.11	29.82	36.02	40.12	42.47	43.86	17.53	28.62	35.24	39.04	40.78	41.89	17.06	27.20	34.14	38.15	39.67	40.77
	40	31.88	44.57	51.51	55.82	58.23	59.65	28.25	41.86	49.46	53.53	55.32	56.46	27.64	39.86	47.80	52.09	53.67	54.81
	50	44.17	57.93	65.14	69.43	71.77	73.15	38.92	54.03	62.07	66.17	67.97	69.10	38.20	51.60	59.96	64.29	65.89	67.02
	60	53.77	67.75	74.90	79.14	81.45	82.81	48.06	63.52	71.55	75.64	77.46	78.61	47.29	60.94	69.27	73.56	75.18	76.32
	70	58.47	71.85	78.80	83.15	85.60	87.04	54.18	68.74	76.40	80.58	82.54	83.80	53.43	66.39	74.34	78.69	80.40	81.64
0.6	0	0.00	0.00	0.00	0.00	0.00	0.00	0.00	0.00	0.00	0.00	0.00	0.00	0.00	0.00	0.00	0.00	0.00	0.00
	10	1.77	6.53	7.77	9.73	10.78	11.38	1.65	5.33	7.75	9.91	11.14	11.90	1.43	5.17	7.64	9.75	10.89	11.63
	20	8.25	17.84	20.30	23.33	24.88	25.69	8.26	15.92	20.57	24.08	25.94	27.04	7.68	15.38	20.17	23.58	25.29	26.35
	30	18.22	31.39	34.69	38.23	40.00	40.89	18.50	29.28	35.39	39.61	41.76	43.00	17.36	28.14	34.47	38.57	40.54	41.75
	40	30.45	46.02	49.84	53.53	55.33	56.23	31.04	44.03	50.97	55.44	57.66	58.93	29.10	42.06	49.26	53.63	55.66	56.90
	50	43.72	60.59	64.64	68.30	70.05	70.93	44.51	58.77	66.04	70.52	72.70	73.96	41.51	55.71	63.26	67.64	69.65	70.87
	60	56.80	73.93	77.97	81.60	83.34	84.22	57.58	72.13	79.36	83.80	85.96	87.22	53.20	67.68	75.19	79.53	81.54	82.76
	70	68.47	84.89	88.73	92.51	94.39	95.35	68.89	82.70	89.67	94.20	96.50	97.85	62.79	76.55	83.77	88.19	90.32	91.63
0.8	0	0.00	0.00	0.00	0.00	0.00	0.00	0.00	0.00	0.00	0.00	0.00	0.00	0.00	0.00	0.00	0.00	0.00	0.00
	10	0.36	0.45	0.50	0.44	0.35	0.32	1.01	5.14	7.29	9.45	10.58	11.24	1.35	4.88	7.37	9.43	10.77	11.59
	20	1.54	1.84	1.92	1.80	1.64	1.59	7.33	15.74	19.42	22.86	24.58	25.50	6.87	14.23	19.00	22.33	24.37	25.57
	30	3.52	4.04	4.14	3.99	3.81	3.74	17.46	29.07	33.64	37.67	39.64	40.67	15.32	25.64	31.91	35.90	38.26	39.63
	40	6.25	6.97	7.08	6.93	6.74	6.67	29.84	43.61	48.59	52.77	54.76	55.79	25.44	37.85	44.96	49.20	51.61	53.02
	50	9.69	10.54	10.67	10.52	10.34	10.28	42.90	57.84	62.92	67.02	68.94	69.94	35.96	49.56	57.00	61.25	63.61	64.99
	60	13.79	14.69	14.83	14.69	14.52	14.46	55.06	70.23	75.27	79.30	81.19	82.17	45.61	59.47	66.88	71.08	73.43	74.80
	70	18.53	19.34	19.47	19.34	19.17	19.11	64.77	79.25	84.27	88.48	90.50	91.54	53.14	66.31	73.44	77.73	80.23	81.69

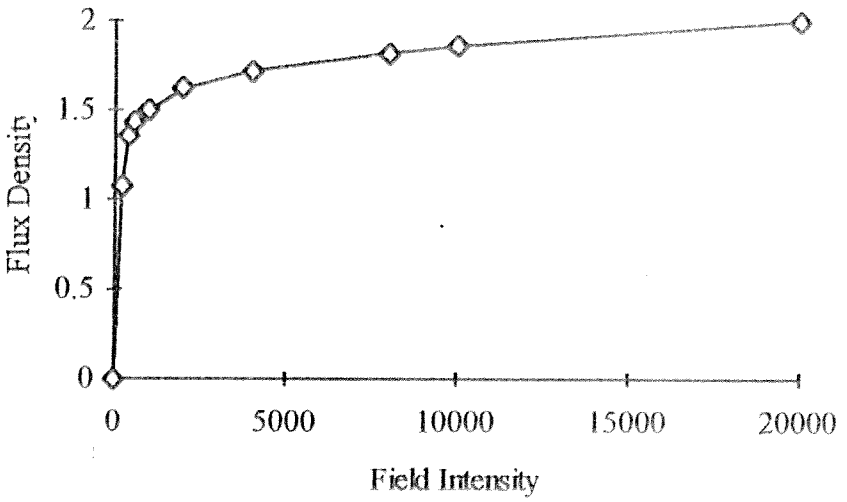

Figure A.1 B-H Curve of the Data Used in Computing the Performance

Table A.3 Data Representing B-H Curve

B	H
0.00	0.0
1.08	200.0
1.36	400.0
1.44	600.0
1.50	1000.0
1.62	2000.0
1.72	4000.0
1.82	8000.0
1.86	10000.0
2.00	20000.0

APPENDIX B

FLUX LINKAGE AND THE INVERSE TABLES

The solution of equation 3.13 to obtain current waveform requires the definition of the magnetic behaviour of the motor in the form of a table $i(\theta,\phi)$ to enable the value of i to be updated after each step of numerical integration of the model equation. In other words, after each integration step, to find a new value of ϕ it is necessary to find the corresponding current which is then inserted in the right hand side of equation 3.13. This table $i(\theta,\phi)$ is obtained by inverting the input table. The values of $i(\phi)$ at equally spaced flux linkages are found by using quadratic interpolation through three successive points.

Table B.1 represents the measured flux linkages for test motor 1 and table B.2 is the inverse table.

Table B.1 Flux Linkage as a Function of Current and Position

	current (A)												
X	0	0.5	1	1.5	2	2.5	3	3.5	4	4.5	5	5.5	6
0.0	0.00	0.40	0.65	0.75	0.80	0.84	0.86	0.88	0.90	0.92	0.93	0.94	0.95
0.1	0.00	0.38	0.63	0.74	0.79	0.83	0.85	0.88	0.89	0.91	0.92	0.93	0.94
0.2	0.00	0.33	0.55	0.68	0.74	0.77	0.80	0.83	0.84	0.86	0.88	0.89	0.90
0.3	0.00	0.27	0.48	0.59	0.66	0.70	0.73	0.76	0.78	0.80	0.82	0.83	0.85
0.4	0.00	0.19	0.34	0.44	0.50	0.55	0.59	0.62	0.66	0.68	0.71	0.73	0.76
0.5	0.00	0.13	0.23	0.30	0.36	0.41	0.45	0.49	0.53	0.57	0.60	0.62	0.65
0.6	0.00	0.05	0.10	0.14	0.19	0.24	0.28	0.33	0.37	0.41	0.45	0.48	0.52
0.7	0.00	0.04	0.07	0.10	0.14	0.17	0.20	0.24	0.27	0.31	0.34	0.37	0.40
0.8	0.00	0.03	0.06	0.09	0.12	0.15	0.18	0.21	0.24	0.26	0.29	0.31	0.34
0.9	0.00	0.03	0.05	0.08	0.10	0.13	0.16	0.18	0.21	0.23	0.26	0.28	0.31
1.0	0.00	0.03	0.05	0.08	0.10	0.13	0.15	0.18	0.20	0.23	0.25	0.28	0.30

Table B.2 Current as a Function of Flux Linkage and Position

	Flux Linkage										
X	0	0.1	0.2	0.3	0.4	0.5	0.6	0.7	0.8	0.9	1.0
0.0	0.00	0.13	0.25	0.38	0.50	0.68	0.89	1.23	2.00	4.00	8.50
0.1	0.00	0.13	0.26	0.39	0.54	0.72	0.93	1.30	2.12	4.33	9.00
0.2	0.00	0.15	0.30	0.45	0.64	0.87	1.17	1.65	3.00	6.00	11.00
0.3	0.00	0.19	0.37	0.57	0.80	1.08	1.56	2.50	4.50	7.25	9.75
0.4	0.00	0.26	0.53	0.86	1.28	2.00	3.15	4.87	6.67	8.33	10.00
0.5	0.00	0.38	0.84	1.50	2.39	3.63	5.00	6.83	8.50	10.17	11.83
0.6	0.00	1.00	2.10	3.22	4.37	5.75	7.00	8.25	9.50	10.75	12.00
0.7	0.00	1.50	3.00	4.39	6.00	7.67	9.33	11.00	12.67	14.33	16.00
0.8	0.00	1.67	3.33	5.23	7.00	8.67	10.33	12.00	13.67	15.33	17.00
0.9	0.00	2.00	3.87	5.83	7.50	9.17	10.83	12.50	14.17	15.83	17.50
1.0	0.00	2.00	4.00	6.00	8.50	11.00	13.50	16.00	18.50	21.00	23.50

SR MOTOR
TORQUE AND FLUX LINKAGE
MEASUREMENTS
AND
FINITE ELEMENT FIELD
CALCULATIONS

BY

FUNDA ŞAHİN & H. BÜLENT ERTAN

1. INTRODUCTION ---- 1

2)FINITE ELEMENTS ANALYSIS SOFTWARE - ANSYS ---- 3

ANSYS PROGRAM: ---- 3

A) BUILDING MODEL: ---- 3

B) APPLYING LOADS AND OBTAINING SOLUTION: ---- 3

Boundary Conditions: ---- 4

Loads: ---- 4

Specifying load step options: ---- 5

C) REVIEWING THE RESULTS: ---- 5

Nodal Data: ---- 5

SWITCHED RELUCTANCE MOTOR MODELING: ---- 6

3) CALCULATIONS OF TORQUE AND FLUX LINKAGE USING FIELD SOLUTIONS ---- 7

3.1) Torque Calculations: ---- 7

3.2) Flux Linkage Calculations: ---- 8

Macro file procedure: ---- 10

4) SOLUTION OF THE FIELD AND CALCULATION OF TORQUE AND FLUX LINKAGE FOR THE TEST MOTORS ---- 11

4.1.) Test Motor 1 (SR1) ---- 12

DIMENSIONS OF THE MOTOR: ---- 12

Step Angle: ---- 13

Position Normalization: ---- 14

Loading: ---- 14

4.1.1 The Effects of Mesh Distribution on Calculations ---- 15

4.1.2. Type of Element and the Distribution of Elements ---- 16

4.1.3. Solution of the Field and Solution Accuracy----------18

1) ANSYS- ANALYSIS OPTIONS:----------18

2) ANSYS-SOLUTION OPTIONS:----------18

3) SOLUTION SEQUENCE- LINEAR ANALYSIS:----------19

4) SOLUTION SEQUENCE - NONLINEAR ANALYSIS:----------19

4.1.4. Rotation of the Rotor: Rotor / Stator Stiching Operation----------20

4.1.5. Calculated Torque and Flux Linkage for SR1 ----------21

Torque Prediction----------21

Flux Linkage Prediction ----------22

4.2. TEST MOTOR 2 (SR2) ----------24

DIMENSIONS OF THE MOTOR: ----------24

4.2.1. Measured Torque and Flux Linkage for SR2 ----------25

4.2.2. Torque Measurements----------25

4.2.3. Flux Linkage Measurement ----------28

4.2.4. The Field Solution and the Mesh Distribution ----------30

5- SR2 MOTOR ----------31

4.2.5 Comparison of Measured and Computed Torque-Position Curves.----------31

4.2.6. Comparison of Measured and Computed Flux Linkage ----------33

5. CONCLUSIONS:----------35

REFERENCES: ----------37

1. INTRODUCTION

Numerical solution of Magnetic fields is an important engineering tool for prediction of performance of various devices. The use of this technique for magnetic design purposes is only about 20 years old and is growingly becoming a very important modern tool for magnetic design. Finite Element method is one of the solution techniques and it has found a more general acceptance than others. Ansys is one such professional Finite Element Field solution tool used by industry.

In this part of the report the use of this software for predicting the performance of switched reluctance motors will be described. In Finite Element field solution program the field is generally devided into number of discrete elements. For each element an equation valid for that mesh is written. Then, the resulting set of equations are solved simultaneously while satisfying the boundary conditions.

The solution therefore greatly depends on how the user discretizes the problem and imposes boundary conditions. For that reason it is essential to test the program and its results for obtaining desired accuracy without excessively increasing the computation time. One of the purposes of this investigation has been to increase experience with the use of such programs for magnetic design purposes.

Although professional programs provide a field solution, often essential software for calculating the desired performance is not readily available. The user develops such 'macro's for the specific problem. Development of such tools for SR motor performance analysis and testing their accuracy has been the other purpose.

The research work has started by solving the field for a SR motor readily available in the laboratory. This was essential since the design of the SR motor for the application here would take time. The tests on this motor (called SR1 in this report) for finding its torque-

position and flux linkage-position-current characteristics was already done in REF [1,2] . The effect of distribution of meshes in the solution area is investigated also on this motor. Another issue investigated was to find out how to use a given mesh distribution for obtaining field solution for different rotor positions. This is extremely important for minimizing the effort to obtain the desired characteristics. The purpose was to identify factors affecting the prediction accuracy, and to find out how to minimize solution time while achieving desired accuracy.

Once the design of the SR motor (This motor is called SR2 in this report) for the application here was done using the software developed in section 1 of this report, the F.E. solution approach is used to verify the design. The two approaches are complementary; the analysis and optimization software gives quick results however, its accuracy is limited. On the other hand using F.E. technique is more tedious and time consuming but its accuracy is greater.

In the study here the following platform purchased within the project budget is used.

HP series 720 Computer Workstation
1 Gbyte SCSI Disk
32 Mbytes RAM
HP - UX 8.07

At a later stage a PC is purchased with the available budget and a PC based version of the program is also studied.

In the following section of this report the ANSYS program is briefly described. Then the test and computation results for each motor is given in separate sections.

2)FINITE ELEMENTS ANALYSIS SOFTWARE - ANSYS

ANSYS PROGRAM:

ANSYS is a computer program for finite element analysis and design. The program may be used to find out how a given design (e.g. a machine) works under operating conditions. It can be also used to calculate a proper design for given operating conditions, through design by analysis technique.

ANSYS program can be used in all disciplines of engineering : structural, thermal, mechanical, electrical, electromagnetic, electronic, fluid and biomedical. In this study only the electromagnetic analysis facilities of the program is used. [3, 4, 5, 6].

In the following sections basic features of ANSYS and the steps to be followed to build a model and solution of the field are described.

A) BUILDING THE MODEL:

The following steps are followed.
Defining element types (four nodded magnetic elements are used for meshing operation)
Defining material properties. Options are as follows

Linear material properties

Nonlinear material properties (BH data of magnetic material is loaded)

Creating the model geometry (dimensions of the motor)

B) APPLYING LOADS AND OBTAINING SOLUTION:

Defining the analysis type and analysis option
Applying loads

Defining boundary conditions ; loads and constraints.
Applying current densities to the conductors.

Boundary Conditions:

*Boundary conditions are considered to be at symmetry planes of a model or at the far-field boundary of the model . Boundary options includes flux-normal, flux-parallel , far-field , far-field zero and periodic.

*Flux normal conditions are used to force flux to flow perpendicular to a surface. This is imposed naturally by the finite element method when no specifications are made at the surface of interest.

*Flux parallel conditions are used to force flux to flow parallel to a surface . This is imposed by setting the magnet vector potential , Az , to a constant value. The constant value is usually zero unless a non-zero field is being imposed.

In this applications flux parallel boundary conditions (A=0) have to be defined on the exterior parts of the motor that surrounded by air. (Drichlet type or flux parallel boundary conditions)

Loads:

*Loads that can be applied to a model include nodal potentials, element current density and nodal current segments.

*Virtual displacements may be specified to indicate a virtual work force calculation

*Maxwell surface "flags" may be set to identify surfaces for evaluation of surface force traction.

*Nodal vector potential loads (A_Z) are used to apply nodal vector potentials to a node. This is generally done to apply an external field to a model by applying potentials at the model boundary.

*Source current density (J_S) loading is used to apply a uniformly distributed source current to an element. The loading is expressed in terms of current "density".

Specifying load step options:

Due to the nonlinear nature of the model, a two load step procedure is used. The first load step is used to ramp on the boundary conditions (nodal potentials and loads) . The second load is used to converge the nonlinear solution. Convergence controls used during solution also have to be defined .

C) REVIEWING THE RESULTS:

Once the solution has been calculated ANSYS postprocessor can be used to review the results. Contour displays , tabular listings and many other postprocessor options are available and there are commands to make some calculations (e.g. line integral, cross product .. etc.)

Nodal Data:

*Nodal vector potential (A_Z) is available for processing.

-Flux lines are lines of constant A_Z in a planar analysis , and lines of constants A in an axisymmetric analysis (r = x coordinate)

- A_Z can be used to visualize flux lines
- Between any two nodes in a model , the flux passing between the nodes may be calculated as :

$$\phi = \int A.\, dl$$

*Nodal magnetic flux density (B) and field intensity (H) are available for processing.

*Nodal Lorentz forces or Maxwell surface forces may be displayed.

SWITCHED RELUCTANCE MOTOR MODELING:

For modeling of switched reluctance motors , full model is used since half symmetry modeling may have some difficulties about rotation of the rotor part. For the exterior nodes of motor (exterior parts of stator and rotor) flux parallel boundary conditions are applied it means parallel component of the magnetic vector potential is defined as zero. It is supposed that only one phase is excited at the time of analysis. Exciting conductors are seen in figure 2.1.

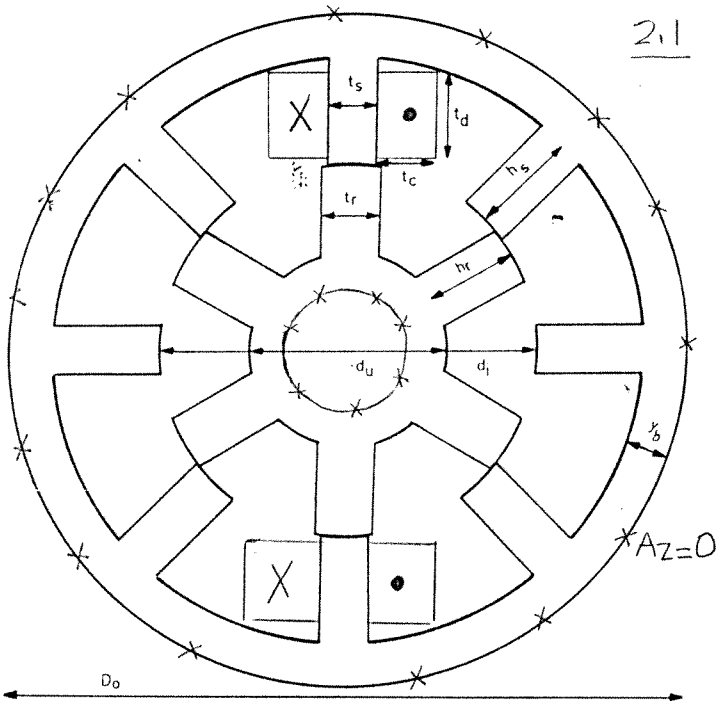

Figure 2.1

3) CALCULATIONS OF TORQUE AND FLUX LINKAGE USING FIELD SOLUTIONS

3.1) Torque Calculations:

A 'Macro' software is developed for calculation of torque produced by the motor at a given position, once the field solution is obtained. The approach used in this software is briefly described below.

The torque on a rigid body can be obtained using the Maxwell stress tensor and is given by;

$$T = \int (\bar{B}.\bar{n})\,(\bar{r} \times \bar{B} / \mu_o) - |\bar{B}|\, 2\,(\bar{r} \times \bar{n}) / 2\,\mu_o)\, ds \qquad (1)$$

For the two dimensional planar case $\bar{r} \times \bar{B}$ has only a single out of plane vector component and can thus be treated as the scalar

$$K = (r_X\, B_y - r_y\, B_X) \qquad (2)$$

therefore equation 1 becomes :

$$|T| = \int (K\bar{B} / \mu_o.\bar{n})\, ds \qquad (3)$$

In the application here a circular integration path is chosen in the center of air gap and for different rotor positions (rotating the rotor nodes without modeling the geometry again) torque is calculated . The path of integration is circular about the origin and number of nodes used to define the path is chosen to be 36 ,it means the angle between nodes is 10 degrees. Integration path is shown in Figure 3.1 . It has to be remembered that the SI unit of calculated torque in this method is Nm/m and resultant torque is calculated by multiplying it with stack length.

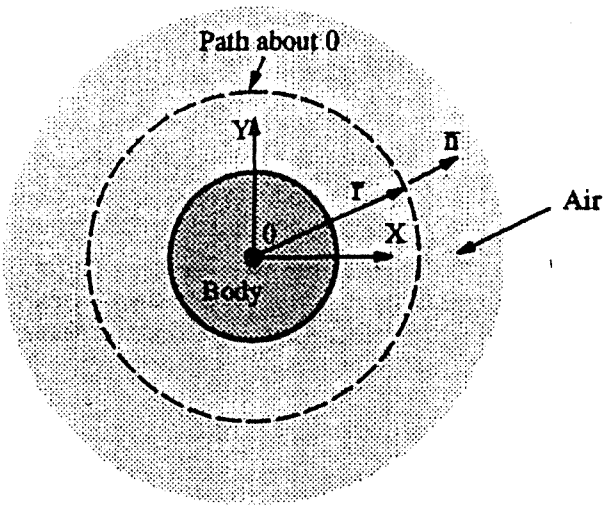

Figure 3.1 Assumed path of integration for torque calculation

3.2) Flux Linkage Calculations:

As discussed in chapter 1 nodal magnetic potential (A_Z) is available in ANSYS postprocessing part. A_Z can also be used to visualize the flux lines . (As seen in the A_Z graphs) . In this study there are two methods used for flux linkage calculations.

METHOD 1:

Between any two node in the model , the flux passing between the nodes may be calculated as :

$$\phi = \int \overline{A}.\ \overline{dl} \qquad (4)$$

In this case the integration is carried out following a closed loop extending into the z direction. Sice A_Z has no component in the x direction. Contribution of the contour along x direction will be zero to the integral. If a unit length of magnetic core is considered in the z direction, it may be concluded that flux through the stator teeth as seen from Figure 3.2 may be calculated from the equation

$$\phi=(A1 - A2).1 \quad (5)$$

where

A1 is the magnetic vector potential of node 1 in Fig 2.3

A2 is the magnetic vector potential of node 2 in Fig 2.3

$\phi 2$ is flux per pole per turn

The flux linkage per phase (Wb-Turns) may be calculated from the equation:

$$\psi = (2 * N) * (\phi 2) * L \quad (6)$$

where

L : Stack length

N : Number of turns

On the other hand flux leakage may be assumed to be

Leakage flux = $2\phi 1 - \phi 2$

where $\phi 1$ is the flux through surface shown in Fig. 3.2 (7)

Leakage fluxes can be seen on A_Z graphs.

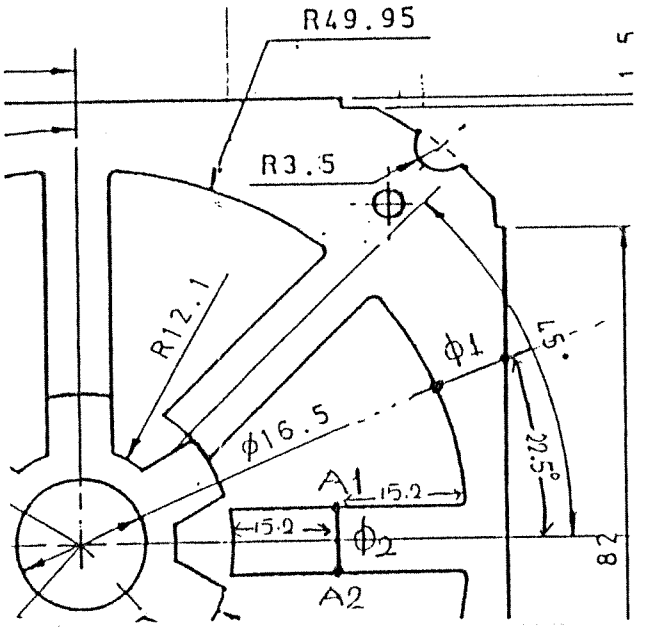

Fig. 3.2 Calculation of flux per pole

METHOD 2:

Moreover a second method recommended by Prof. Jack is also tested . For this purpose a macro file is written to find average magnetic flux density over a coil.

Thus the resultant

flux linkage /pole / turn = Φ = A1 -A2 ... where (8)

A1 is average flux of coil 1

A2 is average flux of coil 2.

Note that this method is similar to method 1 only in this case an average node potential is considered for the calculations. In this study the two methods are found to give almost identical results.

Macro file procedure:

The macro file written for this purpose traces the following steps.

1. From ANSYS magnetic field solution find nodal magetic vector potential A_i for every node on coil 1 (See Fig. 3.3)

2. From ANSYS magnetic field solution find nodal magetic vector potential A_i for every node on coil 2.

3. Find average magnetic vector potential of coil 1 from
   A1 = ($\sum$ Ai) / n , where i= 1, .. n is the node number.

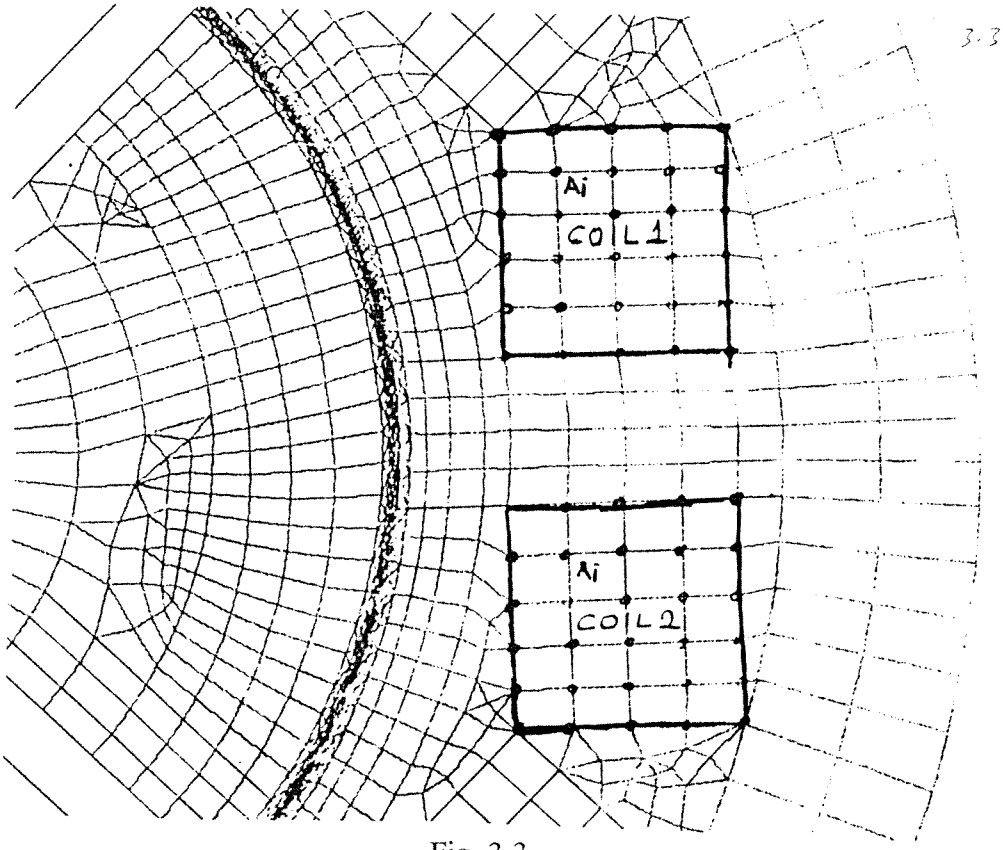

Fig. 3.3

4. Find average magnetic vector potential of coil 2 from

$A2 = (\sum A_i) / n$, where i= 1, .. n is the node number.

(coils have same number of nodes)

5) linkage flux/pole/turn = $\Phi = A1 - A2$

4) SOLUTION OF THE FIELD AND CALCULATION OF TORQUE AND FLUX LINKAGE FOR THE TEST MOTORS

The program used for the solution of the magnetic field with the purpose of calculation of the torque and flux linkage is briefly described in the previous sections.

In this section the application of the field solution technique to the switched reluctance motors in this research is described. The method is first studied on a previously designed

and manufactured SR motor at METU Electrical and Electronics Engineering Department. In this manner time is gained, while other research was pursued to determine specifications and to design the SR motor for the application here.

There experience gained in mesh generation and field solution is later applied to the SR motor developed in this work.

4.1.) Test Motor 1 (SR1)

The effect of the mesh distribution and the factors affecting the accuracy of torque position (T vs θ) and flux linkage- position characteristics (λ vs θ) was investigated on SR1. Measured T ve θ and λ vs θ characteristics of this motor was available from previous work [1,2]. These measurements are not repeated, solution results are compared with these measurements.

The specifications of this motor is as follows.

DIMENSIONS OF THE MOTOR:

Outer diameter of rotor	:	70	mm
Outer diameter of stator	:	135	mm
Core length	:	91.5	mm
Backcore width	:	11	mm
Air gap length	:	0.2	mm
Stator pole width	:	8.5	mm
Rotor pole width	:	10	mm
Stator pole depth	:	21.3	mm
Rotor pole depth	:	17.5	mm
Number of turns	:	300	

Rated Current : 6 Ampere/pole

Maximum are for placing the coil as

a= 6 mm, $t_c = 12.8$ $t_d = 12.6$

The motor structure is shown in Figure 4.1

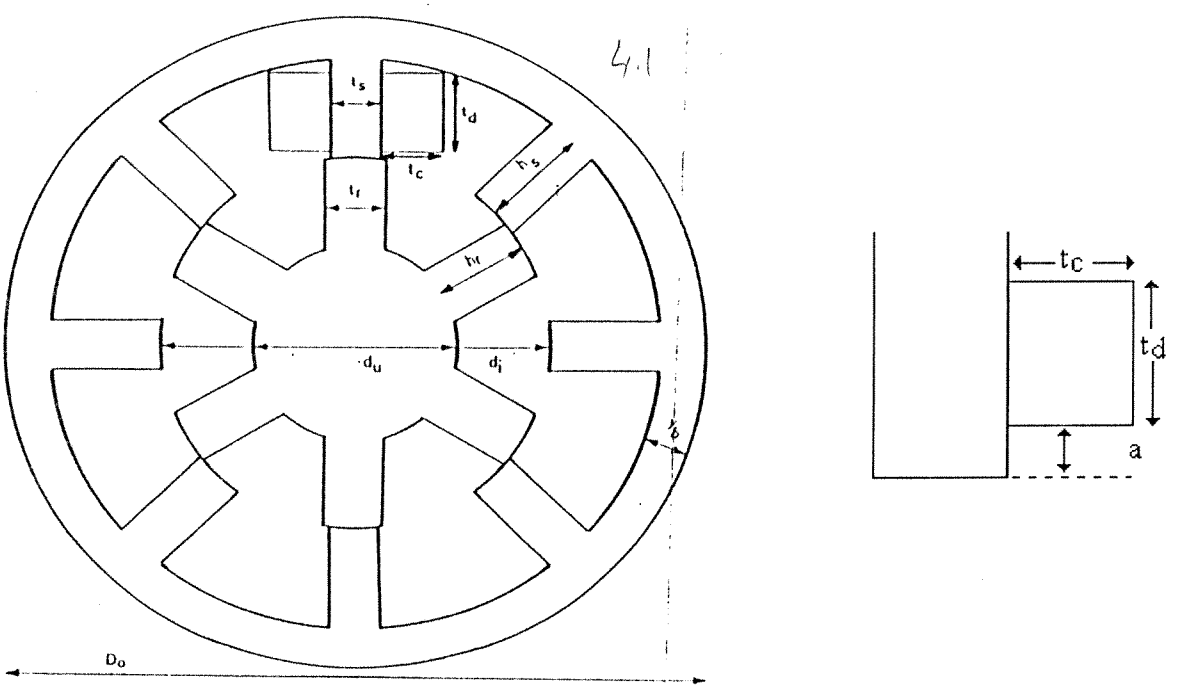

a) SR1 Motor lamination b) A Phase coil of SR1

Fig. 4.1 SR1 motor structure

Step Angle:

The step angle of the motor is simple to calculate

$$\alpha = \frac{360}{n \cdot p} \tag{9}$$

where n is number of phases and p is the number of rotor teeth, therefore

$$\alpha = \frac{360}{4 \cdot 6} = 15^{\circ}$$

Position Normalization:

The torque curve of the motor is periodic over rotor tooth pitch (RTP)

$$RTP = n.\alpha = 4*15 = 60^{o} \quad (10)$$

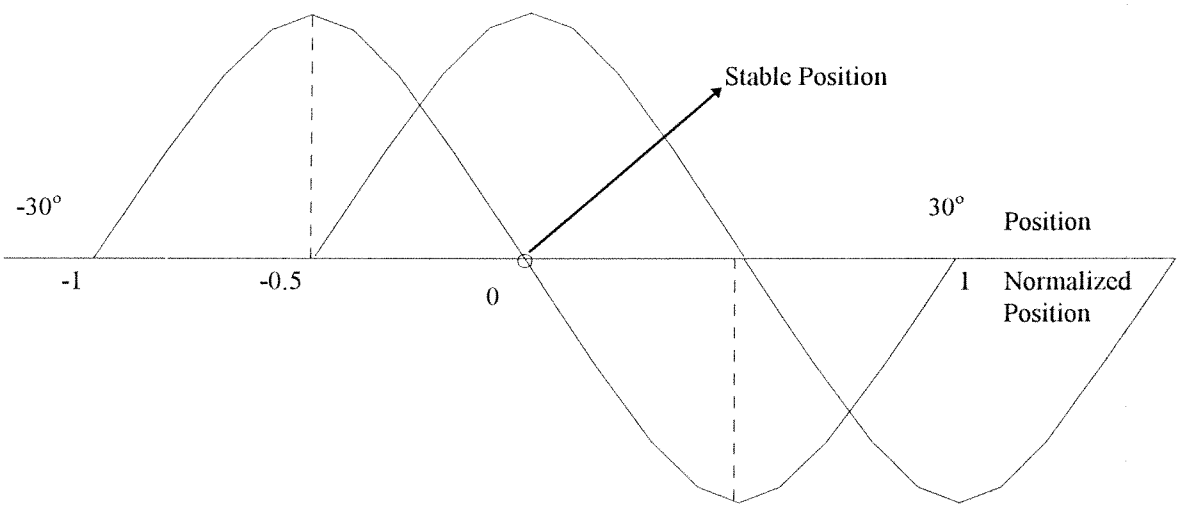

Fig. 4.2

In this study rotor position is expressed in normalized form. The normalization is done over (RTP/2). In this notation, the normalized step angle (α_n) is

$$\alpha_n = \frac{15}{30} = 0.5$$

Loading:

Current density is applied on every element in the area representing the coils of a pole. For SR1 motor for 4 Ampere phase current.

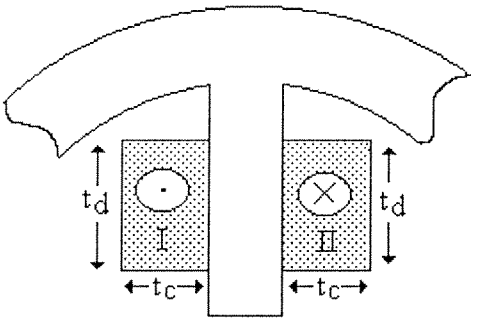

$J = N.I / Area$

$J = 300.4 / (t_c \times t_d)$

$J = 1200 / 1.61.10^{-4}$

$J = 7.44.10^{6}$

For Part II the direction of the current is reserved. $J = -NI / Area \Rightarrow 3 = -7.44.10^{6}$ A/m^2

4.1.1 The Effects of Mesh Distribution on Calculations

The ultimate aim of the field solution is to be able to predict the torque and inductance characteristics of the motor with good accuracy. However, field solution are time consuming even on fast workstation. Therefore, it is highly desirable to minimize number of elements, without loosing the accuracy of solution. To study this issue 3 different meshes are created for SR1. Mesh A and Mesh B as shown below have similar number of elements. The major difference is in the number of elements in the airgap. Mesh B has about 50% less elements in this region.

In the case of Mesh C the number of elements in the airgap are the same as Mesh A. In this case, however, the number of elements in other regions is increased by about 50% to find out its effect on the solution time and accuracy.

MESH A: 8180 elements (total) Fig. (4.3, 4.4)
2160 elements (in the air gap)
**3 ROWS of elements used for air gap mesh
*** Computation Time is approximately 30 minutes

MESH B: 7960 elements (total) Fig . (4.5, 4.6)
1440 elements (in the air gap)

**2 ROWS of elements used for air gap mesh

*** Computation Time is approximately 20 minutes

MESH C: 12140 elements (total) Fig. (4.7, 4.8)

2160 elements (in the air gap)

**3 ROWS of elements used for airgap mesh

*** Computation Time is approximately 45 minutes

The type of element used for meshing, rules followed in creating the mesh are discussed in the following section, as well as the method used for obtaining a solution.

4.1.2. Type of Element and the Distribution of Elements

Element type used for the solution of the problem here is PLANE -13/2-D Coupled-Field Solid.

Plane 13 coupled field solid element is defined by four nodes with up to four degrees of freedom per-node. Magnetic, thermal, electrical and structural field capability may exist in a coupled-field Analysis with limited coupling between the fields. The element has nonlinear magnetic capability for modeling B-H. curves or permanent magnet demagnetization curves.

Plane 13 may be used as a four nodded or three nodded (rectangular or triangular options). element. For airgap meshing, rectangular elements are used. This is called mapped meshing. It requires that an area or volume be "regular" that is, it must meet certain special criteria:

a) The area must be bounded by either three or four lines,

b) It must have equal numbers of element divisions specified on opposite sides rectangular elements for are preferred here meshing the airgap because;

i) For torque calculation, nodes in the same radius have to be taken (accuracy of integration)
ii) For rotation of the rotor without remeshing, there must be equal size of elements on the surface of rotation

In other parts of the motor rectangular elements are prefered But, for non-regular areas, triangular elements are also used.(eg. SR2 stator part)

For meshing other parts of the motor, the shape and distribution of the elements are carefully selected. Using a mesh that has low aspect ratio helps to minimize the discontinuities in the flux density components and the errors in the computed torque of a SRM. For this reason the ANSYS program performs element shape checking (based on aspect ratio and shape angle) to warn user whenever a meshing operation creates on element having a poor shape. Here are some suggestions to decide whether elements shapes are acceptible:

Regions that are flattened or have excessively sharp corners generally cause mesh failure. Hence, mesh should be made dense enough so that elements with high aspect ratio would not be produced.

Low aspect ratio elements should be used to avoid long and sharp triangles. "15°" is a proper lower bound for the internal angles of any element"

In designing the mesh structure of SR motor, the above mentioned principles have been followed. Additionally, since the airgap plays a crucial role in the determination of torque, a special emphesis is given to the mesh design of this region. The design is made such that the elements are smallest of the whole motor structure. Radially moving in both

directions away from the airgap (along the magnetic circuit) first the motor is divided in eccentrical circles such that the radial distance between each successive circle is an increasing multiple of airgap length (x2, x3,....). Then, each ring is meshed automatically by ANSYS in either triangular or rectengular elements. The perimeter of each ring is devided such that the above mentioned 15° constraint is eventually satisfied. This procedure allows us to have a satisfactory accurracy with a considerably low number of elements.

4.1.3. Solution of the Field and Solution Accuracy

1) ANSYS- ANALYSIS OPTIONS:

- Analysis options includes, STATIC, SUBSTRUCTURE analysis, etc.
- Newton-Raphson solution procedure may be selected. (In most cases, the program will choose by default the appropriate option) (NROPT command, adaptive descent procedure)
- Solver options include a FRONTAL EQUATION SOLVER and a JACOBIAN CONJUGATE GRADIENT SOLVER. (EQSLV-command).

2) ANSYS-SOLUTION OPTIONS:

- Number of substeps within a load step may be specified (NSUBST-command)
- Number of equilibrium iterations within a substep to allow for nonlinear convergence may be specified by (NEQIT)-command.
- CNVTOL command is used to set the nonlinear convergence criteria for the analysis.

  - Convergence may be based on the out-of-balance load for the corresponding forcing load (Label=CSG)
  - Convergence may be based on the degree of freedom. (Label=A)
  - Program calculated default reference is recommended

- Solution accuracy has to be set to at last a value 0.001 (0.1%) for the accuracy of the analysis. (Default value is 0.001).
- If convergence is not obtained, program may be terminated (NCNV command)

3) SOLUTION SEQUENCE- LINEAR ANALYSIS:

- Linear analysis accurs when only linear properties are defined (i.e, relative permeability input only, no B-H curve).

- Solution requires only 1 substep.

4) SOLUTION SEQUENCE - NONLINEAR ANALYSIS:

- Nonlinear analysis occurs when B-H curves are input.

- Recommended solution sequence is to solve the problem over two load steps as follows:

a) First load step:

-Obtain approximate solution
-1 equilibrium iteration per substep
-Number of substeps (5-15) is chosen

b) Second load step:

-Obtain converged solution
-Set number of equilibrium iteration (10-20)
-Set convergence tolerance (default value 0.001)

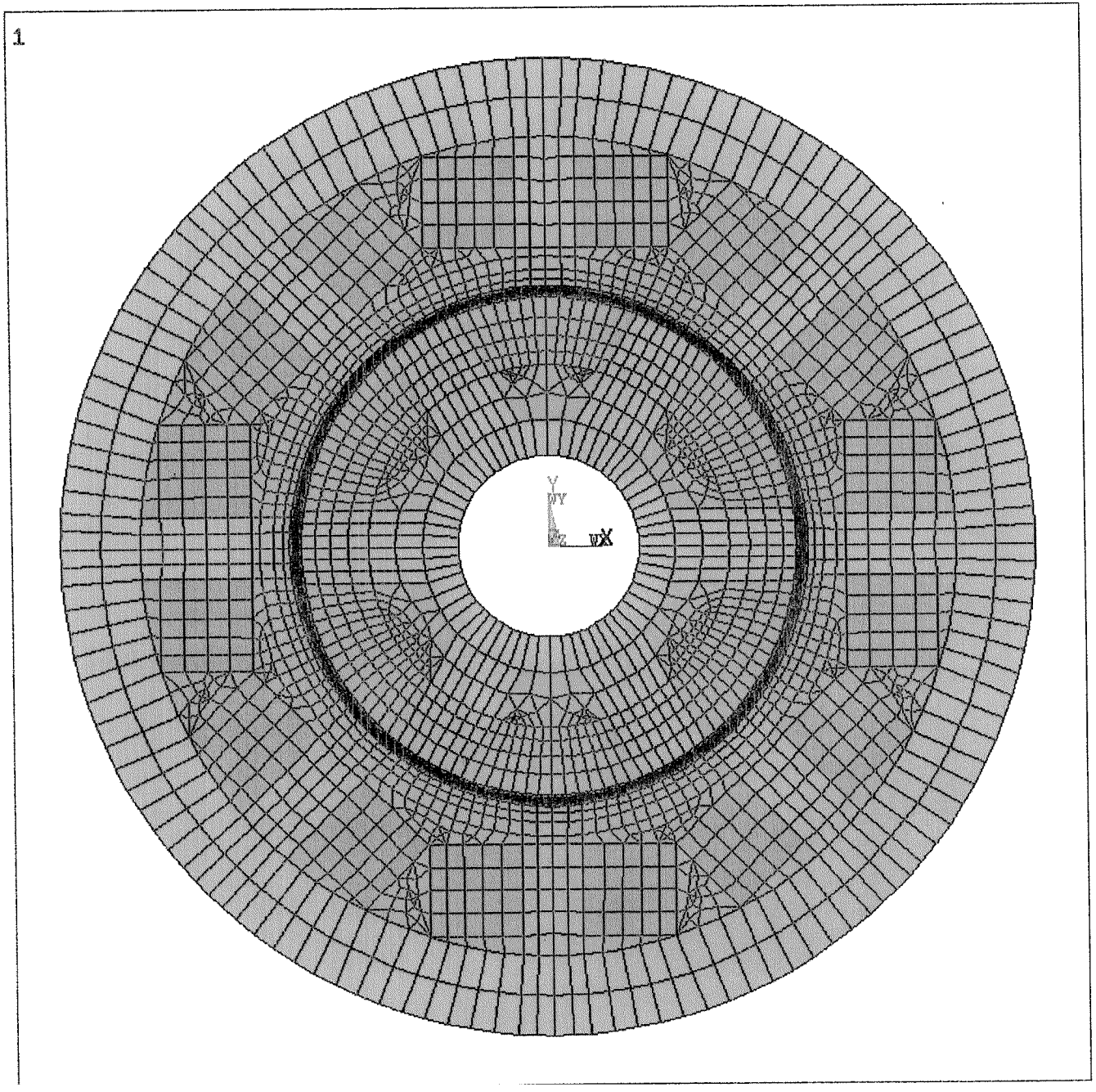

Fig.4.3. Mesh A, Mesh B, general distributic

Fig.4.4 Air gap region meshing for mesh

Fig.4.5. Air gap mesh distribution mesh B

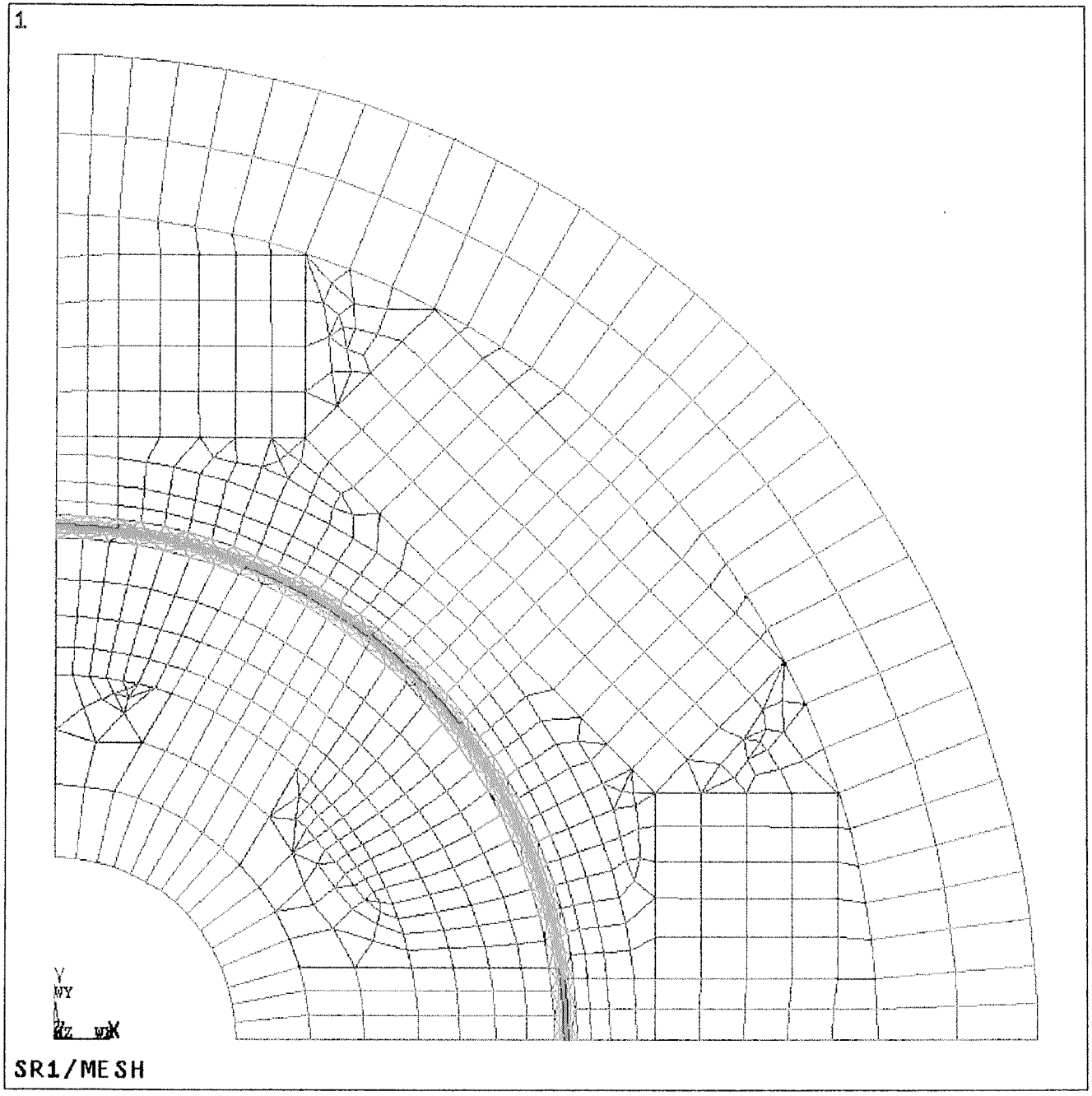

Fig. 4.6. Detail of mesh B

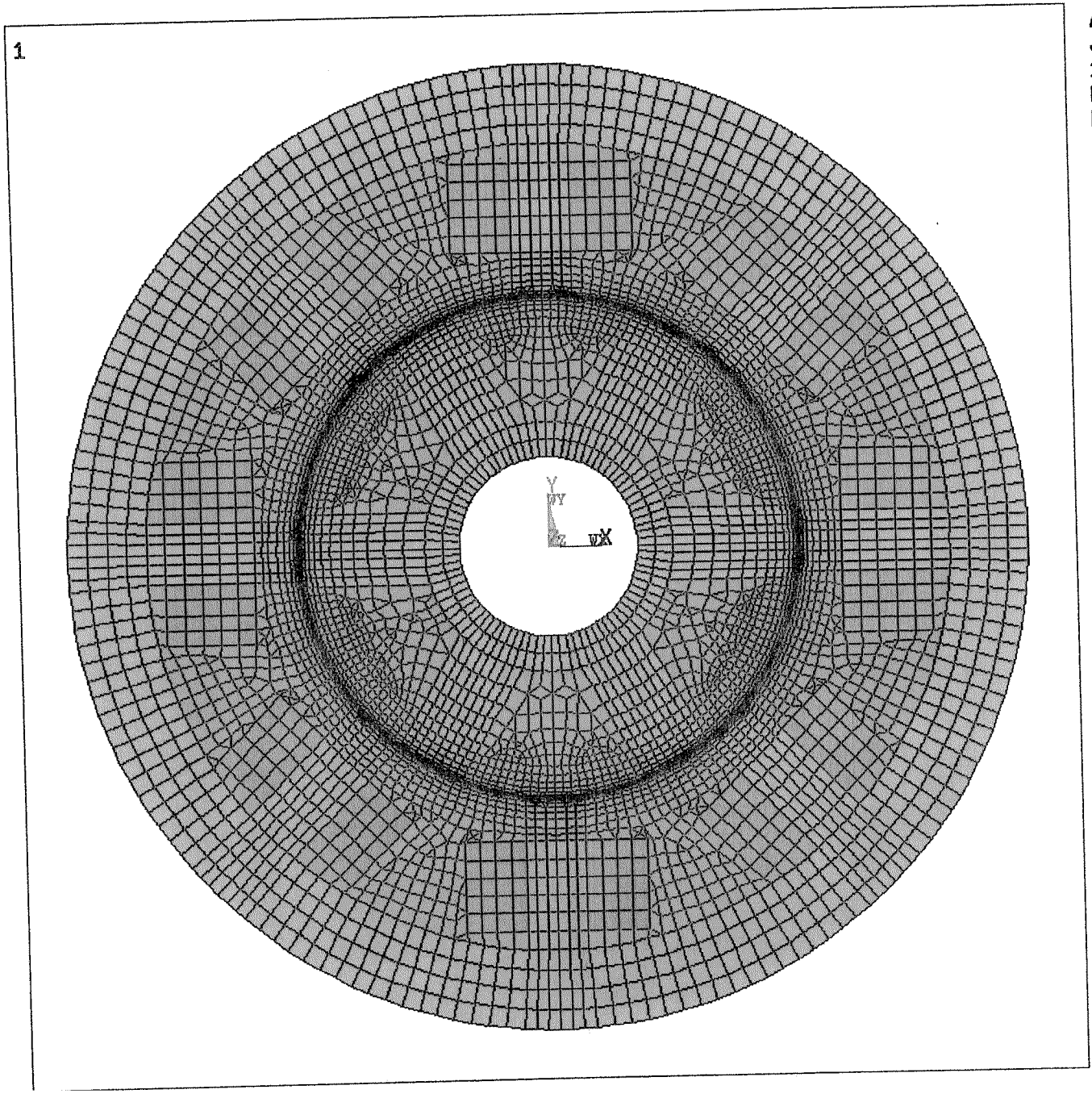

Fig.4.7. General distribution of Mesh C

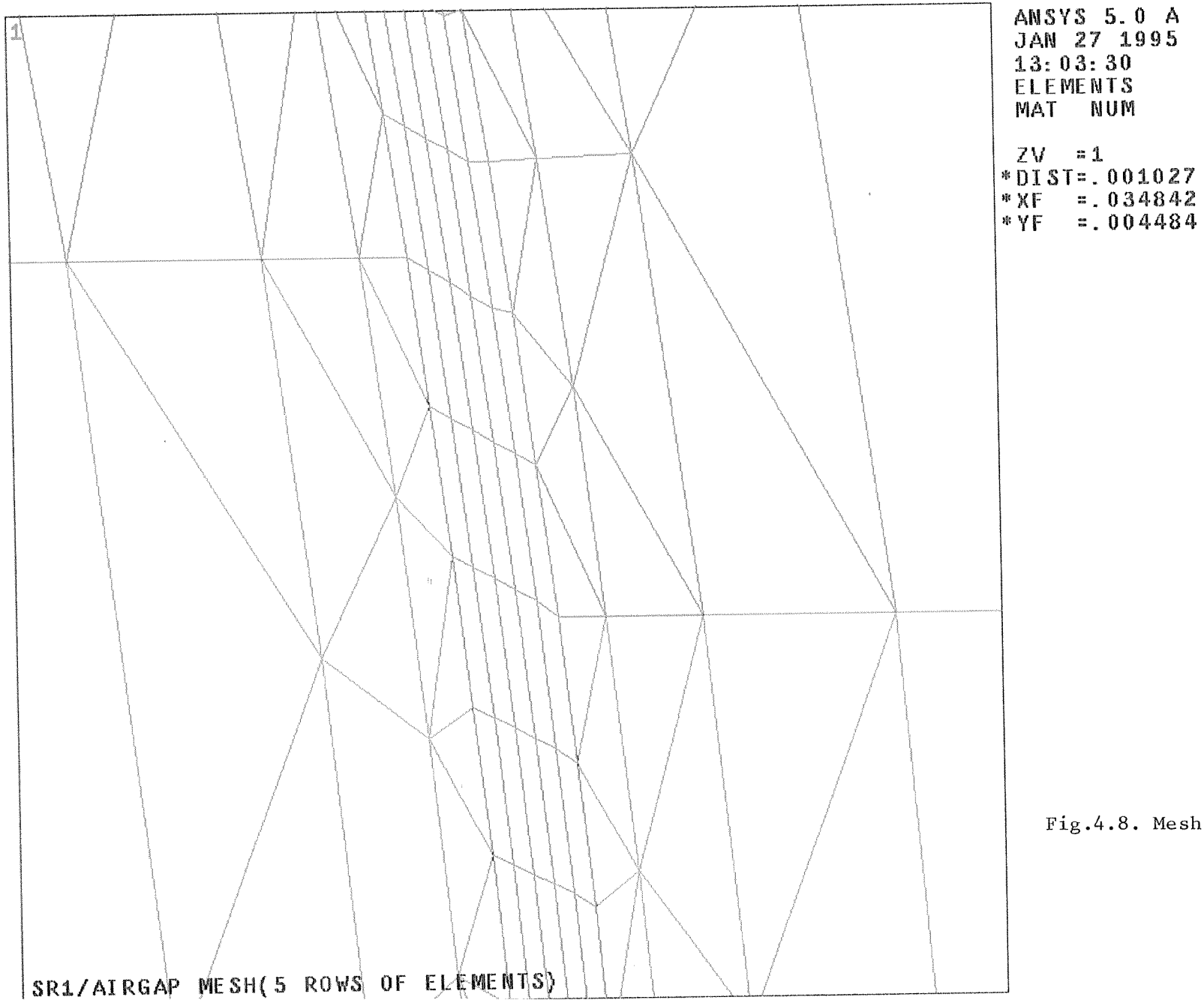

Fig.4.8. Mesh C air gap region

1) Delete constraint equations (stitching)CEDELE command

2) Select rotor nodes

3) Detach solid model

4) Rotate rotor nodes by a specified amont (NGEN-command)

5) Select rotor nodes and stator elements at the surface

6) Generate constraint equations (STITCHING)

7) Solution

4.1.5. Calculated Torque and Flux Linkage for SR1

Torque Prediction

The solution of the field is obtained for all three meshes described in section 4.11 and the static torque curve is computed from Maxwell Stresses, for 5 normalized position of the rotor teeth (see Section 4.1). The measured and computed torque characteristic of the motor (or one phase on excitation at phase current of 4A) is as shown in Fig 4.9 and 4.10 respectively, and is also tabulated in Table 4.1

From these figures it can be observed that the solution obtained for reduced number of meshes in the airgap is unacceptably inancurate (MESH B). However, Mesh A provided a very good accuracy of prediction. The error in predictions from mesh B is obviously due to insufficient number of elements in the ait gap (The rest of the mesh distribution for B is the same as mesh A)

NORMALIZED POSITION	MEASURED (I = 4A)	ANSYS (MESH A)	ANSYS (MESH B)
0.1	3.3	3.16	3.29
0.2	8.0	7.8	4.3
0.3	10.6	10.2	8.27
0.4	11.2	11.9	11.96
0.5	9.1	9.6	13.5

Table. 4.1 Predicted and measured torque for SR1 at various positions.

The solution obtained for MESC C is also found to give a similar accuracy to that obtained from Mesh C However, the computation time was 50% more in this case. For this reason Mesh A is used for further investigation.

The study in this section indicates that the number of meshes in the airgap is extremely important for obtaining acceptable accuracy and 3 rows of elements is highly recommended for the airgap region for an acceptable torque curve prediction.

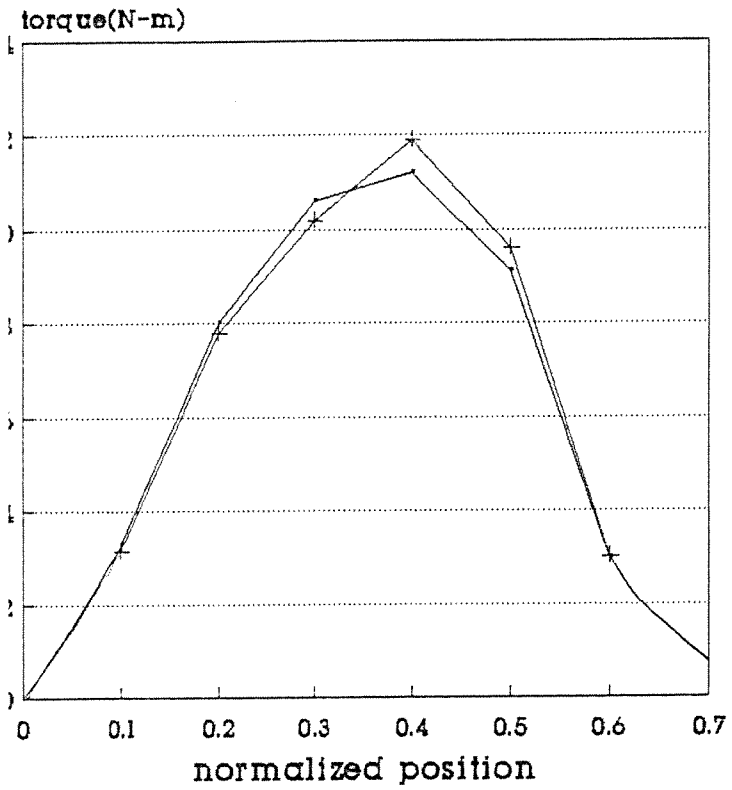

Fig. 4.9 Predicted and measured torque curve for SR1 (Mesh A)

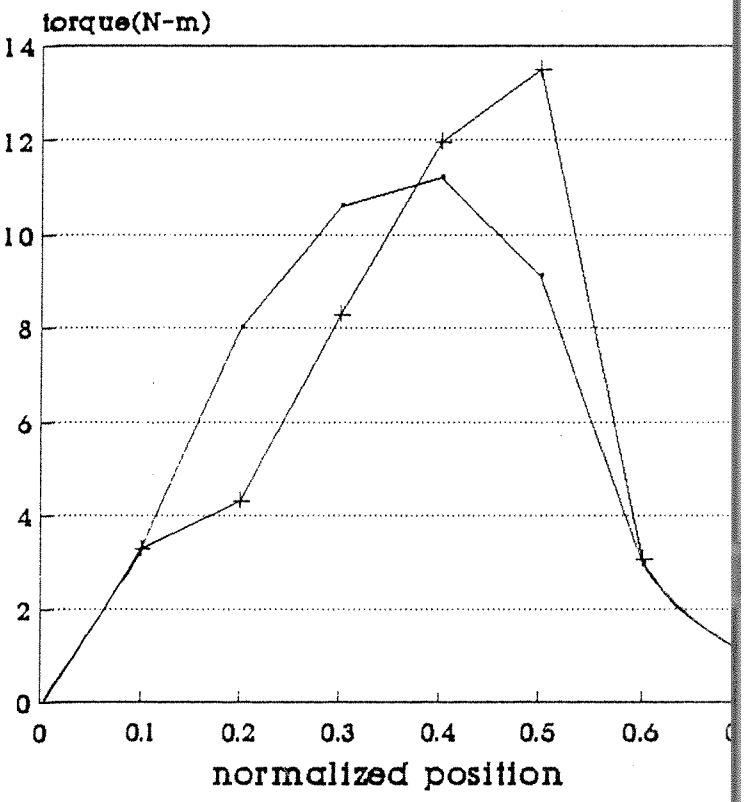

Fig. 4.10 Predicted and measured torque curve for SR1 (Mesh B)

Flux Linkage Prediction

Measured and computed flux linkage position curve is given for the test motor (in

one phase on mode at a phase current of 4A) for Mesh A and Mesh B in Table 2. and plotted in Fig 4.12. The method of flux linkage calculations is as described in section 4.2 Table 4.2 shows that flux linkage is not very sensitive to mesh distribution.

NORMALIZED POSITION	MEASURED (I=4A) weber	ANSYS (MESH A) weber	ANSYS (MESH B) weber
0	0.9	1.02	1.025
0.1	0.89	0.99	1.01
0.2	0.84	0.94	0.956
0.3	0.775	0.86	0.884
0.4	0.655	0.75	0.765
0.5	0.53	0.502	0.504
0.6	0.37	0.346	0.348

Table 4.2 measured and predicted flux linkage for SR1

Investigation of Fig. 4.11 displays a constant discrepancy between measured and computed flux linkage values. This is expectable since the end winding leakage which is independent of rotor position. However, this disprepancy seems to dissapear in normalized positions 0.5 and 0.6.This is likely to be due to a flux or position measurement error for these positions.

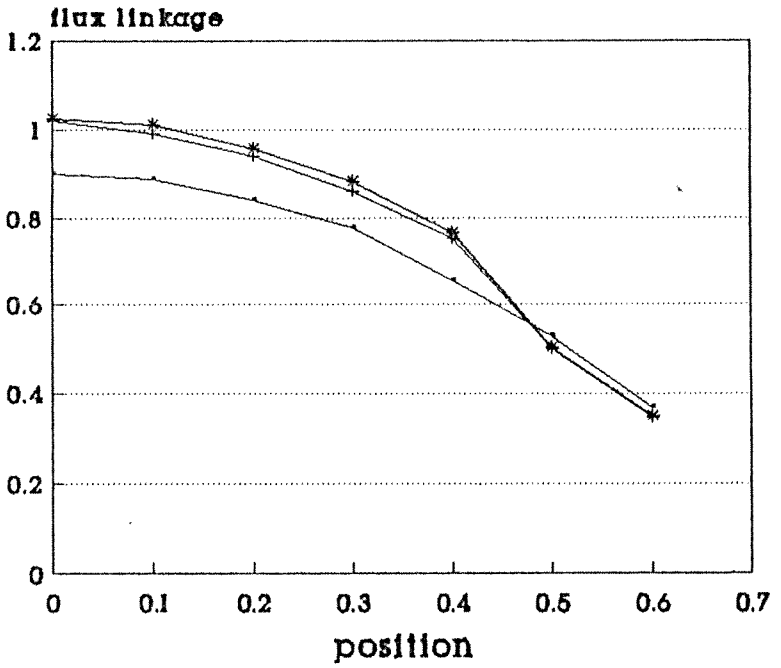

Fig 4.11 Measured and predicted flux linkage for two different meshes for SR1

This point howwever, is not pursued further since the purpose of the exercise at this stage was to gain experience with the field solution programme. In the next section the results obtained for the 2nd test motor (SR2) is givven. In this case the error sources are eliminated with the experience gained in this section and more accurate results are obtained.

4.2. TEST MOTOR 2 (SR2)

This motor is designed with the aid of the analysis optimization software described in section, and is manufactured by project funding.

DIMENSIONS OF THE MOTOR:

Outer diameter of rotor	:	38.6 mm
Outer diameter of stator	:	99.9 mm
Core length	:	40 mm
Backcore width	:	10.1 mm
Air gap length	:	0.255 mm
Stator pole width	:	8.2 mm
Rotor pole width	:	8.2 mm
Stator pole depth	:	30.395 mm
Rotor pole depth	:	7.2 mm
Number of turns	:	322
Rated Current	:	3 Ampere/pole
Wire size	:	0.7 mm

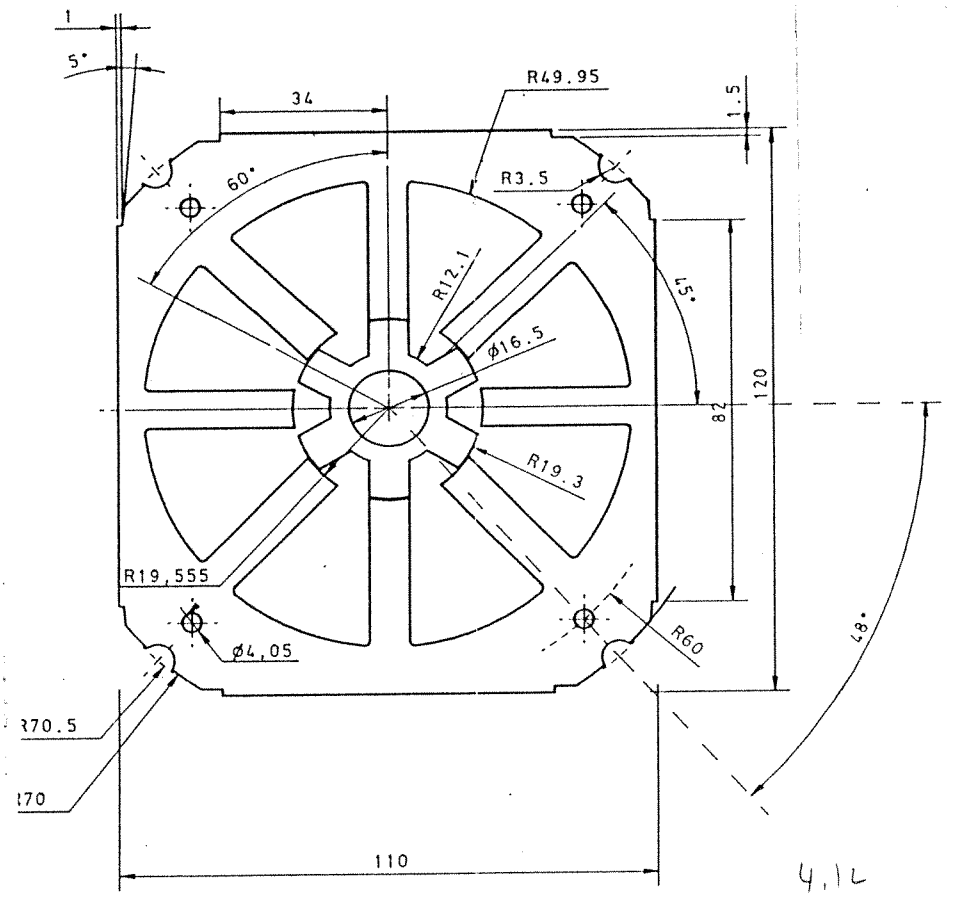

Fig. 4.12 Lamimation of SR2 Air Gap= 0.255mm Stack Length= 40mm

4.2.1. Measured Torque and Flux Linkage for SR2

As discussed in section 4. For SR1 the test data was already available. However, for SR2 torque and flux linkage measurements are made within the project work.

4.2.2. Torque Measurements

The test set up used for torque measurements is shown schematically in Fig. 4.14. The device designed is simple but effective. Fixing rod in the figure stops rotation of the shaft. One of the phases is excited, the rod on which micrometer rests (positioning arm) is set in a horisantal position. The motor is now in the IN position. Than the positioning arm in Fig 4.15 is adjusted with the aid of a screw until it deflects as much as desired. The new position of the rotor can be simply calculated as shown in Fig 4.16

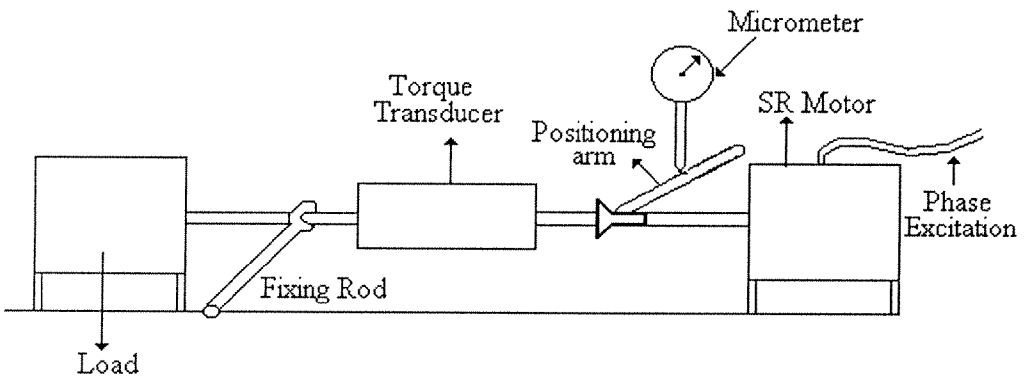

Fig. 4.14. The set-up for measuring static torque

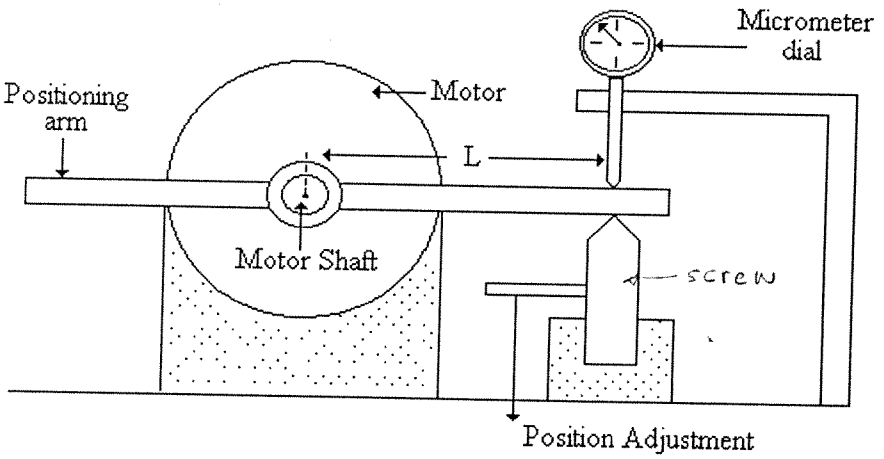

Fig. 4.15. Shaft positioning set-up for torque measurements. (A section of the set-up in Fig. 4.14.)

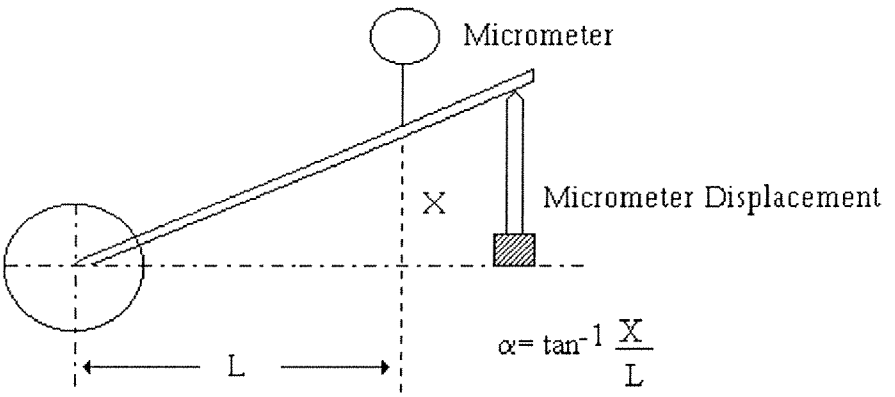

Fig.4.16

The reading of the torque transducer is then recorded and converted to torque at 1m if necessary. The torque transducer used in the tests here is

Brandname: SHC / Himmelstein Model: 24-02T(1-2)

Range: 100 lb-in (11.276 Nm) Max.speed. 15000 rpm

NORMALIZED POSITION	1A Torque (Nm)	2A Torque (Nm)	3A Torque (Nm)
0.1	0.36	0.52	0.61
0.2	0.40	0.72	0.92
0.3	0.41	0.88	1.20
0.4	0.43	1.06	1.50
0.5	0.49	1.16	1.75
0.6	0.45	1.14	1.88
0.7	0.45	1.12	1.85
0.8	0.37	0.91	1.71
0.9	0.20	0.36	0.58

Table 4.3 Measured and predicted torque values for SR2

The measured T-θ curve of this motor is given in Fig 4.17 and Table 4.3 for one phase on excitation at three different excitation levels.

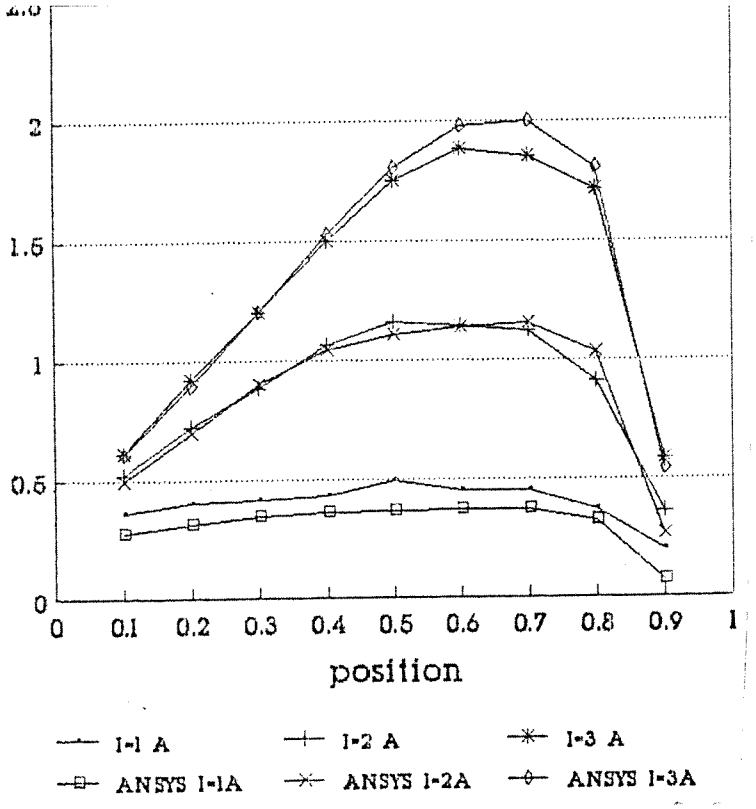

Fig. 4.17. Measured and predicted torque curve for SR2

4.2.3. Flux Linkage Measurement

For flux linkage measurements again the positioning device in Fig. 4.15 is used. For measurement of flux linkage a circuit proposed in reference 9 is used. This circuit is shown in Fig.4.18.

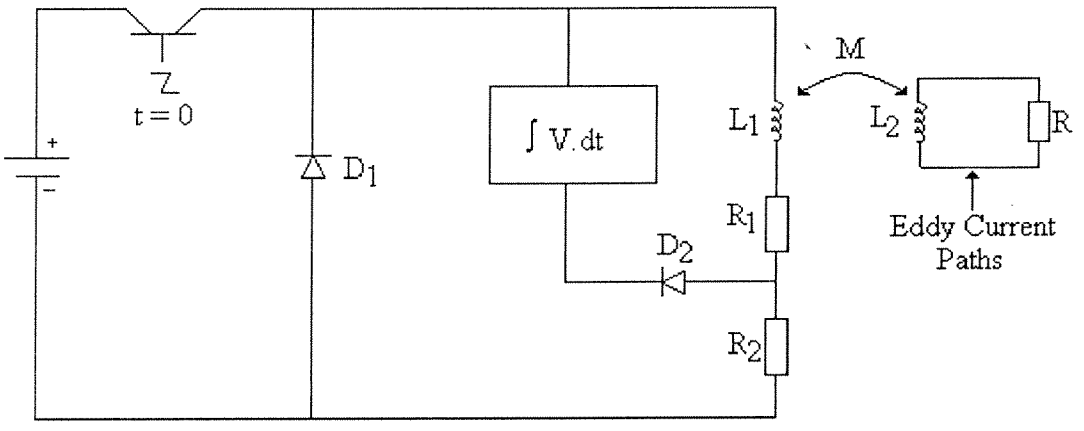

Fig. 4.18 The circuit for measurement of flux linkage

The transistor switch in the circuit was designed after a considerable amount of experimentation with mechanical switches. It is observed that mechanical switches fail to give satisfactory results because of bouncing problems.

The integrator is also very important for obtaining accurate results. Various devices were tested to find out their suitability as an integrator. Drift and noise in the signal received was found to be an important problem. To avoid noise a coaxial cable is used to carry the signal to the integrator

A Gould 1602 digital storage scope with integration facility was found to be most suitable device as integrator in this circuit.

When transitor in the circuit is turned on (manually by supplying its base here) current circulates through the loop formed by the phase coil, resistance R_2 and the champing diode. The indicated voltage-time integral in the figure can be found in terms of the circuit parameters

$$\int V.dt = -Li + Li\frac{R_1}{R_1 + R_2} \tag{11}$$

$$\psi = L\,I$$

$$\psi = -\frac{(R_1 + R_2)}{R_2}.\int V.dt \tag{12}$$

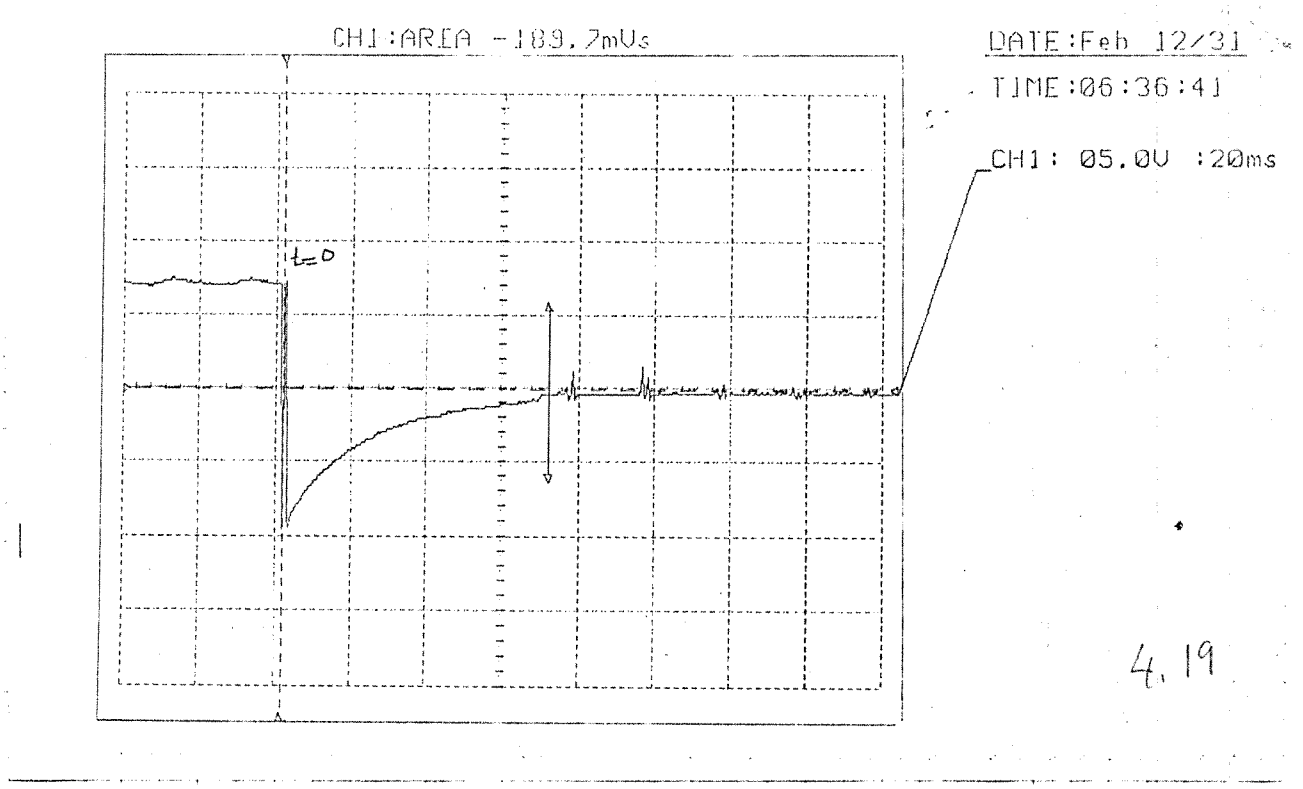

Fig. 4.19 The circuit for measurement of flux linkage: Typical integral signal

4.2.4. The Field Solution and the Mesh Distribution

In the light of the experience obtained in section 4.1.1 the mesh distribution shown in Fig. 4.20, 4.21 is generated. Note that to minimize the number of elements and obtain a reasonable accuracy, the mesh sizes along the pole are increased in a geometric sequence (g, 2g, 4g etc). Behind the poles automatic mesh generation facility was used due to the complex geometry.

Number of Elements 8704

Number of Nodes 7918

Type of Element: rectangular - triangular

rows of elements in air gap 3 (Fig 4.21)

solution accuracy 10^{-6}

5- SR2 MOTOR

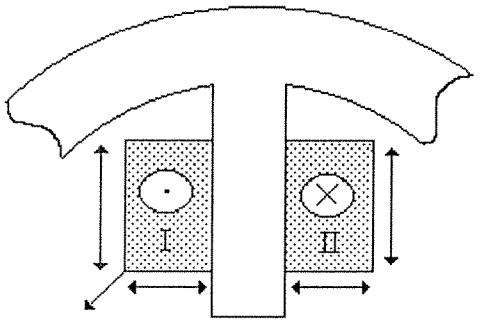

Coil Area = $1.12.10^{-4}$

For I = 1A		For I = 2A		For I = 3A	
I	J = N.I /Area J = (1.322) / $1.12.10^{-4}$ J = $2.8.10^{6}$ A/m^2	I	J = (2.322) / $1.12.10^{-4}$ J =$5.75.10^{6}$ A/m^2	I	J = (3.322) / $1.12.10^{-4}$ J = $8.6.10^{6}$A/m^2
II	J = $-2.8.10^{6}$ A/m^2	II	J =$-5.75.10^{6}$ A/m^2	II	J = $-8.6.10^{6}$ A/m^2

The field solution is obtained with this mesh for 9 different rotor positions at different excitation levels. The solution times are found to charge between 20-35 minutes. A typical solution result is shown in Fig 4.22, 4.23 for 1 phase on excitation at a phase current of 3A.

4.2.5 Comparison of Measured and Computed Torque-Position Curves.

Measured and computed static torque for SR2 are plotted in Fig. 4.17 against normalized position for three different excitation levels, and also tabulated in Table 4.3. The results display an extremely good agreement between measurements and computations. The error is largest for the low excitation level (1A). This is probably because the measured torque is less than 5% of the rating of the torque transducer. For the highest excitation levels (3A) ANSYS prediction gives about an 8% higher value for certain positions (0.6 and 0.7) than measured torque. This is an indication that the airgap size in the manufactured

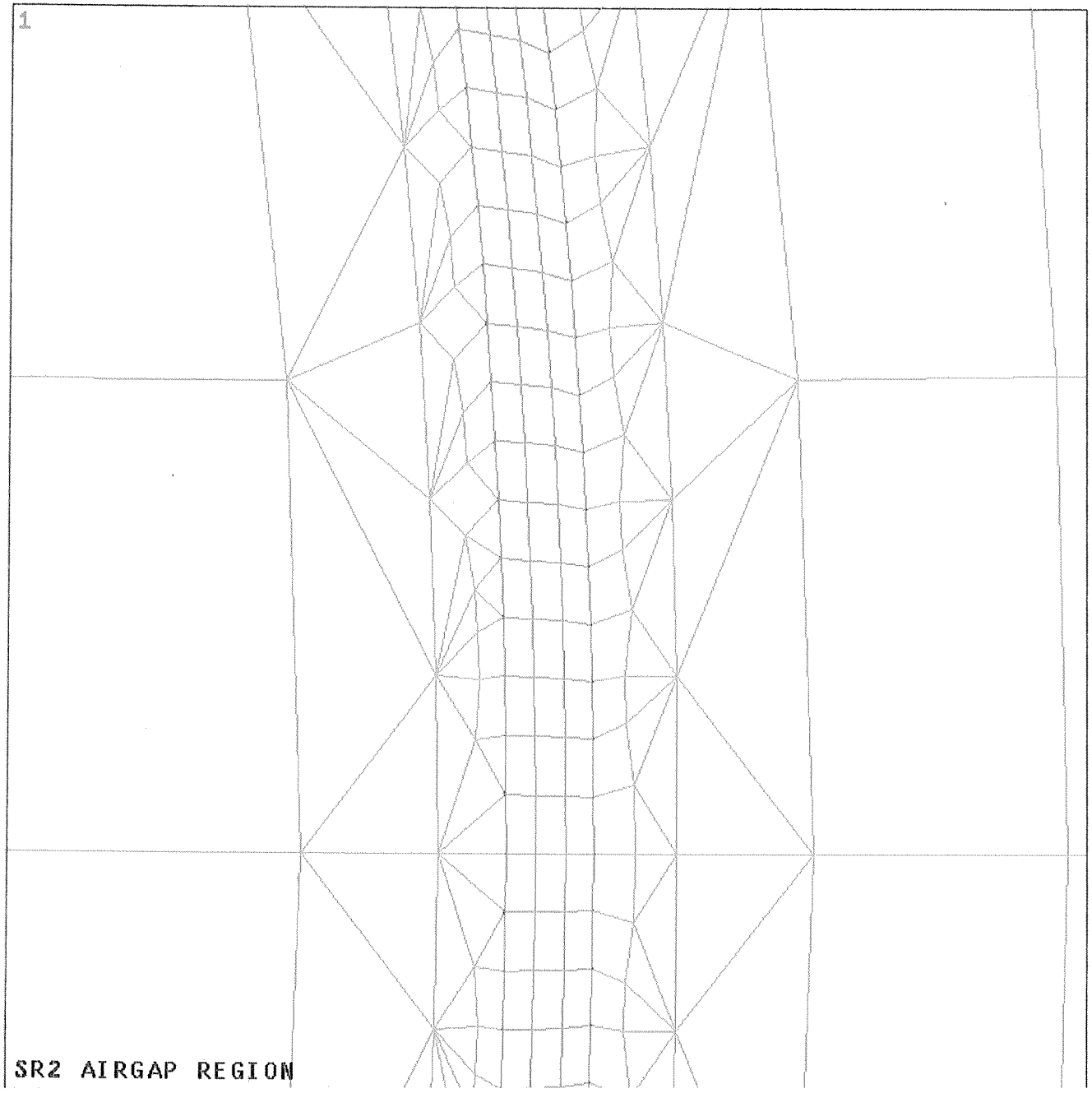

Fig.4.2I.Air gap region mesh distribution for SR2

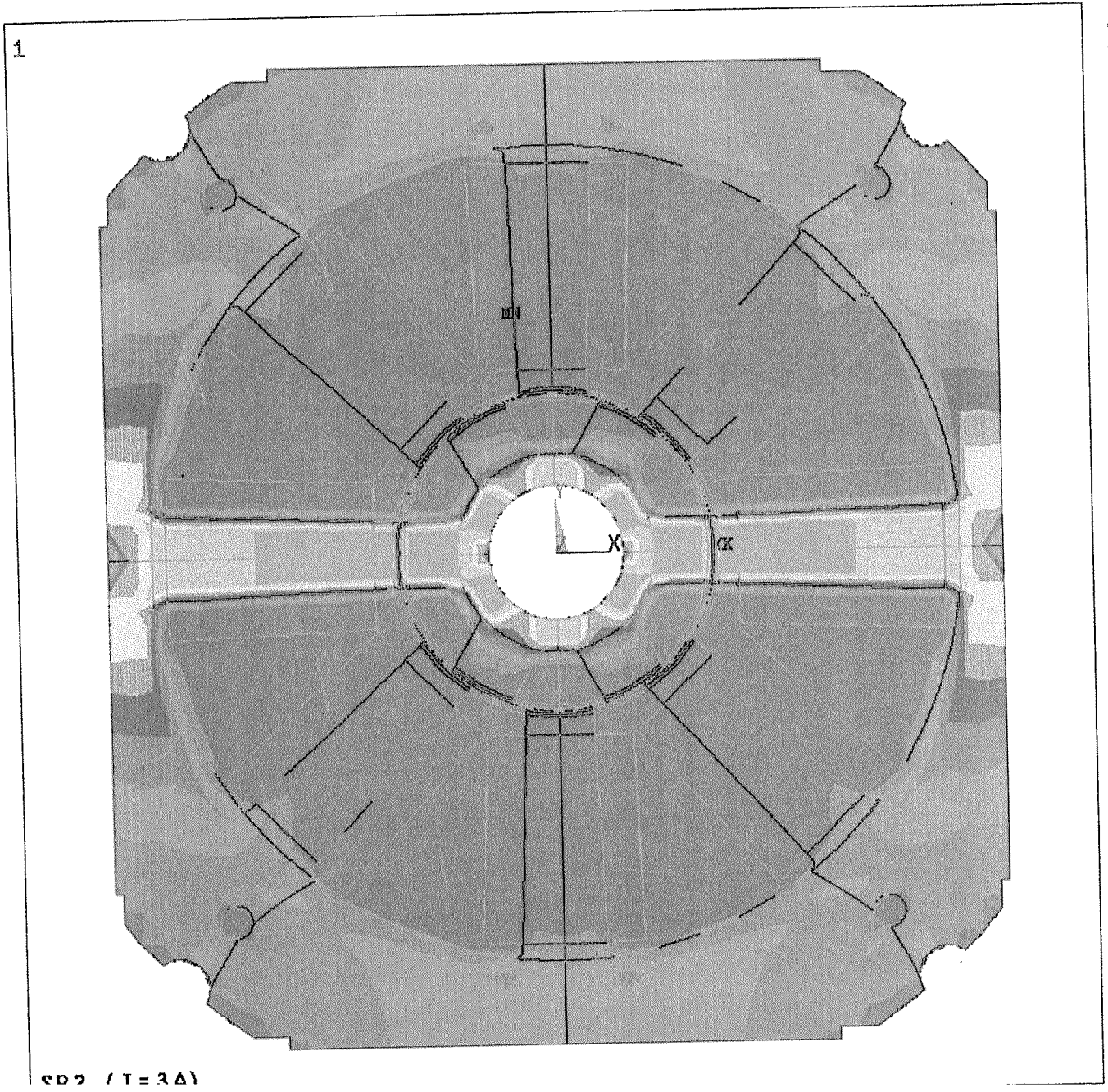

ANSYS 5.0
JAN 27 1994
09:48:58
PLOT NO. 1
NODAL SOLUTION
STEP=2
SUB =1
TIME=2
BSUM (AVG)
SMN =.107E-03
SMX =2.106

	.107E-03
	.234116
	.468124
	.702132
	.936141
	1.17
	1.404
	1.638
	1.872
	2.106

AREAS
MAT NUM

ZV =1
DIST=.066
PRECISE HIDDEN
EDGE

Fig. 4.22. Field distribution for SR2

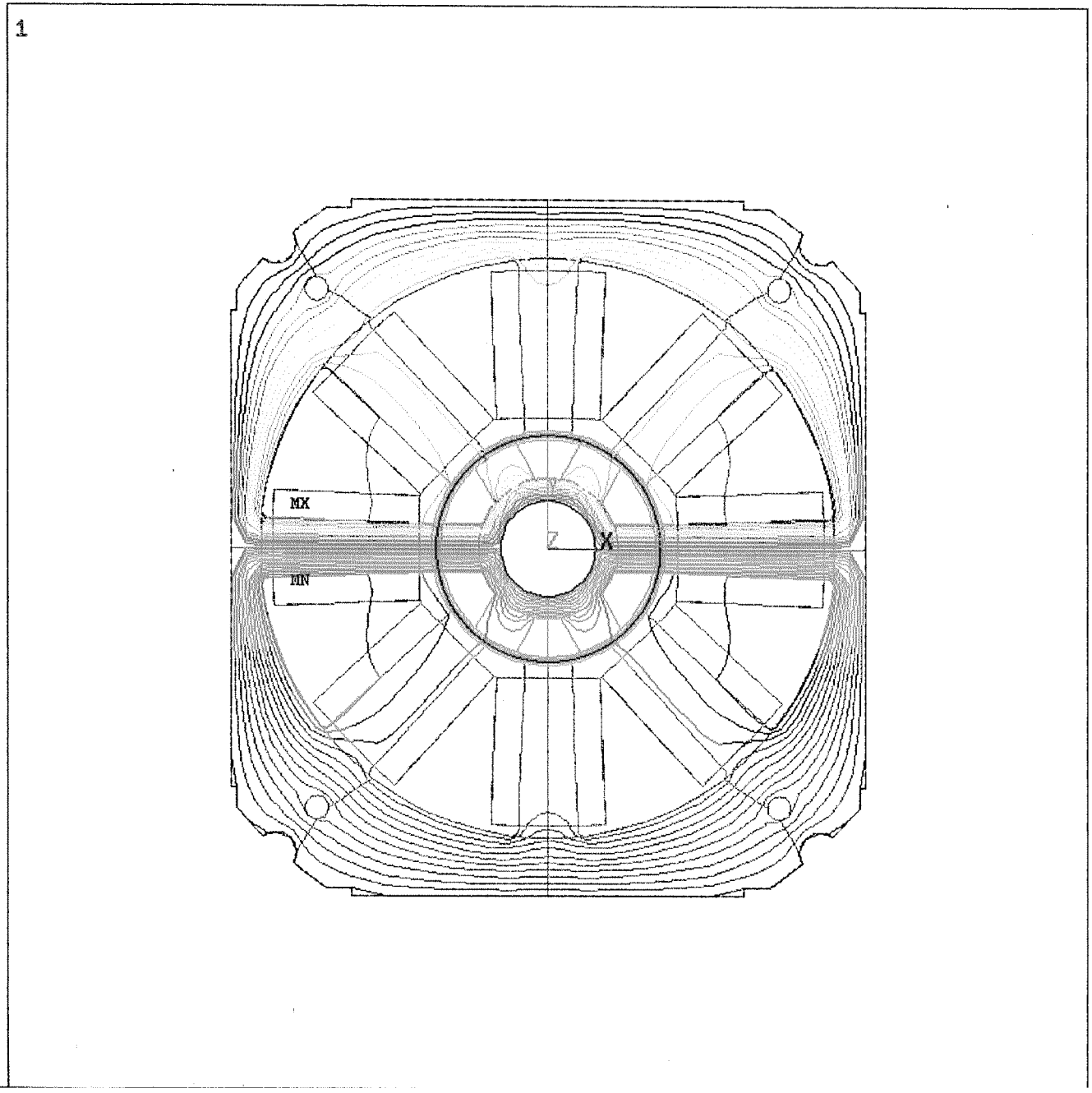

Fig.4.23. Field distribution for SR2

correspond to peak torque due to very small overlap and channeling of tooth flux to this region.

4.2.6. Comparison of Measured and Computed Flux Linkage

The flux linkages of the motor are measured for 8 different positions while the current changes from 0.5 to 3.5 A in 0.5 A steps.

The measured data is given in Table 4.4

POSITION	0.5 A	1 A	1.5 A	2 A	2.5 A	3 A	3.5 A
0.0	0.248	0.386	0.473	0.511	0.576	0.596	0.604
0.1	0.221	0.367	0.452	0.498	0.546	0.574	0.594
0.2	0.195	0.345	0.432	0.478	0.521	0.559	0.577
0.3	0.189	0.324	0.405	0.458	0.505	0.529	0.555
0.4	0.148	0.278	0.378	0.441	0.491	0.519	0.544
0.5	0.123	0.251	0.337	0.406	0.40	0.498	0.531
0.6	0.102	0.218	0.309	0.376	0.438	0.476	0.512
0.7	0.091	0.179	0.249	0.317	0.368	0.406	0.455
0.8	0.088	0.141	0.226	0.295	0.345	0.391	0.425
0.9	0.061	0.113	0.187	0.245	0.315	0.358	0.395

Table 4.5 Measured flux linkage for SR2

Measured and computed flux linkages for SR2 are plotted against position for three phase current values (1A, 2A, 3A) in Figure 4.25 Investigation of this figure show that the shape of the curve is well predicted for all current levels. However, as expected a constant

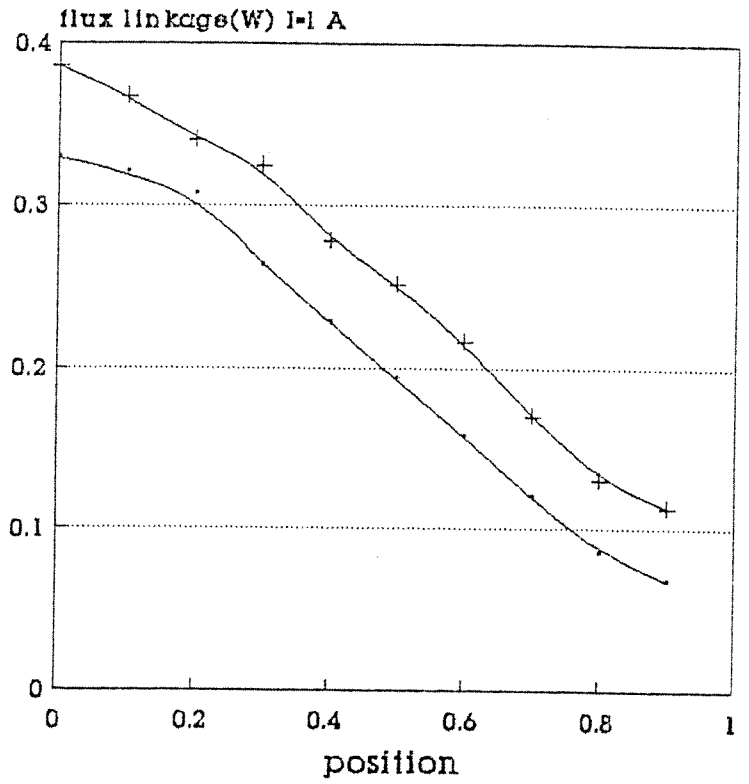

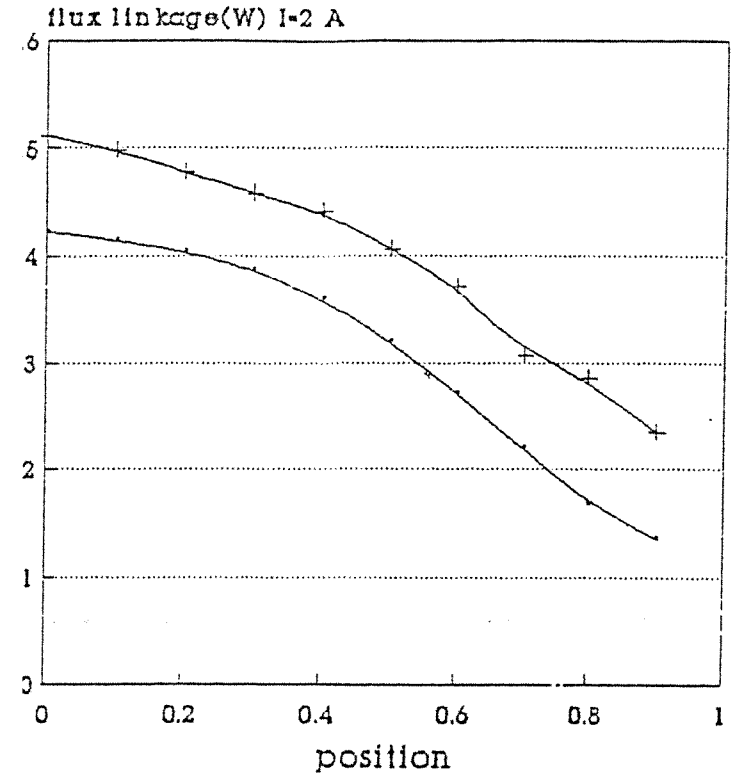

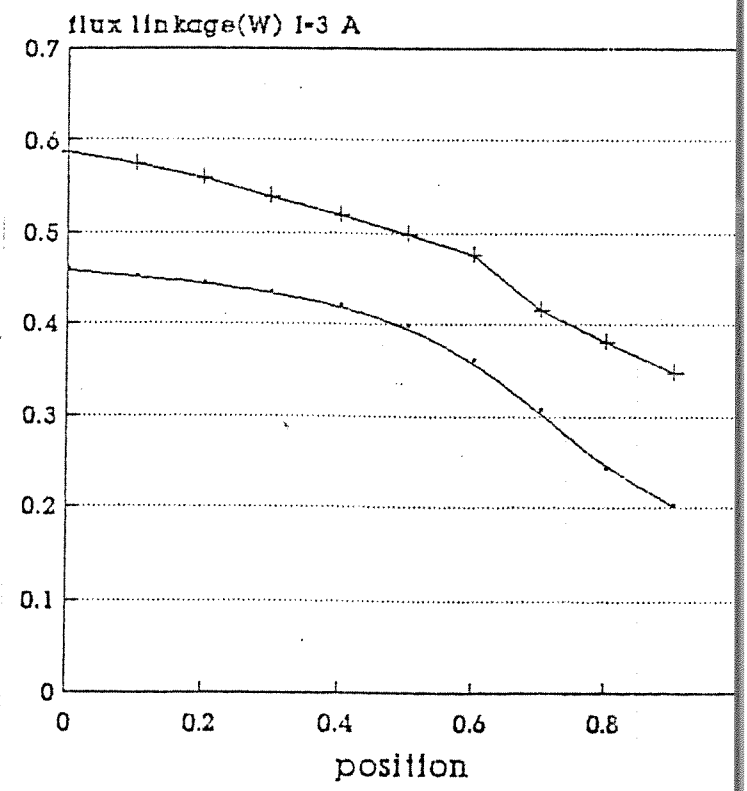

Fig. 4.25 a, b, c Measured and computed flux linkage for SR2

discrepancy exists between measurements and computations. This discrepancy is attributable to the end winding flux linkage which could not be taken into account in two dimensional field solutions. The fact that the magnitude of the discrepancy increases with current level supports this conclusion. It is possible to compute and account for and winding flux leakage if desired [10].

5. CONCLUSIONS:

The study in this part of this research project was aimed to familiarize with the use of professional magnetic field solution sorftware and gain the capability to use such software for design purposes of SR motors.

In the first part of this work, 'macro's are developed for the calculation of flux linkage, leakage flux and torque from the field solution. The effect of mesh distribution on solution accuracy and torque and flux linkage calculation is investigated. Rules are laid out for obtaining accurate results.

Field ssolution software is used for the prediction of torque-position and flux linkage-position curves of two different SR motors.

A set up is developed for measuring the torque and flux linkage characteristics of SR motors. When measured data is compared with computed torque curves the agreement is found to be very good.

Comparison of measured and computed flux linkage- position curves displayed that a constant discrepancy exists between measurements and predictions due to the end winding leakage which can not be taken into account in two dimensional field solutions.

However, it must be noted that often the difference in the area under the curves is required in performance computations and in that case the constant end winding leakage

plays no role. If necessary though the end winding leakage can be calculated using analytical and numerical techniques.

The study in this section clearly displayed that magnetic field solution technique and the routines developed for torque and flux linkage calculation are reliable and can be used to verify the performance of designs from the (design) software developed in this project.

In short an exteremely valuable experience is gained on the use of magnetic field solution software in this study.

REFERENCES:

1. Müjdat Tohumcu, **"Optimum Design of Switched Reluctance Motors"**, A Doctor of Philosophy Thesis, 1985

2. Necip Besenek , **"Numerically Calculated Force and Permeance Data for Doubly Salient Geometries",** Ms. Thesis

3. ANSYS - Theoretical Manual

4. ANSYS - Commands Manual

5. ANSYS - Magnetics Manual

6. ANSYS - Users Manual.

7. Moallem, M., Ong, C. M., **"Predicting the Torque of a Switched Reluctance Machine from its Finite Element Field Solution"** IEEE Transections on Energy Conversion, Vol. 5, No.4, December 1990, pp:733-739

8. Marinescu, M.,Marinescu, N.," **Numerical Computation of Torques in Permanent Magnet Motors by Maxwell Stresses and Energy Method"**. IEEE Transections on Magnetics, Vol. 24, No.1, January 1988, pp:463-466.

9. Mellitt, B., Rashid, M.,H. **"Voltage-Time Integral Method for Measuring Machine Inductance"** Proc. IEE, Vol.121, No.9, September 1974, pp:1016-1017

10. Corda J. Stephenson J.M. "**Analytical Estimation of the Maximum and Minimum Inductances of Doubly-Salient Motor**", Proc. of the International Conference on Stepping Motors and Systems, University of Leeds UK. pp 50-59 September 1979

A CONTROL STRATEGY FOR SPEED CONTROL OF S.R. MOTOR

Program Description:

The software that has been designed and implemented, consists of three parts, communicating with user, acceleration, constant speed. These parts are explained separately with their corresponding flowcharts. Before doing that a general explanation of the software is given first.

General Explanation:

The main aim of the software is to accelerate the motor to the desired speed and keep the motor running at that speed.

For this purpose the user enters the desired speed of the motor and the switch angle at which the motor accelerates. Moreover the user is asked to mention whether the overall time of running is limited or not. If limited then the user should enter the desired time of running which has been set up to 500 seconds presently.

The program accelerates the motor to the desired speed. This is done while comparing the speed of the motor with desired speed, each time when the software receives a feedback from the motor. The feedback is received when the rotor pole and stator pole are aligned where is called stable position. when the rotor reaches to the desired speed, constant pulses are applied to the motor phases.

Communicating With User:

Timer 2 is used as a baud rate generator with 2400 bits/sec. By using timer 2, characters are sent and received to and from Microcontroler. A PC can be used as terminal which is connected to the Evaluation board through port 2.

The speed should be entered in the digit form from 50 to 9990 rpm. The entered speeds should be a multiple of 10. The corresponding time period is found from a look up table. This restriction is because of look-up table managed in the program in which the time corresponding to the speeds from 50 to 9990 are saved. This time has been found from the relation T= 5/(2*N) . Where T is the time of completion of one step angle in sec and N is the speed of the motor in rpm.

While entering the switch angle, the number of switch angle should be entered, not itself. So that the integers from 1 to 9 are entered therefore the switch angle corresponding to these numbers would be selected.

If the time of running is limited then a multiple of 50 msec is entered which has been limited to be 9999 presently and this corresponds to 500 minutes. After this time elapse the software directs towards deceleration routine and motor stops.

Acceleration:

In the acceleration routine, first a phase of the motor is excited and this is followed by a one second pause. This is needed to assure that the motor always rotates in the desired direction.

As mentioned before for starting, constant pulses with a frequency below the starting/stopping region are given to the motor phases in the designed software the Frequency has been selected to be 20 steps/sec. The initial number of pulses are set to be three. But this number can easily be modified by changing the value of the register R0. After giving these pulses to the motor, the rotor accelerates therefore the PCA timer can be used for measuring the time between two stable position. So the next phase can be switched on with the corresponding switch angle. The motor accelerates with the entered switch angle and during this, the speed of the motor is compared with the operating speed entered with user each time that a step is traveled.

During the speed comparison, the time between two feedback's which corresponds to the time of the one step angle is compared with the corresponding time of the entered speed.

The time of the entered speed has been found from look-up table since the exact equivalence of these two time may not be possible, the comparison is done between 93.75% and 106.25% of the entered speed. These two bounded values are calculated at the end of the communicating with user section. The speed of the motor at the end of each step angle travel is checked to find out weather it is inside the mentioned range or not. If not acceleration goes on and the next pulse is given to the motor, if yes then the motor has approximately the speed of the desired speed so that the software jumps to constant speed part.

Constant Speed:

For keeping the speed of the motor at the desired speed, constant pulses of the same frequency as the desired speed frequency are applied to the motor phases. This is done by using timer 2 in the autoreload mode. So the time corresponding to the desired speed is loaded to timer 2 and when this time is passing one phase of the motor is being excited. After completion of the time, next phase starts excitation and is being excited until set time in timer 2 elapses again.

While giving constant frequency pulses to the motor phases, the speed of the motor is compared each time that a feed back is received. But at the beginning of the constant speed section, three pulses are applied to the motor without measuring the speed of the motor, this is done because the motor has not reached desired speed exactly. For this reason comparing the speed of the motor just after the first pulse in the constant speed section may give a wrong result.

In the duration where constant frequency (3) pulses are applied to the rotor manages itself to follow the constant pulses applied to motor phases. After this duration, the speed of the motor is compared with reference speed and if the motor is still in the mentioned range, applying constant pulses is continued. But if the speed of the motor has increased or decreased which might have been caused due to the variation of the load, the program directs to the Dec-Con or Acce-Con routines respectively. Before directing to these routines the reference switch angle should be obtained, which are used in the above routines to control the speed. This is done by measuring the time of timer 2 from the last feedback up to it's overflow. This time is measured by timer 1 reloaded to data memory.

Routines and Interrupts:

In the section the routines and interrupts are explained.

PUT-CHAR: Will send a single character to the terminal

GET-CHAR: Will receive a single character from the terminal

PUT-CRLF: Will send carriage return and line feed.

PUT-STRING: Will strings to the terminal. Strings are saved in the memory and the address of the first character of the string is in the DPTR register.

GET-NUM: Will read a BCD number up to 4 digits from the terminal. Digits are located one by one in the data memory. The start location is addressed by the contents of the R0 register. But it should be noted that the number of the digits are saved in the location addressed by the contents of the R0 and digits themselves are saved in the successives locations.

GET-BINNUM: Will convert the entered BCD number to the binary number and output the binary number through the locations named as OUTBINH & OUTBINL.

FIND-TIME: Will output the time found from the look-up table, through TREFH & TREFL

LOCATION: Will find the time from the look up table.

TIMERO-INT: Will increment a 16- bits register named as COPMH & COPML and compare this register with LIMTIMEH & LIMTIMEL register which content is the total time of running. When these two 16-bits registers become equal then the routine changes the interrupted address saved in the stak. And load the address 4040 H where the program jumps to the deceleration routine.

PCA-INT: Will output the time between two positive transition events which in our case are the feedback's taken from the stable positions of the motor. The found time is output through CAPTUREH & CAPTUREL.

COMPARE: Will compare the 16-bits value found in the PCA-INT with two 16-bits registers named as LTREFH & LTREFL and HTREFH & HTRFL respectively. Some flags are set up after comparing. If the 16-bits value is greater than HTREFH & HTREFL then the speed is below the desired range and the BELOW flag is set acceleration goes on. If it is less than HTREFH & HTREFL then it is compared with LTREFH & LTREFL and if it is greater than this value then the speed is inside the desired range so the MIDDLE flag is set. And the program jumps to constant speed section. If it is also less than LTREFH & LTREFL so the speed of the motor is the out off the desired range and the ABOVE flag is set. The speed should be brought to the desired range. This is done by using DEC1.

SW-ANG: Will find the required time which should be elapsed for switching the next phase. The time found from the PCA-INT which corresponds to the time between two stable position, is devided by 8. this is done by using the shift instruction three times. The devided value then is multiplied by the entered number of the switching angle and the multiplied value is loaded to the timer 1's registers TH1 &TL1.

STEP-COMMAND: Will send pulses to the port 1pins 4, 5, 6, 7 are corresponded to the transistors 1, 2, 3, 4 respectively Value 0 turns on transistor and value 1 turns off transistors. The corresponding pulses for turning on the next phase are saved in the register POSITION. Before sending pulses through port 1, the high nibble value of the accumulator is masked. This should be done because pin 3 of the port 1 is used as an input to the microcontroler. This input comes from the encoder connected to the motor and encoder sends the feedback taken from the stable position.

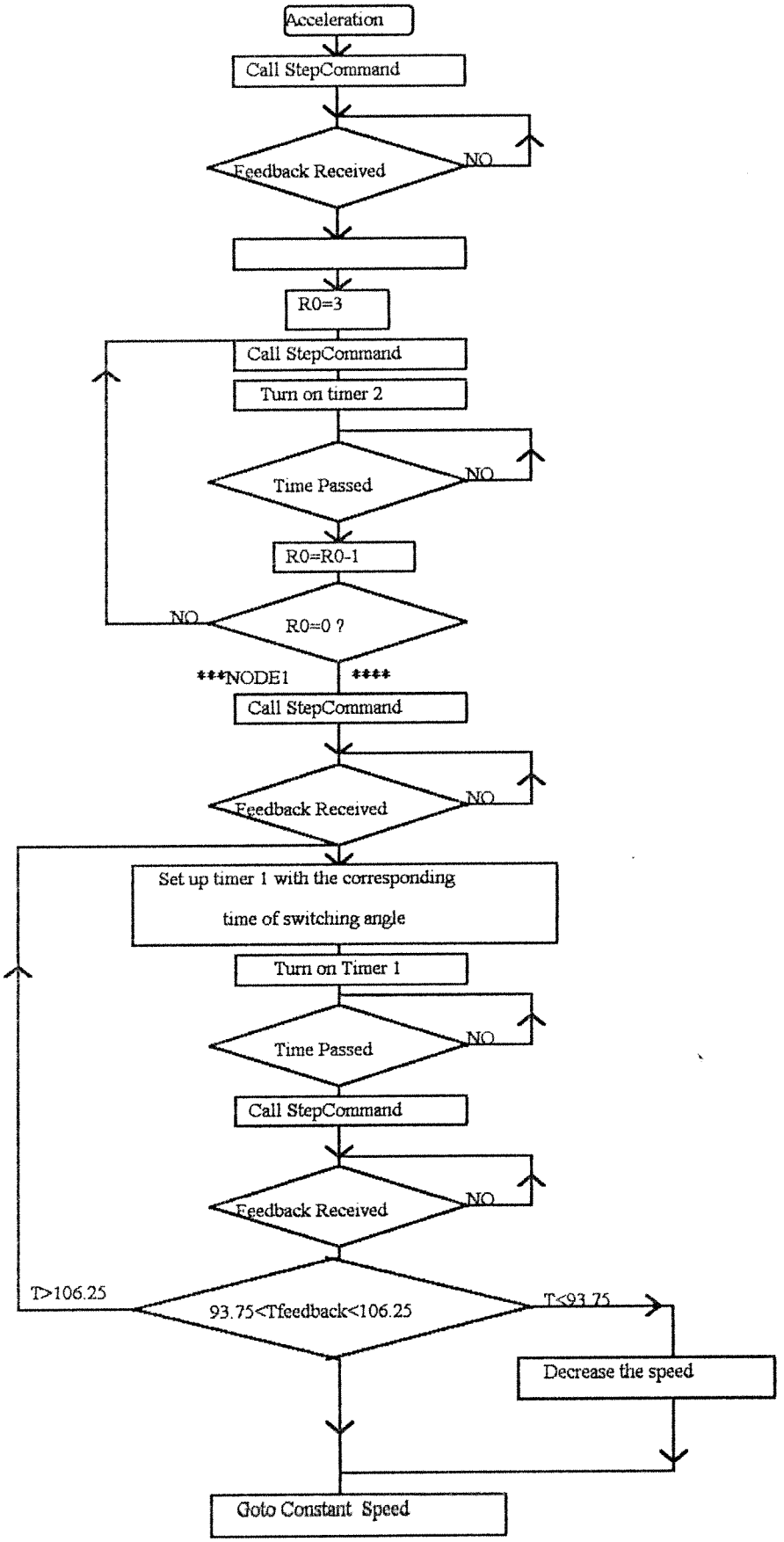
Acceleration
Call StepCommand
Feedback Received
NO
R0=3
Call StepCommand
Turn on timer 2
Time Passed
NO
R0=R0-1
NO
R0=0 ?
***NODE1
****
Call StepCommand
Feedback Received
NO
Set up timer 1 with the corresponding
time of switching angle
Turn on Timer 1
Time Passed
NO
Call StepCommand
Feedback Received
NO
T>106.25
93.75<Tfeedback<106.25
T<93.75
Decrease the speed
Goto Constant Speed

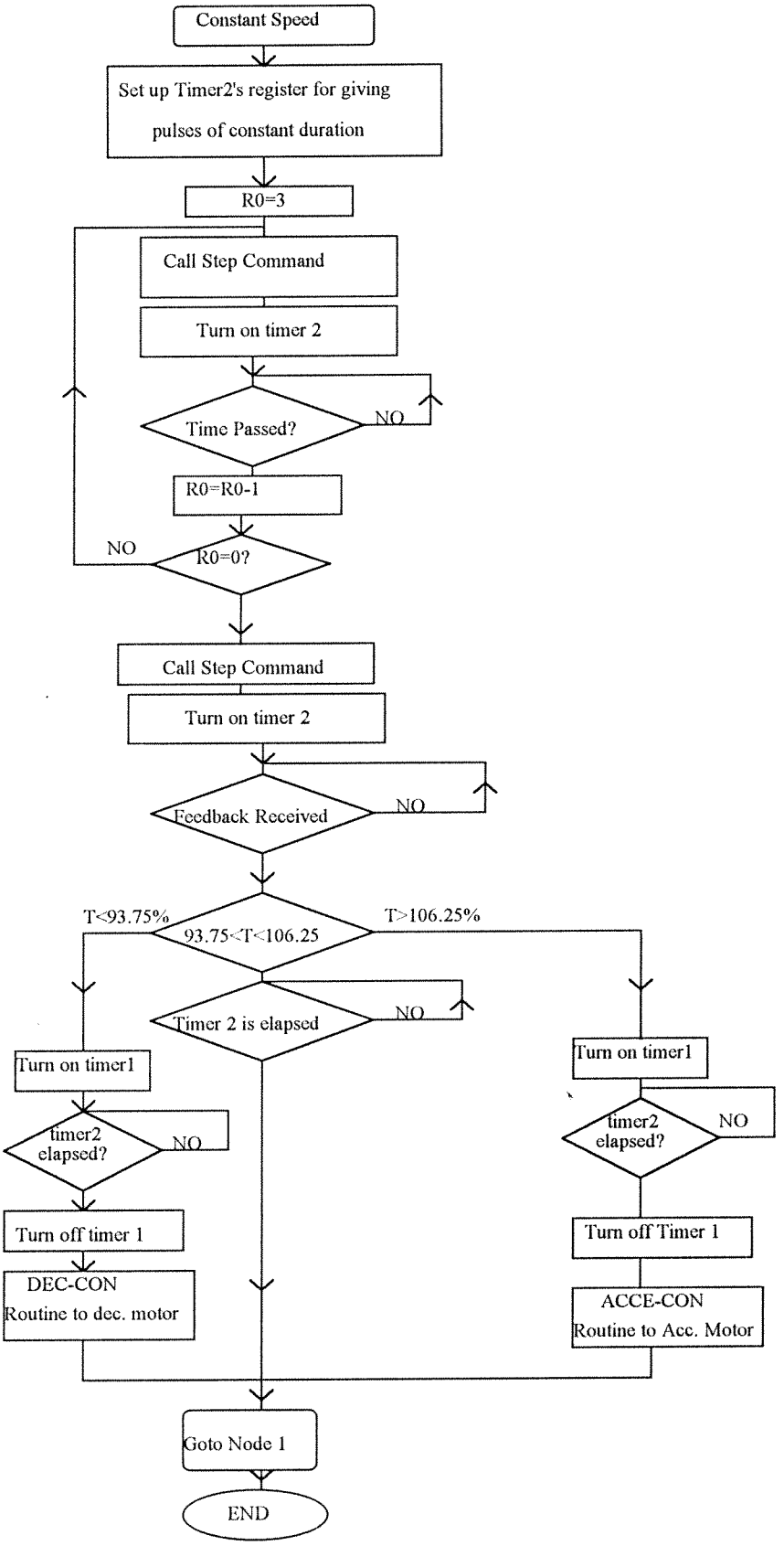
Constant Speed
Set up Timer2's register for giving pulses of constant duration
R0=3
Call Step Command
Turn on timer 2
Time Passed?
NO
R0=R0-1
NO
R0=0?
Call Step Command
Turn on timer 2
Feedback Received
NO
T<93.75%
93.75<T<106.25
T>106.25%
Timer 2 is elapsed
NO
Turn on timer1
timer2 elapsed?
NO
Turn off timer 1
DEC-CON
Routine to dec. motor
Turn on timer1
timer2 elapsed?
NO
Turn off Timer 1
ACCE-CON
Routine to Acc. Motor
Goto Node 1
END

EK 6

Hız Kontrolü Yazılımı

A CONTROL STRATEGY FOR SPEED CONTROL OF S.R. MOTOR

Program Description:

The software that has been designed and implemented, consists of three parts, communicating with user, acceleration, constant speed. These parts are explained separately with their corresponding flowcharts. Before doing that a general explanation of the software is given first.

General Explanation:

The main aim of the software is to accelerate the motor to the desired speed and keep the motor running at that speed.

For this purpose the user enters the desired speed of the motor and the switch angle at which the motor accelerates. Moreover the user is asked to mention whether the overall time of running is limited or not. If limited then the user should enter the desired time of running which has been set up to 500 seconds presently.

The program accelerates the motor to the desired speed. This is done while comparing the speed of the motor with desired speed, each time when the software receives a feedback from the motor. The feedback is received when the rotor pole and stator pole are aligned where is called stable position. when the rotor reaches to the desired speed, constant pulses are applied to the motor phases.

Communicating With User:

Timer 2 is used as a baud rate generator with 2400 bits/sec. By using timer 2, characters are sent and received to and from Microcontroler. A PC can be used as terminal which is connected to the Evaluation board through port 2.

The speed should be entered in the digit form from 50 to 9990 rpm. The entered speeds should be a multiple of 10. The corresponding time period is found from a look up table. This restriction is because of look-up table managed in the program in which the time corresponding to the speeds from 50 to 9990 are saved. This time has been found from the relation T= 5/(2*N) . Where T is the time of completion of one step angle in sec and N is the speed of the motor in rpm.

While entering the switch angle, the number of switch angle should be entered, not itself. So that the integers from 1 to 9 are entered therefore the switch angle corresponding to these numbers would be selected.

If the time of running is limited then a multiple of 50 msec is entered which has been limited to be 9999 presently and this corresponds to 500 minutes. After this time elapse the software directs towards deceleration routine and motor stops.

Acceleration:

In the acceleration routine, first a phase of the motor is excited and this is followed by a one second pause. This is needed to assure that the motor always rotates in the desired direction.

As mentioned before for starting, constant pulses with a frequency below the starting/stopping region are given to the motor phases in the designed software the Frequency has been selected to be 20 steps/sec. The initial number of pulses are set to be three. But this number can easily be modified by changing the value of the register R0. After giving these pulses to the motor, the rotor accelerates therefore the PCA timer can be used for measuring the time between two stable position. So the next phase can be switched on with the corresponding switch angle. The motor accelerates with the entered switch angle and during this, the speed of the motor is compared with the operating speed entered with user each time that a step is traveled.

During the speed comparison, the time between two feedback's which corresponds to the time of the one step angle is compared with the corresponding time of the entered speed.

The time of the entered speed has been found from look-up table since the exact equivalence of these two time may not be possible, the comparison is done between 93.75% and 106.25% of the entered speed. These two bounded values are calculated at the end of the communicating with user section. The speed of the motor at the end of each step angle travel is checked to find out weather it is inside the mentioned range or not. If not acceleration goes on and the next pulse is given to the motor, if yes then the motor has approximately the speed of the desired speed so that the software jumps to constant speed part.

Constant Speed:

For keeping the speed of the motor at the desired speed, constant pulses of the same frequency as the desired speed frequency are applied to the motor phases. This is done by using timer 2 in the autoreload mode. So the time corresponding to the desired speed is loaded to timer 2 and when this time is passing one phase of the motor is being excited. After completion of the time, next phase starts excitation and is being excited until set time in timer 2 elapses again.

While giving constant frequency pulses to the motor phases, the speed of the motor is compared each time that a feed back is received. But at the beginning of the constant speed section, three pulses are applied to the motor without measuring the speed of the motor, this is done because the motor has not reached desired speed exactly. For this reason comparing the speed of the motor just after the first pulse in the constant speed section may give a wrong result.

In the duration where constant frequency (3) pulses are applied to the rotor manages itself to follow the constant pulses applied to motor phases. After this duration, the speed of the motor is compared with reference speed and if the motor is still in the mentioned range, applying constant pulses is continued. But if the speed of the motor has increased or decreased which might have been caused due to the variation of the load, the program directs to the Dec-Con or Acce-Con routines respectively. Before directing to these routines the reference switch angle should be obtained, which are used in the above routines to control the speed. This is done by measuring the time of timer 2 from the last feedback up to it's overflow. This time is measured by timer 1 reloaded to data memory.

Routines and Interrupts:

In the section the routines and interrupts are explained.

PUT-CHAR: Will send a single character to the terminal

GET-CHAR: Will receive a single character from the terminal

PUT-CRLF: Will send carriage return and line feed.

PUT-STRING: Will strings to the terminal. Strings are saved in the memory and the address of the first character of the string is in the DPTR register.

GET-NUM: Will read a BCD number up to 4 digits from the terminal. Digits are located one by one in the data memory. The start location is addressed by the contents of the R0 register. But it should be noted that the number of the digits are saved in the location addressed by the contents of the R0 and digits themselves are saved in the successives locations.

GET-BINNUM: Will convert the entered BCD number to the binary number and output the binary number through the locations named as OUTBINH & OUTBINL.

FIND-TIME: Will output the time found from the look-up table, through TREFH & TREFL

LOCATION: Will find the time from the look up table.

TIMERO-INT: Will increment a 16- bits register named as COPMH & COPML and compare this register with LIMTIMEH & LIMTIMEL register which content is the total time of running. When these two 16-bits registers become equal then the routine changes the interrupted address saved in the stak. And load the address 4040 H where the program jumps to the deceleration routine.

PCA-INT: Will output the time between two positive transition events which in our case are the feedback's taken from the stable positions of the motor. The found time is output through CAPTUREH & CAPTUREL.

COMPARE: Will compare the 16-bits value found in the PCA-INT with two 16-bits registers named as LTREFH & LTREFL and HTREFH & HTRFL respectively. Some flags are set up after comparing. If the 16-bits value is greater than HTREFH & HTREFL then the speed is below the desired range and the BELOW flag is set acceleration goes on. If it is less than HTREFH & HTREFL then it is compared with LTREFH & LTREFL and if it is greater than this value then the speed is inside the desired range so the MIDDLE flag is set. And the program jumps to constant speed section. If it is also less than LTREFH & LTREFL so the speed of the motor is the out off the desired range and the ABOVE flag is set. The speed should be brought to the desired range. This is done by using DEC1.

SW-ANG: Will find the required time which should be elapsed for switching the next phase. The time found from the PCA-INT which corresponds to the time between two stable position, is devided by 8. this is done by using the shift instruction three times. The devided value then is multiplied by the entered number of the switching angle and the multiplied value is loaded to the timer 1's registers TH1 &TL1.

STEP-COMMAND: Will send pulses to the port 1pins 4, 5, 6, 7 are corresponded to the transistors 1, 2, 3, 4 respectively Value 0 turns on transistor and value 1 turns off transistors. The corresponding pulses for turning on the next phase are saved in the register POSITION. Before sending pulses through port 1, the high nibble value of the accumulator is masked. This should be done because pin 3 of the port 1 is used as an input to the microcontroler. This input comes from the encoder connected to the motor and encoder sends the feedback taken from the stable position.

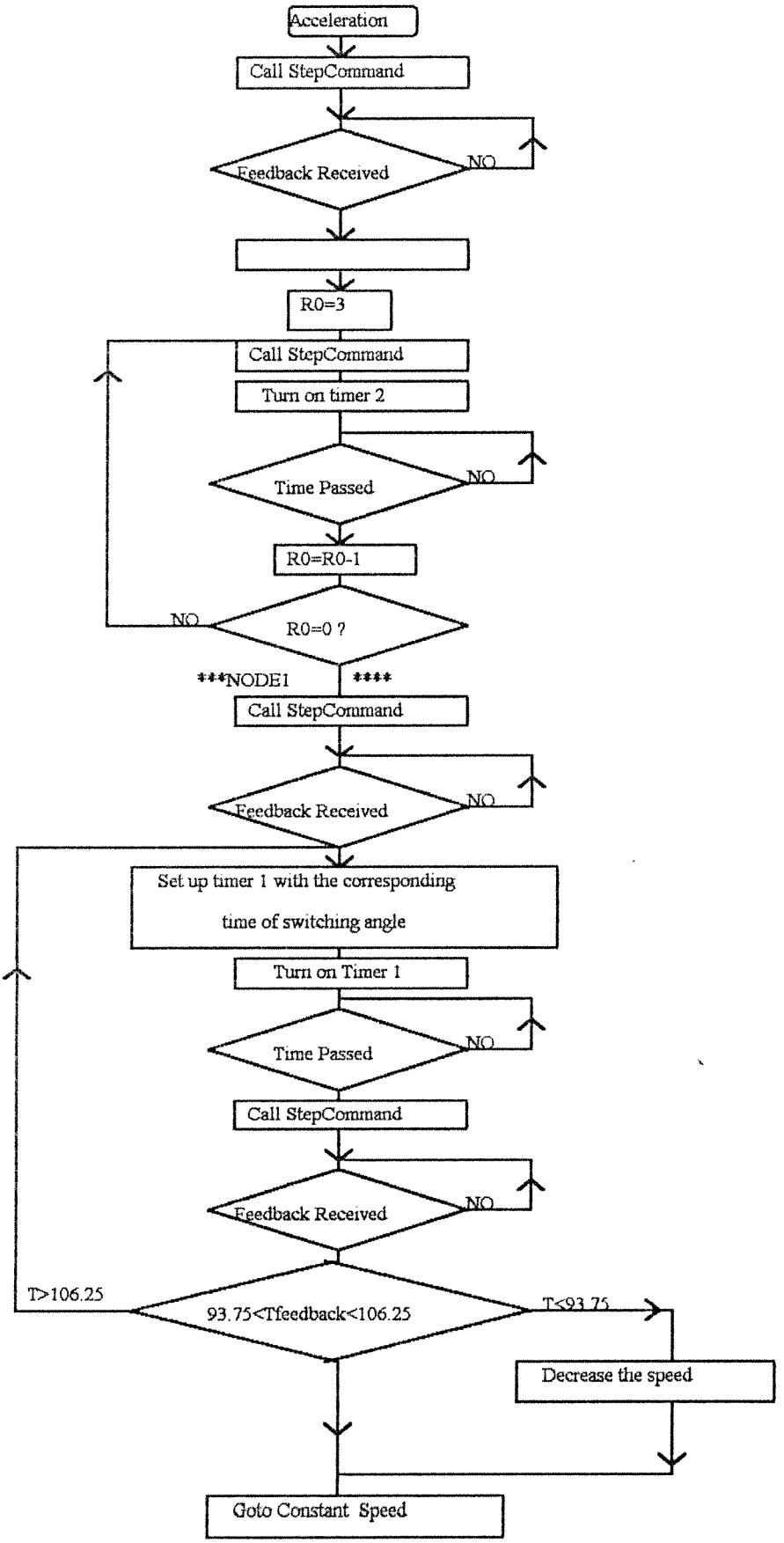
Acceleration
Call StepCommand
Feedback Received
NO
R0=3
Call StepCommand
Turn on timer 2
Time Passed
NO
R0=R0-1
NO
R0=0 ?
***NODE1
****
Call StepCommand
Feedback Received
NO
Set up timer 1 with the corresponding time of switching angle
Turn on Timer 1
Time Passed
NO
Call StepCommand
Feedback Received
NO
T>106.25
93.75<Tfeedback<106.25
T<93.75
Decrease the speed
Goto Constant Speed

LIST OF FIGURES

Page

Figure 2.1. Basic Structure of a Four Phase SRM 5

Figure 2.2. A Typical Current Waveform Showing Excitation Parameters θ_{on}, θ_{con}, I_{chop} 7

Figure 2.3. A Typical Limiting Torque Speed Characteristics 9

Figure 2.4. Typical Torque Speed Curves for a SRM Operating From a Fixed Supply by Fixed Switching Conditions 10

Figure 2.5. Typical Torque Speed Curves For a SRM Operating From a Fixed Supply by Variable Switching Conditions 11

Figure 2.6. Typical Torque/Speed/Switching Angle Characteristics of a SR Motor 11

Figure 2.7. Typical Torque Speed Curves for a SRM Operating From a Controlled Supply by Fixed Switching Conditions 13

Figure 2.8. Currents in a Phase of SRM when a) Chopping Has Started at Time t_1. b) Chopping Has Started at Time t_3 14

Figure 2.9. Typical Torque Speed Curves for a SRM Operating From a Controlled Phase Current by Fixed Switching Conditions. 15

Figure 2.10. Typical Torque Speed Curves for a SRM Operating From a Controlled Phase Current, by Variable Switching Conditions 15

Figure 2.11. Power converter Configurations: a) Three Wire Supply
b) Bifilar 18

Figure 2.12. Power Converter With Asymmetric Half Bridge 19

Figure 2.13. Power Converter With Split DC Supply 20

Figure 2.14. Section of Novel Converter 21

Figure 2.15. Novel Power Converter and Four Phase Motor 22

Figure 2.16. Switching States and Base Currents in One Phase On
Excitation Mode 24

Figure 2.17. Switching States and Base Currents in Two Phase On
Excitation Mode 25

Figure 2.18. Switching States and Base Currents in Half Step
Excitation Mode 26

Figure 2.19. Four Phase Power Converter With Six Switches 30

Figure 3.1. General Block Diagram of the System 34

Figure 3.2. Circuit Used for Finding Values in Table 3.1 37

Figure 3.3. Snubber Circuit 38

Figure 3.4. Microcontroller and Power Converter of SR Motor 41

Figure 3.5. Isolation and Inversion Circuit Used Between IGT's and
Controller Circuits 43

Figure 3.6 General Block Diagram of the Current Limiter 47

Figure 3.7. Detailed Diagram of Current Limiter 48

Figure 3.8. Enable Circuit of Current Limiters 53

Figure 4.1. Closed Loop Control Employing Encoder 56

Figure 4.2. Waveform Detection Closed Loop Control 57

Figure 4.3. Current Waveform, When Chopping at Rated Current 60

Figure 4.4. Current Waveform, When Chopping at Zero Current 61

Figure 4.5. Flow Chart for Closed Loop Control with Rotor Position Detection Using Sense Pins of IGTs 63

Figure 4.6. Circuit Diagram of the Modified Encoder 65

Figure 5.1. General Block Diagram of the Microprocessor Based Closed Loop Control System 67

Figure 5.2. EV80C51FB Board: a) Block Diagram b) Printed Circuit Board 69

Figure 5.3. Connection of the Evaluation Board to the Computer, Terminal and Power Circuitry 71

Figure 5.4. General Block Diagram of the Software 73

Figure 5.5. a) Flow Chart of General Strategy Used
b) Closed Loop Control's Timing Diagram 75

Figure 5.6. Detailed Diagram of the DAC Circuitry 77

Figure 5.7. Microprocessor Based Control of Switching Angle
a) Flow Chart for Software b) Timing Diagram For
1/4 Step Ignition Advance 79

Figure 5.8. Microprocessor Based Control of Conduction Time Period

a) Flow Chart for Software b) Timing Diagram for 2/3 Period Conduction 81

Figure 5.9. Flow Chart of Main Module 82

Figure 5.10. Flow Chart of Initialization Module 84

Figure 5.11. Flow Chart of Data Module 86

Figure 5.12. Flow Chart of PCA Module 91

Figure 5.13. Flow Chart of Step Command Module..... 92

Figure 6.1. a) Microcontroller Pulses for Switching a Transistor b) Corresponding Gate Pulses Applied to the Transistor. 96

Figure 6.2. Delay Between Processor Signal and Corresponding Gate Signal of an IGT a) Microcontroller Signal for Switching a Transistor b) Corresponding Gate Signal Applied to the Transistor 96

Figure 6.3. a) Gate Emitter Voltage of a Transistor b) Corresponding Collector Emitter Voltages 97

Figure 6.4. Collector Emitter Voltage of an IGTs at Turn ON Instant.97

Figure 6.5. Collector Emitter Voltage of an IGTs at Turn OFF Instant.98

Figure 6.6. Turn On Delay of an IGT a) Gate Emitter Voltage b) Collector Emitter Voltage 98

Figure 6.7. Turn Off Delay of an IGTa) Gate Emitter Voltage b) Collector Emitter Voltage 99

Figure.6.8. Power Converter Circuitry and the Carbon Resistor in Series With Phase 1 100

Figure 6.9. a) Phase Current Waveform b) Waveform of $V_{ce'}$ When Speed of Motor is 500 RPM and Lead Angle is Zero 101

Figure 6.10. a) Phase Current Waveform b) Waveform of $V_{ce'}$ when speed of Motor is 2000 RPM and Lead Angle is Zero 101

Figure 6.11. a) Phase Current Waveform b) Waveform of $V_{ce'}$ when speed of Motor is 500 RPM and Lead Angle is 1/2 (7.5^0) 102

Figure 6.12. a) Phase Current Waveform b) Waveform of $V_{ce'}$ when speed of Motor is 2000 RPM and Lead Angle is 1/2 (7.5^0) 102

Figure 6.13. a) Output of Senturk's Encoder b) Output of Modified Encoder When Motor Speed is 500 rpm 104

Figure 6.14. a) Output of Senturk's Encoder b) Output of Modified Encoder When Motor Speed is 1000 rpm 104

Figure 6.15. a) Output of Senturk's Encoder b) Output of Modified Encoder When Motor Speed is 2000 rpm 105

Figure 6.16. a) Output of Senturk's Encoder b) Output of Modified Encoder When Motor Speed is 3550 rpm 105

Figure 6.17. Position Feedback Pulses When Speed Is 3000 rpm 107

Figure 6.18. Position Feedback Pulses When Speed Is 1500 rpm 107

Figure 6.19. a) Feedback Pulses b) Transistor Gate Pulses for Zero Lead Angle (Advance Angle = 0^0) 109

Figure 6.20. a) Feedback Pulses b) Transistor Gate Pulses for 1/8 Step Ignition Advance (Advance Angle = 1.875^0) 109

Figure 6.21. a) Feedback Pulses b) Transistor Gate Pulses for 1/4 Step Ignition Advance (Advance Angle = 3.75^0) 110

Figure 6.22. a) Feedback Pulses b) Transistor Gate Pulses for 1/2 Step Ignition Advance (Advance Angle=7.5^0) 110

Figure 6.23. A Section of the Power Converter Circuit 111

Figure 6.24. a) Reference Voltage of Current Limiter
b) Transistor Gate Pulses When Phase Current Value Is Set to Be 5 Amps 112

Figure 6.25. a) Reference Voltage of Current Limiter
b) Transistor Gate Pulses When Phase Current Value Is Set to Be 1 Amps 112

Figure 6.26. a) output of the schmit trigger b) input of the schmitt trigger when voltage of the sense pin has not reached the reference voltage 114

Figure 6.27. a) output of the schmit trigger b) input of the schmitt trigger when current in the phase has reached the rated current 114

Figure 6.28. Input versus output waveform of current limiter 115

Figure 6.29. Transfer function characteristics of the current limiter 115

Figure 6.30. a) Microcontroller Pulses for Switching a Transistor
b) Corresponding Gate Pulses Applied to the Transistor When Current Limiter Tries to Fix Current by Chopping. 116

Figure B.1. PCB of Snubber Circuit (Soldering Side)..... 129

Figure B.2. PCB of Isolation and Inversion Circuit (Soldering Side).129

Figure B.3. PCB of Current Limiter Circuit. a) Soldering Side
b) Component Side 130

Figure B.4. PCB of Enable Circuit. a) Soldering Side
b) Component Side 131

Figure D.1. JP2 Memory Expansion Connector 140

Figure D.2. JP3 I/O Expansion Connector 141

Figure E.1. General Outlook of the Drive Circuit 142

Figure E.2. The Prototype Motor and the Test System 143

CHAPTER I

INTRODUCTION

1.1. General

The Switched reluctance motor (SRM) has evolved to near maturity over several decades and is now finding applications in general industry. Therefore the importance of designing the best controller for these motors is essential. The literature on SRM drives concentrates mainly on the analysis of the machine [1-12] and the configuration of the power converters [13-18], but very few papers discuss the control aspects [19-20]. "The SRM drives discussed in the literature are mainly open loop control with angle and current amplitude regulation and have usually been designed with discrete components and dedicated hardware" [19]. The motor and controller equipment together is considered to form a drive. Due to the small size, cheapness and huge abilities of microprocessors, it seems that the best and most flexible controller could be made using microprocessors.

A transistorized SRM drive was made by Senturk [21] in 1989. This drive has some disadvantages. One can mention its size in this respect, which is quite large. Other problems are its limited flexibility since it is hardware based and limited access to control parameters such as phase current which can be fixed and only changed by hand. Furthermore, advance angle which is another control parameter, can only be changed manually. That is, controller doesn't have any control on it. The mode of operation of the motor should also be changed by hand.

The SRM drive designed in this work doesn't have any of the above mentioned problems. In fact the design is based for achieving the

purposes which are explained below.

1.2. Objective

The object of this work is to design and implement a general purpose microprocessor controlled high performance switched reluctance motor drive system. The system is aimed to drive a four phase SRM, which has eight stator poles and six rotor poles. Optimal design of the drive is an important and difficult task. In this work, the design is based on achieving the following purposes:

i) Use minimum number of switches.

Drive cost is dominated by converter cost, and hence is closely coupled to the number and cost of the controllable switches in the drive. Therefore to minimize drive cost, one can think of minimizing number of switches, as is done in the implementation here. But unfortunately as will be explained later, this minimization has the drawback of increase in the number of power supplies in the drive circuitry.

Note also that size of the drive is completely dependent on the number of switches in the power converter. Less switches means less number of heat sinks for these switches and hence smaller drive circuit. So using minimum number of switches results in reduction in cost and size of the drive.

ii) Software controllability of various modes of operation.

In this work a microprocessor based control philosophy is adopted to achieve flexibility of adapting the controller-driver for various applications. In this manner various drive modes (one phase on, two phase on and half step) can be software selected by the user.

iii) Hardware closed loop control (with a view for sensorless operation eliminating hardware)

Closed loop control has lots of advantages over open loop control. In a closed loop switching motor system the instantaneous rotor position is detected and fed back to the control unit. Although

in this work a specially designed position encoder is used, the drive is designed to be also suitable for position feedback through waveform detection and, Hence eliminating position encoder hardware.

iv) User programmable software

It is desired that user be able to operate the motor under various conditions. That's why the software written in this work should be a user programmable software. By user programmable it is meant that user be able to enter his desired values for some control parameters. Giving this facility to the user enables him to investigate motor performance in detail under various advance angles and phase currents. Hence important results may be obtained for a sophisticated control in future.

Furthermore one of the aims is to create a hardware such that any control strategy designed by a user can be easily implemented, since all control variables are measured and interfaced with the microprocessor. Similarly all microprocessor control signals are interfaced with the power stage for this purpose.

1.3. Outline of The Work

As the aim of this work is design and implementation of a microprocessor controlled Switched reluctance motor drive, it seems reasonable to start first by understanding what a switched reluctance motor is. That is understand its basic structure and principles of operation. Since our aim is to control this motor we should also see what are the basic principles of control for a SRM, and explain the independent variables which may be kept under control by means of a controller (chapter II). The final aim of the work is to speed control the motor in a wide range. The work here is however, restricted to operating the motor under user defined conditions. For this reason the torque speed characteristics of SRM is investigated to find out how one can operate the motor to get required characteristics. Therefore, In Chapter II SRM characteristics and operating modes are investigated to identify the type of program to be implemented for control purposes also find out a drive circuit to accomplish this task.

Chapter III discusses the power stage designed to achieve the purposes outlined previously.

In chapter IV, two methods of rotor position detection are explained. A literature survey is also done on waveform detection schemes using phase current, motional voltage and phase inductance.

Chapter V explains the microprocessor hardware and software designed. This chapter shows how a microprocessor based control philosophy is adopted to achieve flexibility of adapting the controller-driver for various applications. In this manner various drive modes can be software selected. The microcontroller software is explained in detail in this chapter and its flow charts are presented. The software here is a user programmable software which enables user to investigate the motor performance in detail under various conditions. This chapter also explains possible control parameters and shows how it is possible to change these parameters by a microprocessor.

In chapter VI the operation of the controller is tested and some waveforms are presented to illustrate the operation of the drive. Finally some recommendation for future works are presented.

CHAPTER II

SWITCHED RELUCTANCE MOTOR
STRUCTURE, PRINCIPLES OF CONTROL AND DIFFERENT DRIVE TYPES

2.1. Basic Structure and Principles of Operation

The switched reluctance motor (SRM) is a doubly salient variable reluctance motor. A typical four phase SRM with eight stator poles and six rotor poles is shown in Fig.2.1. In this figure only a single phase winding is shown. Simple concentrated stator coils are wound on each stator pole. The absence of coils on the rotor means that torque is produced purely by the saliency of the rotor laminations. The direction of the torque produced is independent of the direction of the flux through the rotor and, hence, the direction of the current flow in the stator phase windings is not important. Therefore, each phase of SRM can be excited both by bipolar and unipolar drives. In this work each phase of SRM is excited by unidirectional currents. As a result of this only a single power switch is required per phase. Moreover,

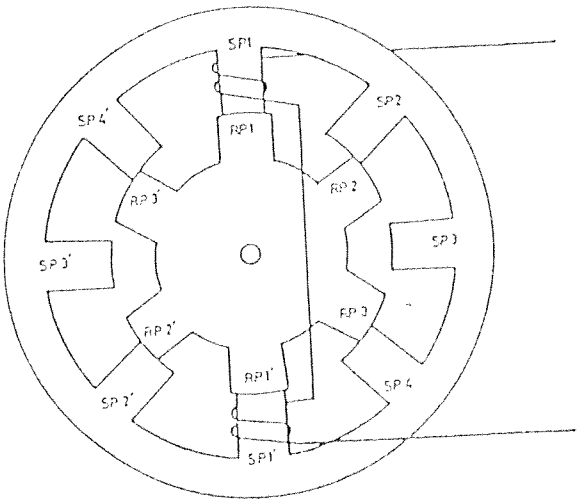

Figure 2.1. Basic Structure of a Four Phase SRM

with a unipolar drive short circuit current is limited but with a bipolar drive it is not. Hence, a unipolar drive is preferred here as unipolar phase current in the reluctance motor results in simpler and more reliable power converter circuits. The salient pole and brushless design of the rotor combine to produce a reliable and cheap motor. The movement of the rotor is maintained by switching DC voltage to each phase one by one by means of a switching circuitry.

When a phase is excited the rotor tends to align with the corresponding pole of the excited phase with the effect of the reluctance torque. If the phases are excited continuously in a sequential manner continuous motion of the rotor will be attained. After a complete period, which is equivalent to excitation of all phases, rotor will have moved by an angular displacement of $2\pi/6$ radian or 60 degrees. The angular displacement of the rotor for one change of excitation is 15 degrees, for this example, which is called the step angle [11]. The step angle for a SRM is normally large compared to that of commonly encountered step motor since a SRM is designed for speed control in a wide range, rather than fine position control [11,12].

2.2. Basic Principles of Control for a SRM

Since the direction of motion does not depend on the direction of phase currents, it is sufficient to excite each phase by unidirectional currents.[13]. This is an important feature resulting in simplicity of the controller. The average torque produced by a SRM depends on independent variables which may be kept under control by means of a controller. Those parameters are the terminal voltage, supply current, switch on position or angle (θ_{on}) and switch off position or angle (θ_{off}). Note that instead of switch off angle we can use its equivalent, the conduction period or angle (θ_{cond}). The control may be achieved throughout controlling above mentioned parameters. In this manner a number of different torque/speed characteristics may be obtained from the same motor. The control modes for a SRM is discussed in next section.

For a given phase, switch on instant is the instant at which this phase is energized. After the switch on instant, energy begins to flow from the supply to the phase winding belonging to the excited phase. Switch off instant is the instant at which the main switching element carrying the phase current is turned off. After the switch off instant energy begins to flow from the phase winding to the supply. Conduction period for a given phase is the total period between switch on and switch off instants. The controller is responsible for enforcing the excitation at desired instant for the specified direction. The excitation is designed to produce the required drive output of speed and torque. $I(\theta)$ is specified completely by the selection of the turn on angle θ_{on}, the phase conduction angle θ_{cond}, the reference level above which current chopping occurs I_{chop} (mean phase current reference) and the supply voltage, as was mentioned previously. These four are the variables which should be controlled.

There is no control on the current until it reaches the hysteresis band limit. Rate of rise of current is determined by the switch on instant, phase current parameters and the back EMF induced in the phase which is speed dependent.

A typical chopped current waveform is presented in Fig.2.2 to show the relationship between the excitation parameters [14]. At low

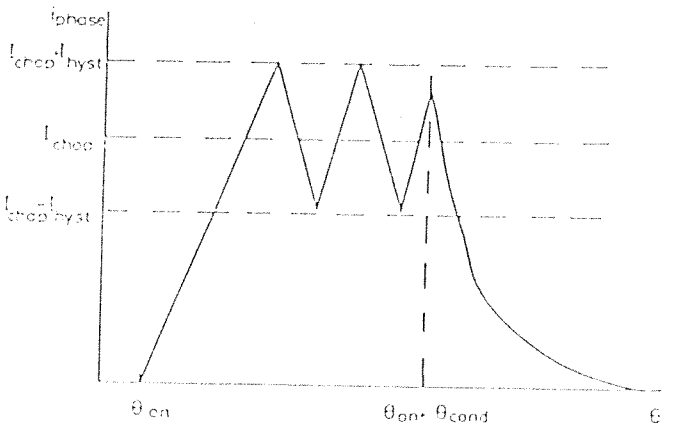

Figure 2.2. A Typical Current Waveform Showing Excitation Parameters θ_{on}, θ_{con}, I_{chop}

increase well beyond the current capabilities of the power switches (given a fixed supply voltage). Note that when back EMF is sufficiently large the drive will never get into this mode of operation since current can not reach the limit of hysteresis band. That is, at sufficiently high speeds, where the machine back EMF exceeds the DC supply voltage, the machine is operated without current chopping.

We would like to have speed control in this application. At this stage therefore, it is desired to observe the effect of each control variable on the torque speed characteristics of the motor.

2.3. Limiting Torque Speed Characteristics for a SRM

Theoretically the natural torque speed characteristics of a SRM operating from a fixed supply with fixed switching position will be a curve which drops with the square of the speed.[11]. The limiting natural torque speed characteristics will be achieved for the limiting case where the supply voltage is chosen as the maximum allowable value and switchings are adjusted so that maximum maintainable torque is produced at any given speed. For practical drives however, there exists a constant torque zone for low speeds. The reason for the existence of this zone is explained in [11]. At speeds beyond the constant torque zone the motor operates in its usual switched mode. A typical limiting torque speed characteristics is as shown in Fig.2.3. Here the rated motor speed is denoted by w_r.

As can be seen from the figure the limiting characteristics is determined by the maximum possible supply voltage value (curve A) and the maximum possible current value (curve B). Note that this defines an area which is called the operating region. Different control facilities are available in order to achieve different torque speed characteristics in the area under limiting torque speed curve. That is in the operating region.

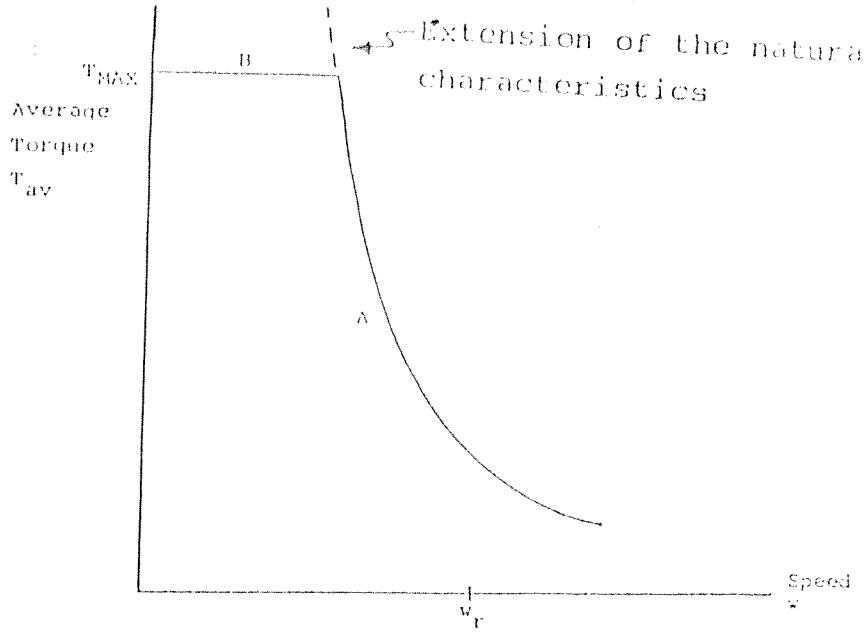

Figure 2.3. A Typical Limiting Torque Speed Characteristics.

2.3.1. Operation From a Fixed Supply by Fixed Switching Conditions

We said that for a SRM if the supply voltage and switching positions are fixed the torque will be inversely proportional with speed. Therefore for various fixed switching positions a family of curves which lay under the limiting curve may be achieved [11]. Typical curves are shown in Fig.2.4. Here the control variable is the conduction period. Curve 1 of Fig.2.4, is the limiting curve of Fig.2.3. As the conduction period is decreased different torque speed curves may be achieved (curves 2 and 3). Here, conduction period for curve 3 is less than that of curve 2. This type of operation is suitable for loads whose torque demand decrease with increasing speed, such as traction.

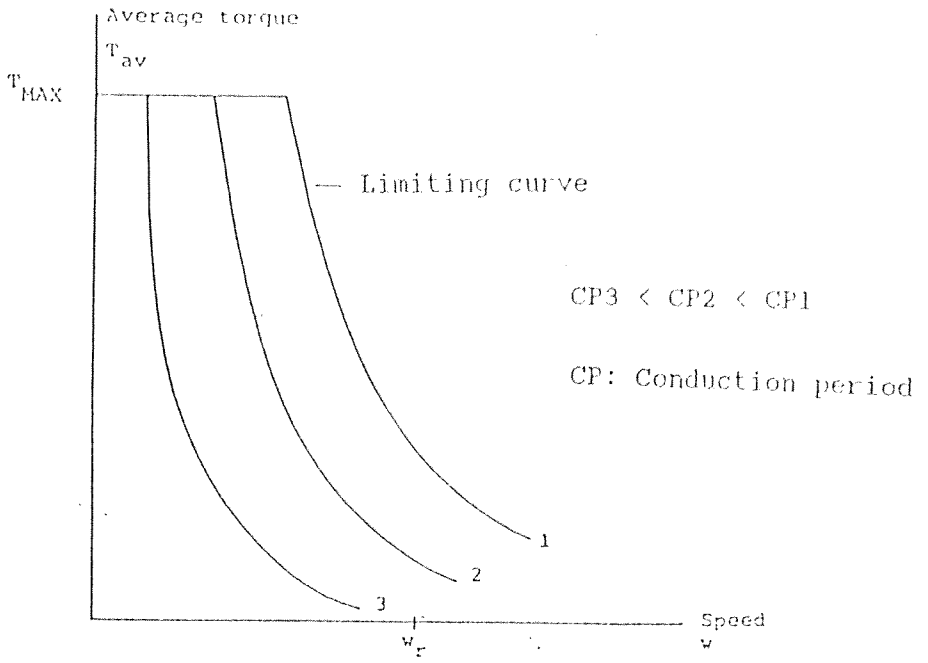

Figure 2.4. Typical Torque Speed Curves for a SRM Operating from a Fixed Supply by Fixed Switching Conditions.

2.3.2. Operation From a Fixed Supply by Variable Switching Conditions

If as the speed is increased switching positions are varied the torque will fall in a more controlled manner. Therefore different types of torque speed curves may be achieved [11]. Two typical torque speed curves corresponding to this type of operating mode is shown in Fig.2.5. Here the control variable is the switching angle. For curve 4 in Fig.2.5, torque varies with the inverse of the speed and constant power is developed above the constant torque zone. For curve 5, a linear relationship exists between torque and speed. Since there is an upper limit for conduction period, ie. unity. After a certain speed the fall in torque can no longer be compensated and the torque starts to fall more rapidly as will be encountered for the case of fixed switching positions. This type of control is also suitable for loads whose torque demand drops with increasing speed.

Note that Fig.2.5 is a direct prediction of linear theory.

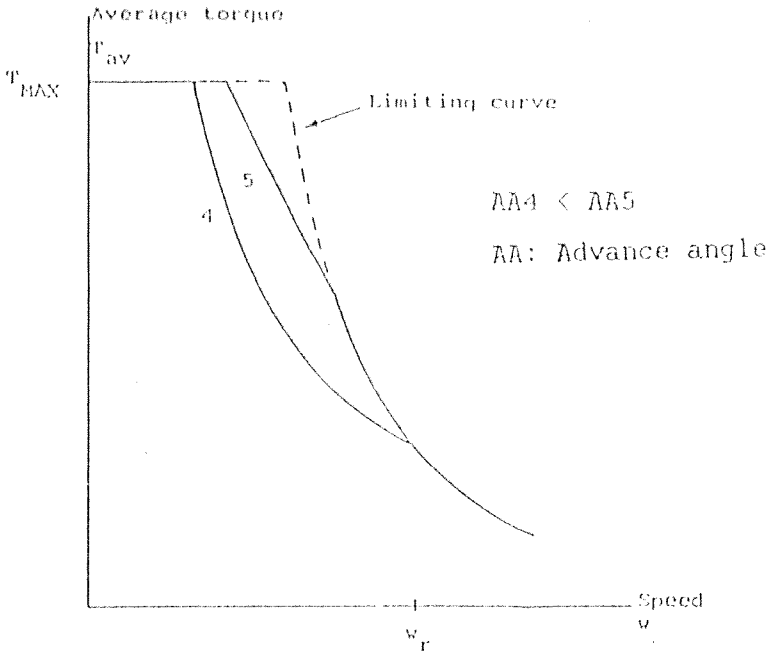

Figure 2.5. Typical Torque Speed Curves for a SRM Operating from a Fixed Supply by Variable Switching Conditions.

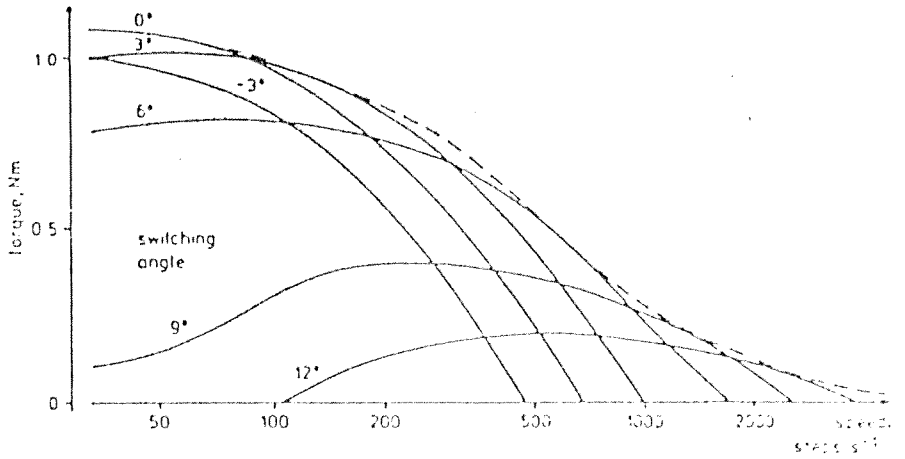

Figure 2.6. Typical Torque/Speed/Switching Angle Characteristics of a SR Motor.

However, in practice the variation of torque with switching angle and speed for a motor is as shown in Fig.2.6. [12]. Theses characteristics include a negative value of switching angle, for which the phase excitation is changed after the static torque/position "crossover" points. Figure 2.6. shows quite clearly that an injudicious choice of switching angle may prevent the motor from producing any torque at certain speeds, e.g. switching angle=12 degrees at speeds, below 100 steps per second.

For small switching angles a high torque is developed at low speeds, so the system accelerates rapidly from rest, but the maximum speed is restricted. Conversely if a large switching angle is chosen the torque is small at low speeds and the initial rate of acceleration is slow, but ultimately higher running speeds can be attained. Hence, although large switching angles must be used to attain high pull-out rates, these angles are inappropriate for low speed operation. Note that when switching angle is fixed to a value, motor operates on the torque speed characteristics related to that switching condition, depending upon what the load behavior is.

2.3.3. Operation From :

1) Controlled Supply by Fixed Switching Condition
2) Controlled Phase Current by Fixed Switching Condition

This kind of operation of SRM is suitable for industrial loads demanding constant torque over a wide speed range. The instantaneous phase current for a SRM is directly proportional with supply voltage and inversely proportional with speed (i.e. v\w ratio). [11]. So one method of controlling the phase current is to control the terminal voltage as speed varies such that the voltage to speed ratio stays constant.

For fixed switching conditions the phase current will assume a similar waveform as long as the current exceeds the limit value of the hysteresis band. Therefore for fixed switching conditions, the torque speed characteristics may be represented by a constant torque

curve. However after a certain speed at which the maximum voltage is applied to the motor, since the voltage can no longer be increased, the torque begins to decrease with increasing speed. Typical curves corresponding to this type of operation are shown in Fig.2.7. Each curve on that figure corresponds to a different V to w ratio. As this ratio is increased the highest speed at which torque may be kept constant decreases.

Above, a method was illustrated for controlling the phase current. Below another method of phase current control is explained. As soon as a phase is turned on current will increase on that phase until the upper limit of hysteresis band after which chopping action starts (to keep the current fixed at reference level). In Fig.2.8a, one phase of a SR motor is turned on at time t_1. The current has risen to I_{chop1} at time t_2, at which chopping has started to keep current fixed at I_{chop1}. Note that if chopping had been started at some earlier time, for example at t_3 (see figure 2.8B) , then since the time for current build up was less compared to that of previous case (i.e. keeping the

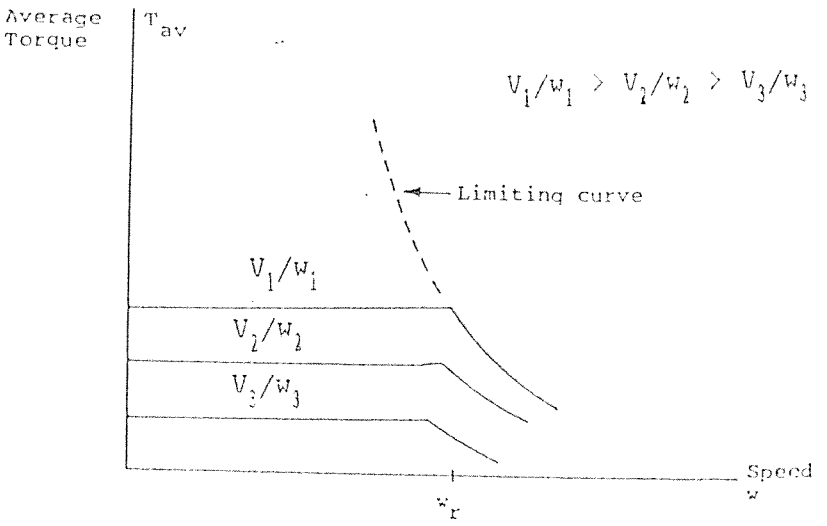

Figure 2.7. Typical Torque Speed Curves For a SRM Operating from a Controlled Supply by Fixed Switching Conditions.

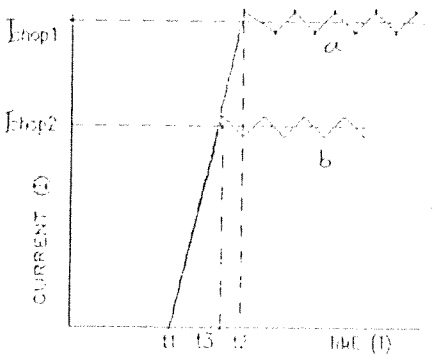

Figure 2.8. Currents in a Phase of SRM When a) Chopping Has Started at Time t_1. b) Chopping Has Started at Time t_3 ($t_1>t_3$, $I_{chop1}>I_{chop2}$)

phase on until time t_1 ($t_1>t_3$)) the value of I_{chop2} would be lower than that of I_{chop1}. Hence different phase current values can be obtained just by keeping the phase on ,at the beginning, for different time values. Therefore a microprocessor can control the phase currents by controlling the time that chopping of switches should start.

In Fig.2.9, typical torque speed curves for a SRM operating from a microprocessor controlled current by fixed switching conditions are shown. Each curve on that figure corresponds to a different mean phase current reference value. As the current is increased the highest speed at which torque may be kept constant decreases. For each curve in figs.2.7 & 9, it is assumed that the switching positions are chosen so that maximum attainable torque is produced at a given speed.

2.3.4. Operation from a controlled phase current by variable switching conditions

It should be noted that by varying switching positions it is possible to shift each curve in Fig.2.9, downwards as a whole. For different mean phase current reference values, typical curves obtained by varying switching positions are shown in Fig.2.10.

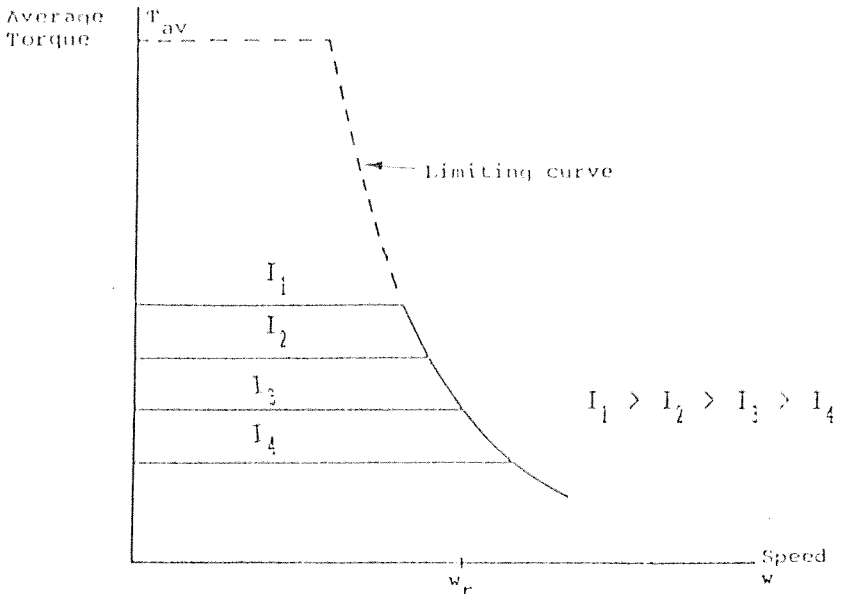

Figure 2.9. Typical Torque Speed Curves for a SRM Operating from a Controlled Phase Current by Fixed Switching Conditions.

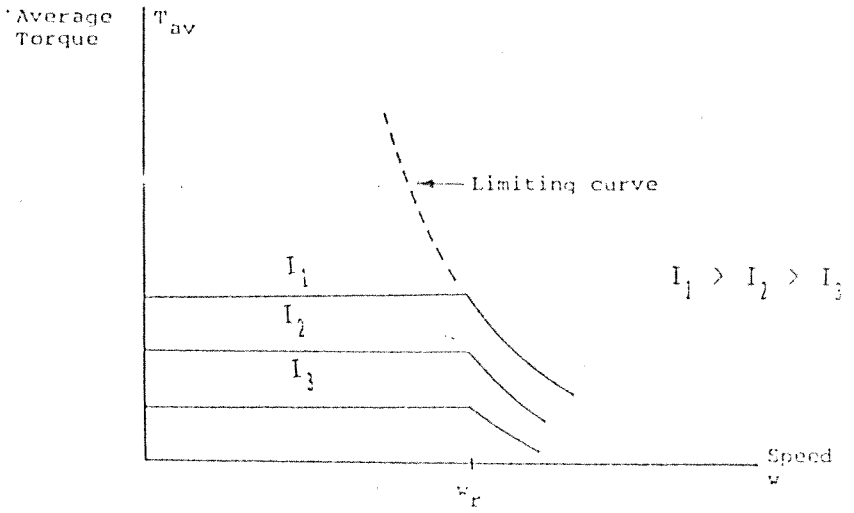

Figure 2.10. Typical Torque Speed Curves for a SRM Operating from a Controlled Phase Current, by Variable Switching Conditions.

Above, the effect of different control variables on the torque speed characteristics of the SR motor were observed. We said that we would like to have speed control in this application. One may ask why a SRM drive is chosen for the application here. In other words, why a Dc or Induction motor drive is not used here? Now that the structure and principles of operation and control of a SR motor are explained, we can answer this question. Below a comparison is done between a SRM drive and other drives to show advantages of SRM drive compared to other drive types.

2.4. Comparison of Different Drive Types

In this section a comparison is done between a SRM drive, a DC drive and an induction motor drive to describe why a SRM drive is preferred for the application here. Table below presents a brief comparison of the three drives [11].

Table 2.1. Comparison of SRM Drive With Other Drives

	SRM DRIVE	DC DRIVE	INDUCTION MOTOR DRIVE
Motor structure	Extremely simple without any rotor winding	Complicated due to commutator and rotor winding	Rather simple structure
Driver	Unidirectional phase currents so rather simple controller	Extremely simple controller	Complicated controller
Feedback scheme	Is necessary. For switching control from rotor position, For speed count # of pulses	Depending on application, is or is not necessary	Depending on application is or is not necessary
Maintenance problem	Rare due to simplicity of structure	Often, due to commutator	Rare due to simplicity of structure

Some advantages and disadvantages of the SRM drive may be summarized as follows:

Advantages:

The motor has a very simple and robust construction.

The motor consists of a very simple doubly salient magnetic circuitry.

_The rotor does not have a winding of any type.
_The stator windings are concentrated windings.
_The constructural features of SRM's are very simple compared to induction motors and especially to DC motors.
_The reliability of the drive is good, needing less maintenance.
_The driver configuration is rather simple.
_Only a single power switch is required per phase since each phase of a SRM is excited by unidirectional currents.

Disadvantages:
_The speed of the rotor can not be fixed exactly at a given speed, although the average speed will be, the required speed, the instantaneous speed of the rotor oscillates around the required speed.
_High frequency Noise may be a disadvantage of SRM drive.
_A feedback is required from the rotor position for an efficient drive operation.

Studying Table 1.1 and considering advantages of SRM drives, explains the reason of preferring these drives in this work. Below different power converter circuit for the SR motors is described and after comparison a power converter requiring only a single switch for each phase is chosen to be implemented.

2.5. Driver Configurations

Switching reluctance motor is generally designed for continuous running. A power converter is required to control the unipolar phase current in the phase windings and able to increase and decrease the current in the windings as fast as possible (to avoid contribution of negative torque in the phase which is off). In this section different driver circuits will be considered. Then a comparison is done and a driver circuit which has minimum number of switches is selected.

The motor windings must be arranged both to accept power from a source and return power to it [13]. A motor with a single winding per phase uses it for both functions, like the three wire supply configuration shown in Fig.2.11a. In practice due to the necessity of two different dc sources, this circuit is never used. Bifilar windings avoid the need for a three wire supply, although retaining the advantage of only one transistor and one diode per phase, Fig.2.11b. One of the bifilar windings is connected to a single switching device and the other to a freewheel diode. Current builds up in the main winding when the switching device is turned on and transfers to the secondary winding when the switch is turned off. Depending on the degree of coupling between the two windings and their turns ratio, the voltage across the switching device may rise to over twice the supply voltage at the instant of turn off. The switching device must be rated to withstand this. Although this driver has only one switch per phase, the voltage rating of that device must be at least twice the rating of the motor windings.

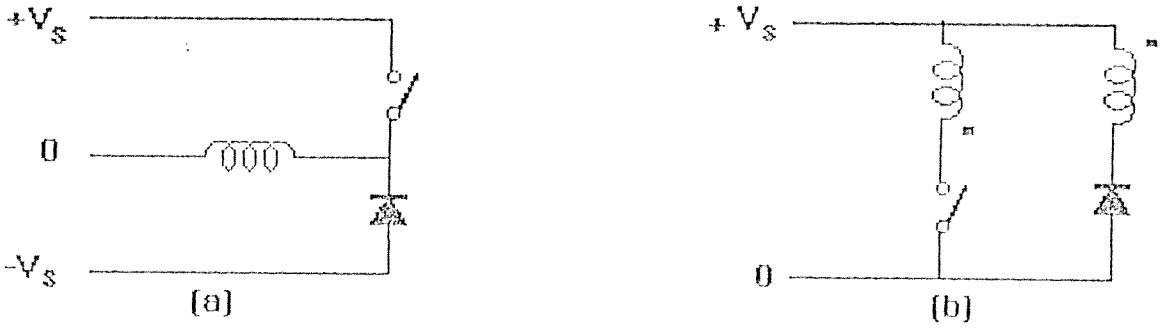

Figure 2.11. Power converter Configurations: a) Three Wire Supply b) Bifilar

The asymmetric half bridge Fig.2.12, uses two power semiconductor switches for each phase winding. The switching devices and freewheeling diodes must be rated to withstand the supply voltage plus any switching transients. The motor windings are rated at the supply voltage. This circuit therefore allows the motor to be rated at close to the maximum switch voltage. This is important where the DC supply voltage or available switch voltage may be limited. The asymmetric half bridge has three main modes of operation [15,16]. The first, a positive voltage loop, occurs when both switching devices S_a and S_b are turned on. The supply voltage is connected across the phase winding and the current in the phase winding increases rapidly supplying energy to the motor. The second mode of operation is a zero volt loop. It corresponds to current control. This occurs if either of the two switching devices is turned off while current is flowing in the phase winding. In this case the current continues to flow through one switching device and one diode. Energy is neither taken from nor returned to the DC supply, minimizing the current ripple rating of the supply capacitor. The voltage across the phase winding during this time is equal to the sum of the on state voltages of the two semiconductor devices. This voltage is small and the flux linkage associated with the phase winding decays slowly. The third mode of operation is a negative voltage loop. Both of the switching devices are turned off. The current is forced to flow through both freewheel diodes. The flux linkage associated with the phase winding decreases rapidly as energy is

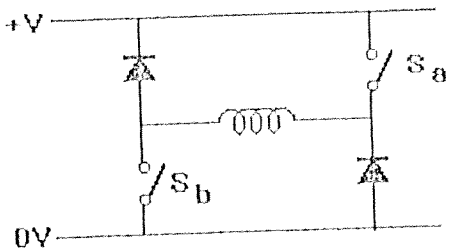

Figure 2.12. Power Converter with Asymmetric Half Bridge.

returned from the motor to the supply.

The major advantage with this circuit is that all of the available supply voltage can be used to control the current in the phase windings. As each phase winding is connected to its own asymmetric half bridge, there is no restriction in the number of phase windings. However as there are two switches per phase winding it is best suited to motors with few phase windings.

2.5.3. Power Converter With Split DC Supply

A power converter employing a split DC supply has been proposed to provide the positive and negative voltages needed to increase and decrease the current in the phase windings. In Fig.2.13 two phase windings are shown. [15,16]. The position of the switching devices and freewheel diode are transposed for each phase winding to ensure that there is no power flow imbalance between the two supply capacitors. This arrangement means that this power converter circuit is only suitable for motors that have an even number of phases. Each switching device and freewheel diode must be rated to withstand the complete supply voltage plus any transient voltages due to the switching. However, only half of this voltage can be applied across the motor winding. Although this circuit requires only one switch per phase

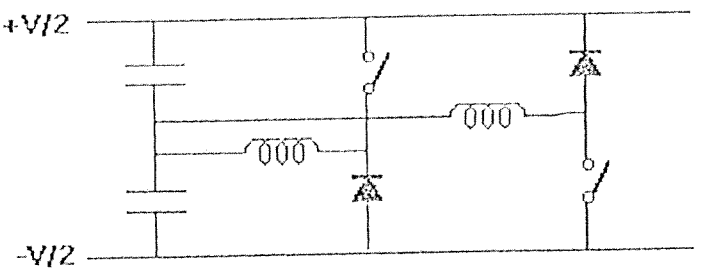

Figure 2.13. Power Converter with Split DC Supply

winding, this advantage is outweighed by under use of the switch voltage, the need for extra capacitive components in the DC supply and the requirement for an even number of phase windings.

2.5.4. The Novel Power Converter

The novel power converter is based on the asymmetric half bridge hence the advantages of asymmetric half bridge are retained. The simplest form of this circuit is shown in Fig.2.14. Two phase windings are connected to three switching devices [16]. (Note that this converter is referred to as the novel converter throughout thesis to differentiate it from others. The circuit is in fact the same as described in reference [16]). The central switch in the diagram S_b is connected to two phase windings, rather than one as in the conventional asymmetric half bridge. The proposed circuit for a four phase reluctance motor is shown in Fig.2.15. It contains two semiconductor switches, S_b and S_d, each one connecting two of the phase windings to the positive supply rail, and two further switches, S_a and S_c, to connect the other ends of the phase windings to the lower supply rail. In this circuit when two switches are turned on there could be two possible current paths through the phase windings. The rectifying diodes connected in series with each phase winding prevent these unwanted circulating currents from flowing [15,16]. Below a switching

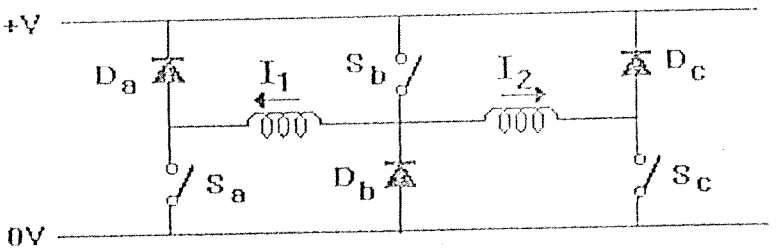

Figure 2.14. Section of Novel Converter.

algorithm is described that allows the current in two phase windings to be controlled simultaneously. In other words, A switching algorithm has been developed that maintains independent control of all the phase currents in the drive circuit of Fig.2.15. Table 2.2 shows the operation of the switches in Fig.2.14, during a normal pulse of current in phase winding 1 [16]. First switches S_a and S_b turn on and current I1 (phase 1's current) starts increasing. To hold the current I1 at its rated value switch S_b starts chopping. Till now switch S_c was off and current I2 (phase 2's current) was zero. In order to increase current in phase winding 2 and also hold current I1 at its rated value, switches S_b and S_c become on and switch S_a starts chopping. Therefore, current I2 increases and to hold it at the rated value switch S_c should start chopping, while S_b is on and S_a is chopping (see fourth line of table 2.2). Now comes the most important feature of the switching strategy used here, Which is illustrated by the fifth line of table 2.2. It shows how it is possible to decrease current I1 which maintains

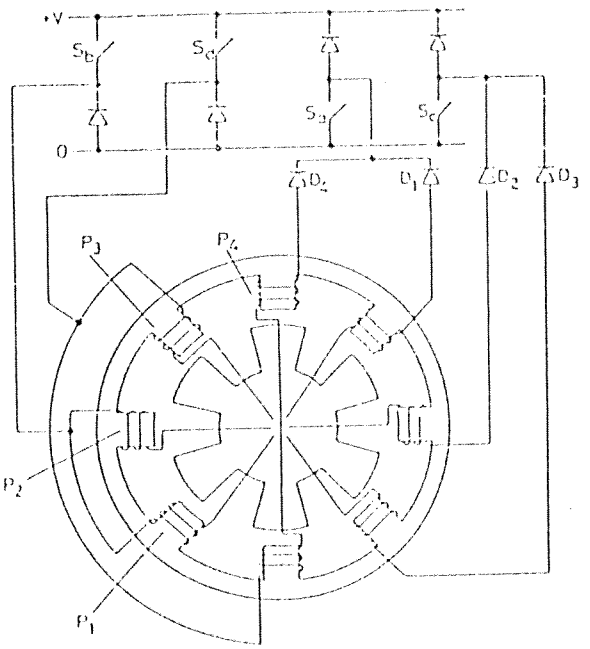

Figure 2.15. Novel Power Converter and Four Phase Motor.

the level of current I2. Switch S_a is turned off and the operation of switches S_c and S_b is interchanged. Hence current I1 decreases while current I2 is hold. The duty cycle of the switch current waveforms of the novel converter are greater than those of drive based on a split DC rail [16]. The switches are therefore better utilized than in other drives.

Table 2.2. Operation of the Switches in Fig.2.14. during one period of I1.

I1	I2	Sa	Sb	Sc
Increase	Zero	On	On	Off
Hold	Zero	On	Chop	Off
Hold	Increase	Chop	On	On
Hold	Hold	Chop	On	Chop
Decrease	Hold	Off	Chop	On

2.6. Excitation Modes For The Novel Converter

There are three modes of operation of the motor. The phase currents and switch states of the Novel power converter, for one phase on, two phase on and half step sequence mode operations are given in Fig.2.16, 2.17 and 2.18 respectively. Here ' H ' means phase is excited, and 'L' means phase is not excited.

2.6.1. One Phase On Excitation

Phase 1	H	L	L	L
Phase 2	L	H	L	L
Phase 3	L	L	H	L
Phase 4	L	L	L	H
Sa	On	Off	Off	On
Sb	On	On	Off	Off
Sc	Off	On	On	Off
Sd	Off	Off	On	On

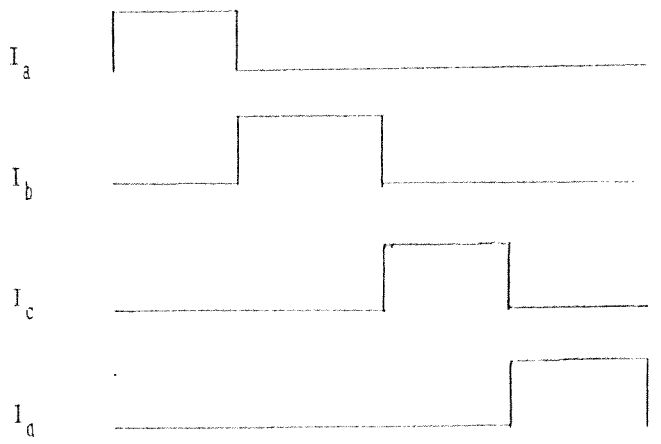

Fig.2.16 Switch States and Base Currents in One Phase On Excitation Mode.

2.6.2. Two Phase On Excitation

Fig.2.17 shows the phase currents and switch states of the Novel power converter for two phase on mode. It is shown by Acarnley [12] that the maximum peak static torque is produced when two of the phases of a four phase motor are excited simultaneously.

Phase A	H	H	L	L
Phase B	L	H	H	L
Phase C	L	L	H	H
Phase D	H	L	L	H
Sa	On	On	Off	On
Sb	On	On	On	Off
Sc	Off	On	On	On
Sd	On	Off	On	On

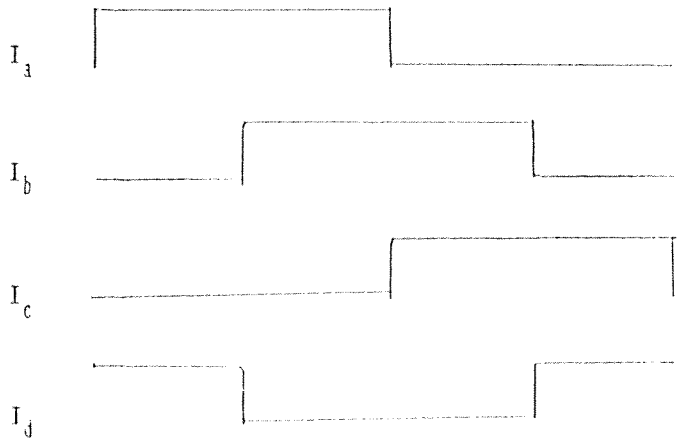

Fig.2.17 Switch States and Base Currents in Two_Phase_On Excitation Mode.

2.6.3. Half Step Excitation

In half step operation mode the motor operates with alternate one and two phase on excitation. i.e.A, AB, B, BC, C, ... Each excitation change produces an incremental movement which is half the length of a normal step and therefore the excitation is known as the half stepping mode of operation [12]. Fig.2.18 shows the phase currents and switch states of the Novel power converter for half step mode.

Phase A	H	H	L	L	L	L	L	H
Phase B	L	H	H	H	L	L	L	L
Phase C	L	L	L	H	H	H	L	L
Phase D	L	L	L	L	L	H	H	H
Sa	On	On	Off	Off	Off	On	On	On
Sb	On	On	On	On	Off	Off	Off	On
Sc	Off	On	On	On	On	On	Off	Off
Sd	Off	Off	Off	On	On	On	On	On

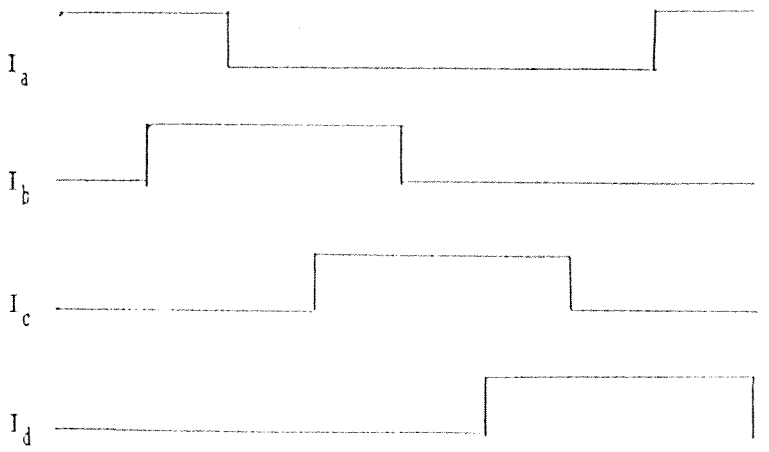

Fig.2.18 Switch States and Base Currents in Half Step Excitation Mode.

2.7. Comparison of Various Driver Configurations

Ideally a driver circuit for the switched reluctance motor would have:

a) The minimum number of switches.

b) Complete flexibility in the number of phase windings.

c) The full supply voltage applied to the motor phase windings

d) Switching devices rated at close to the motor voltage.

e) An ability to increase the phase current rapidly.

f) Effective means for current control by modulation of the switches.

g) Some method to return the energy to the supply while the flux linkage is decreasing.

Six of these requirements are met by the asymmetric half bridge, but as it uses two switches per phase winding it does not satisfy the first criterion. The split DC supply is restricted to motors with an even number of phases and also it doesn't satisfy requirement c. However the Novel power converter satisfies all the above requirements [16]. Table 2.3. compares different driver circuits mentioned before. Studying this table, shows that the Novel converter is the best one among others.

If one takes the current flowing a phase (when voltage across the phase is Vs) as the base current I_{base}, and take the supply voltage Vs as V_{base} then for discussed converters the per unit current and voltages shown in Table 2.4 are obtained. This table is drawn under the condition that the same motor is driven by different types of converter configuration. Note that split DC supply now has to supply twice the current to produce same output current if motor losses are neglected.

For the case of comparison of efficiencies, let's take 1 pu output power for each converter and find out the losses of the five converters. In the Table 2.5, one unit transistor switching loss is denoted by Pt1, one unit core loss by Pc, and one unit ohmic loss by

Table 2.3. Comparison of Various Driver Configurations.

	3 Wire supply	Bifilar winding	Asym. half bridge	Split DC supply	Novel
# of transistors in four phases	4	4	8	4	4
# of diodes in four phases	4	4	8	4	8
Semiconductor's voltage rating	2Vs	2Vs	Vs	2Vs	Vs
Semiconductor's current rating	I	I	I	I	2I
Drive can be used in chopping mode	Yes	Yes	Yes	Yes	Yes
Efficiency for a given supply	High	High	Mid	Mid	High
# of voltage sources necessary per phase	2	1	1	2	1
Efficient usage of copper in the motor	Yes	Yes	Yes	Yes	Yes
Restriction on # of phases	No	No	No	Yes	No
Voltage applied across motor winding	Vs	Vs	Vs	Vs/2	Vs
Energy returned to supply when phase switched off	Yes	Yes	Yes	Yes	Yes
Energy returned during chopping	Yes	Yes	No(*)	Yes	No(*)
Ohmic losses	Same	Same	Same	Same	Same
Core losses	Same	Same (**)	Same	Same	Same
Dynamic response switch to motor voltage ratio	Mid	Mid	High	Mid	High
Duty cycle of the switch current waveform	Mid	Mid	High	Mid	High

(*):Neither taken nor returned.

(**): The core losses are same since the flux waveforms are same for a SR motor with monofilar and bifilar windings [11].

Table 2.4 Per Unit Phase Current and Voltages of Different Converters

	3 wire supply	Bifilar winding	Asym. half bridge	Split DC supply	Novel converter
PU phase current	1	1	1	1/2	1
PU phase voltage	1	1	1	1/2	1

Table 2.5 Comparison of Losses and Efficiencies of Explained Converters.

	3 wire supply	Bifilar winding	Assymmet half bridge	Split DC supply	Novel converter
Transistor switching losses	Pt1	Pt1	2Pt1	Pt1	Pt1
Ohmic losses	Po	Po	Po	Po(*)	Po
Core losses	Pc	Pc(***)	Pc	Pc	Pc
Phase voltage	Vs	Vs	Vs	Vs/2	Vs
Phase current	I	I	I	2I(**)	I
Total losses	Low	Low	Mid	Mid	Low
Efficiency	High	High	Mid	Mid	High

(*):Here since the current for this converter is 2I i.e. double, one may think that the ohmic losses be four times Po, But since the cross section and number of turns is changed the Po will stay same as that of other converters, i.e. it will be Po.

(**):Reason for this is that, one of our assumptions is to have always same power output Po. Since phase voltage for split DC converter is Vs/2 phase current should be 2I in order to get VI as output power, assuming a lossless machine.

(***): As explained before, since flux waveforms are the same for bifilar and monofilar windings [11], the core losses will also be the same.

Po. Note that switching losses arise from the energy lost during turn-on and turn-off, of transistors. One assumption at this stage is that switching times are identical. Note that more loss means lower efficiency. Below efficiencies of power converters with four switches is compared in more detail.

Let 'a' be the efficiency of a driver employing a 240 V split DC supply (120 V of which can be applied across the phase winding) and 'b' be the efficiency of the Novel converter with four switches operating from a supply voltage of 120 V. The efficiency of motor connected to the power converter with a split DC supply of 120 volts (60 volts of which can be applied across the phase winding) is 'c'. Experimental results has shown that [16]: a > b > c

The reason for 'b' being less than 'a' can be attributed to the factor that Each phase current flows through three conducting semiconductors, at least one of which is a diode.

The efficiency of b would be improved at higher supply voltages and could be increased further by using the circuit shown in Fig.2.19 which does not require series diodes, but uses a total of six

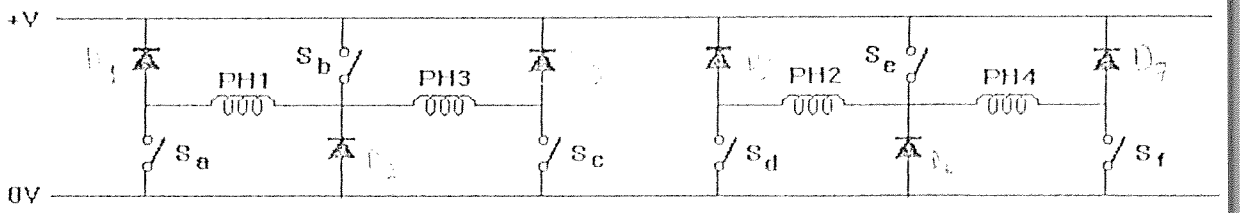

Figure 2.19. Four Phase Power Converter With Six Switches.

switching devices and is a four phase power converter with six switches [16]. As the current in phases 1 and 3 do not overlap, this circuit ensures that only one phase current has to flow through each switch at any one time. The peak current through the switch is equal to the peak phase current. The heating losses are no longer equally distributed between devices.

In this work, since one of the objectives is to use minimum number of switches (to minimize drive cost and size), the novel converter which has only four switches is used as the power converter circuit.

CHAPTER III

DESIGN OF THE POWER STAGE

3.1. Design Criteria

In this section specifications of the drive will be given and the design procedure will be described. The drive to be designed in this work is intended for driving a four phase, switched reluctance motor. To achieve this purpose it is desired to satisfy the following requirements;

The system must be capable of driving a SRM having four phases with unipolar excitation. It must be able to reach high speeds (12000 rpm), also be able to operate in different modes. The power stage should be isolated from controller for protection purposes. It should be also compatible to the outputs of the microcontroller. The power stage should have current limiting capability in order not to let current passing a phase increase beyond the rated value. Switching elements used in the power drive stage should be suitable for the rated voltage 280 Volts and rated phase current 5 Amps. Moreover they should be quite fast switches and if possible have some means of sensing the current passing them (in order be able to know current passing a phase without insertion of any resistors in the circuit).

Since it is desired for the motor to rotate for speeds till 12000 rpm, each switch should be able to operate at frequency 2.4 KHZ. This value is found using formula (3.1).

$$f = N_s * S / 60 \qquad (3.1)$$

where; f is the frequency at which switchings should occur, S is the

switching element for one complete rotation of motor (it is 12 for the novel converter used here. Studying Figs.2.16, 2.17 and 2.18, which show the switching states of the novel converter for different modes of operation, show that for 60^0 rotation of the motor each switch switches 2 times. Hence, for one complete rotation of motor, 360^0, each switch switches 12 times).

3.2. Basic Structure of The Power Drive

In this thesis the novel power converter circuit described in the previous chapter is preferred as the power drive stage. This power drive system is primarily designed to achieve a unipolar drive circuit form. Reasons for preferring this drive to other drives, were explained in detail in the second chapter but the most important reason is usage of only one switch per phase in this converter.

The general block diagram of the system is shown in Fig.3.1. Here, microprocessor is like the brain of the system. Four of its output pins are used for switching the four transistors of the power converter. It is not possible and wise to connect these outputs directly to the gate of the four IGTs, since Output voltage of the processor is 5 V and this voltage is not enough to turn on the IGTs. Moreover, there should be an isolation between controller part and high voltage part to protect controller from any damage if somehow one of the switches burns out. For these purposes the isolation circuit is placed at the gate of the IGTs (see Fig.3.1).

When one phase is on as there is a high voltage supply and low resistance, current passing the phase will be higher than the rated phase current. For a supply voltage of 300 volts and phase resistance of 7.5 ohms, the phase current will reach 40 amperes. To limit the current at rated phase value a "Current Limiter" is required. The value at which current will be limited can be determined both by software (microprocessor) and hardware. In the general block diagram of the system there is a block called "Enable Circuit of Current Limiter". The

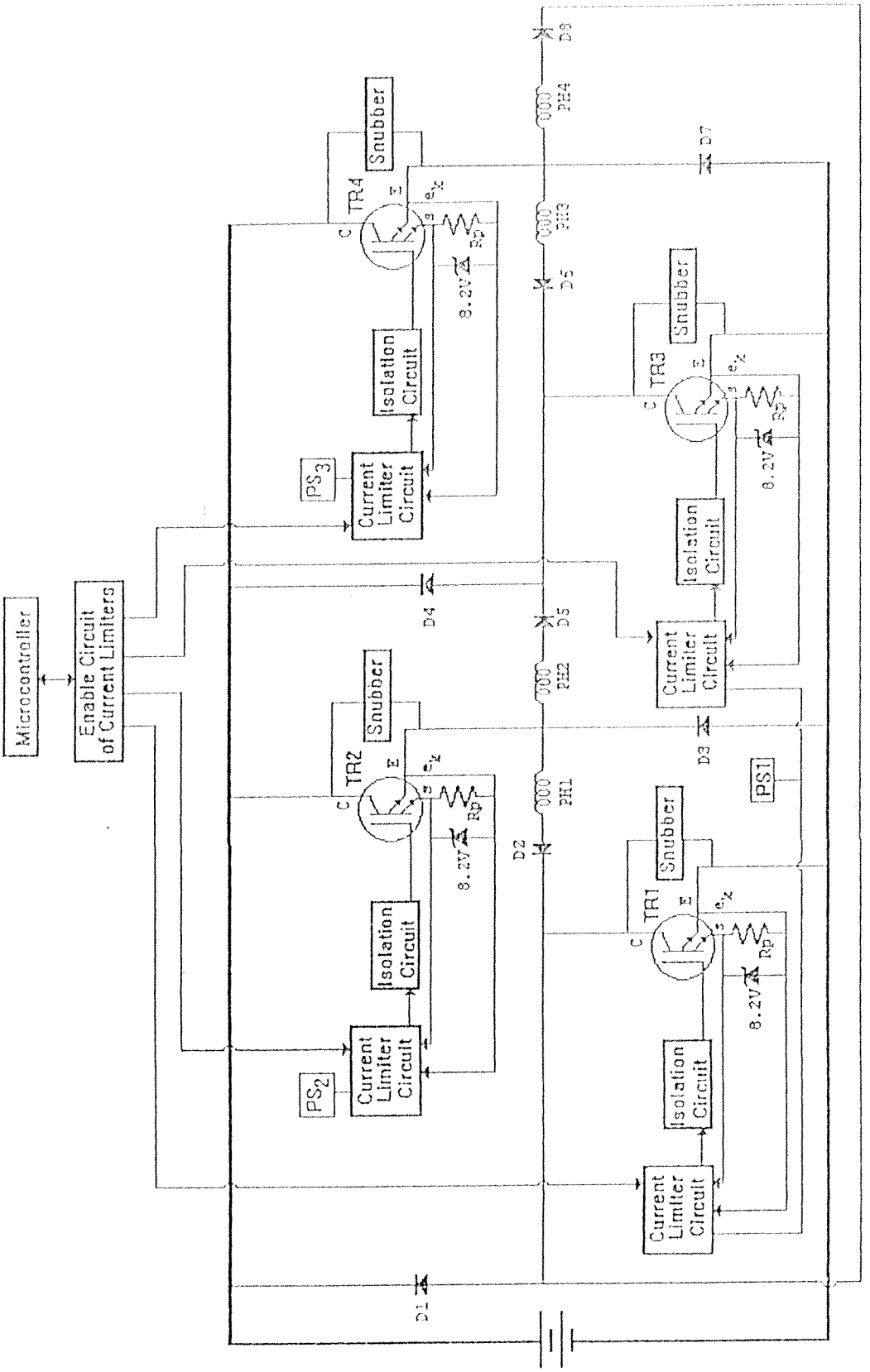

Figure 3.1 General Block Diagram of the System.

(PS : Power Supply)

at each time, since it is not required for all the limiters be active all the time. Even sometimes (e.g. in two phase on operation) some of them should be inactive as will be explained later. The "Snubber" block in the Fig.3.1 is used to reduce the turn off switching losses for the IGTs and protect them from over voltages. In Fig.3.1 PS1, PS2 and PS3 are 10 Volt power supplies.

Explanation and detailed circuit diagram of all the blocks shown in Fig.3.1 will be given in the coming sections.

There are four switching elements controlled by the microprocessor. In the section below the choice of these switching elements are discussed.

3.3. Selection of Switching Elements

In section 3.1 it was stated that the switching elements which can be quickly switched on and off must be used. Thyristors are disadvantageous when the switching speed is concerned, as generally they are slow devices. Also the cost of a high speed thyristor is much more than a BJT or MOSFET. A MOSFET is faster than BJT also to turn on and off a MOSFET is very easy compared to BJT. MOSFETs are voltage controlled devices. Their on state resistance r_{dson} is rather high and causes considerable power dissipation. On resistance of a 15 A, 450 V MOSFET is typically 0.3 - 0.4 ohms [21]. The power loss on the MOSFET is 7.5 - 10.0 W for a current of 5A. The gate drive circuits of MOSFETs are simple, as they require a low current injected from the gate. MOSFETs are very expensive. From the point of power losses BJT has a lower dissipation. V_{cesat} of a BJT is typically 0.3 - 0.5 V and for a current of 5 A the power loss is 1.5 - 2.5 W [21] which is lower than a MOSFET. To drive this BJT a base current of 0.7 - 0.9 is needed [21]. The base drive circuit of BJTs is expensive compared to the gate drive circuit of a MOSFET.

An IGT (Insulated Gate Transistor) is a power switching

device that combines the advantages of BJTs and MOSFETs. An IGT has high input impedance, like MOSFETs, and low on state conduction losses, like BJTs. The gate characteristics of the IGT transistor are similar to power MOSFETs but its equivalent r_{dson} drain resistance is ten times lower. It is a voltage controlled device and requires only a small input current. This simplifies and reduces the number of discrete elements required.

Consider the IGT7E20CS transistor (25 A ,500 V) which is a current sensing IGT. This transistor is a MOS-Gated power switching device combining the best features of power MOSFETs and bipolar transistors with current sensing pilots. The result is a device that has the high input impedance of MOSFETs and the low on state conduction losses of bipolar transistors. Data sheets of this transistor are in the appendix A. The transistor features are as follows:

- Ultra fast turn on,150 ns typical
- Voltage controlled turn on/off
- Current sensing pilot

One important facility of this IGT is that the voltage at the sense pin of this transistor is proportional to the current $I_{collector}$. Hence By using this transistor one can find the value of current in the windings without any need for insertion of a resistor. Therefore it seems that this IGT satisfies all the requirements for the switch that is suitable for our power drive. Therefore, in this work IGT7E20CS transistors are used as the switching elements.

In data sheet of this transistor the variation of collector current and the sense pin voltage for currents below 10 Amps is not shown precisely. On the other hand ,in this work, it is required to know the value of collector current (hence phase current) precisely. Using test circuit shown in Fig.3.2. one can find the voltages at current sense pin of this transistor (Vp values) corresponding to different $I_{collectors}$. These values are found and tabulated as shown in Table 3.1.

Table 3.1 Voltages at Sense Pins Corresponding to Various Collector Currents.

Collector current I_c (Amps)	Sense pin voltage Vp (mvolts)	Collector current I_c (Amps)	Sense pin voltage Vp (mvolts)
0.5 A	400 mv	4.5 A	810 mv
1 A	630 mv	5 A	820 mv
1.5 A	700 nv	5.5 A	840 mv
2 A	740 mv	6 A	860 mv
2.5 A	760 mv	6.5 A	880 mv
3 A	780 mv	7 A	900 mv
3.5 A	790 mv	7.5 A	920 mv
4 A	800 mv	8 A	940 mv

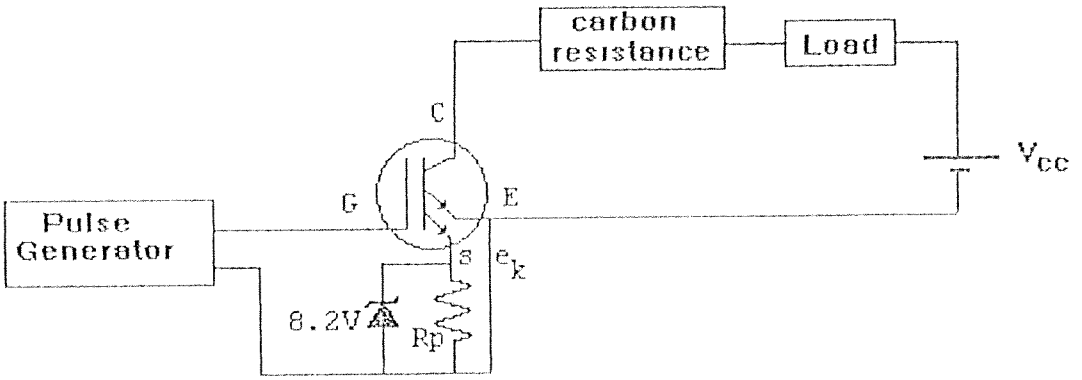

Figure 3.2. Circuit Used for Finding Values in Table 3.1

In power transistor switching circuits, shunt snubbers (dv/dt limiting capacitors) are often used to reduce the turn off switching loss or prevent reverse biased second breakdown. Other names of shunt snubber are current snubber and turn off snubber. The snubber circuit designed for the IGT used is shown in Fig.3.3. Here energy is stored in the capacitor and is dissipated during its discharge. During turn off the capacitor will charge by the load current. The capacitor voltage will appear across the transistor and the dv/dt is:

$$dv/dt = I_{load}/C \tag{3.2}$$

During turn off the collector emitter voltage must rise in relation to the fall of the collector current and dv/dt is:

$$dv/dt = V_{cc}/T_f \tag{3.3}$$

From equations (3.2) & (3.3) we have: $C = I_{load} * T_f / V_{cc}$ (3.4)

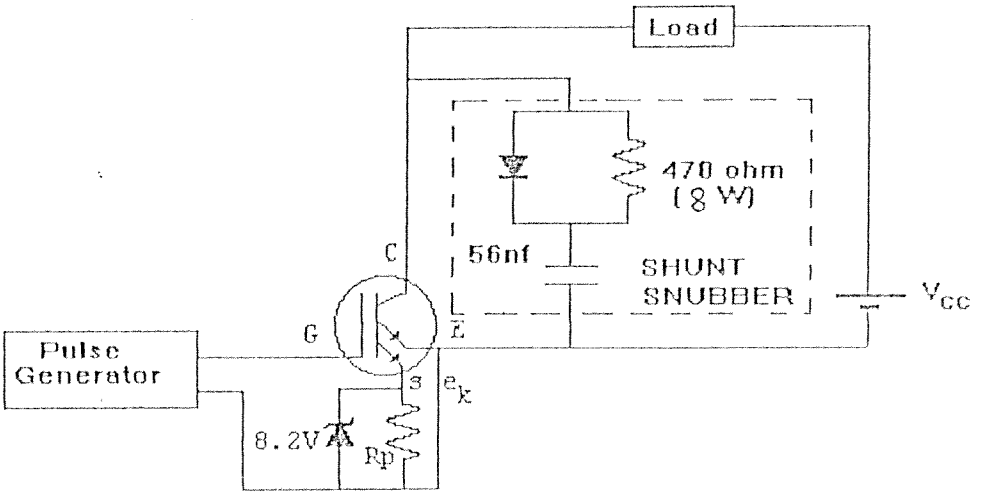

Figure 3.3. Snubber Circuit

In the following page numerical values of R and C of the snubber are calculated.

Design parameters:

$T_{fi(max)}$:Current fall time 90% to 10%.

$T_{fi(max)}$ =1.6 microsec. (see appendix A)

$I_{c(max)}$:Maximum load current.

$I_{c(max)}$ =10 Amps (We take it as 10 Amps for our SRM)

$V_{ce(max)}$:Maximum collector emitter voltage.

$V_{ce(max)}$ =310 Volts (Supply Voltage is 280 V)

f : Maximum operating frequency

f = 2.5 KHZ (Although for speed 12000 rpm this value is 2.4 KHZ, for safety it is taken as 2.5 KHZ)

Using formula (3.5) (The derivation of this formula is shown in reference [26], and it is shown that it guarantees that the current in the transistor will be reduced to near zero by the time V_{ce} has risen to $V_{ce(max)}$) the minimum value of the capacitor is found as 51.6 nf.

$$C_{min} = I_{c(max)} * T_{fi(max)} / V_{ce(max)} \qquad (3.5)$$

Let's take the capacitor value as: C = 56 nf

In choosing the value of R, the discharge time RC should be considered. We would prefer that the capacitor be essentially discharged (through RC) at the end of switching period T_s. A discharge time of one third the switching period T_s, is usually adequate [26], that is:

$$3RC = T_s = 1/f \quad \text{therefore} \quad R = 1/3fC \qquad (3.6)$$

Hence $R_{(max)}$ =2380 Ohms.

The discharge of C is limited by R. Increasing R increases the discharge time which will be about 4RC. We take the value of R as: R = 470 Ohms (8 Watts), Reason for choosing such a value for R , in addition for its simplicity to be found in local market, is that the discharge time of the capacitor when the transistor is turned on is:

$4RC = 1.0526*10^{-4}$ i.e. $4RC = 0.1$ ms ,and this is less than T=1/2*2.5KHz=0.2 ms (So it is guaranteed that the capacitor is fully discharged before the switch is turned off). Therefore, these values of R & C satisfy required conditions. Now let's check that the turn on current in the transistor due to the capacitor discharge , I_{dis} is not a significant portion of $I_{c(max)}$.

$$I_{dis}(max) = V_{ce(max)}/R = 0.659 << 10 \text{ Amps} \qquad (3.7)$$

Therefore these R and C values satisfy this condition also. It is Shown in [22,23] that the maximum dissipation of RC can be found using formula (3.8) as:

$$P_{r(max)} = CV_{ce(max)}^2 f/n = 8 \text{ W} \qquad (3.8)$$

Note that if we had used higher value capacitors, then value of $P_{r(max)}$ would come out to be higher. This is not a desired thing since a power resistor with high heat dissipation ratings is expensive and is a heat source in the system. By examining the V_{ce} figures shown in the test results chapter one can assure that the design is correctly made.

3.5. Isolation of IGT Transistor and Microprocessor

Fig.3.4. shows the microprocessor and the power converter of our SR motor. For operating IGTs as switches, an appropriate gate voltage must be applied to drive the transistors into the on state. The control voltage should be applied between the gate and emitter terminals. In the power converter circuitry of this work, four transistors exist. Two of these transistors have their emitters connected to the ground terminal of the main DC supply. Emitters of the other two transistors are connected to different places (see Fig.3.4). Therefore, the control voltage which should be applied between the gate and emitter terminals of four transistors, faces the grounding problem (as microprocessor has one ground but emitters of the four transistors aren't connected to the same place). In order to get rid of this

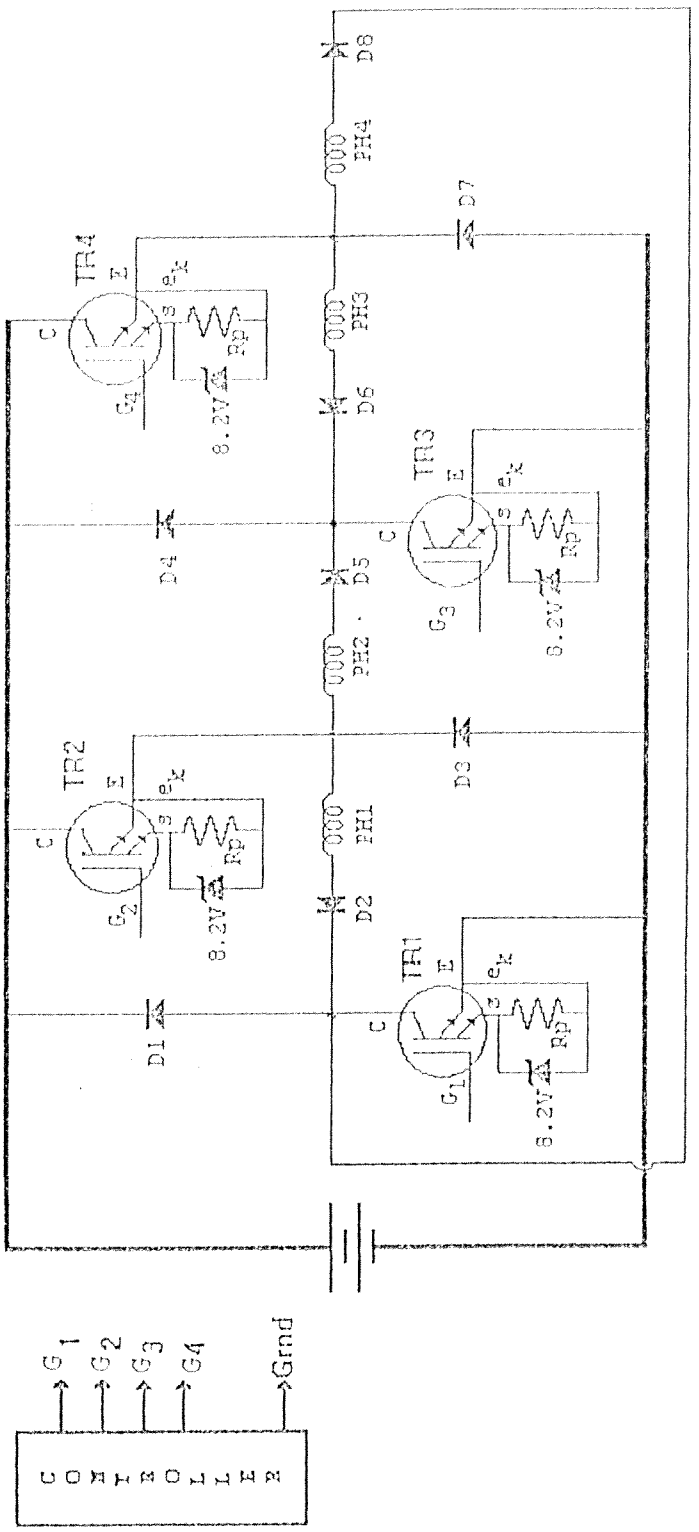

Figure 3.4. Microprocessor and Power Converter of SR Motor

grounding problem and also isolate (hence protect) controller circuits from high voltage part an isolation circuitry is designed. Note that if by some unknown reason, one of the transistors burns out, the isolation circuits will protect microprocessor from any damage.

Isolation stage: There are basically two ways of floating or isolating the control or gate signal with respect to ground. i.e. using;

1. Pulse transformers
2. Optocouplers

In this work optocouplers are used in the power drive. Optoelectronic components transmit electronic signals without electrical connections.

For operating IGTs used in this work as switches, a minimum gate voltage of 7 Volts must be applied to drive the IGT into the on state. Microprocessor voltage is 5 Volts. Therefore, in order for microprocessor to turn ON IGTs an interface circuitry is required to change the 5 V signals to 7 V signals suitable for turning on the IGTs. The isolation circuitry designed here does this function also. That is, it produce 9 V pulses to be applied to the gate of the IGTs. Note that although 7 Volts is sufficient to turn on the IGTs, here for safety purposes the isolation circuit applies 9 Volts to the gate of IGTs. Here, 4N25 optocoupler is used in the implementation. The optocoupler works in the phototransistor operating mode to give 9 volt output to the gate of IGTs.

Note that when at start microprocessor turns on, all its pins will be set (5 Volts), and since four of these pins should be connected to four IGTs, it means that when one turns on the system all the motor phases will be energized. To prevent this event an inversion circuitry is required. Function of this circuitry is to invert the signals coming from the processor. For this purpose a transistor (here, BC237) in the inverting mode is used.

Fig.3.5 shows the isolation and inversion circuit designed for inverting processor pulses, also producing 9 V pulses to be applied

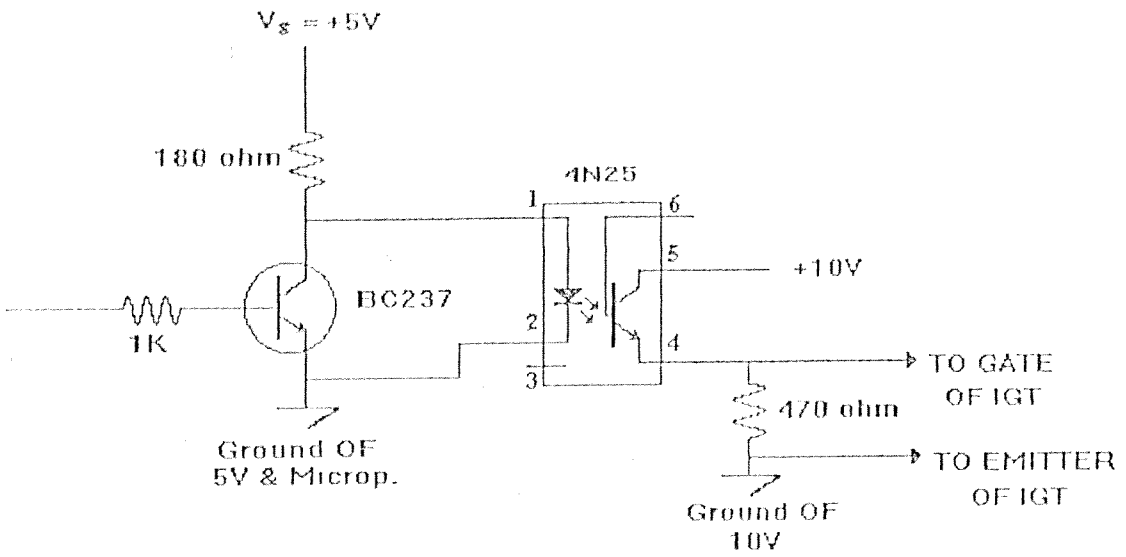

Figure 3.5 Isolation and Inversion Circuit Used Between IGT's and Controller Circuits.

to the gate of the IGTs. The PCB layout of this circuit is given in appendix B. As seen in data sheet, the voltage drop of the diode is 1.2 V. Here pulses with 5 Volts peak are applied to the base of BC237. When the transistor BC237 becomes SAT, the input current I_{diode} will be: I_{diode} =21 mAmps. (Which is quite higher than the 3.2 mAmps that is the minimum I_{diode} that can make the transistor inside the optocoupler enter saturation.)

3.6. Power Dissipation and Heat Sink Calculations

Transistor is an expensive and critical item in the power converter circuit. For this reason, power dissipation over it has to be calculated and on the basis of calculation, necessary cooling of transistors has to be arranged by proper means. However if other heat dissipating elements as in this case diodes exist their dissipations should also be considered in order to implement proper cooling.

Power dissipation in the switching transistor consists of:

i) power dissipation on the transistor due to switching losses, i.e. turn on and turn off switching losses which is found from the formula (3.9) [23].

$$P_s = [V_{ce(max)} * I_c * f_s * (t_r + t_f)]/4 \qquad (3.9)$$

Where; $V_{ce(max)}$ is the maximum collector emitter voltage, I_c is the max collector current (taken as 5 Amps). f_s is the switching frequency ,and t_r & t_f are the rise time and fall times of the transistor respectively.

Hence : $P_s=(250*5*5KHz*(150*10^{-9}sec+3*10^{-6}sec))/4=4.92$ W

which is approximately 5 Watts.

ii) Power dissipation due to conduction losses during saturation which can be found from formula (3.10) (leakage losses, during non_conduction times can be neglected since they are very small).

$$P_{on} = [V_{cesat} * I_c * (\text{duty cycle})] + [I_b * V_{be} * (\text{duty cycle})] \qquad (3.10)$$

P_{on} =1.3*5*50%=3.25 W (Since I_b is very small the second part in the equation is neglected). Hence, total transistor losses will be:

$$P_{transistor} = P_s + P_{on} = 5+3.25=8.25 \text{ W} \qquad (3.11)$$

For safety it is taken as 10 Watts. In this work one heat sink is used for two transistors. Therefore the total power dissipation of the heat sink for two transistors will be:

$$P_{HS,2tran.} = 2 * 10 = 20 \text{ Watts}$$

Power dissipation of the diodes is found using formula (3.12) as:

$$P_{diode} = I * V_{drop} * (\text{duty cycle}) = 5*1.5*50\% = 3.75 \text{ W} \qquad (3.12)$$

Now its time for determination of thermal resistance. Thermal resistance is the single most important parameter in heat sink selection, apart from mechanical considerations. For determination of thermal resistance first lets explain symbols below and find their values from data sheets in appendix A.

T_j : Maximum operating junction temperature
T_j =150 ^{0}C (from data sheet) For safety take it as 140 ^{0}C
T_c : Maximum allowable case temperature
T_A = 40 ^{0}C (Ambient temperature)
R_{JC} : Junction to case Thermal resistance
R_{JC} =1 ^{0}C/W (from data sheet)

Case temperature of each transistor is found using formula (3.13) [24].

$$T_c = T_J - P_{transistor} * R_{JC} = 140-10 = 130\ ^0C \qquad (3.13)$$

Using formula (3.14) [24] thermal resistance between case and ambient can be found.

$$T_c - T_A = P_{transistors} * R_{CA} \qquad (3.14)$$

$$130-40=20*R_{CA} \qquad \text{Hence: } R_{CA}=4.5$$

In this work two transistors are mounted on same heat sink. Therefore, to have electrical isolation between them insulators (Washers) are used between transistor case and heat sink. Thermal grease is used between the insulator and heat sink, also insulator and IGT, for better conduction of heat to and from washer. Thermal resistance of the insulator 0.002" film is 0.47 ^{0}C/W per square inch of area. Since area of the insulator for two transistors is one square inch, the thermal resistance of the insulator is : R_w =0.47 ^{0}C/W
So the thermal resistance of the heat sink becomes:

$$R_{HS} = R_{CA} - R_W = 4.5 - 0.47 = 4\ ^0C/W \qquad (3.15)$$

For the diodes thermal resistance of the heat sink is calculated by formula (3.16) [24].

$$T_C - T_A = P_D * R_{CA} \qquad (3.16)$$
$$R_{CA} = 125-40/4 = 21.25 \ {}^0C/W$$

So thermal resistance of diodes is 21.25 ^{0}C/W. Therefore, in the circuit implemented proper heat sinks are used for them.

For two transistors the thermal resistance of the heat sink was calculated to be 4 ^{0}C/W (In the circuit implemented V 6716 Z/K heat sink which has 2.3 ^{0}C/W thermal resistance value is used for safety, two transistors are mounted on the same heat sink).

3.7. Current Limiter

When one phase is on as we have a high voltage supply and low resistance, current passing the phase will be higher than the rated phase current. For a supply voltage of 300 volts and phase resistance of 7.5 ohms, the phase current will reach 40 amperes. To limit the current at rated phase value a "Current Limiter" is designed. This circuit limits current at some reference value by turning off the transistor when current exceeds the reference level. Then as current reduces to a specified value it turns on the transistor and lets current increase again. This procedure repeats and as a result of these chopping it is as if current is fixed at the rated value. The general block diagram of the current limiter is given at Fig.3.6. To limit the current at rated phase value a feedback of the phase current is required. As current sensing IGT transistors are used in our converter, we are able to know the collector current, hence the phase current ,by just considering the voltage at the sense pin (see chapter 3.3). So the current limiter designed here is based on the use of the voltage at sense pin. Here, as it is shown in Fig.3.6, this voltage is first amplified and then compared with a reference voltage which corresponds to the reference current at which current should be limited. The reference voltage can be the output of a hardware circuitry "Voltage

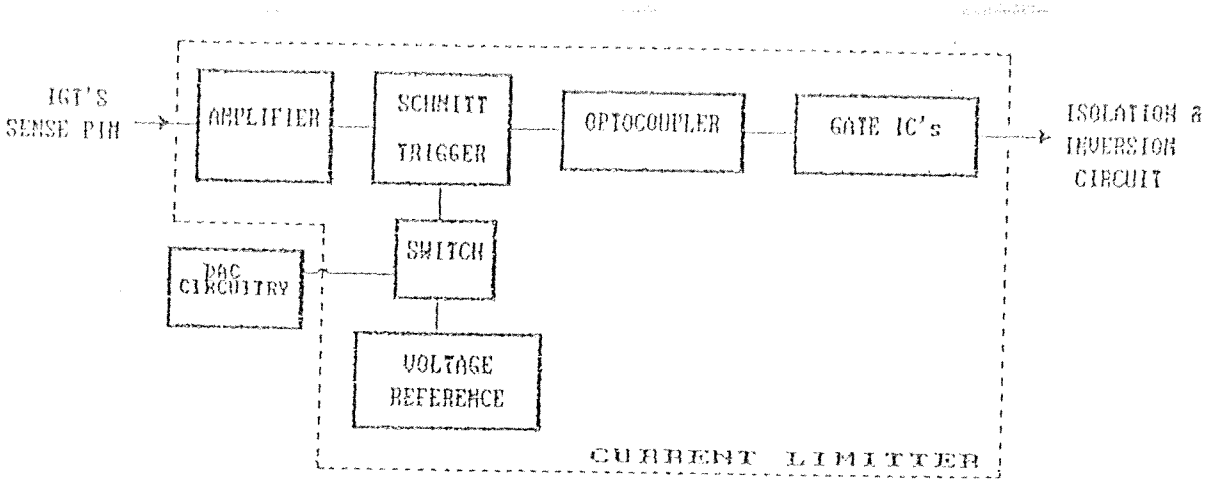

Figure 3.6 General Block Diagram of the Current Limiter.

Reference" (its value should be change manually) or it can be controlled by software (using microprocessor and a DAC circuitry). There is a switch to choose one of these. There is an optocoupler in the current limiter circuitry to prevent grounding problems and making grounds same for the +5 Volt V_{cc} of gate ICs and other inputs of the block "Gate IC's" which will determine the state of the transistor to be off or on. This is explained in detail as follows.

The detailed circuit diagram of the current limiter is given at Fig.3.7 and its PCB is in the appendix B. As was mentioned previously, current feedback is taken from the sense pin of IGT. Since the voltage at the sense pin is low it should be amplified in order to be able to compare it with the reference voltage V_r. Amplification is done using an opamp in non-inverting configuration. Reference voltage is set to 4.7 volt (for 5 A phase current). Gain of the amplifier is set to 5.7 in order to produce the 4.7 V at the time that phase current is 5 A (the sense pin voltage is 0.82V when phase current is 5 A (see Table 3.1) hence 5.7 * 0.82V = 4.7V). V_r can be produced by two

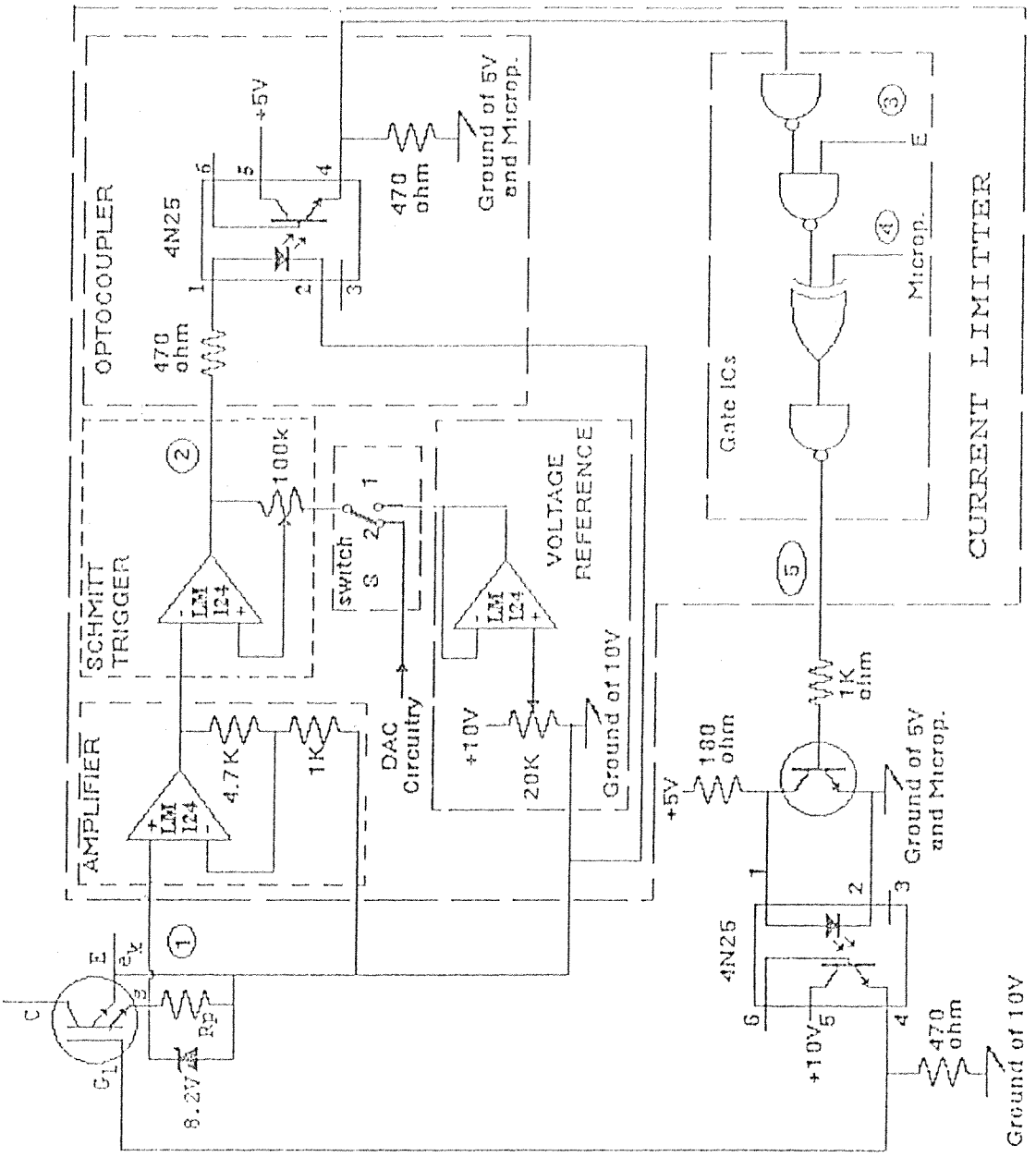

Figure 3.7 Detailed Diagram of the Current Limiter.

different circuits. One can choose one of these circuits be active by placing the switch 'S' in positions 1 or 2. If the switch 'S' is at position 1, V_r will be produced by the " Voltage reference circuit " as shown in the figure. Here V_r is controlled by a potentiometer so the current limit level of the windings can be changed according to the rated current values required. Therefore one should play with the potentiometer manually in order to set V_r to a new value. If the switch 'S' is brought to position 2, V_r will be the output of the DAC circuitry. In this case, as will be explained in detail in chapter V, value of V_r is determined by the microcontroller. That is, the microcontroller changes the current limit level according to the software decision and there is no manual adjustments. The output of the schmitt trigger enters an optocoupler to prevent grounding problems and having same ground for the +5 Volt V_{cc} of gate ICs and the 'E' and 'm' inputs to the gates which come from "enable circuit" and microprocessor respectively. Optocoupler's output is inverted and then NANDed with enable signal, and result is EXCLUSIVE ORed with the data coming from the microprocessor and result is inverted. Now let's give some more explanation on the operation of this current limiter. Consider one phase of our motor. When transistors T1 & T2 are on, the phase current and corresponding to it the voltage at the sense pin of T2 increases. While the phase current is below its rated value the output of the schmitt trigger is high and the output of the current limiter is same as microprocessor port. When the phase current goes above rated value, output of the schmitt trigger becomes low causing change of output of the current limiter, hence turning off the transistor. As T2 turns off the phase current decreases below its rated value. Therefore transistor 2 switches on again. The full supply voltage is applied to the winding and the current increases to slightly above rated. This cycle is repeated through out the excitation time of this phase, so that the winding current is held near its rated value by an ON/OFF state closed loop control. Since all four transistors in the converter should be able to chop, for each transistor a current limiter is required. That's why there are four current limiters in the power drive system. Each current limiter circuit has an 'E' (enable) signal that enables or disables that current limiter. This signal is the output of the "ENABLE

CIRCUIT" ,which is explained in the next section. When this signal is HIGH that current limiter is enabled and when it is LOW the current limiter is disabled hence current can increase above the rated value which is 5 Amps. In other words, when the current limiter of an IGT is disabled, current passing through that transistor can go above 5 Amps. This a desired property when for example the motor operates at two phase on mode. (for example phases one and two are on and hold at 5 Amps. (Transistors 1 and 3 chop and current passing them is 5 A, but transistor 2 is on and its current will be 10 Amps.)

Table 3.2 is the truth table of the current limiter circuit. Note that when microprocessor port is set high the related transistor is desired to be OFF and when the port is set to zero the transistor is ON.

When $I_{collector}$ > 5 Amps then (1) >0.52 Volts and (2) becomes LOW.

When $I_{collector}$ < 5 Amps then (1) <0.52 Volts and (2) becomes HIGH.

Table 3.2 Truth Table of the Current Limiter Circuit.

Point (2)	Point (3)	Point (4)	Point (5)	TR gate
L I_c>5A	L Disabled	L TR ON	L	H TR ON
L I_c>5A	L Disabled	H TR OFF	H	L TR OFF
L I_c>5A	H Enabled	L TR ON	H	L TR OFF
L I_c>5A	H Enabled	H TR OFF	(*)	(*)
H I_c<5A	L Disabled	L TR ON	L	H TR ON
H I_c<5A	L Disabled	H TR OFF	H	L TR OFF
H I_c<5A	H Enabled	L TR ON	L	H TR ON
H I_c<5A	H Enabled	H TR OFF	H	L TR OFF

(*):Impossible to occur.

Function of this circuit is to determine which current limiters be active at each time. In the previous section it was explained that for each transistor in the power converter a separate current limiter is required. Therefore there exist four current limiter circuits in the power drive. Now the question that arises here is: Which current limiters should be enabled and which ones be disabled at a time? In order to be able to answer this question transistor states and current waveforms of phases for different operating modes and different direction of rotations are considered and results obtained are put in Table 3.3. In fact this table shows the truth table of the enable circuit. Using the table following state equation for enable signals of four current limiters is found.

E1,E3=a+a'.[(T1.T2.T4'+T2'.T3.T4).b+(T1.T2'.T4+T2.T3.T4').b']
E2,E4=E1',E3'

Fig.3.8 shows the circuit diagram of the "ENABLE CIRCUIT" that produces the four enable signals of the four current limiters. In the appendix B you can find the PCB of this circuit.

Table 3.3 Truth Table of the Enable Circuit.

TR1 (T1)	TR2 (T2)	TR3 (T3)	TR4 (T4)	CW (b)	1PHON (a)	E1,E3	E2,E4	
1	1	*	0	1	0	1	0	For 2PHON
0	1	1	*	1	0	0	1	CW also
*	0	1	1	1	0	1	0	Half step
1	*	0	1	1	0	0	1	CW
1	1	0	*	0	0	0	1	For 2PHON
1	0	*	1	0	0	1	0	CCW also
0	*	1	1	0	0	0	1	Half step
*	1	1	0	0	0	1	0	CCW
*	*	*	*	*	1	1	0	For 1PHON

* : Don't care

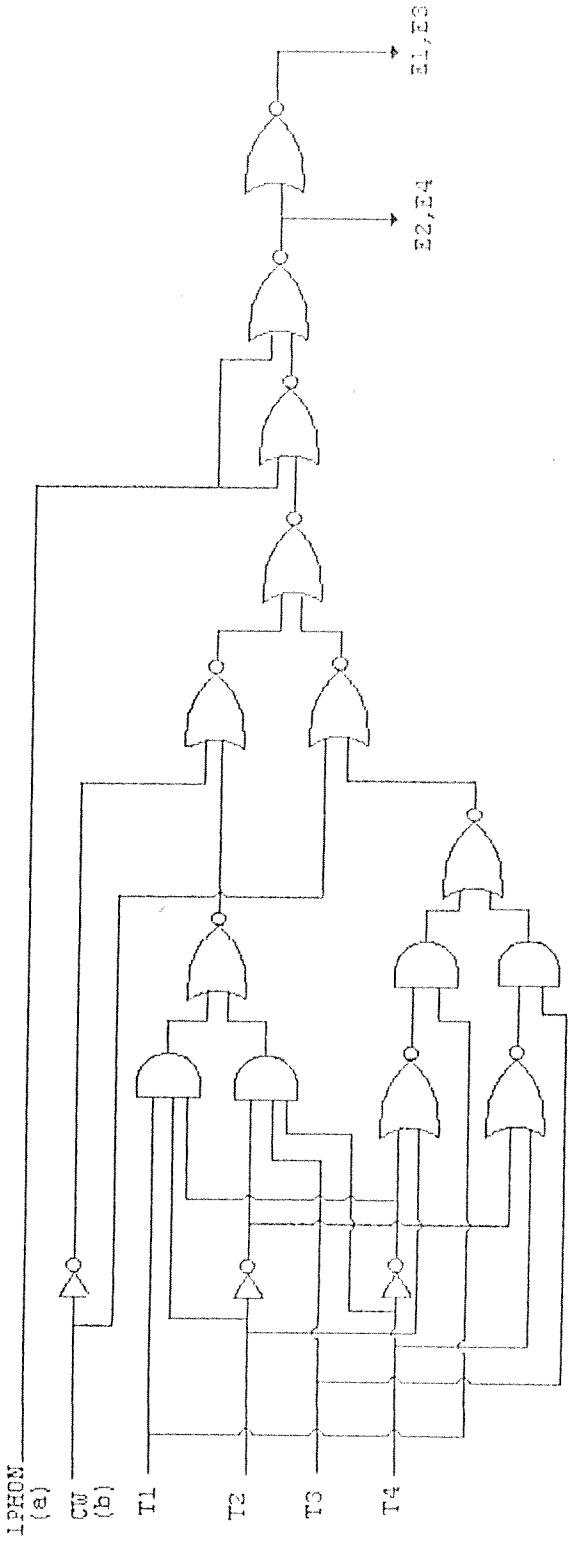

Figure 3.8 Enable Circuit of Current Limiters.

CHAPTER IV

CLOSED LOOP CONTROL AND POSITION DETECTION OF ROTOR

4.1. Introduction

Closed loop control has lots of advantages over open loop control. Some of these advantages are as follows:

- Providing maximum system reliability and repeatability
- Providing maximum performance from a given motor
- Permits operation over the entire speed range capability of the motor.
- Versatility of control
- Smoother speed

Although closed loop control has all these advantages it has one important disadvantage which is the need for a feedback device. That is, in a closed loop switching motor system the instantaneous rotor position should be detected and fed back to the control unit. There are mainly two methods of rotor position detection; These are using an incremental optical encoder or waveform detection. In this chapter, these two techniques are discussed and compared. A literature survey is also done on waveform detection schemes using phase current, motional voltage and phase inductance. Moreover, a comparison is done between three different methods of rotor position detection based on the use of phase inductances.

Although the survey has shown that for detection of position of rotor, waveform detection method is the best method, the aim here is restricted to implementing a flexible drive which can be easily modified to accomodate waveform detection. In the implementation here, the position feedback is obtained from a specially designed position

encoder (Senturk [21]).

4.2.Position Detection Techniques

In a closed loop system a position detector generates a pulse which signals to the control unit that a step has been completed. There are two types of position detection techniques:

1. Incremental encoder.
2. Waveform detection.

In the section below these topics are discussed.

4.2.1. Encoders

A position encoder translates the motor displacement information into an electrical signal in pulse form. The pulses generated by the encoder are then fedback to the motor driver via a controller. Thus the motor is normally started by a single pulse, and the pulse which causes phase switchings and consequently continuous motor shaft rotation are derived from the encoder. The timing of these pulses is a function of the mechanical position and the speed of rotation of the motor [25].

The encoder used may be a high resolution encoder or a low resolution one. With a low resolution encoder only position of some specified fix points of the rotor are specified. But, by using some hardware position of other points of the rotor can be determined as well. A high resolution encoder is more expensive than a low resolution encoder. It determines continuously position of different points of the rotor.

Figure 4.1 shows the block diagram representation of a closed loop control scheme for motors employing an encoder, usually of the optical or magnetic type, mounted on the motor shaft.

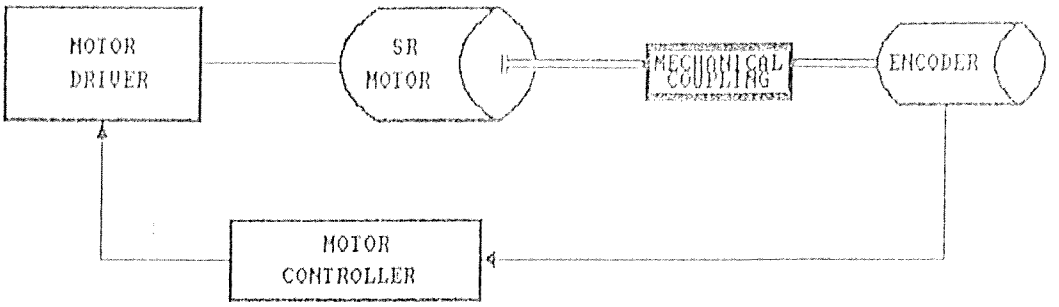

Figure 4.1. Closed Loop Control Employing Encoder.

4.2.2. Waveform Detection

The block diagram of a closed loop waveform detection system is shown in Fig.4.2. The feedback pulses in Fig.4.2 are generated by WAVEFORM DETECTOR inserted between the MOTOR DRIVER and the MOTOR.

The waveform detector extracts positional information from the electrical variables of the motor phases. These pulses are used to drive the motor in a closed loop sense. The waveform detector is an entirely electronic device with no moving parts, and therefore no mechanical linkage to the motor. This allows the motor to be located remotely, while the detector, power supplies, and driver circuitry can be located away from adverse environmental conditions. If desired, the detector can be built directly into the controller logic. It is physically very small and inexpensive.

The waveform detector can be one that senses the peaks, slopes , points of inflection, or zero crossings of the currents, voltages or fluxes that exist in the motor. For instance, it has been shown by Kuo [23,24] that the positive or negative peaks of the phase currents of a variable reluctance motor have predictable and

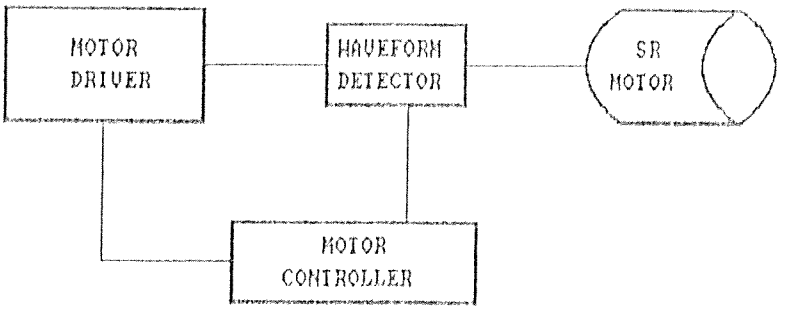

Figure 4.2. Waveform Detection Closed Loop Control.

controllable properties for feedback control purposes. Other signals of possible use for waveform detection are induced voltages or the back in the phase windings. These topics will be discussed later in this chapter.

4.3. Advantages of Waveform Detection Over Optical Encoder

Several advantages of waveform detection over incremental optical encoders are presented in table 4.1.

Table 4.1 Advantages of Waveform Detection Over Incremental Optical Encoder.

	Incremental optical encoder	Waveform detection
Additional mechanical connections to the motor required	Yes	No
Cost	Higher	Lower
Needs mechanical adjustments	Yes	No
Needs electrical adjustments	Yes	No
Size	Large	Small
Needs set up or additional circuitry	Yes	No
Reliable	No	Yes
Position information	Quantized	Continuous
Can be located remotely from rotor	No	Yes

4.4. Waveform Detection Using Motional Voltage and Using Phase Inductance

Waveform detection can be based on the modulating effect on the phase current of the motional voltage (which in turn is a function of rotor position), or can use the rate of change of phase current (since the rate of current change is dictated by the incremental inductance of the phase circuit, and the incremental inductance is in turn a function of rotor position and phase current, rotor position can be deduced from a knowledge of phase current and its rate of change).

In article [29] the self synchronization with a measured induced voltage, obtained by a bridge circuit is explained and a motion induced voltage is detected by a specific auxiliary winding. In article [30] the angular position determination by means of a suitable measurement method of the back electromotive force induced in the winding is explained. Table 4.2, compares the waveform detection scheme using motional voltage and using phase inductances.

Table 4.2 Comparison of Waveform Detection Scheme Using Motional Voltage, and Using Phase Inductance.

	Using motional voltage	Using phase inductance
Operate successfully at low speeds	No	Yes
Operate successfully with chopper	No	Yes
Cost	Higher	Lower

The waveform detection scheme using motional voltage is unable to operate successfully at low speeds, because the motional voltage is zero, or with chopper drives, because the phase current is almost constant. But the waveform detection using phase inductance doesn't suffer from these problems.

In switched reluctance motors the inductance variation occurs

The rate at which changes in phase current occur is dictated by the position dependent winding inductance, so rotor position can be detected whenever phase currents are changing. Below we explain two methods for rotor position detection, based on the use of phase inductances. Note that the inductance method gives us the minimum inductance position. Only software can allow us to find other excitation points, on the assumption of constant speed.

4.5. Rotor Position Detection Using Variation of Chopping Characteristics.

We know that during chopping, the phase current swings around the required level at a rate dictated by the incremental inductance of the phase at that current level, and as the incremental inductance is rotor position dependent, the instantaneous rotor position can be deduced from the chopper characteristics . For normal operation of SR motor the phase current is either held at its rated value or reduced to zero, and, therefore there is the possibility of detecting rotor position from variation of chopping characteristics in a phase which is either ON (with phase current at rated) or OFF (with phase current zero). That is:

1. Chopping at rated current
2. Chopping at zero current

These two cases are discussed below.

4.5.1. Chopping at Rated Current

In this operating condition the phase current varies between $I+\delta I/2$ and $I-\delta I/2$,so during the rise time T_{rise} the current increases δI, and during the decay time Tdecay the current decreases δI. (see Fig.4.3)

In reference [28] it is shown that the current rise and decay times are proportional to incremental inductance. However, the most

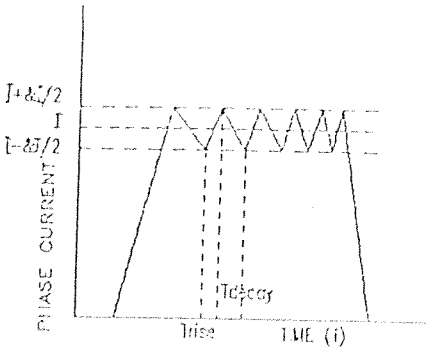

Figure 4.3. Current Waveform, When Chopping at Rated Current.

notable feature of the incremental inductance/rotor position characteristic at rated current is that around the position where stator/rotor teeth are misaligned there are four rotor positions corresponding to each value of incremental inductance [28]. Because of this ambiguity, continuous position detection is unreliable for this operating condition [28]. However, detection of a specific rotor position is possible. with the machine producing maximum motoring torque, for example, each phase is switched on at the misaligned teeth position and switched off at the aligned teeth position. The phase turn off position corresponds to the minimum incremental inductance [28], so this position may be detected at the low speed, by seeking the minimum rise or decay times in the chopping of the excited phase. The current rise and decay times are independent of speed at the aligned and misaligned torque positions as shown in reference [28]. In short, by monitoring the chopping characteristics for an excited phase it is possible to detect a single rotor position per step, and the most reliable indicator of rotor position is the current rise time at aligned and misaligned tooth positions.

4.5.2. Chopping at Zero Current

An alternative strategy for direct position detection with a chopper drive is to observe chopping behavior in a phase which is turned off. During normal operation of the drive, of course, the current in such a phase would be zero, but by setting the required current level to be a small fraction of the rated current, chopping behavior can be observed without diminishing the torque producing capability of the motor. Here continuous monitoring of rotor position is possible. In this situation the phase current increases from zero to δI during the rise time T_{rise} (see Fig.4.4). In summary, monitoring of chopping behavior in a phase which is turned off has the advantages that the rotor position can be deduced with no ambiguity and immunity from errors due to motional emf. However one should have rapid current decay and high sampling rate. Note that since in general a SR motor drive has a chopping mode, direct detection of rotor position by monitoring chopping behavior is a reliable and cost effective alternative. For detection of the position from chopping in a turned off phase, maximum immunity from motional effects is obtained by observing current rise time.

One important disadvantage of on_phase chopping and off_phase chopping for rotor position detection is that they are unable to detect position at the very highest speeds, where chopping operation may have ceased because the current build up time exceeds the phase excitation period. Below we explain a rotor position detection method which doesn't suffer above mentioned disadvantage.

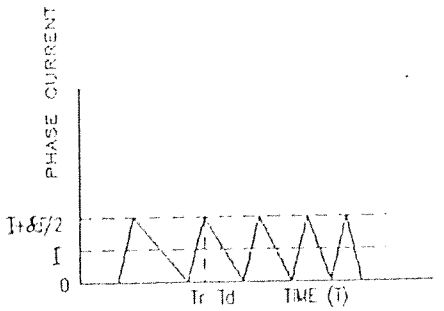

Figure 4.4. Current Waveform, When Chopping at Zero Current. (I Is a Small Fraction of the Rated Current.)

In general, the slope and/or the magnitude of the voltages or currents in the motor windings may be sensed to provide detections . If current is to be sensed, it should first be converted into a voltage. This is done by inserting a small resistor of known value in the current path and measuring the voltage across it. Then V/R gives the value of current. Consider the situation when the phase is first turned on. The phase current and flux linkage are zero, so the resistive voltage drop and motional are negligible, and the initial rate of current rise is, [28]:

$$di/dt(\text{at } i=0) = V/L \qquad (4.1)$$

In this expression the relevant incremental inductance is that associated with low phase current which leads to a well defined unambiguous relationship between current gradient and rotor position independent of operating speed. Winding current waveforms for a switched reluctance motor appear to be irregular, especially with a stationary rotor and at low speeds. However an analysis of current data [31] shows that simple mathematical models describe the relationship between the rate of rise of current and rotor position. Examining the rising part of current in a winding, with a stationary rotor, has shown that simple relationships can be found for describing the rate of rise of current as a function of rotor position.[31].

Closed loop control with a series resistance drive is implemented by repeatedly turning on the next phase in the excitation sequence and examining the initial current gradient. If the gradient matches the gradient obtained by turning on at the optimum rotor position for excitation change then the excitation change is allowed to proceed. However, if the optimum position has not been attained, the current gradient is incorrect, and the small phase current is reduced to zero, in preparation for another turn on attempt a short time later. So just by knowing the optimum switching angle (hence optimum rotor position for excitation changes) using a microprocessor one can control

the switching by above mentioned method. The technique of monitoring initial current gradient in the next phase to be excited is applicable to chopper drives. In that situation the technique has the advantages, over monitoring of chopping characteristics, that it is able to detect position even at the very highest speeds, where chopping operation may have ceased because the current build up time exceeds the phase excitation period. Note that the switches used in our drive are current sensing IGTs, hence we don't need to insert sensing resistors in series with phases and can use the voltage at the sense pins of the IGTs directly. Fig.4.5 shows the flow chart for closed loop control with rotor position detection using sense pin of IGTs.

Table 4.3, summarizes above mentioned characteristics of the three types of rotor position detection, based on the use of phase inductances.

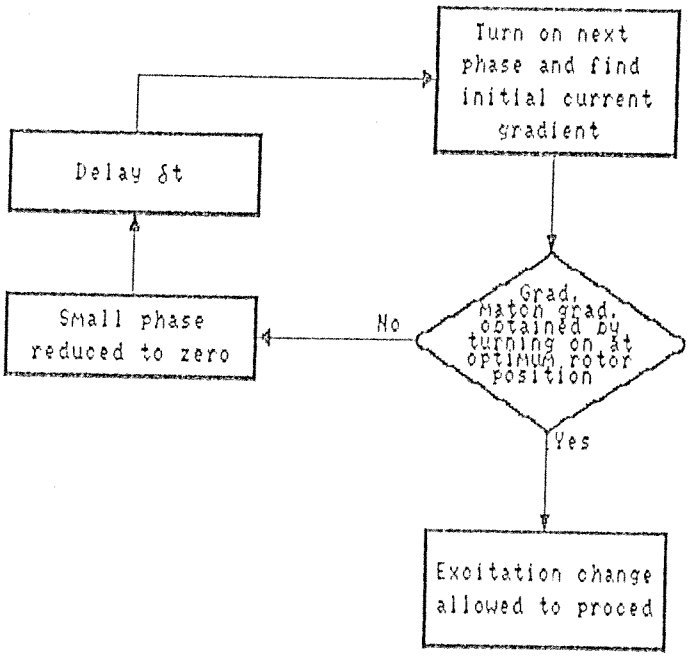

Figure 4.5. Flow Chart for Closed Loop Control with Rotor Position Detection Using Sense Pins of IGTs.

Table 4.3 Comparison of Different Methods of Rotor Position Detection Based on the Use of Phase Inductances.

	On phase chopping	Off phase chopping	Initial current rise
Reliable continuous position detection	No	Yes	Yes
Immune from errors due to motional	No	Yes	Yes
Able to detect position at very highest speeds (where current build up time is grater than phase excitation period)	No	No	Yes
Applicable to chopper	Yes	Yes	Yes
Circuit must ensure rapid current decay and high sampling rate	No	Yes	No

4.7. A Specially Designed Encoder Used in This Work

In previous sections different rotor position detection techniques were compared. It was concluded that waveform detection method is preferred to using optical encoders. But, position detection by waveform detection method is not in the scope of this thesis. That's why, in the application here, an optical encoder that was designed by Senturk [21] is used. Some modifications are done on this encoder to make the output of it compatible to the input of the microprocessor. The circuit diagram of the modified encoder is in figure 4.6. This modified encoder produce a pulse at the stable equilibrium position of each phase. Position information on intermediate positions is obtained as described in section 5.4.2.2. In chapter VI, operation of the modified encoder is tested and figures are presented showing the encoder's output for different speeds of the motor.

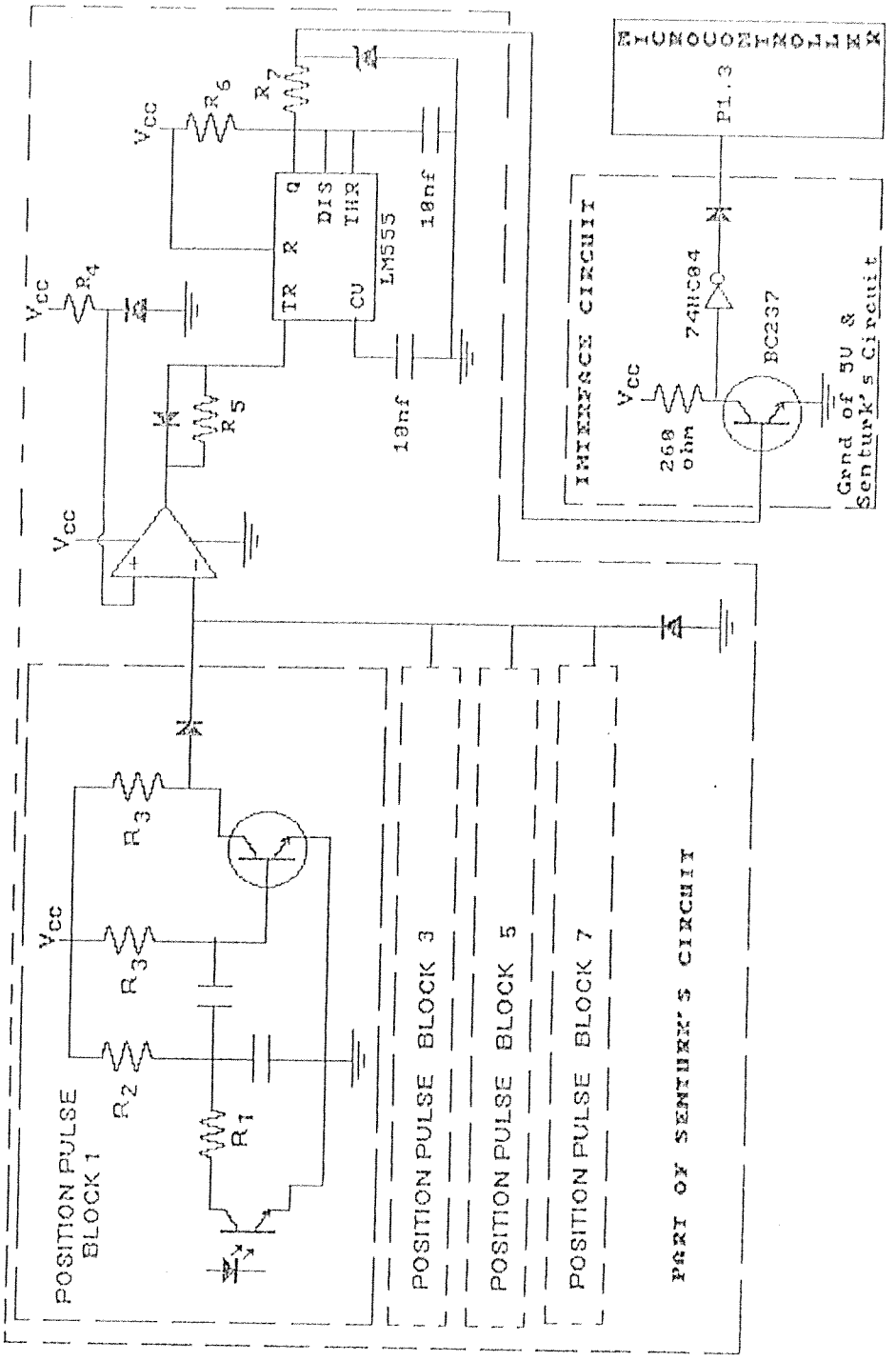

Figure 4.6. Circuit Diagram of the Modified Encoder

CHAPTER V

MICROCONTROLLER BASED CLOSED LOOP CONTROL OF A SRM

5.1. Introduction

Advantages of closed loop control to open loop control are obvious to everyone. One important advantage of a closed loop controlled SRM to an open loop controlled one is reliability of the drive. In a closed loop SRM system a position detector feedbacks the position of the motor to the controller. Each step command is issued only when the motor has responded satisfactorily to the previous command and so there is no possibility of the motor loosing synchronism.

At this stage the aim is to implement a flexible system on which any desired microprocessor based speed control may be achieved in future, and that involves development of control strategy either through models or using approaches which rely on knowing input and outputs of the system.

In any microprocessor based system, software has an important role and it should be written cleverly. The software written in this work is aimed to be a user programmable software. That is user be able to communicate with the software and determine the value of different control parameters, under which motor should be rotated. Therefore one can investigate motor performance in detail, under various control parameters. Hence important results may be obtained for a sophisticated control in future.

It is tried for the software written to be in modular form in order to be able to use its modules in future softwares.

In this chapter it is also explained how the microcontroller can change the three control parameters; phase current, advance angle, and conduction time.

5.2. Microprocessor Based Closed Loop Control

Nowadays, microprocessors are available cheaply. They have huge capabilities and some of them are designed specially for control purposes. Therefore, utilization of a microprocessor in control of a SR motor seems to be essential. This chapter discusses a microprocessor controlled closed loop system designed to drive a four phase SRM. The general block diagram of the system is shown in Fig.5.1. Here the microcontroller sends out signals to the "Power Stage" and "DAC Circuitry" to switch transistors (energize the phases) and also determine the phase current reference level. The "Power Stage" block was explained in detail in the third chapter. Its inputs are signals from microprocessor and its outputs are the signals to the gates of the transistors, hence energizing phases and rotation of motor. The "DAC circuitry" produces a voltage as the output. This voltage is the reference voltage at which current limiter limits the phase current. The value of this voltage is determined by the signals coming from

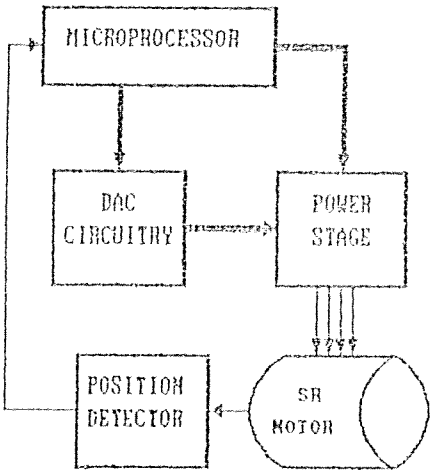

Figure 5.1. General Block Diagram of the Microprocessor Based Closed Loop Control System.

microprocessor to inputs of the DAC circuitry. The "Position Detector" block sends pulses to the processor when rotor is at some specified positions. In short determines position of rotor. Therefore when microprocessor sends a signal to energize a phase (rotate the motor), this signal goes through some blocks. Whether motor has rotated or not is shown by "Position Detector" block which sends a signal to microprocessor to show rotation is done. Now microprocessor can decide what to do next.

The microprocessor is, of course, the central component in any microprocessor based systems. Below the processor and the card used here is described. Note that in this work aim is not to design a processor card, which nowadays has become a fairly standard process, but, is to develop a system which is controlled by the microprocessor. That's why, the Intel's EV80C51FB Evaluation board is used as the processor card. Although using this ready card has saved our time and has given us debugging capabilities (for the programs written), it has unfortunately put some limitations for us as are explained below.

5.3. Description of The Microcontroller and EV80C51FB Board

The microprocessor used in the implementation here is the Intel 80C51FA which is an 8 bit control oriented microcontroller based on the 8051 architecture. Being a member of the MCS-51 family the 80C51FA uses the same powerful instruction set, has the same architecture, and is pin compatible with the existing MCS-51 products [32]. In addition to all the facilities of 8051 this microcontroller has Programmable Counter Array (PCA), which provides more timing capabilities with less CPU intervention than the standard timers, hence reduced software overhead and improved accuracy.

In this work Intel's EV80C51FB Evaluation board is used as the processor card. This card is based on the Intel 80C51FA processor. Block diagram of the EV80C51FB board and its printed circuit board are shown in Fig.5.2a & b. The pin diagram of the board is shown in Appendix D. There are two serial ports available on this board [33].

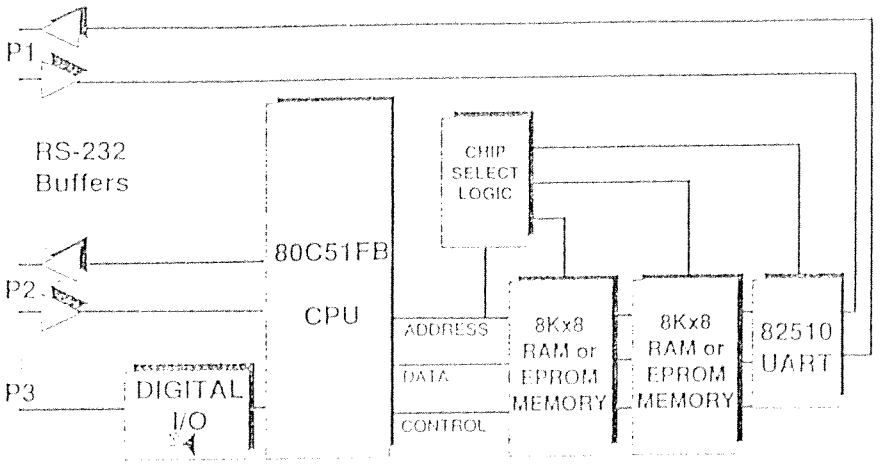

(a)

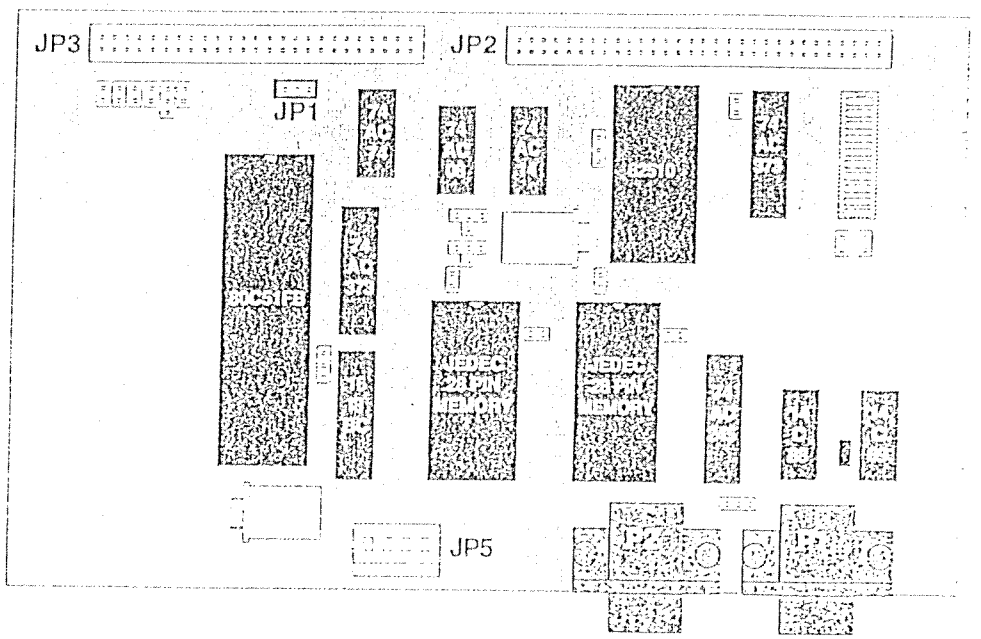

(b)

Figure 5.2. EV80C51FB Board: a) Block Diagram
b) Printed Circuit Board

The first (P1) is an external 82510 used as the primary communication port to the host PC. One loads the program to the EPROM of the card using the PC connected to (P1).

The second (P2) is the CPU's on-chip UART. This port is connected to a terminal (see Fig.5.3). It is as if a keyboard and a display are connected to the drive system through which user communicates with the controller.

Parallel I/O pins of Ports 1 and 3 of the 80C51FA are brought out unbuffered along with power and ground to connector JP3 (which is a 50-pin ribbon cable header). Four of these I/O pins (P1.4, P1.5, P1.6, P1.7) are used for switching ON and OFF the four transistors of the power circuitry. One I/O pin (P1.3) is used as an input pin to receive the feedback pulses coming from the optical encoder. The remaining Port 1 pins, (i.e. P1.0, P1.1, P1.2) together with three pins of Port 3 (P3.2, P3.4, P3.5) are used as output ports and connected to the DAC circuitry which is explain in section 5.5.1. Note that other Port 3 pins can not be used by the user of the card. For example P3.3 which is the external interrupt 1 pin is not available to the user and it is used in the card to signal the computer that a receive data character is available [33]. Some other restrictions are as follows: Locations 2E through 3E of the internal data RAM should not be used by the user. Eight bytes of user stack must be reserved for use by the iECM-51 software (a resident software in the internal ROM) [33]. Register Bank 3 is also not available to user. User should start writing program from address 4000H. All the interrupts and the reset vectors are remapped to an offset of 4000H. Therefore RESET begins execution at address 4000H [33]. As some advantages of using this ready card one can mention program debugging and control facilities (like Breakpoints) available to user. Also displaying and modifying program variables by user. Moreover one saves time from dealing with the preparation of a processor card. Note that after the system is developed, one can design the microprocessor card suitable to the system.

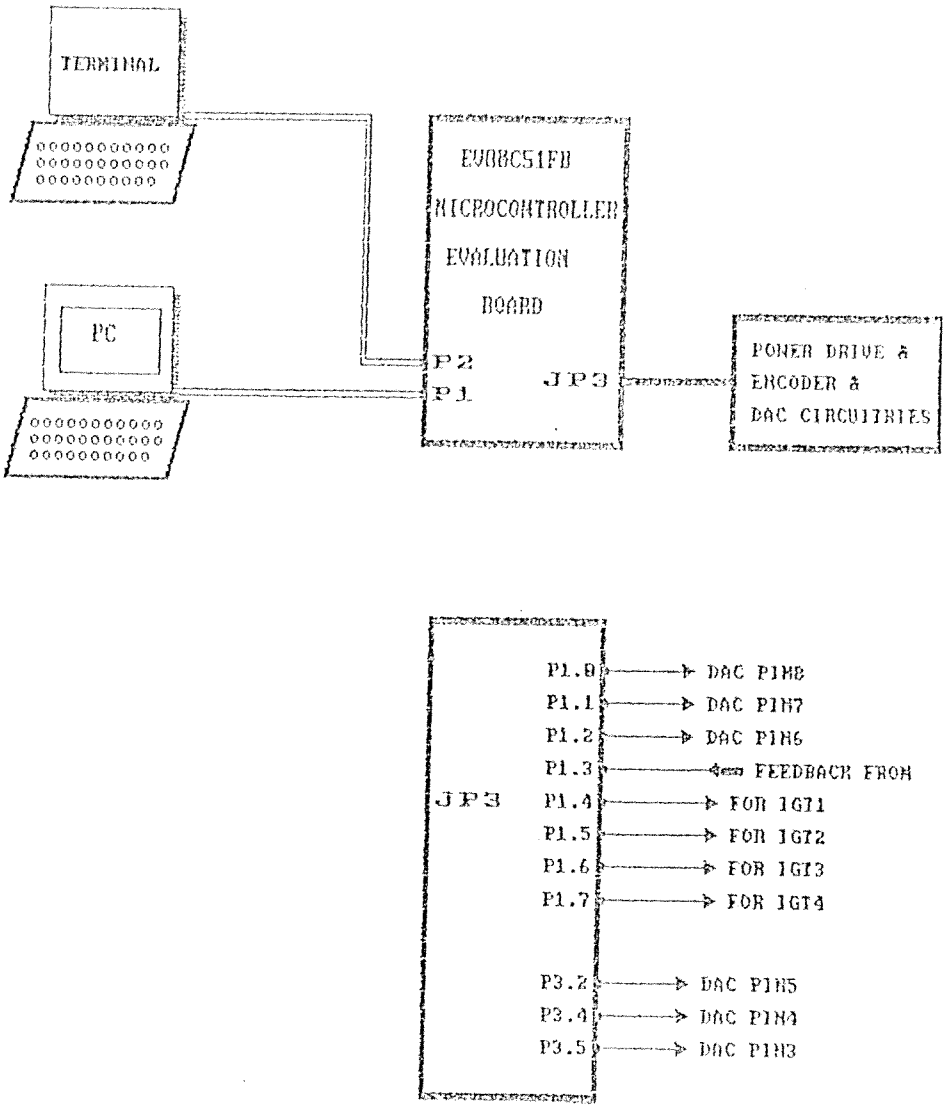

Figure 5.3. Connection of the Evaluation Board to the Computer, Terminal and Power Circuitry

5.4. Description of the Software

The purpose of the software written in this work is to rotate the motor under different advance angles and different phase current values. In this manner one can investigate motor performance in detail under various advance angle and phase currents. Hence important results may be obtained for a sophisticated control in future.

It is desired for the software to be a user programmable software. By user programmable it is meant that, user should be able to enter values of some control parameters, determine mode of operation and direction of rotation of the motor. Therefore, program should be able to communicate with user.

Moreover, the software written should be in modular form in order to be able to use its modules in the software written in future.

Fig.5.4 shows the general block diagram of the software (The listing of the assembly program is in the Appendix C). The software is composed of the following modules (see Fig.5.4):

1) Main module
2) Initialization module
3) Data module
4) PCA module
5) Step command module

Here, initialization module performs all the usual tasks associated with the setting up of a microprocessor system. Data module is responsible for communication with user. It is the function of the PCA module to receive the feedback pulses coming from the position detection system and find the times between these pulses (this is an important data used in other modules as will be discussed later). This module also informs main module that feedback has come and motor has rotated. Hence main module understands completion of previous command and continues issuing new commands (e.g. energizing next phase) as will

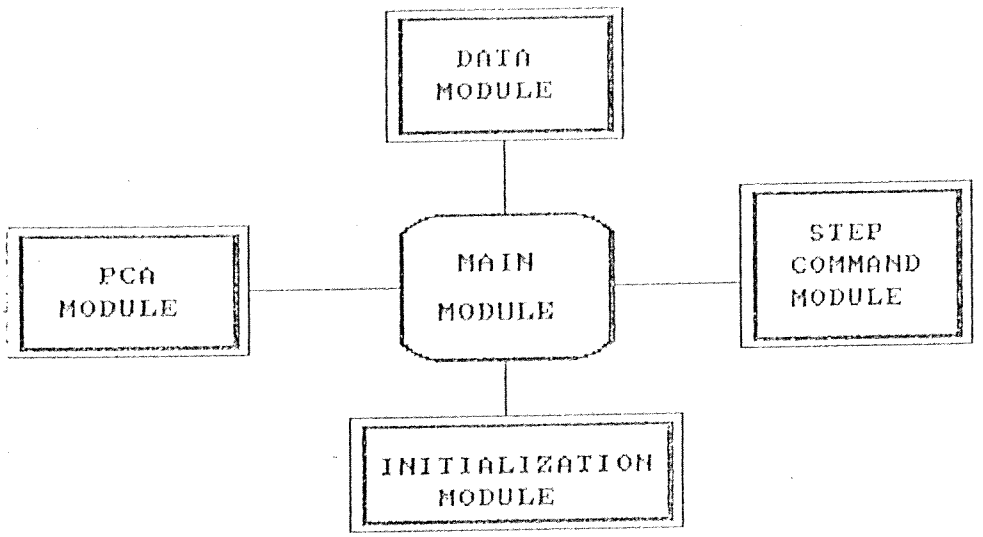

Figure 5.4. General Block Diagram of the Software

be explained below, while explaining the main module. Step command module does the task of exciting the motor phases in the sequence appropriate to the direction of rotation. It also sends data out to ports which are connected to the DAC circuitry (to determine the phase current value). Main module is the most important module of the program. It is responsible for calling the appropriate module to perform the desired task. It first calls the Initialization and Data modules. Then it starts rotation of the motor by calling the Step command module. It waits till PCA module informs the reception of the feedback. Therefore main module understands that previous commands have been completed. So, it starts issuing new commands and calling appropriate modules to rotate the motor.

The details of each module will be given incorporating their flow-charts. But, first a general overview of the program is given below and the closed loop control strategy used is explained.

5.4.1. General

Figures 5.5a & b show the flow chart of the general strategy used here and the closed loop control's timing diagram respectively. The basic part of the program is to energize a phase and wait for the reception of the feedback pulse (from encoder), then repeat this procedure again and again. In other words, One phase is turned on and only after receiving the feedback signal, next phase will be turned on. This will go on and the motor will run while it is self triggered by its own rotation. Note that there is no possibility of loosing any step and system is a closed loop controlled system.

5.4.2. Control Parameters

In the second chapter different torque speed characteristics of SRMs were examined and the variation of these characteristics with three independent parameters were explained. These three parameters are:

a) Phase current
b) Advance angle
c) Conduction time period

Microprocessor technology can be usefully employed for the control of these parameters. The following sections discuss the way the control parameters are adjusted by the microprocessor.

5.4.2.1. Microprocessor Based Control of Phase Current

In section 3.7 it was explained that the current limiter circuitry limits the phase current of the motor by turning on/off the IGTs. The limit at which phase currents are kept is determined by the reference voltage applied to the current limiter. Therefore one can change the phase current just by changing the reference voltage applied to the current limiter circuitry.

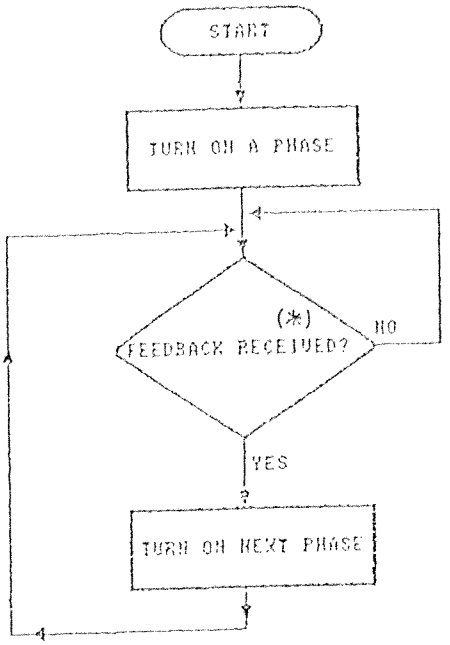

(a)

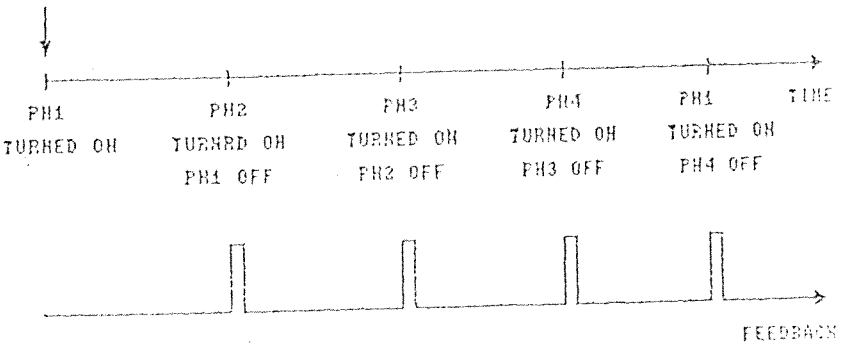

(b)

Figure 5.5. a) Flow Chart of General Strategy Used
b) Closed Loop Control's Timing Diagram
(*) : Feedback Pulse from Encoder

In this work, it is desired to change the phase currents by the microprocessor. In other words, the microprocessor should somehow be able to change the reference voltage of the current limiter circuitry. So the following problem arises: How the microprocessor can change this reference voltage. Answer to this problem is as follows. If microprocessor can produce a digital data for a reference voltage then by sending different digital data different reference voltages can be obtained. In this manner the phase current can be changed by the processor, if this information can be converted to an analog voltage. This function is performed by the DAC circuitry designed. That is, It takes the digital data as its input (from microprocessor) and produces an analog voltage as its output (corresponding to the digital input data). Note that in this work, since number of available output ports of the Evaluation board are restricted (as was explained in section 5.3), the digital data sent by microcontroller is a 6 bit digital data (000000 - 111111). Corresponding to this digital input (000000 - 111111) DAC circuitry produces analog voltages in the range 3 - 4.7 Volts (which corresponds to phase currents 1 - 5 Amps). Note that since digital data is 6 bits wide, each increment of digital data corresponds to an increment of 0.0265 Volts (62.5 mA) at the analog output. The detailed circuit diagram of the DAC circuitry designed is shown in Fig.5.6. Here microcontroller sends a 6 bit digital data (000000 - 111111) to a digital to analog converter DAC 02. Corresponding to each digital input the DAC 02 produces an analog voltage at its output. The voltage at the output pin of the DAC should be applied to the four current limiters in the power drive system. But since three different supplies are employed with different grounds, for the four limiters, in order to be able to apply DAC's output voltage to all current limiter circuitries without facing any grounding problem, three optocouplers are used as shown in figure 5.6. Therefore, after buffering the output of DAC three optocouplers are used, the outputs of which can be connected to the reference voltages of the four current limiters.

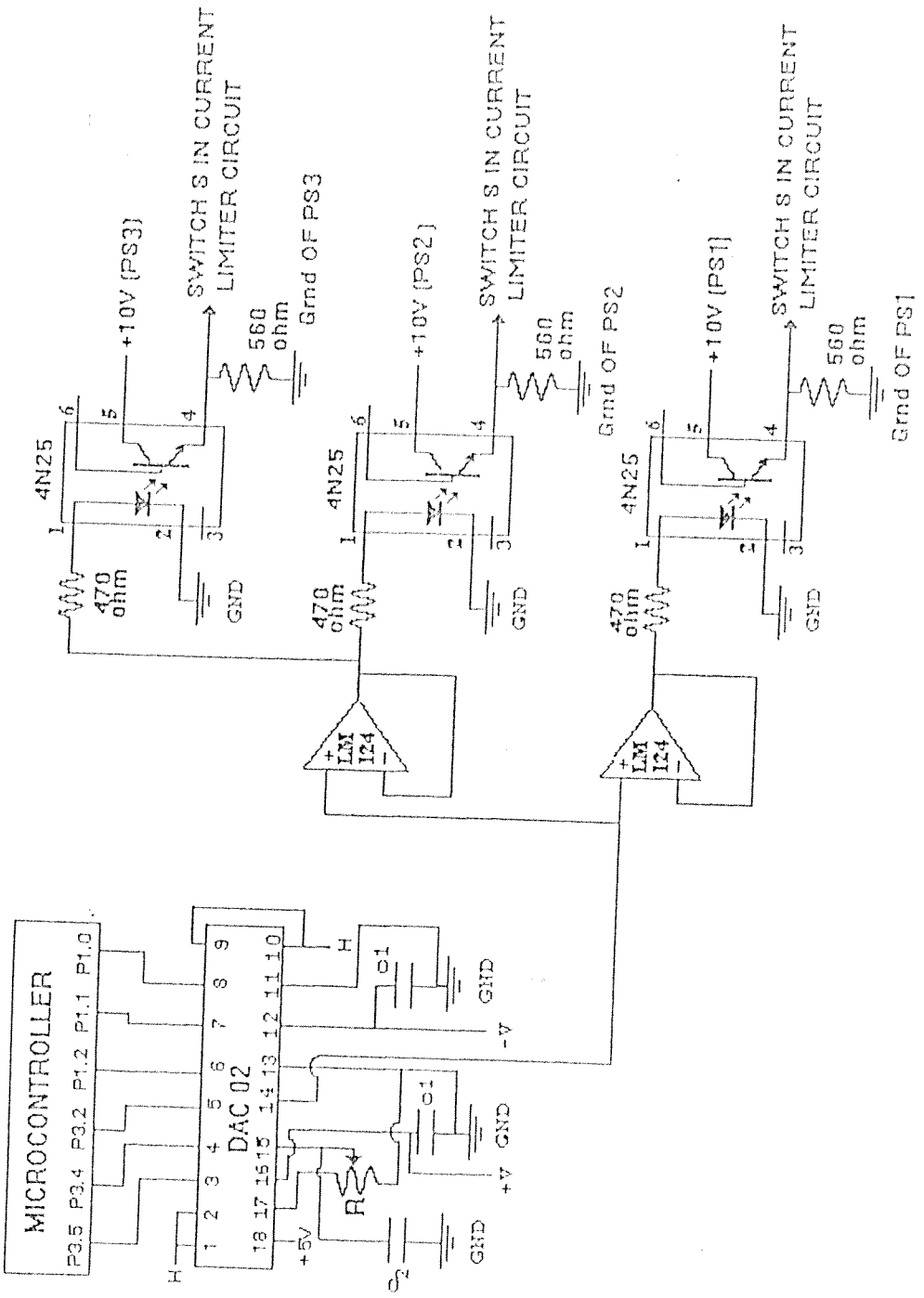

Figure 5.6. Detailed Diagram of the DAC Circuitry

Microprocessor technology can be usefully employed for the control of ignition advance. That is, varying the switching angle with motor speed. The aim here is to obtain intermediate position data. Motor speed is assumed constant in the interval to the next position pulse. The position to which the desired ignition angle corresponds is found using one timer of the microprocessor and some software. As shown in Fig.5.7, a dedicated microprocessor receives position signals from the motor and finds value of time T1 loaded into timer1. Then timer1 is turned on and when this time is passed a step command is issued. Then, processor will wait for the reception of the feedback signal and enter the loop again.

Note that here phases are energized before the reception of the feedback pulses. Hence ignition advance is done. If the advance angle was zero (no advance), step commands were issued at the time of reception of the feedbacks.

In the software written in this work, advance angles of 0, 1/2, 1/4, 1/8, 1/16 and 1/32 are selected. Reason for choosing these angles, is the simplicity in calculating the value of time T1 (corresponding to these angles) which should be loaded to timer1. Note that for dividing a binary number (placed in an accumulator) by 2 it is enough to rotate right the accumulator. Therefore, for half step ignition advance it is enough to divide the time between two feedback pulses by 2 (rotate right accumulator once), for 1/4 ignition advance rotate right accumulator two times and for advance angle of 1/8 rotate right accumulator three times, etc.

Note that any lead angle can be obtained by proper initialization of timer1. That is, calculating proper value of time T1.

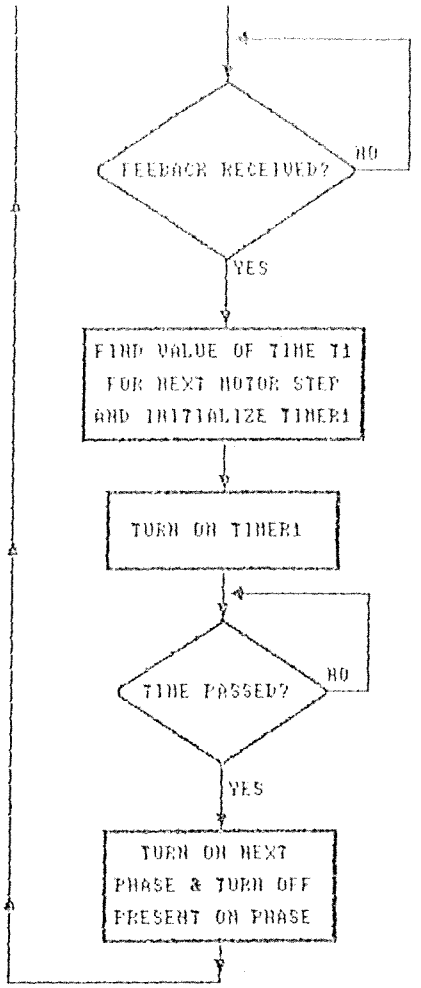

(a)

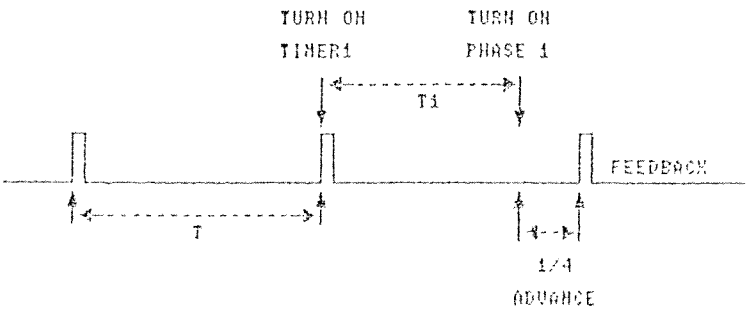

(b)

Figure 5.7. Microprocessor Based Control of Switching Angle
a) Flow Chart for Software
b) Timing Diagram for 1/4 Step Ignition Advance

Conduction time period can be easily varied using one of the timers of the microprocessor and knowing the conduction time. Fig.5.8. shows the timing diagram and the flow chart of the software written for this purpose. Here, as soon as the feedback is received, value of the conduction time for the next phase is determined and loaded into the timer0. The appropriate phase is energized and timer0 is turned on. When time is passed, energized phase turns off and program waits for the reception of the feedback to energize next phase. Here one can choose any conduction time period in the range zero and full conduction just by puting value of desired conduction time the timer0.

5.4.3. Description of Program Modules

As was said in section 5.4, the program written in this work is composed of five modules. Understanding the program requires understanding function of these modules. In the following sections these modules are explained in detail, incorporating their flow charts.

5.4.3.1 Main Module

Main module is responsible for calling the appropriate module to perform the desired task. The overall flow chart of the program (main module) is illustrated in Fig.5.9. It first calls the Initialization module and then starts communication with user. In other words it calls the DATA module (The explanation of each module used here is given in detail, incorporating their flow charts, in the coming sections).

Actually a SRM is switched on and off by using feedback signals taken from position of rotor. However, when the rotor is at standstill, it is impossible to obtain positional feedback. Therefore starting, different excitation scheme should be used. At start one phase is energized (e.g. PH1) and a timer (here T1) is also turned on. If a feedback is received, next phase (PH2) will be energized and the

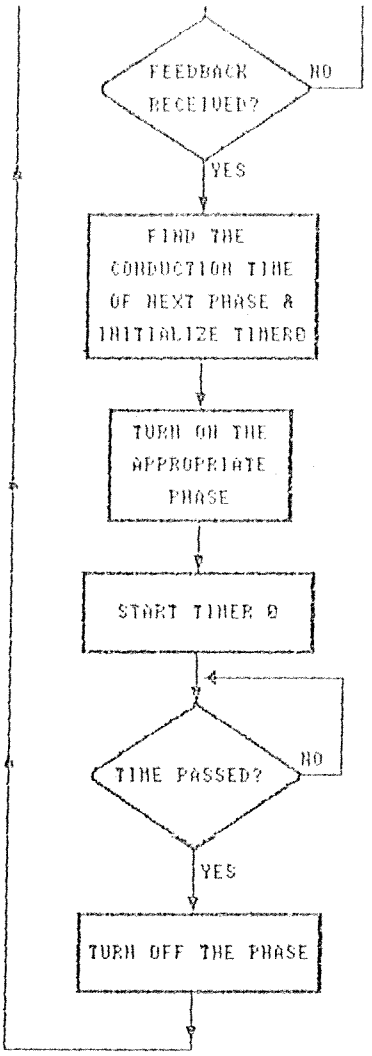

(a)

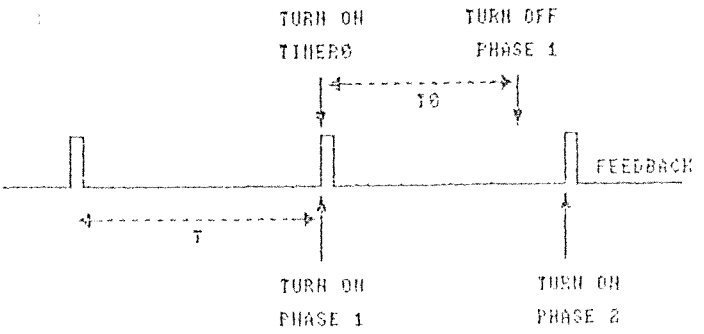

(b)

Figure 5.8. Microprocessor Based Control of Conduction Time Period
a) Flow Chart for Software
b) Timing Diagram for 2/3 Period Conduction during

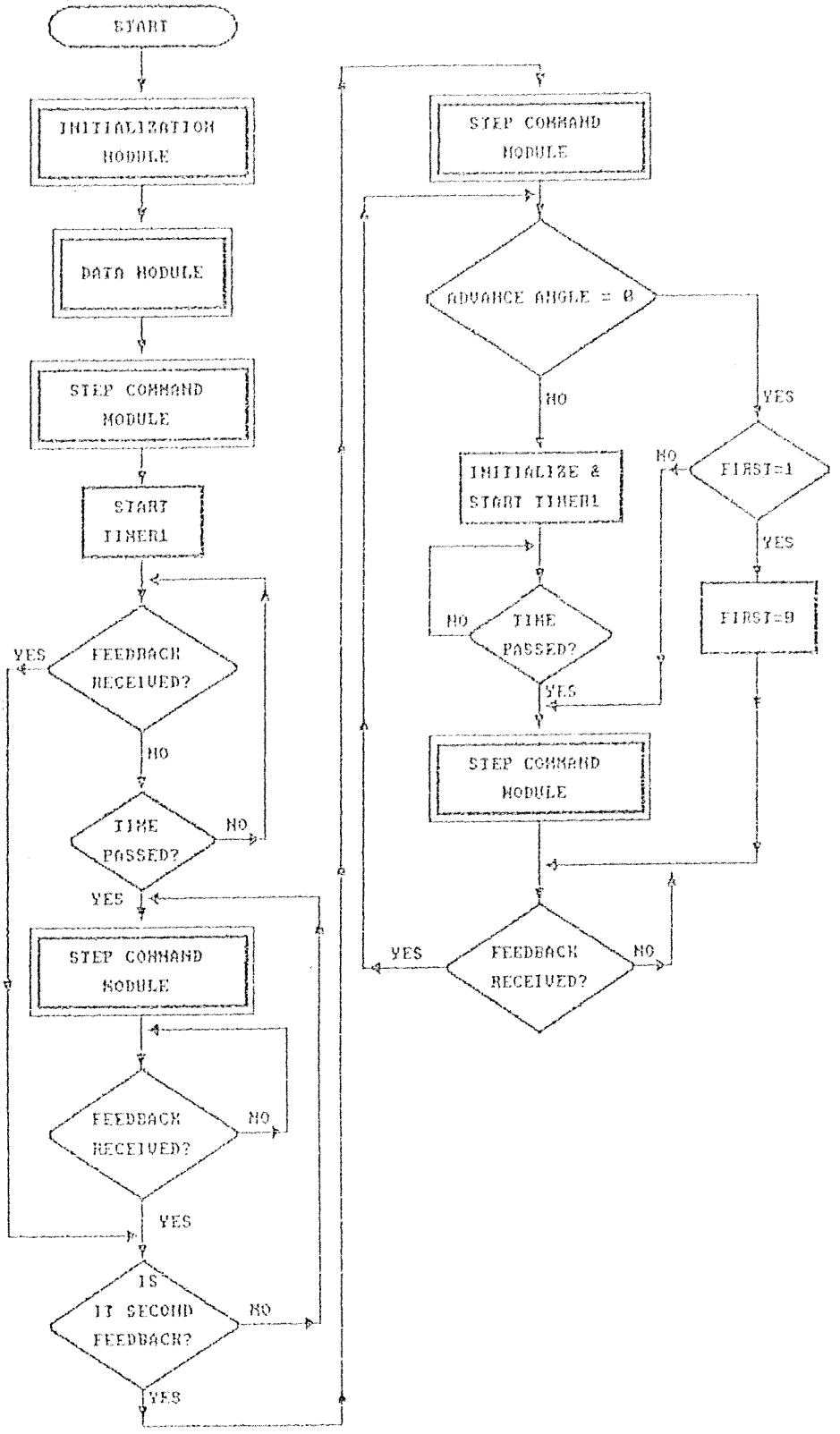

Figure 5.9. Flow Chart of Main Module

PCA timer also turns on. But, if timer (T1) goes off and still no feedback was received, (This happens only when the angle between energized phase and the rotor pole is exactly 30 degrees) next phase (PH2) is turned on and from now on it is for sure that feedback pulse will be received. So program waits for the reception of the feedback and As soon as the feedback is received the PCA timer is turned on and next phase is also energized (PH3). Then program will wait for reception of the second feedback. This time as soon as feedback is received the value of the PCA timer is stored (it is the time between the two feedback pulses). This time is used for ignition advance. That is, if it is desired to have an advance angle. Therefore as was explained in section 5.4.2.2, if advance angle is not zero timer1 is turned on and when time is passed next phase is energized. But if advance angle is zero next phase is energized immediately as soon as feedback is received. Then, program will wait for the reception of the feedback pulse to make sure that rotation is performed and after receiving feedback it is time for energizing next phase. Program will loop again and again until user stops program by pressing the key 's' of the keyboard.

In the following sections modules that were used in the main module are explained.

5.4.3.2. Initialization Module

This module performs all the usual tasks associated with the setting up of a microprocessor system. For example, instructions are executed for initialization of Programmable Counter Array (PCA) to work in internal clock Fosc/12 mode, module 0 to work in capture mode, timers 0 and 1 as 16-bit timers, timer2 as a baud rate generator, serial port for 8-bit UART, interrupt enable and interrupt priority special function registers and control parameter values appropriate for starting the motor. In figure 5.10 the flow chart of this module is shown.

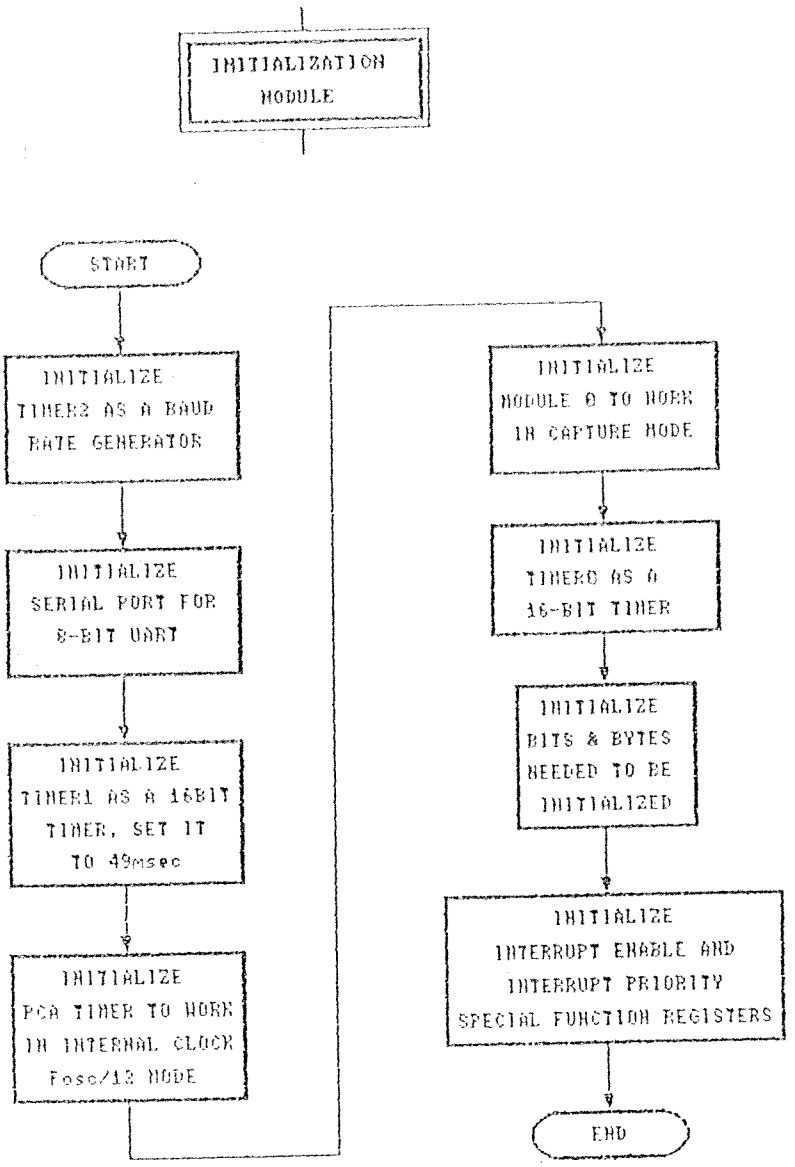

Figure 5.10. Flow Chart of Initialization Module

5.4.3.3. Data Module

Here the data module represents the user controls (a terminal through which user communicates with controller). This module performs a background task and the port generating the interrupt has the lowest priority. The flow chart of data module is shown in figure 5.11. This module enables the user to communicate with microcontroller. It is the function of this module to ask user whether he wants to enter control parameter values or just rotate the motor at the phase current and advance angle stored in the program. Then it will initialize required bits and locations in RAM according to values entered. User also determines mode of operation and direction of rotation of the motor using this module. Questions that are asked from user are as follows:

- Do you want to enter control parameter values? (y/n)

If answer is yes then following questions appear:

- Enter advance angle: (0,1/2,1/4,1/8,1/16,1/32)
- Enter phase current: (1.0,1.5,2.0,2.5,3.0,3.5,4.0,4.5,5.0)
- Enter mode of operation: (O,T,H)
- Do you want rotation be CW? (y/n)

If answer to first question was no then program fixes the phase current and advance angle to some specified value and continues with asking the last two questions.

Note that although the program asks user to choose one of the specific phase current and advance angle values written in the questions, user can choose any phase current values in the range 1 to 5 Amps and any advance angles just by specifying required values for the program (which is a very simple task).

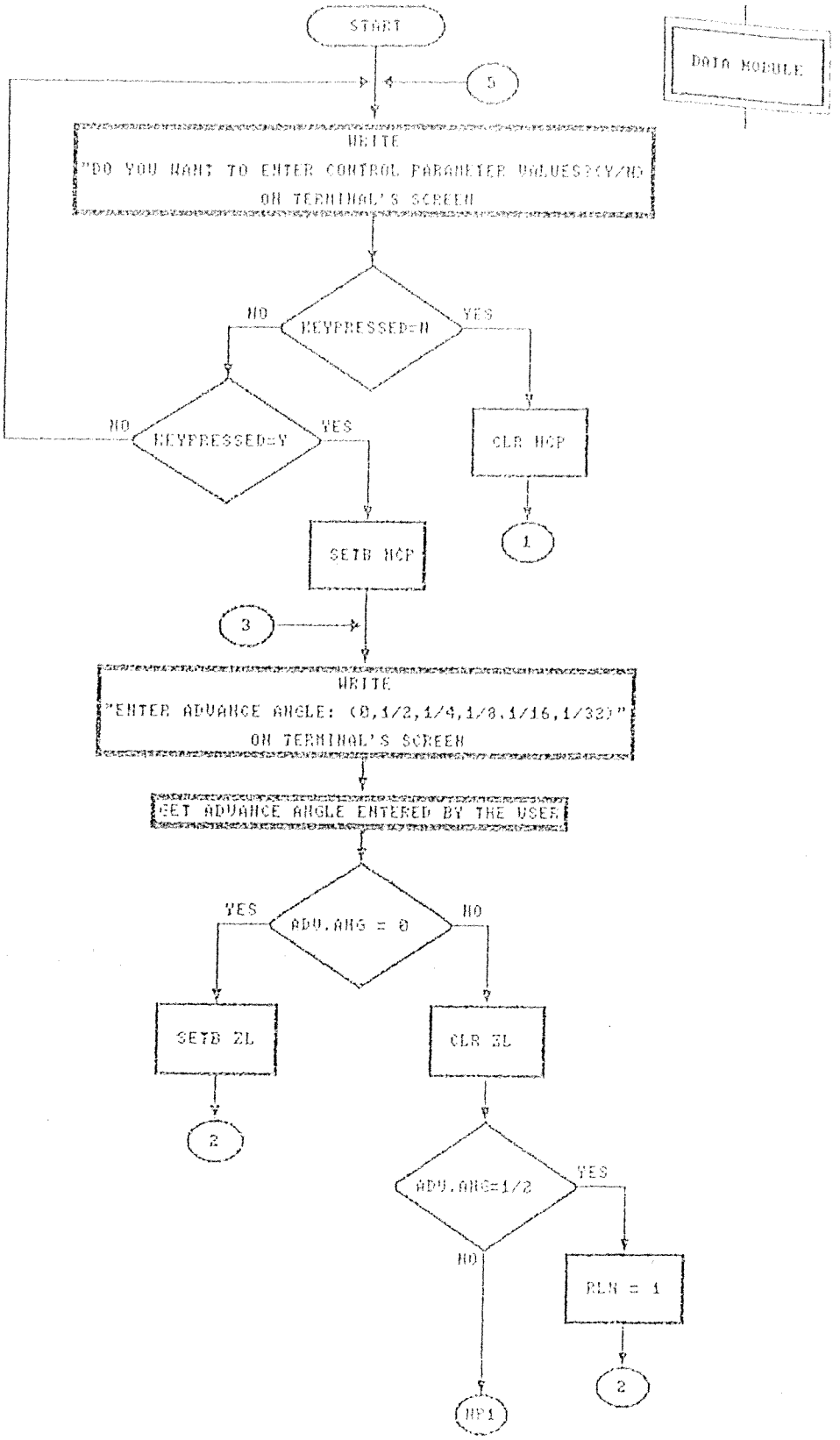

Figure 5.11. Flow Chart of Data Module

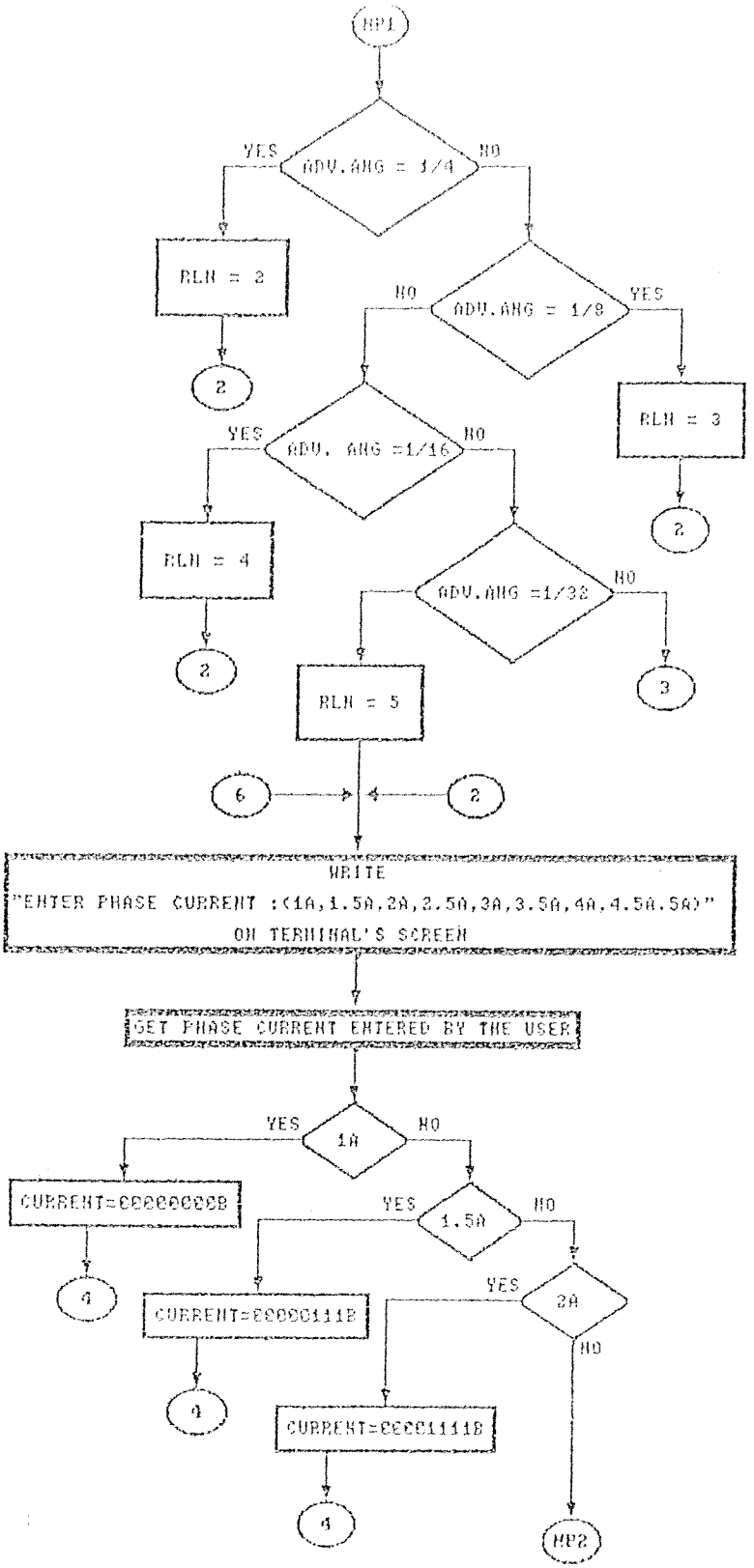

Figure 5.11. Flow Chart of Data Module (cont'd)

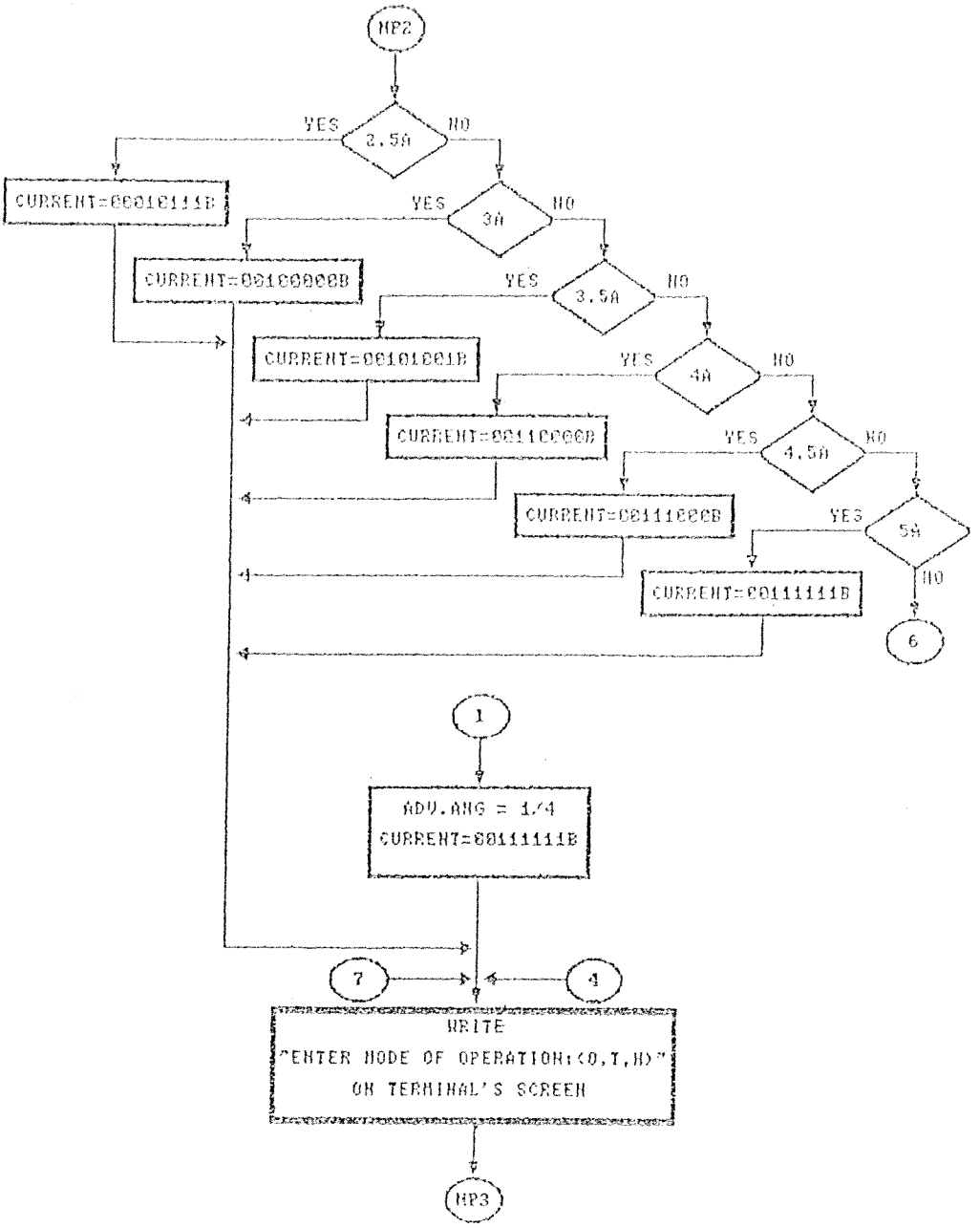

Figure 5.11. Flow Chart of Data Module (cont'd)

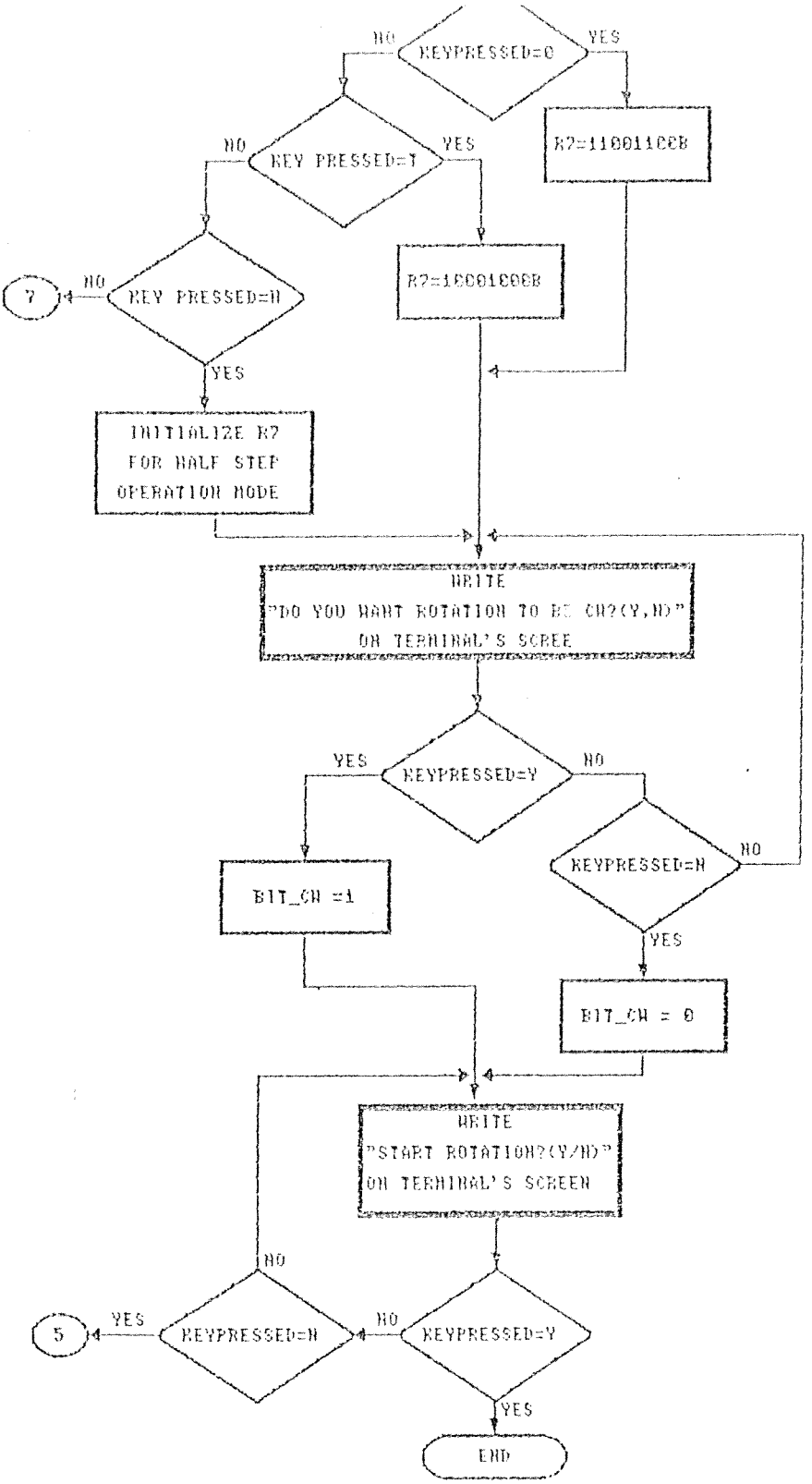

Figure 5.11. Flow Chart of Data Module (cont'd)

The function of the PCA module is to receive the feedback pulses coming from the position detection system and find the times between these pulses as explained below. This module also informs main module that feedback has come and motor has rotated. Hence main module understands completion of previous commands. Figure 5.12 shows the flow chart of this module. AS said previously, the task of this module is finding the time between the feedback pulses. This time is found as follows. The feedback signal is input to P1.3 as was explained in section 5.3 (in the program here module 0 is used). As soon as a transition is detected on that pin, the 16-bit value of the PCA timer (CH, CL) is loaded into the capture registers (CCAPOH, CCAPOL). Module 0's event flag is set and an interrupt is flagged. In the interrupt service routine the 16-bit capture value is saved in some location in RAM before the next event capture occurs; a subsequent capture will write over the first capture. After the second capture,a subtraction routine calculates the period in units of PCA time ticks (0.75 microsec). In this manner the time between two feedback pulses is found. This data is very important and is used for ignition advance. That is after calculating the period if lead angle required is not zero, the PCA module will find the value to be loaded to timer1 for the specified lead angle as was explained in section 5.4.2.2.

5.4.3.5. Step Command Module

This module is responsible for exciting the motor phases in the sequence appropriate to the direction of rotation. It also sends data out to ports which are connected to the DAC circuitry (to determine the phase current value).

The flow-chart of the step command module is illustrated in Fig.5.13. As it is seen in the flow chart the logic sequencer function is implemented by checking a flag for understanding the direction of rotation. Then according to the state of this flag program will either rotate right or left content of the accumulator (which contains the

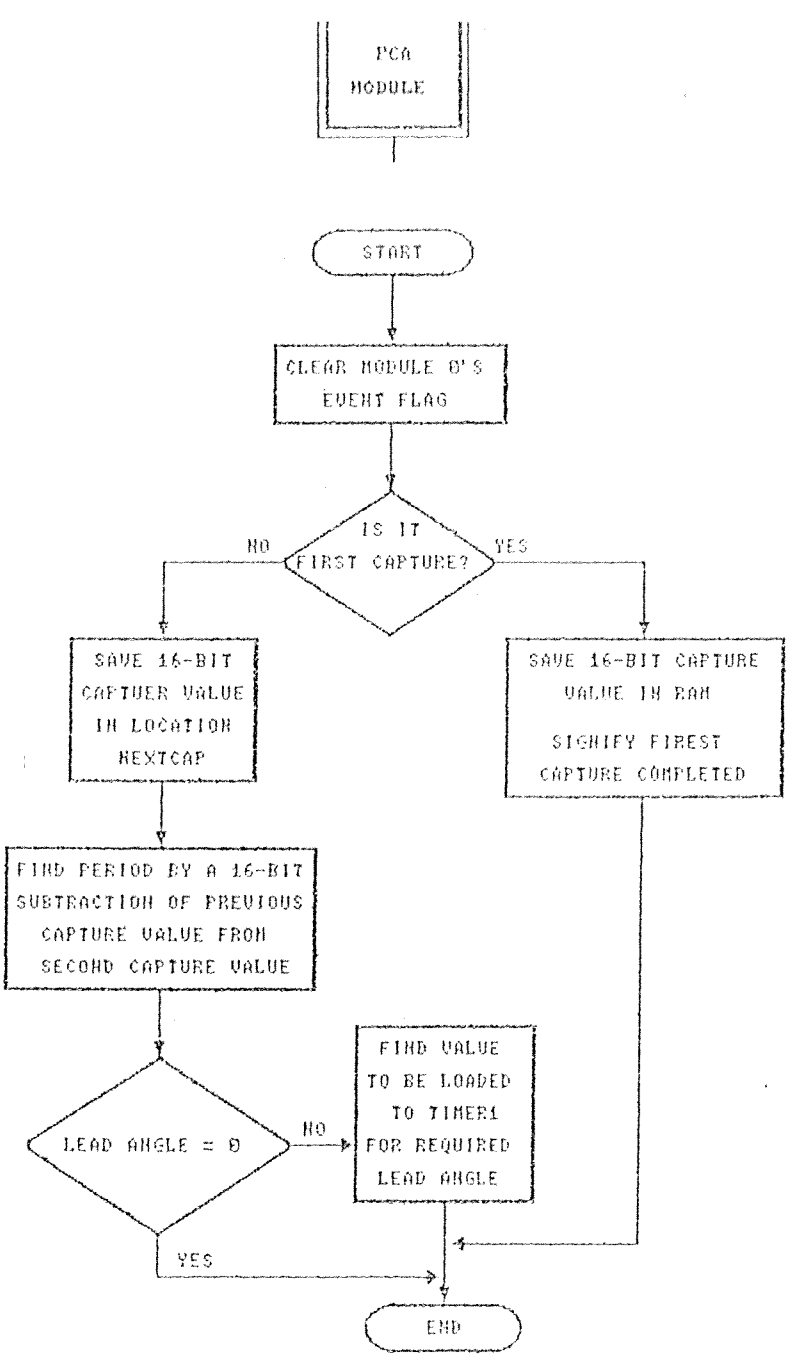

Figure 5.12. Flow Chart of PCA Module

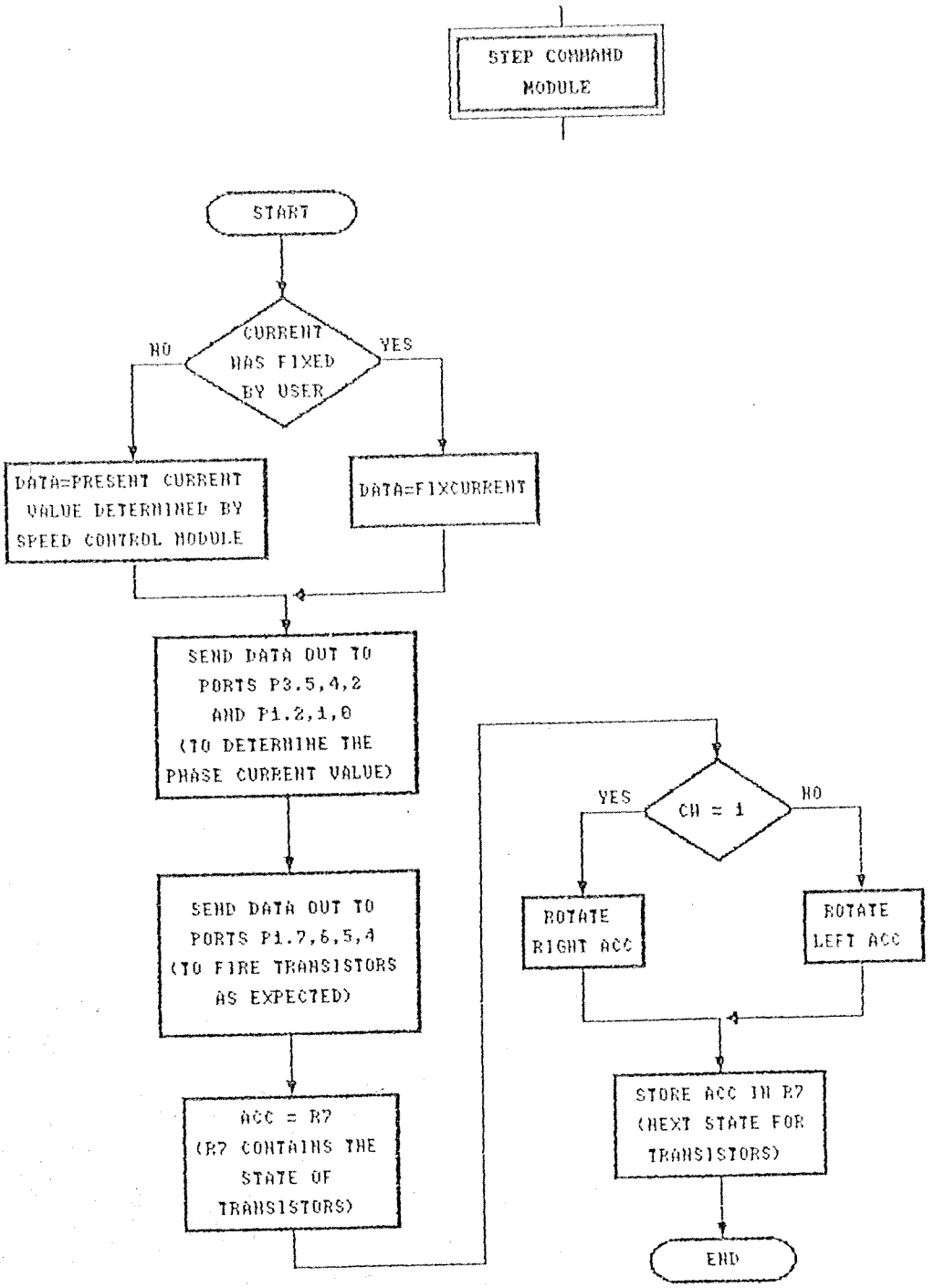

Figure 5.13. Flow Chart of Step Command Module

the next state of switches. This data is stored in a register to be sent out to ports when next phase should be turned on.

CHAPTER VI

TEST RESULTS

6.1. Introduction

The motor used here is a four phase SRM, which has eight stator poles and six rotor poles. This motor was designed by Mujdat Tohumcu as a doctor of philosophy thesis at Middle East Technical University. It has a nominal rating of 1.1 kw at 1500 rpm and is designed to be supplied from a DC voltage source of 280 Volts [11]. The number of turns per pole is equal to 300. The wire size which fills the winding space is 0.7 mm. In appendix E photographs of the motor and drive circuitry are presented.

To test the SRM drive, an adjustable DC power supply is needed. We have used the DC Supply of Senturk's drive [21]. This supply contains a variac for adjusting the DC voltage output, an uncontrolled bridge rectifier as AC to DC converter and a second order filter. The ripple content of the supply is low enough to neglect the effects of ripple in the motor performance. The peak to peak ripple output versus DC line current is shown in reference [21].

For capture and record the waveforms shown in this chapter, DSO 450 storage oscilloscope is used (the probe used is a 10/1 probe). These waveforms are obtained when the motor was rotated in one phase on mode. Similar results can be obtained for other modes of operation.

The following sections illustrate that the microprocessor produces commands as required by the software, the operational characteristics of the power stage, encoder operation, accuracy of the advance angle calculation, the current limit operation, phase currents,

6.2. Power Stage Operation

As was explained in previous chapters microcontroller is responsible for switching of transistors. The pulses that it sends go through some circuitry (current limiter, isolation and inversion circuits) and applied to the gate of IGTs. Fig.6.1a shows the microcontroller pulses and Fig.6.1b shows the corresponding gate pulses applied to a transistor. Here, As it is expected, when microprocessor signal is high, That is 5 volts (note that at start when microcontroller is turned on all its pins are high) the signal applied to the gate of transistor is low, hence transistor is off. When microprocessor output becomes low (0 volts) a 9 volt pulse applies to the gate of the transistor and makes it on.

Figure 6.2 shows the delay (due to intermediate circuits between the processor and the IGTs) between microprocessor signal for turning on an IGT and the corresponding gate signal of the IGT. This delay is about 8 microseconds.

The IGBT's gate emitter and collector emitter waveforms are shown in Fig.6.3. Here one can see the perfect operation of these switches. By examining the collector emitter waveform shown in Fig.6.3 one can see the perfectness of the snubber designed, as there is no sparks at all, when switching occurs.

Figures 6.4 and 6.5 show voltage waveforms of the IGTs at turn on and turn off, respectively. In these figures the IGTs operation at switching instants can be seen. The turn on time of the IGT is about 0.9 microsec, and turn off time is about 5 microsec.

Figures 6.6 and 6.7 show the turn on and turn off delays of the IGTs. Turn on delay of the IGT from the recordes is about 0.7 microsec, and turn off delay is about 3 microseconds.

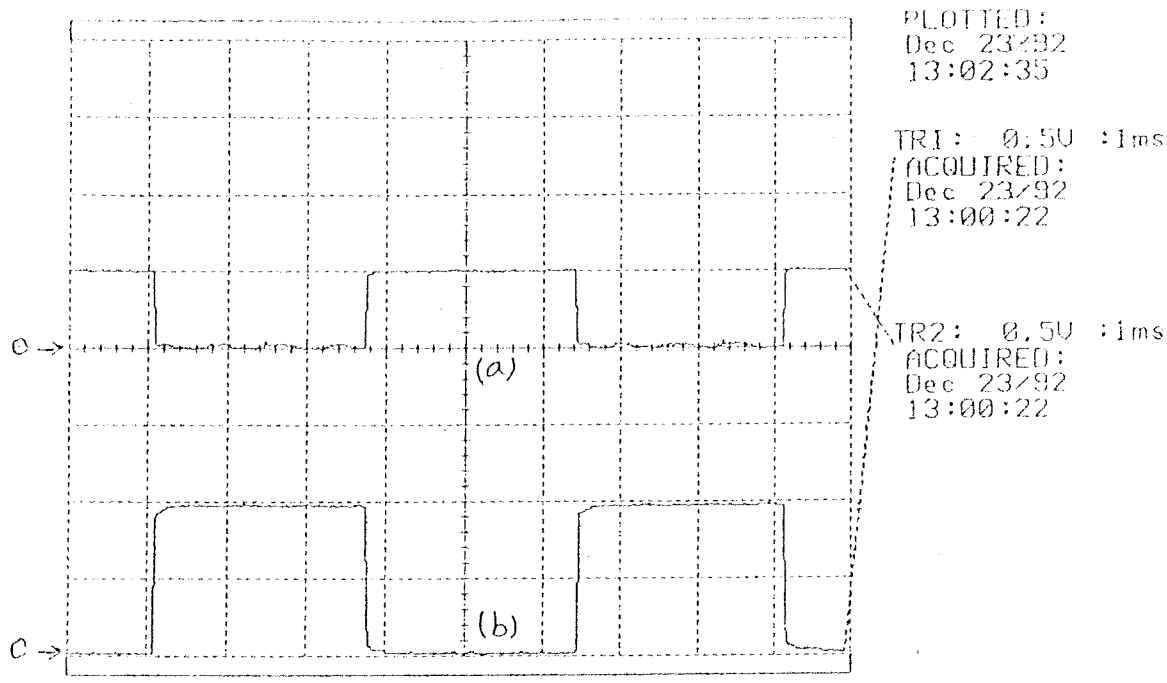

Figure 6.1. a) Microcontroller Pulses for Switching a Transistor
b) Corresponding Gate Pulses Applied to the Transistor.

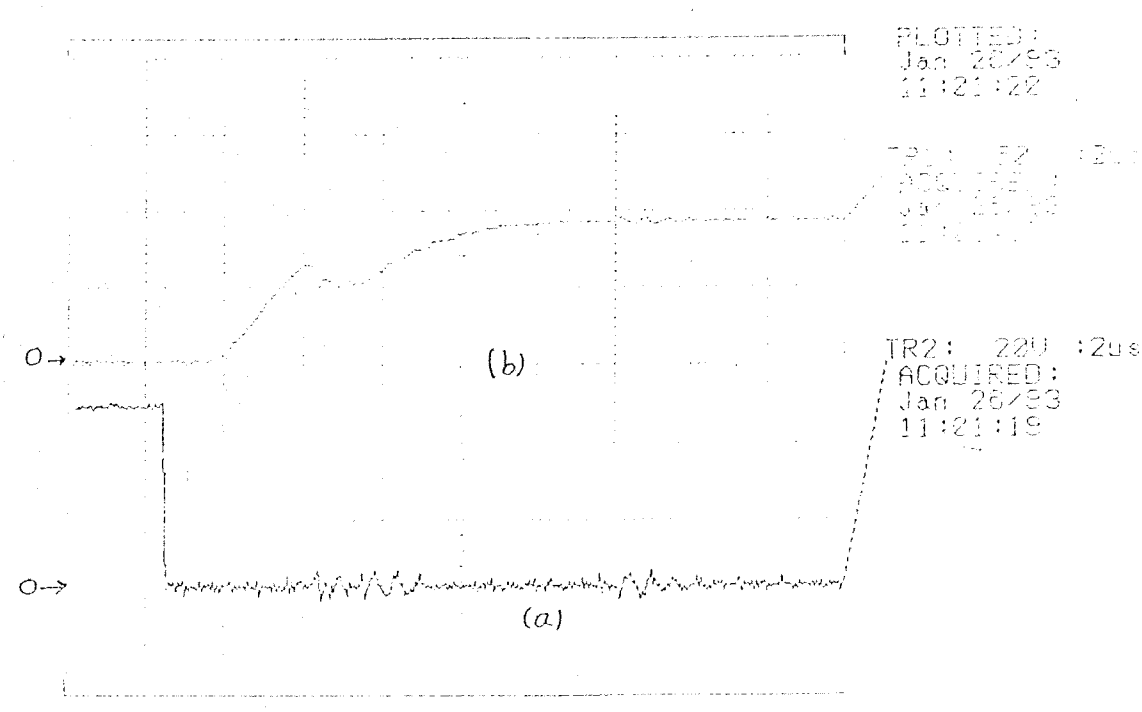

Figure 6.2. Delay Between Processor Signal and Corresponding Gate Signal of an IGT a) Microcontroller Signal for Switching a Transistor
b) Corresponding Gate Signal Applied to the Transistor.

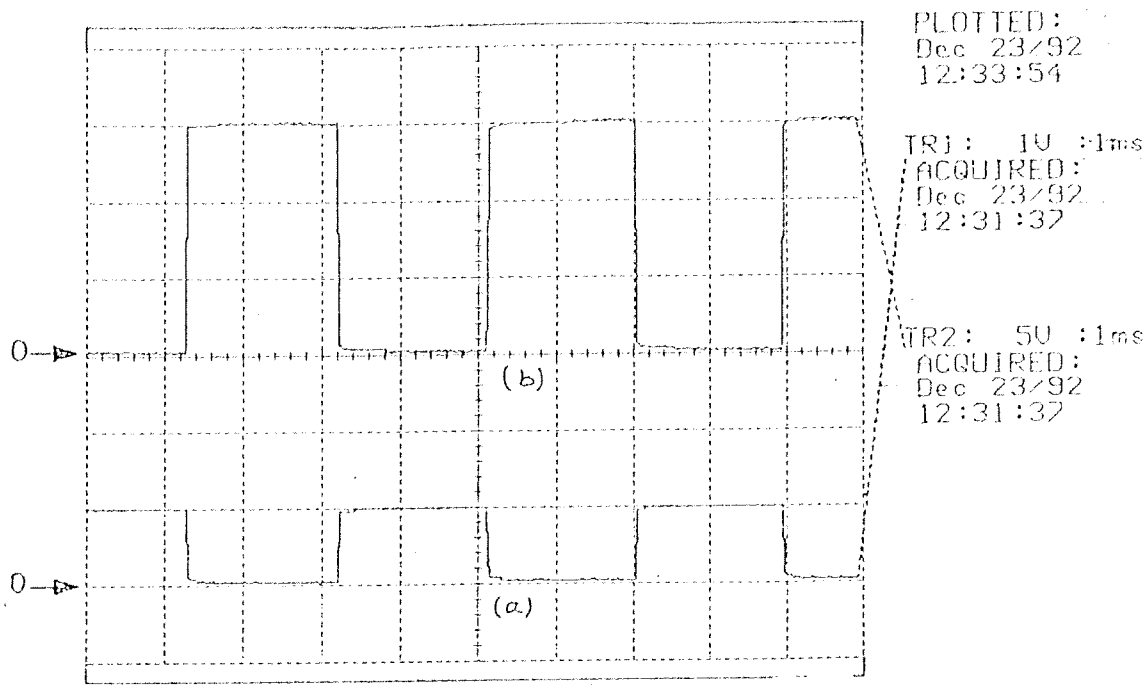

Figure 6.3. a) Gate Emitter Voltage of a Transistor
b) Corresponding Collector Emitter Voltages

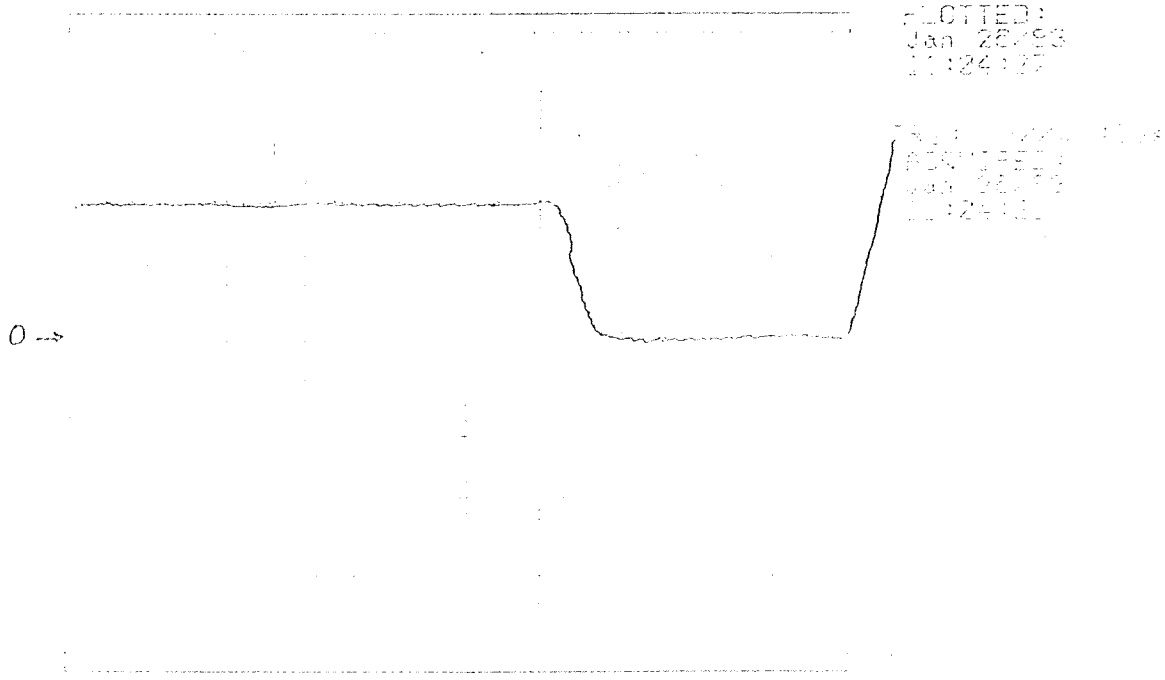

Figure 6.4. Collector Emitter Voltage of an IGTs at Turn ON Instant

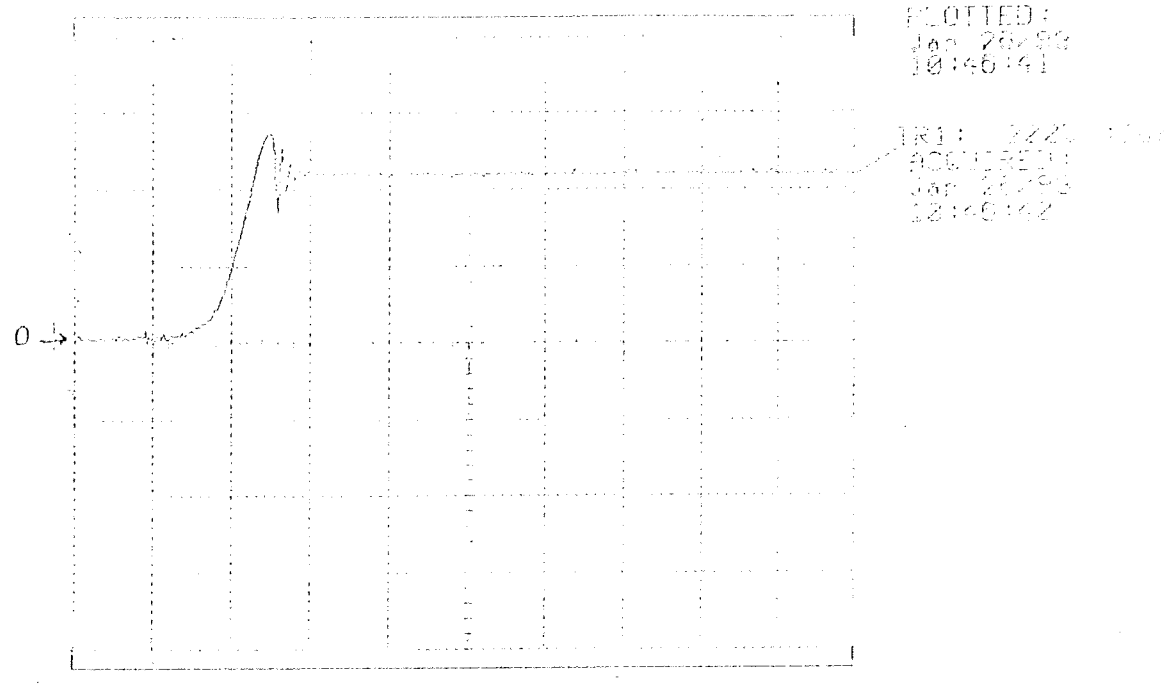

Figure 6.5. Collector Emitter Voltage of an IGTs at Turn OFF Instant

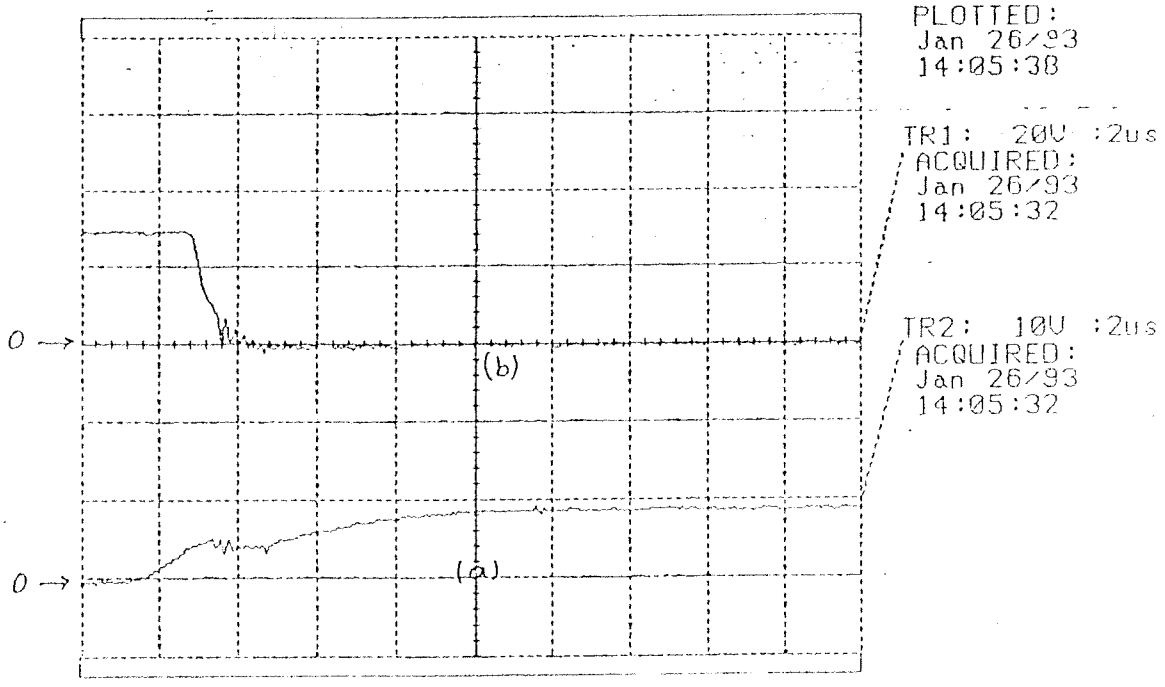

Figure 6.6. Turn On Delay of an IGT a) Gate Emitter Voltage
b) Collector Emitter Voltage

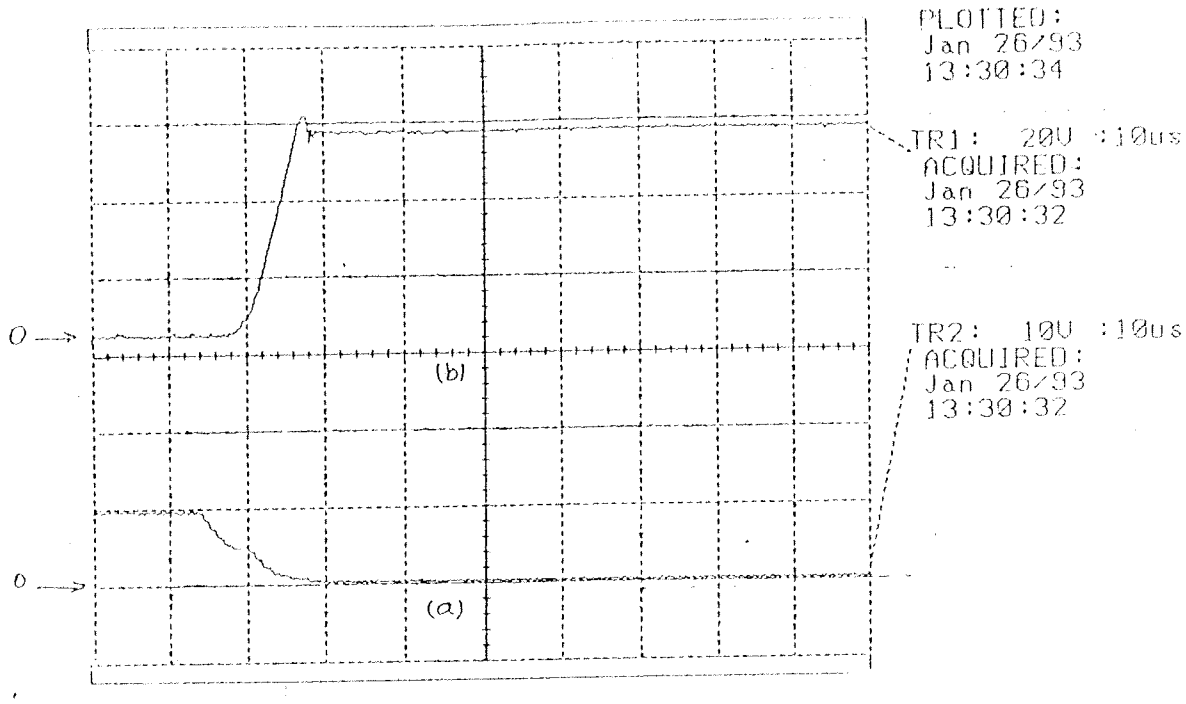

Figure 6.7. Turn Off Delay of an IGT a) Gate Emitter Voltage
b) Collector Emitter Voltage

6.3. Phase Current Waveforms

Current passing through a phase can be measured by using a carbon resistor of known value (e.g. 0.25 ohm) in series with a phase winding. Figure.6.8 shows the power converter circuitry and the carbon resistor in series with phase 1. Two scope probes are used here. One is connected across the carbon resistor and the other one is connected to the emitter of transistor 1, as shown in Fig.6.8 (the second probe output is inverted in order to give us the waveform V_{j1}, which is V_{ce} plus V_{d1}, diode D2. We call V_{j1} as $V_{ce'}$). Then motor is operated at speeds 500 and 2000 rpm (with zero advance angle). Figures 6.9 and 6.10 show the phase current and $V_{ce'}$ waveforms obtained when motor rotates at these speeds and zero advance angle. Consider Fig.6.9. Each period of current is composed of 5 regions. First region corresponds to the case that both transistors are on and diode D2 is closed (conducts). That is, at point u transistors turn on and a voltage applies across the phase winding (see Fig.6.9b). Hence current starts rising in the winding. In the second region which starts at point v (which is the mid

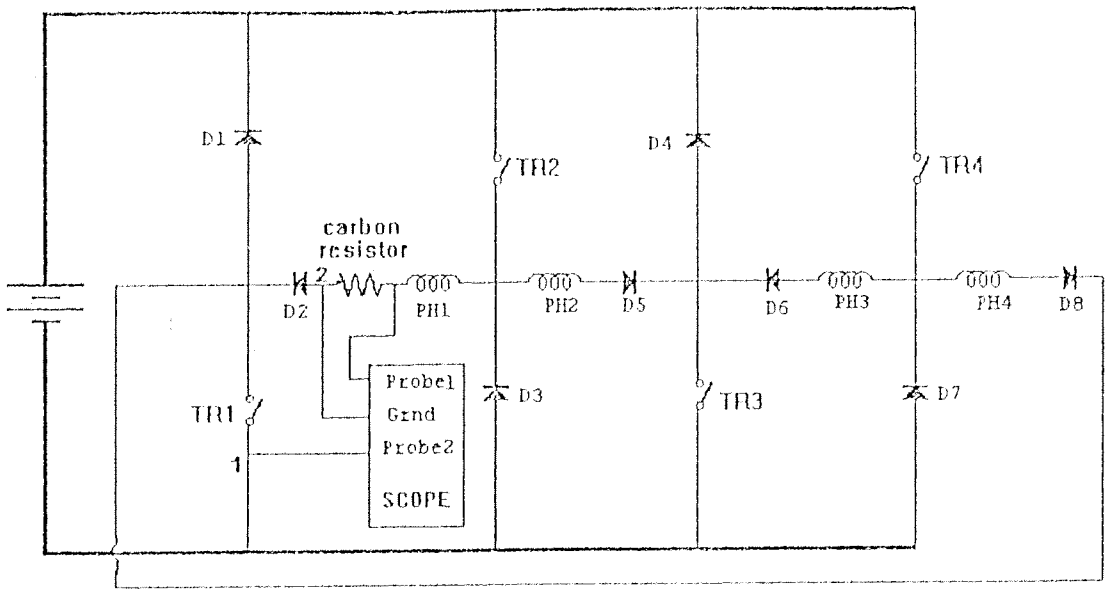

Figure.6.8. Power Converter Circuitry and the Carbon Resistor in Series With Phase 1.

point between u and w, see figure) transistor TR1 turns off and diode D2 is still conducting. Hence as seen in Fig.6.9a current starts decreasing. Note that in this region TR2 and TR3 are on and phase 2 is energized. Region III corresponds to the time that both TR1 and TR2 are off and diode D2 is closed. Hence current is forced to flow through both freewheeling, diodes D1 & D3, and current in the winding 1 reaches zero. In this region TR3 and TR4 are on and phase 3 is energized. Region IV starts from point x and it is when both transistors are off and diode D2 is open. In this region still TR3 and TR4 are on. Then comes region V in which transistors 4 and 1 are on and phase 4 is energized. Note that TR2 is off and again diode D2 is open but this time transistor 1 is on. Here is Fig 6.9b the small voltage seen at V_{ce}, corresponds to the v_0 of the open diode D1. After the fifth region again first region reaches and current starts increasing in phase 1.

Figures 6.9 and 6.10 were obtained when advance angle was zero. If advance angle changes the phase current waveforms will also change. The phase current and V_{ce}, waveforms For the advance angle of

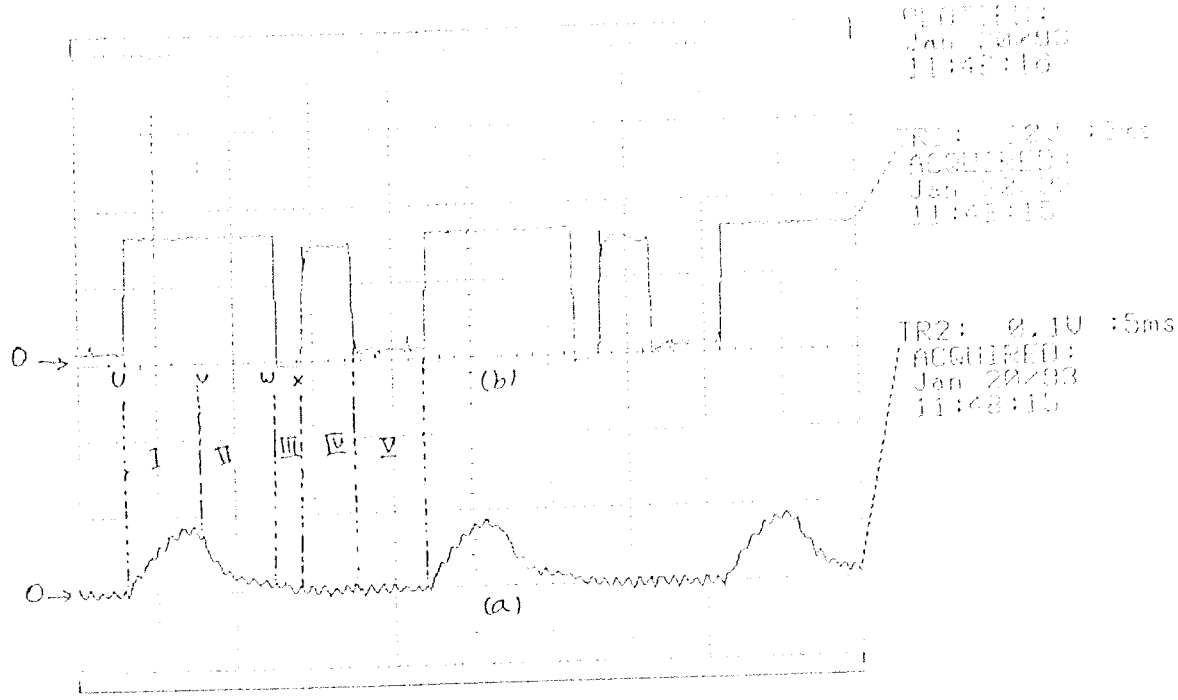

Figure 6.9. a) Phase Current Waveform b) Waveform of V_{ce}, When Speed of Motor is 500 RPM and Lead Angle is Zero

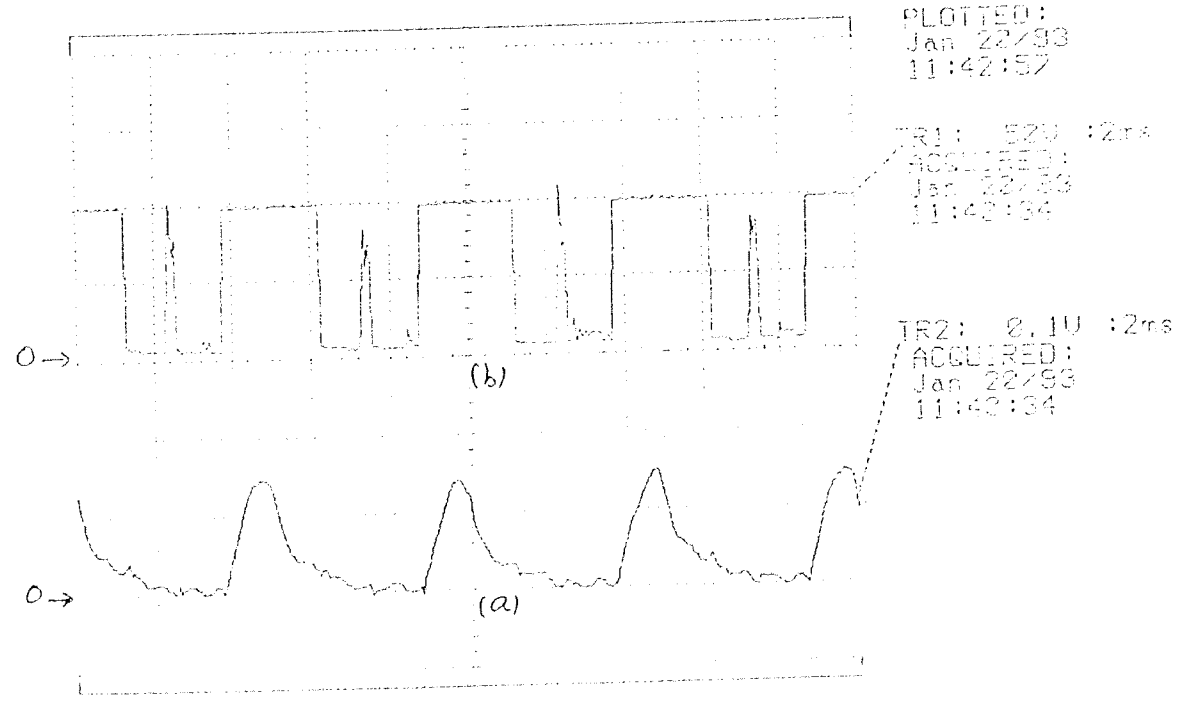

Figure 6.10. a) Phase Current Waveform b) Waveform of V_{ce}, when speed of Motor is 2000 RPM and Lead Angle is Zero

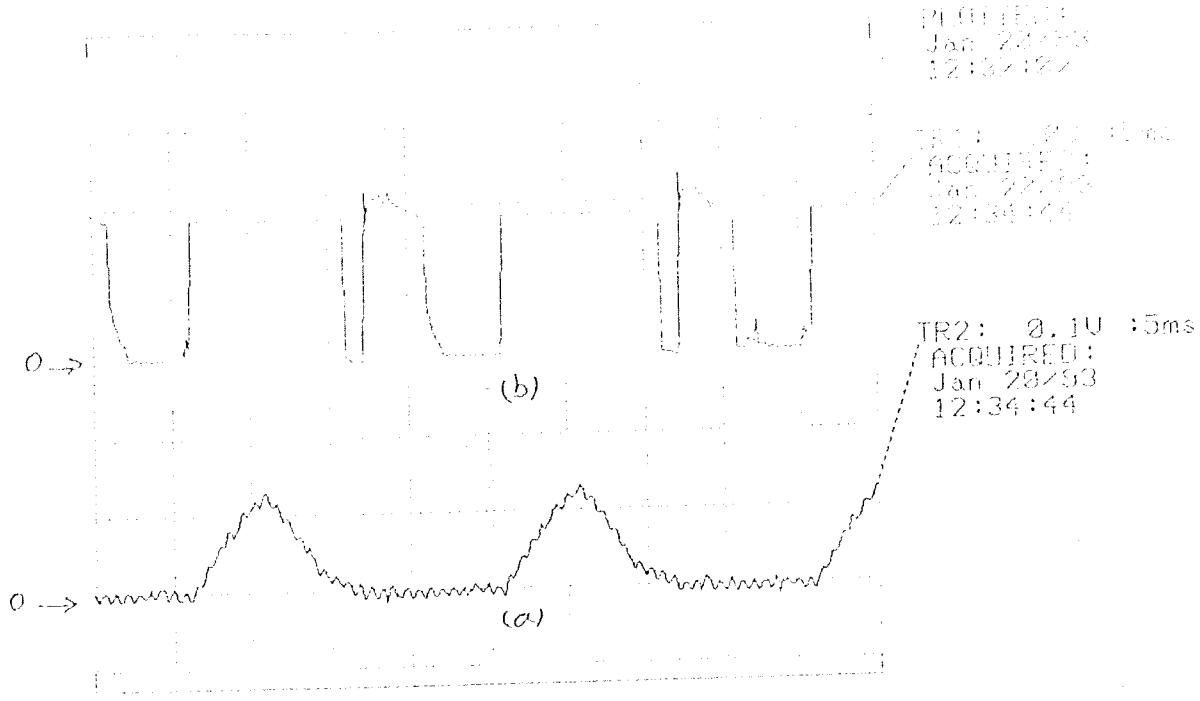

Figure 6.11. a) Phase Current Waveform b) Waveform of V_{ce}, when speed of Motor is 500 RPM and Lead Angle is 1/2 (7.5^0)

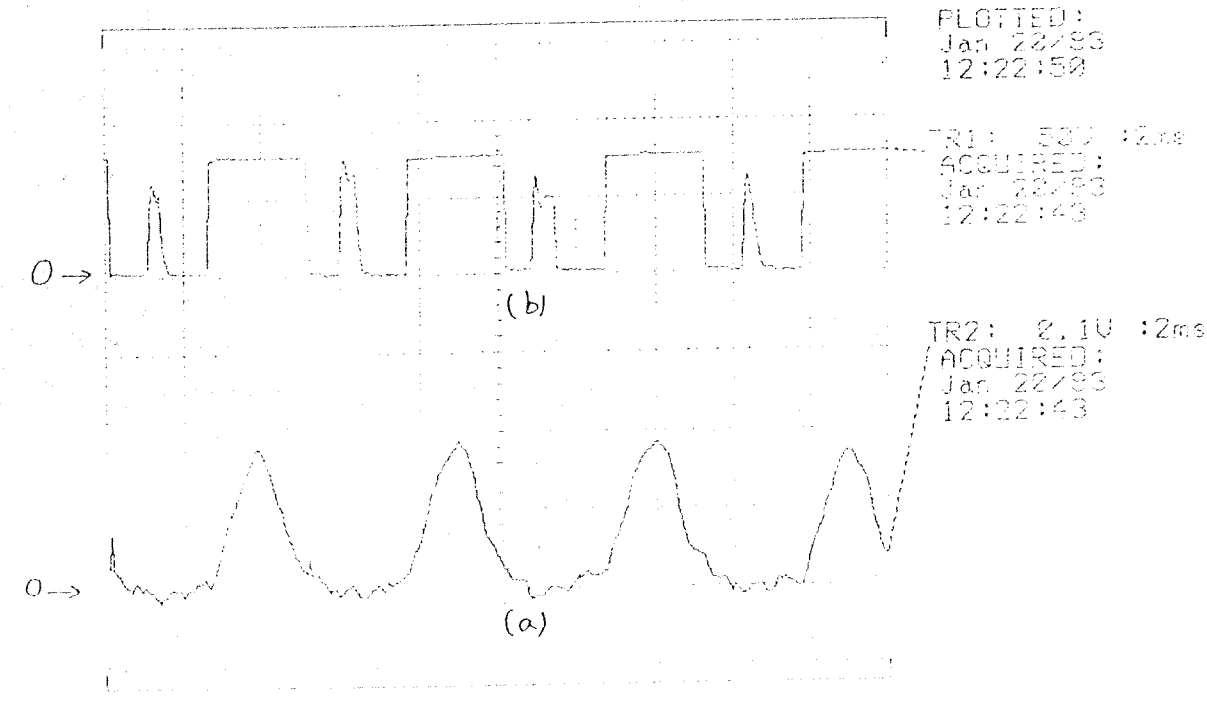

Figure 6.12. a) Phase Current Waveform b) Waveform of V_{ce}, when speed of Motor is 2000 RPM and Lead Angle is 1/2 (7.5^0)

1/2 (half step, i.e. 7.5 degrees lead) are shown in Figures 6.11 and 6.12 for speed of 500 and 2000 rpm. The difference between current waveforms for zero lead and half step lead angle is especially obvious for high speeds (see Figs. 6.10 and 6.12). Reason for this is that; current build up in a phase takes some time. With zero lead angle, at high speeds, current will not have enough time to reach its maximum value as phase turns off very fast. But, when there exists a lead angle phase will be energized earlier and there will be enough time for current to reach its maximum.

6.4. Encoder Operation

In section 4.7 it was explained that in this work an optical encoder that was designed by Senturk [21] is used and in order to make the output of this encoder compatible to the microcontroller an interface circuitry is made. The outputs of Senturk's encoder and corresponding microcontroller inputs (out puts of interface circuitry) are shown in Figs.6.13 to 6.16 for motor speeds of 500, 1000, 2000 and 3550 rpms respectively. Fig.6.13a shows the output of the Senturk's encoder when the motor speed is 500 rpm. As it can be seen in this figure, the outputs of Serdars's encoder are not shaped properly. Moreover one of the four phototransistor's output has a lower voltage compared to others. Figure 6.13b shows the modified encoder outputs (which is input to the microcontroller) for the signals shown in Fig.6.13a. As it is seen in this figure the interface circuitry has shaped the input signals and made them suitable for being applied to the microcontroller.

In Fig.6.16a the output of the Senturk's encoder when motor speed is 3550 rpm is shown. As seen here the peak values of the output signals vary a lot and are not same. Although this has not made any problem for motor rotation at this speed (as outputs of the interface circuitry are shaped properly) it is advised to use a magnetic encoder (as a future work) instead of the optical encoder used here because due to the distance between the light emitting diodes and phototransistors and the dust in the air, the intensity of the light coming to

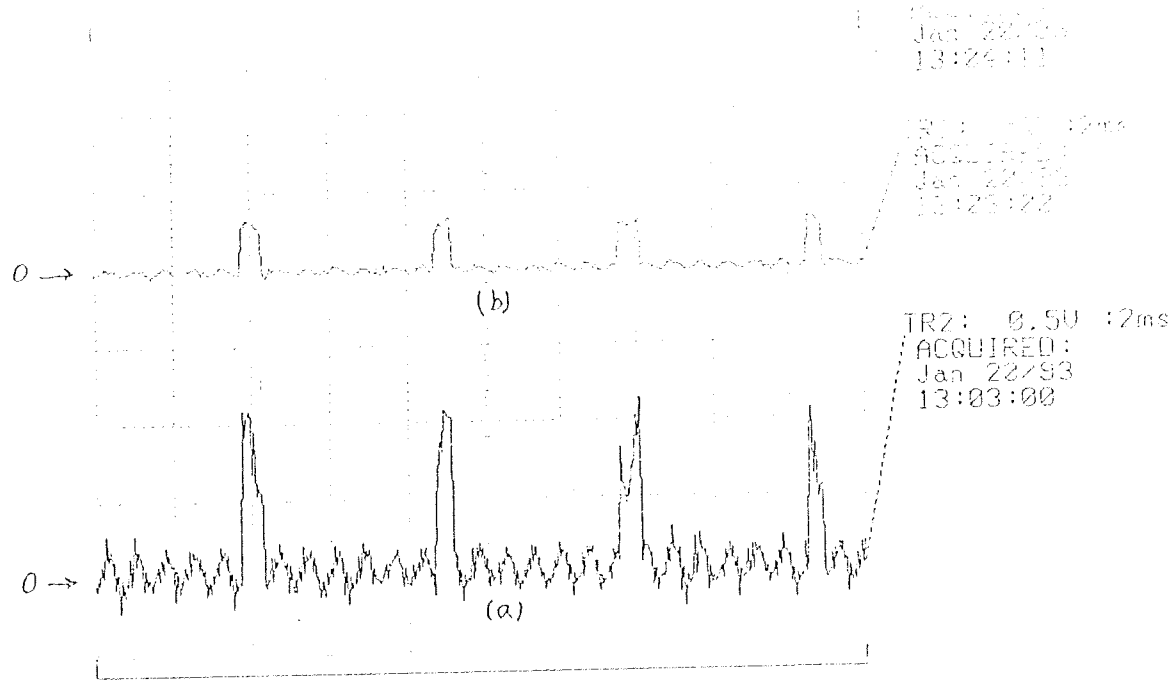

Figure 6.13. a) Output of Senturk's Encoder b) Output of Modified Encoder When Motor Speed is 500 rpm

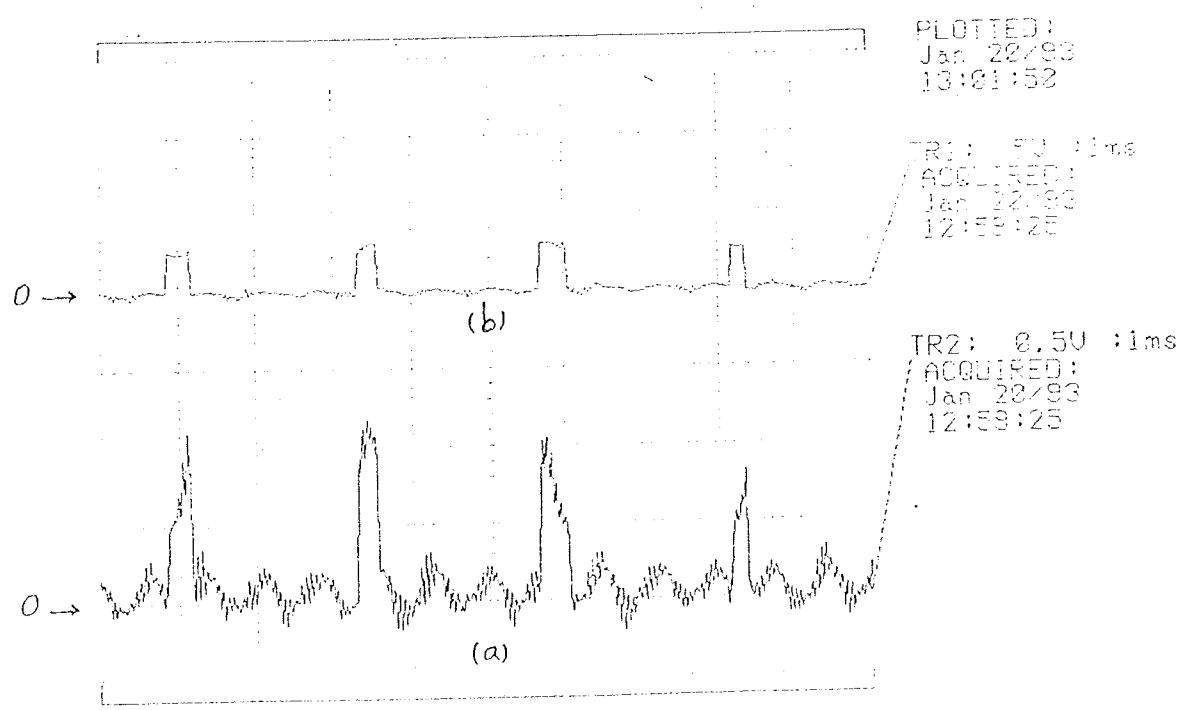

Figure 6.14. a) Output of Senturk's Encoder b) Output of Modified Encoder When Motor Speed is 1000 rpm

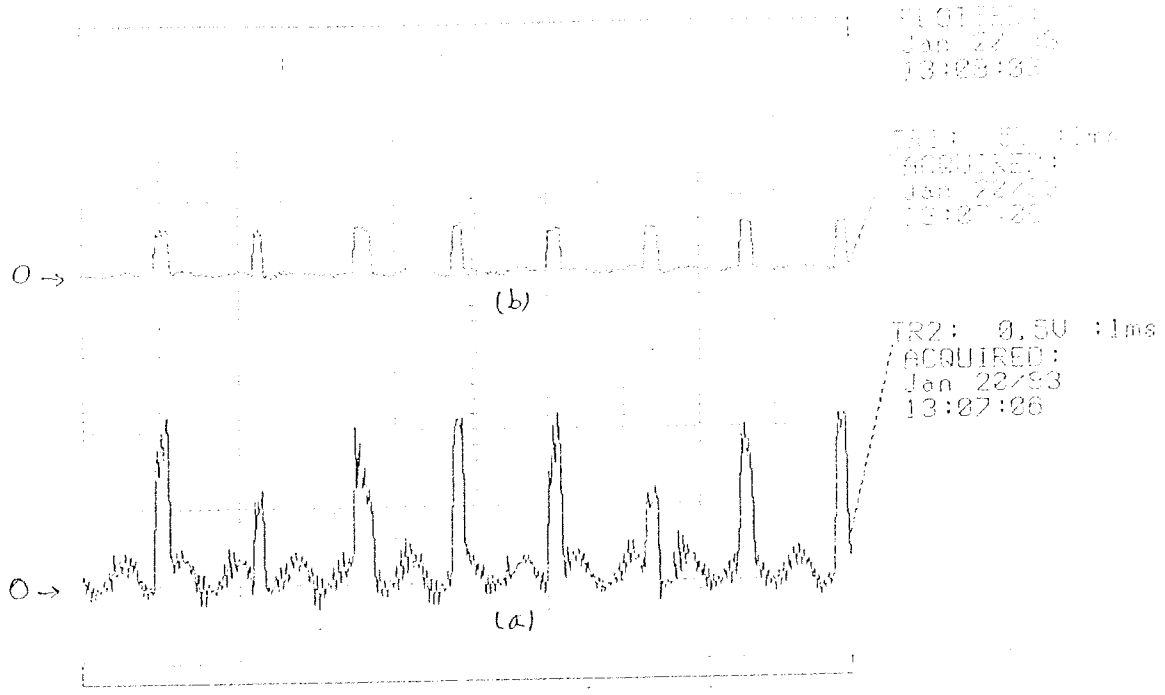

Figure 6.15. a) Output of Senturk's Encoder b) Output of Modified Encoder When Motor Speed is 2000 rpm

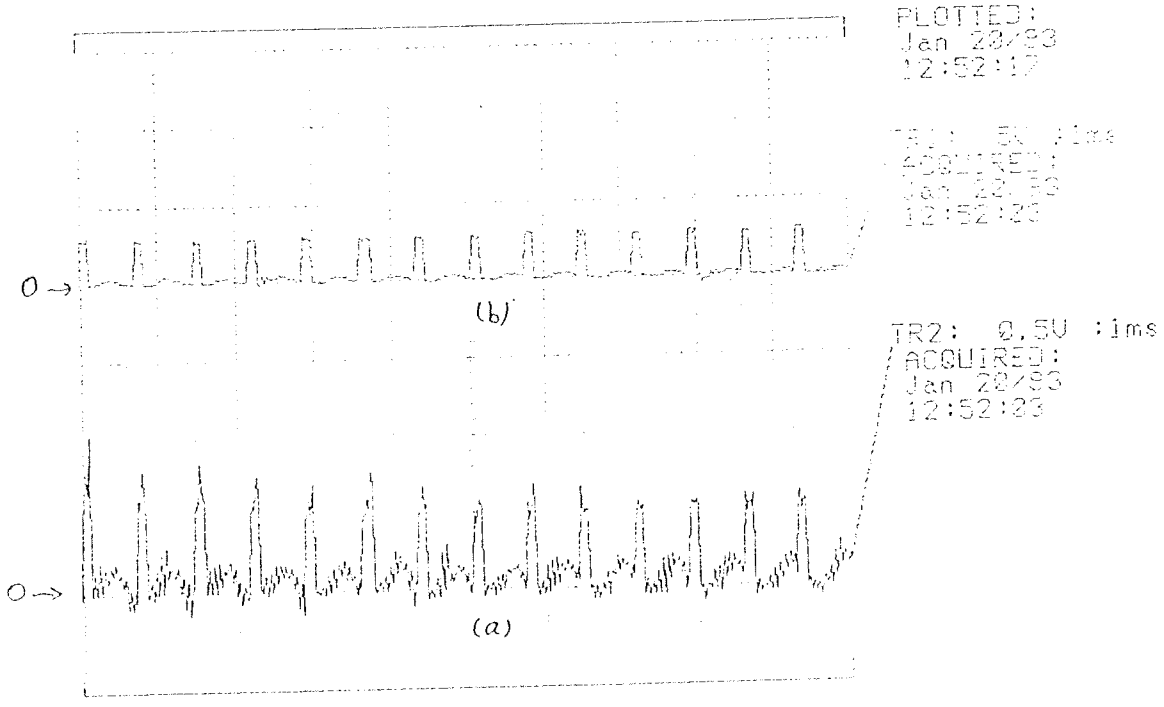

Figure 6.16. a) Output of Senturk's Encoder b) Output of Modified Encoder When Motor Speed is 3550 rpm

phototransistor may be so low that it may produce problems at high speeds. But, with a magnetic type encoders these problems does not exist.

In the second chapter it was explained that one step of our SRM is 15 degrees. So one complete rotation of the rotor (360^0) consists of 24 steps. The position detection system used here gives a feedback pulse each time a step is completed. Hence 24 feedback pulses for one complete rotation of the rotor. Therefore one can drive the formula (6.1) for the relation between speed of the motor in rpm and time T (time between feedback pulses), which is the time between the feedback pulses.

$$T(\text{seconds}) = 60 / 24 * \text{Speed(rpm)} \qquad (6.1)$$

Theoretically (using above formula) for speeds 3000 and 1500 rpm value of T is calculated as 0.833 and 1.66 msec respectively. In Figs.6.17. and 6.18. Position feedback pulses for speeds 3000 and 1500 rpm are recorded. Examining these figures and finding the time between the feedback pulses show the coincidence between theoretical and practical results. Note that as speed of the motor increases, number of feedback pulses also increases (time T between the feedback pulses decreases).

6.5. Verification of the Software

As was explained in chapter V, the software written in this work is a user programmable software and can be used to investigate the motor performance under various advance angle and phase currents. In the coming sections advance angle change and microprocessor setting of current reference is explained.

6.6. Changing Advance Angle

The waveforms of the position pulses and the transistor gate pulses are recorded for the operation of the motor under various

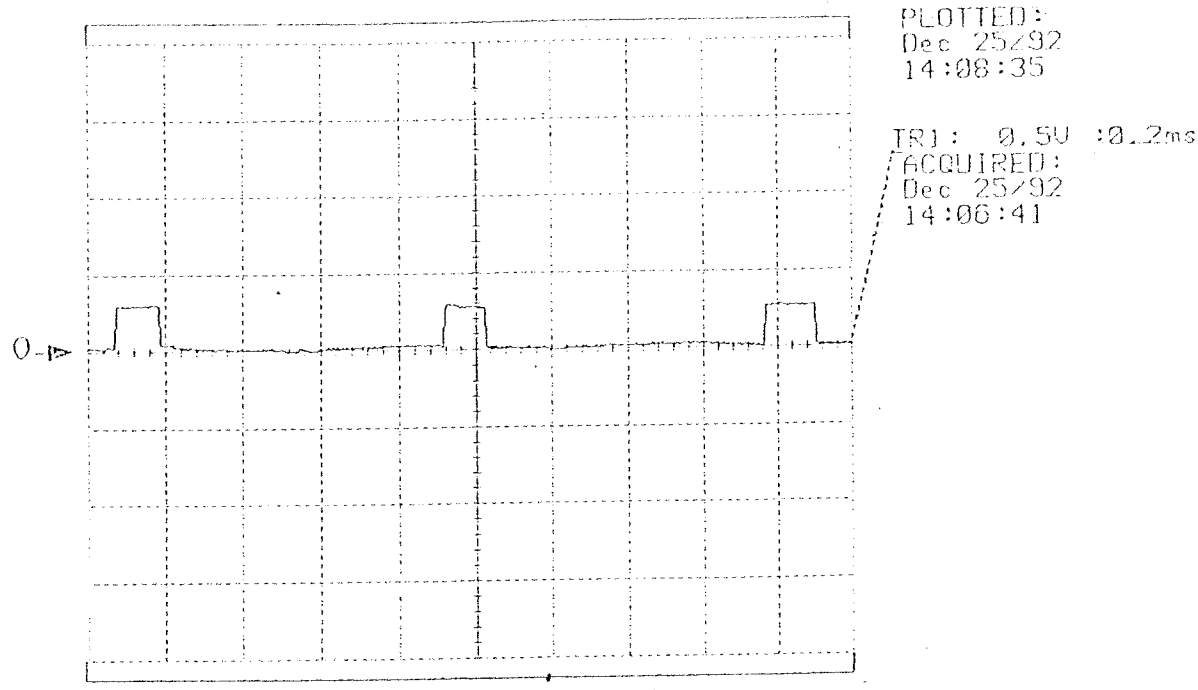

Figure 6.17. Position Feedback Pulses When Speed Is 3000 rpm

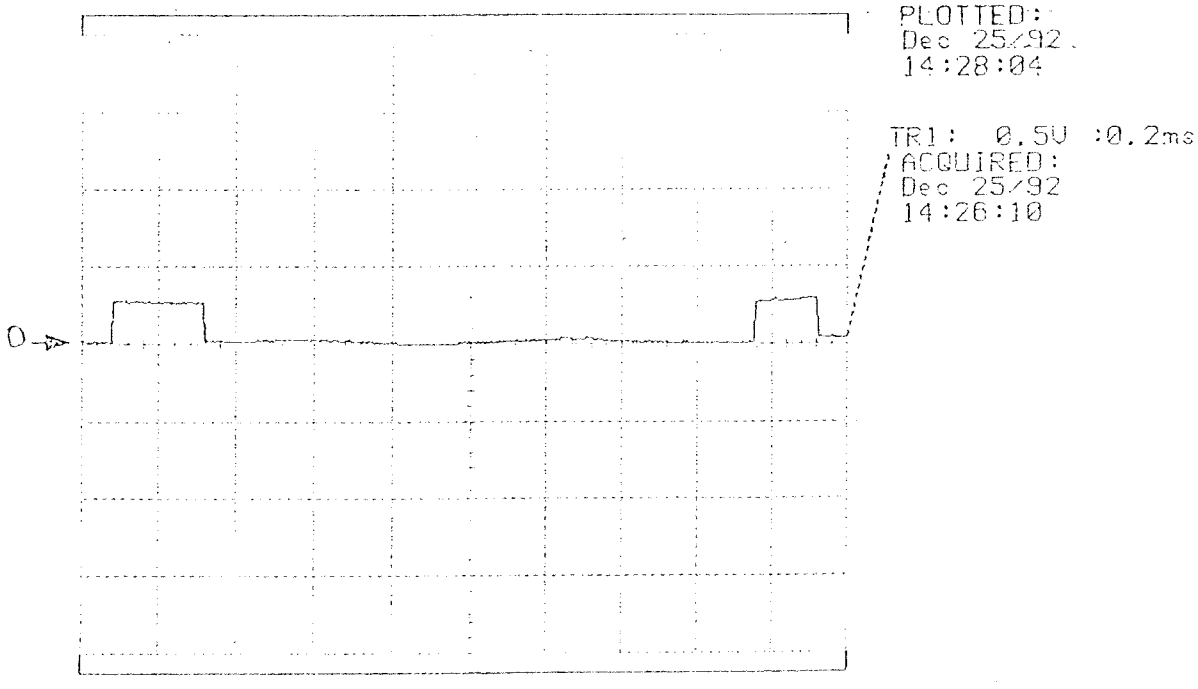

Figure 6.18. Position Feedback Pulses When Speed Is 1500 rpm

advance angles (See Figs.6.19 through 6.22). In Fig.6.19 Feedback pulses and transistor gate pulses for Zero lead angle (Advance angle = 0^{o}) are shown. As it is seen in this figure, as soon as position feedback pulse is received an step command is issued and energized phase is changed. One may wrongly think that when feedback pulses f_2 & f_4 in the Fig.6.19 are received no phase change has occured. This is not the case and it fact phase change has occured when those signals are receiced. This is explained as follows: Since motor is rotated in one phase on mode, each transistor in the power converter is ON while energizing two phases and OFF while energizing the next two phases. For example, consider TR2 in Fig.6.23 which shows a section of the power converter circuitry. This transistor is ON when phase 1 is energized. It will be again ON when phase 2 is energized. Then it will be OFF when two other phases are energized.

Fig.6.20 ,6.21 and 6.22 show the Feedback pulses and transistor gate pulses for 1/8, 1/4 and 1/2 step ignition advance (Advance angles 1.875^{0}, 3.75^{0}, 7.5^{0}) respectively. In these figures one can see the difference between reception time of the feedback and energization of a phase. Hence the advance angle program works perfectly.

Experimental results showed that speed reaches 3800 rpm when advance angle is set to 1/2, supply voltage is 280 V and rated current 5 Amps. For 1/4 advance angle speed is 3500 rpm for the same supply voltage and phase current. For zero advance angle speed is 3200 rpm for the 280 V supply voltage and rated current of 5 Amps. From these results one concludes that higher running speeds are reached when motor operates with higher advance angles. Therefore, The test results here coincides with the theory, as theoretically, at high speeds each change in phase excitation must occur earlier relative to the rotor position, to let the phase current to have sufficient time to become established before the rotor reaches the position of maximum average phase torque.

With this motor and power supply the above values seem to be the top speeds and encoder seems to function well for the speed range

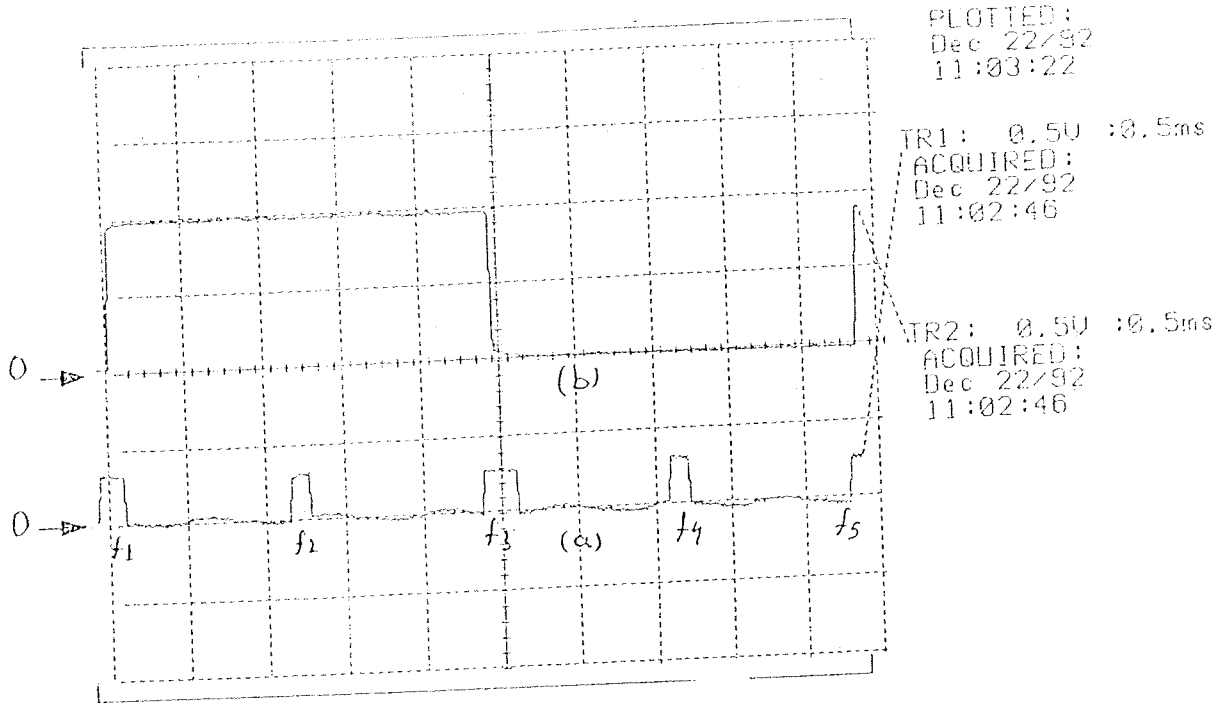

Figure 6.19. a) Feedback Pulses b) Transistor Gate Pulses for Zero Lead Angle (Advance Angle = 0^0)

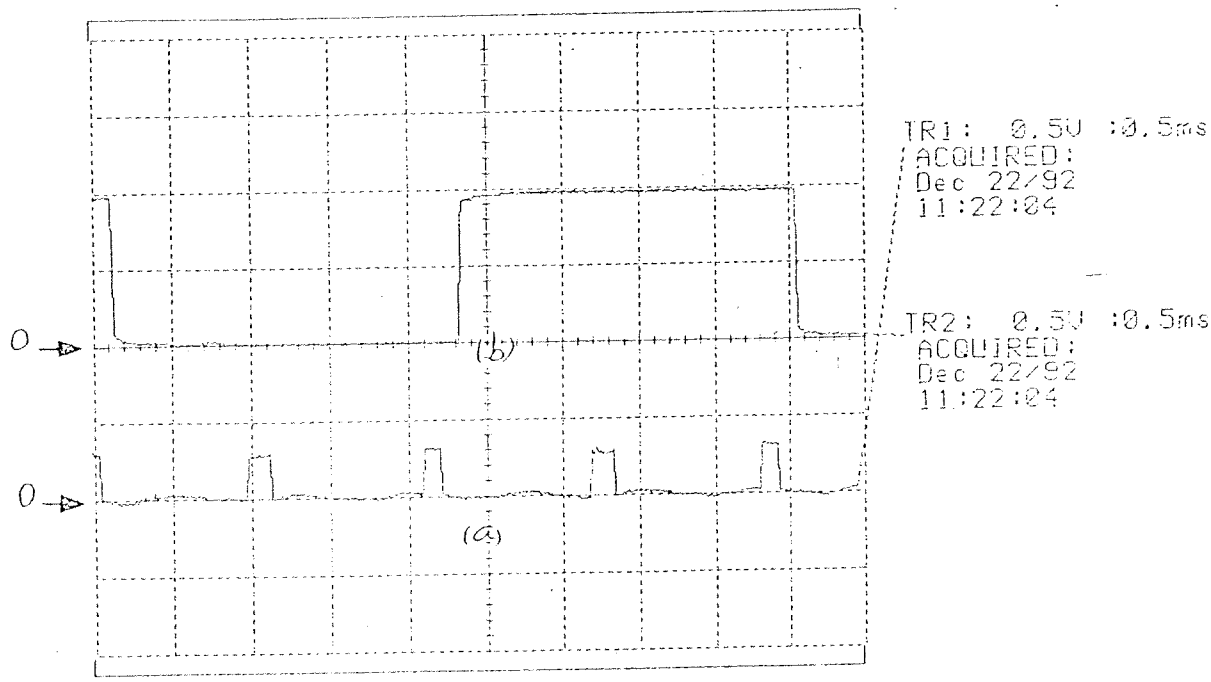

Figure 6.20. a) Feedback Pulses b) Transistor Gate Pulses for 1/8 Step Ignition Advance (Advance Angle = 1.875^0)

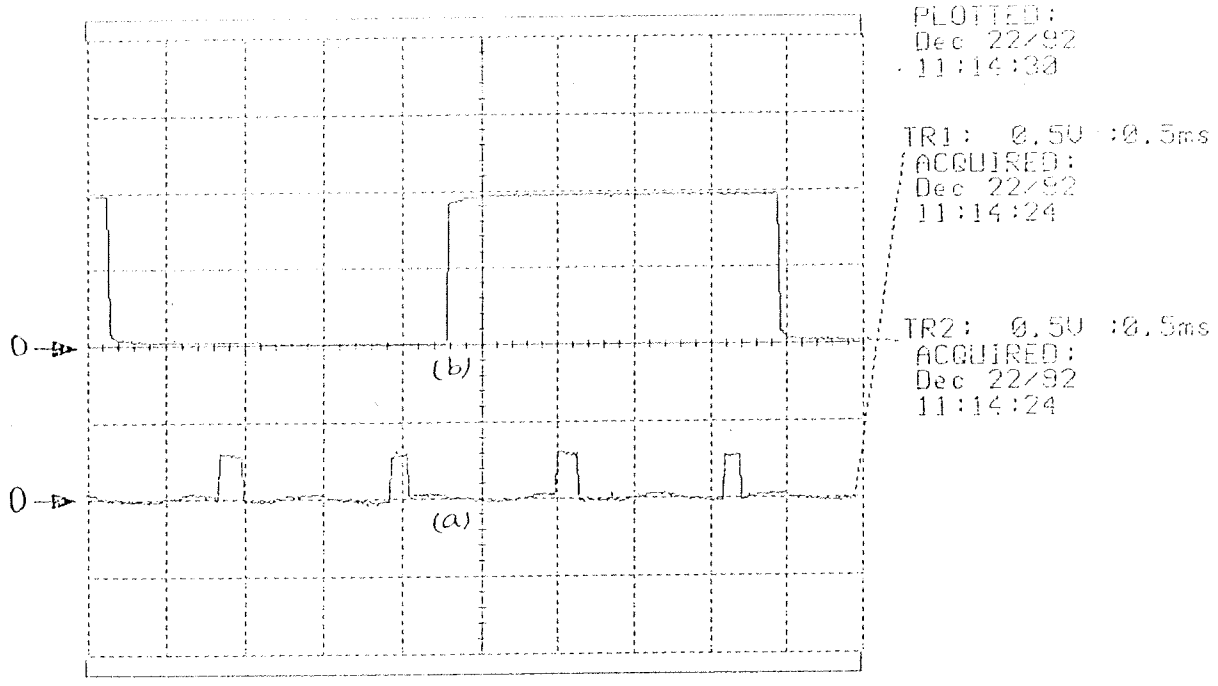

Figure 6.21. a) Feedback Pulses b) Transistor Gate Pulses for 1/4 Step Ignition Advance (Advance Angle = 3.75^0)

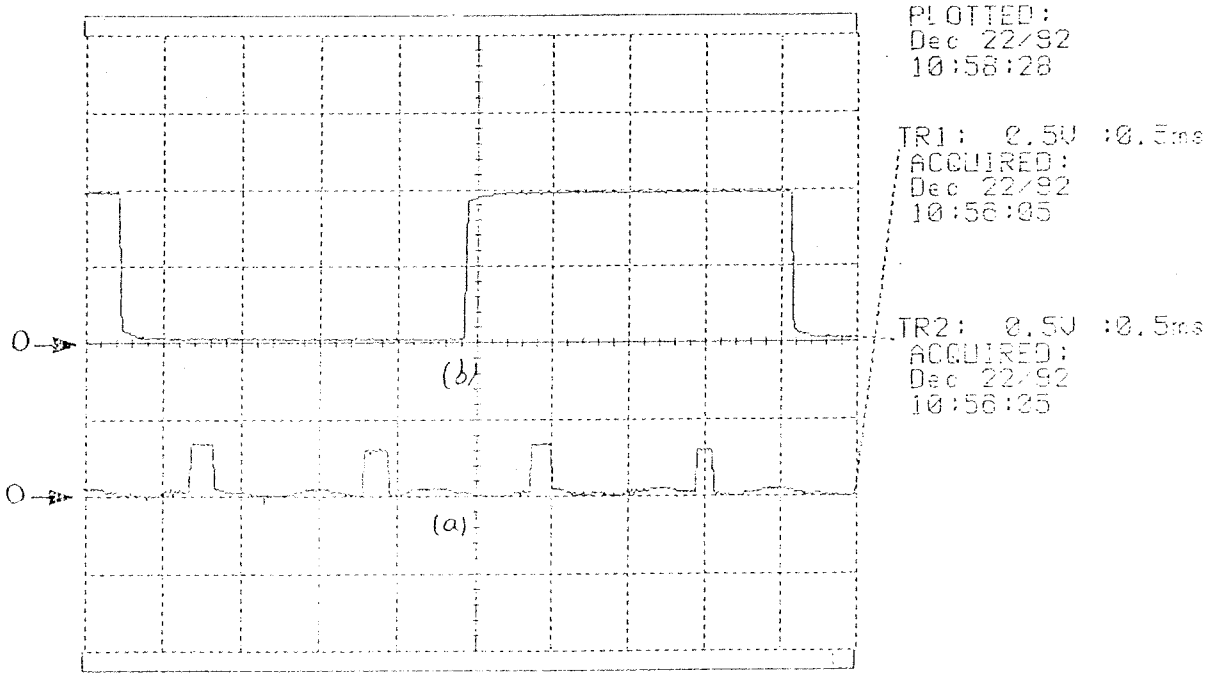

Figure 6.22. a) Feedback Pulses b) Transistor Gate Pulses for 1/2 Step Ignition Advance (Advance Angle=7.5^0)

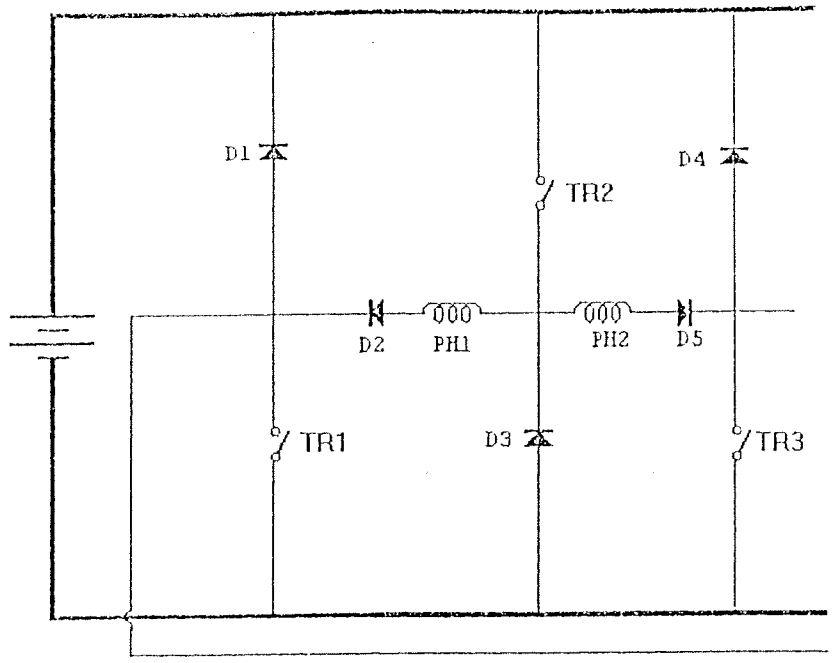

Figure 6.23. A Section of the Power Converter Circuit

it is designed for. However, it is not clear whether it will function satisfactorily when a motor capable of operating at higher speeds is tested. For high speeds it is advised to use a magnetic encoder instead of the optical encoder as was explained in section 6.13.

6.7. Microprocessor Setting of Current References

In previous chapters It was explained how phase current value is related to the reference voltage of the current limiter circuit and this reference voltage is the output of the DAC circuitry whose inputs are the 6-bits coming from microprocessor. In this section accuracy of this setting is illustrated.

Fig.6.24 is obtained when microprocessor has set the phase current to 5 Amps. Here microprocessor has sent a digital data (corresponding to 5 Amps) to the DAC circuitry. Fig.6.24a shows the output of the DAC circuitry which is the reference voltage of current limiter. Here this output is an analog voltage whose value is 4.7 (see

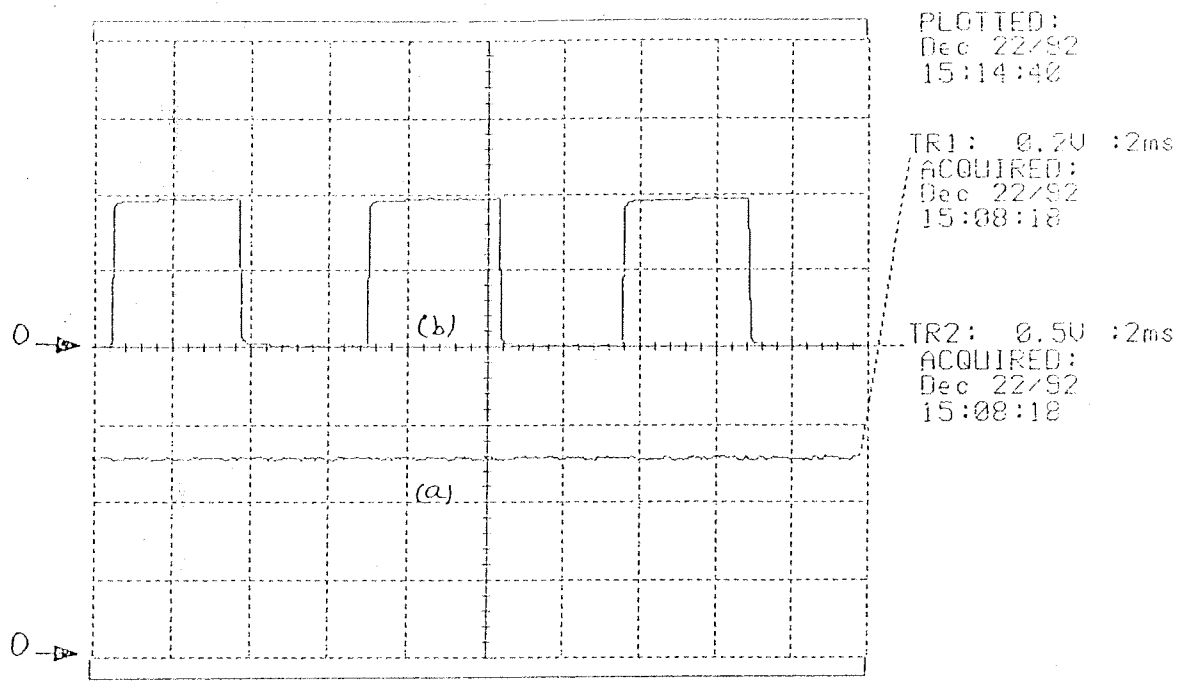

Figure 6.24. a) Reference Voltage of Current Limiter b) Transistor Gate Pulses When Phase Current Value Is Set to Be 5 Amps.

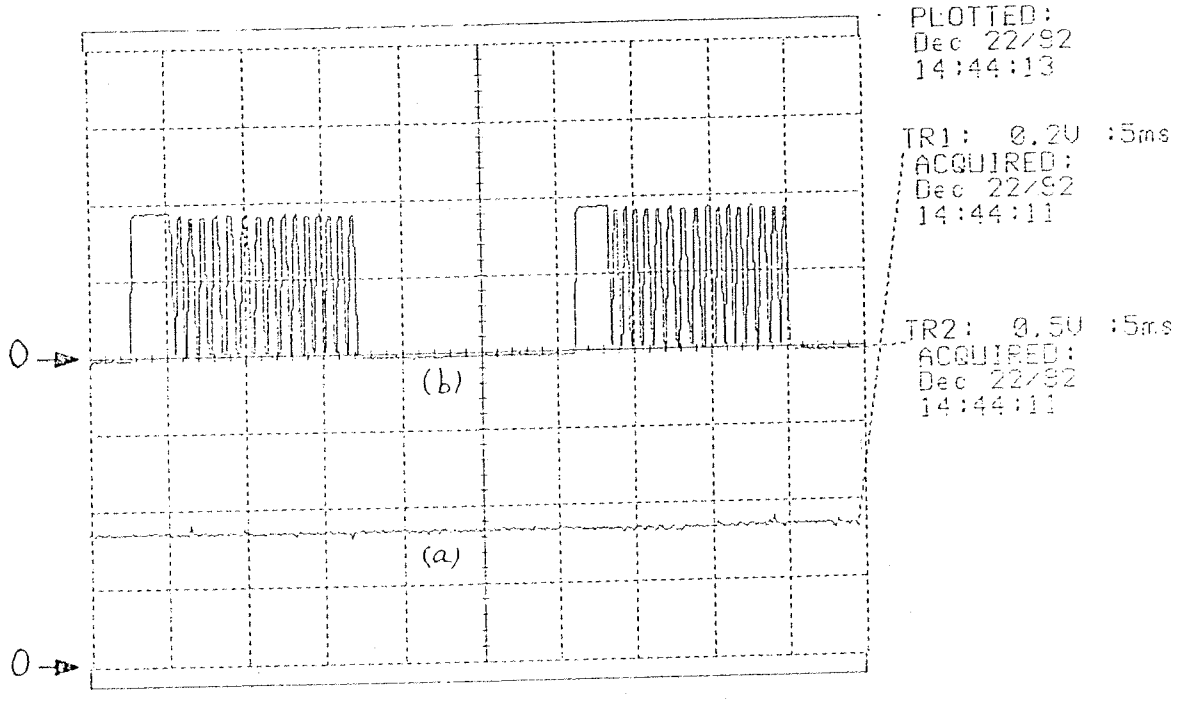

Figure 6.25. a) Reference Voltage of Current Limiter b) Transistor Gate Pulses When Phase Current Value Is Set to Be 1 Amps.

figure). It was explained in section 5.4.2.1 that this value of reference voltage corresponds to phase current of 5 Amps.

Fig.6.25 shows the transistor gate pulses and the reference voltage of current limiter. Here microprocessor was required to change the phase current to 1.5 Amps. As it is seen in the figure the reference voltage is at 3.8 Volts which corresponds to the phase current of 1.5 Amps (see section 5.4.2.1). Note that here transistor is chopping as current limiter tries to fix current at 1.5 Amps.

6.8. Current Limiter Operation

In section 3.7 the operation of the current limiter was explained and its detailed circuit diagram was shown. The proper operation of the current limiter is tested and the results are given in this section. Figure 6.26a shows the output of the schmit trigger when its input is as shown in Fig.6.26b. Note that the input of the schmitt trigger (Fig.6.26b) is the output of the amplifier which amplifies the voltage of the sense pin of the IGT. Figure 6.26 corresponds to the case that; voltage of the sense pin has not reached the reference voltage. In other words, current has not passed the rated value. Note that the output of the schmitt trigger is always high. Hence, transistor switching is completely dependent on the microprocessor signals to the transistor.

Figure 6.27 corresponds to the case that current in the phase has reached the rated current and current limiter tries to fix current. As it is seen in Fig.6.27a the output of the schmitt triger is not always high. During the times that this output is low the transistor will be off (although the processor commands for the transistor to be on). Fig.6.28 shows input vs. output waveforms of the current limiter. This data was obtained when the limiter was trying to fix current. Fig.6.29 shows the transfer function of the limiter for the same conditions.

Fig.6.30 shows the operation of the current limiter

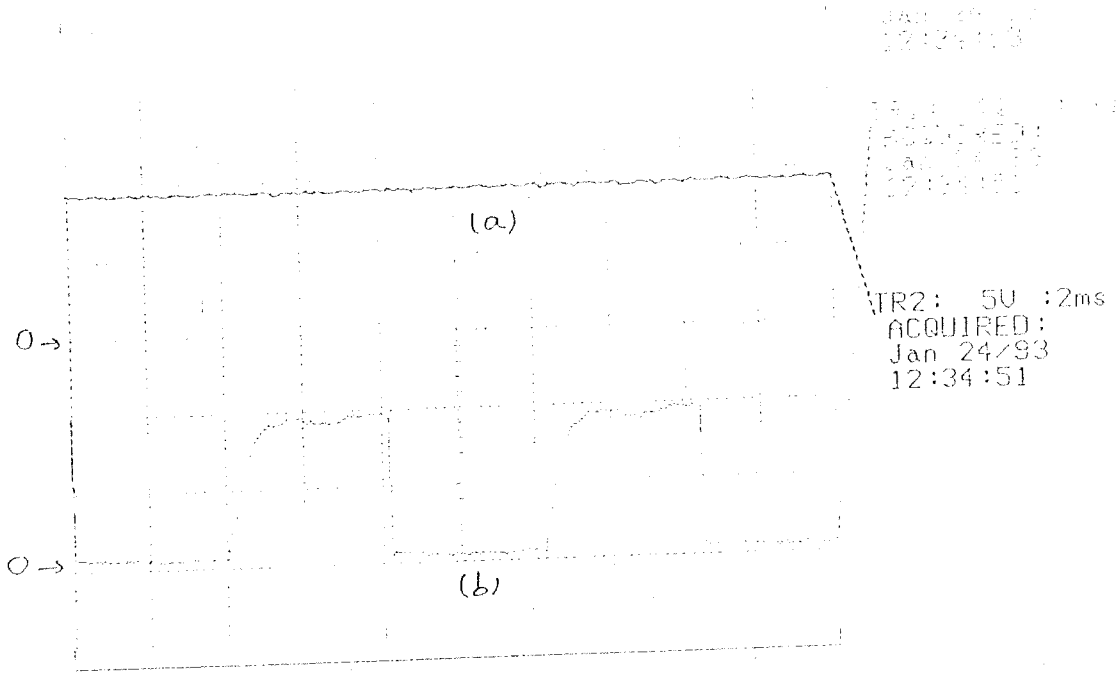

Figure 6.26. a) output of the schmit trigger b) input of the schmitt trigger when voltage of the sense pin has not reached the reference voltage

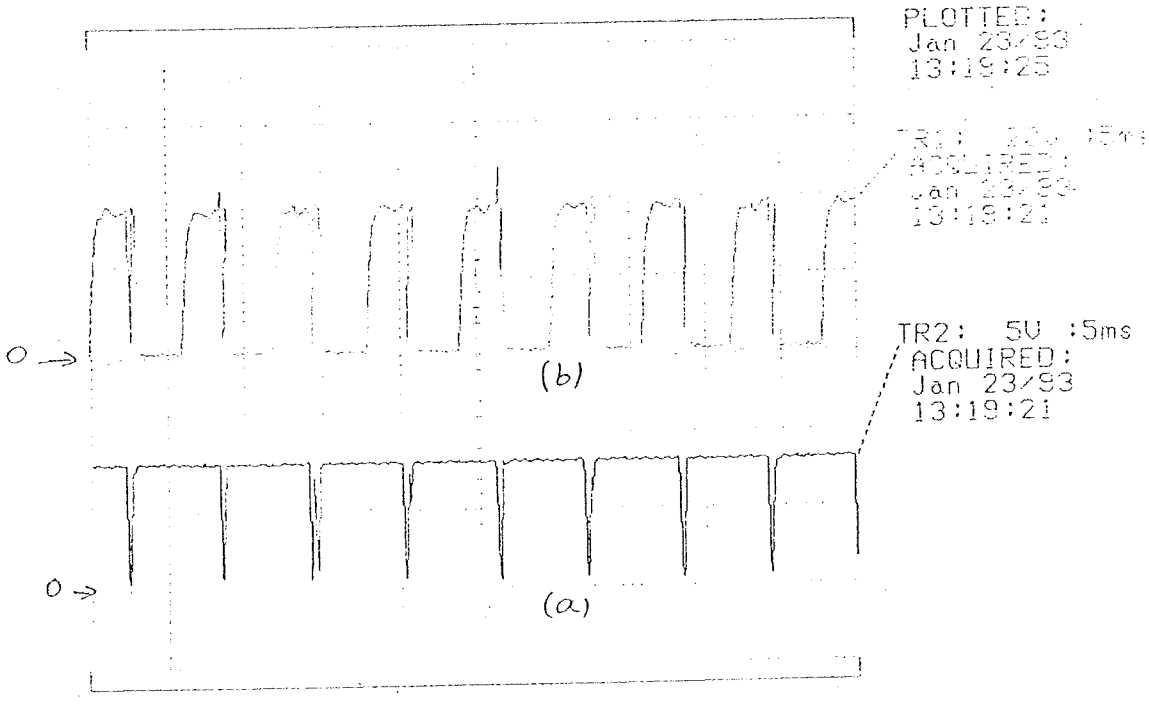

Figure 6.27. a) output of the schmit trigger b) input of the schmitt trigger when current in the phase has reached the rated current

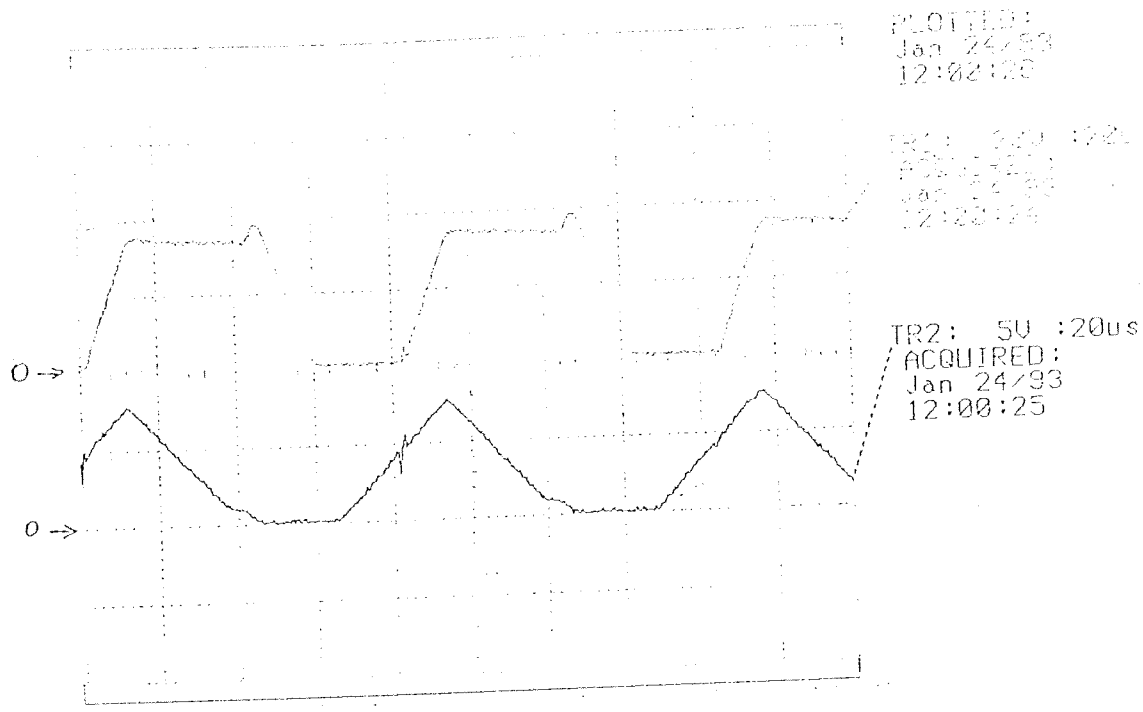

Figure 6.28. Input versus output waveform of current limiter

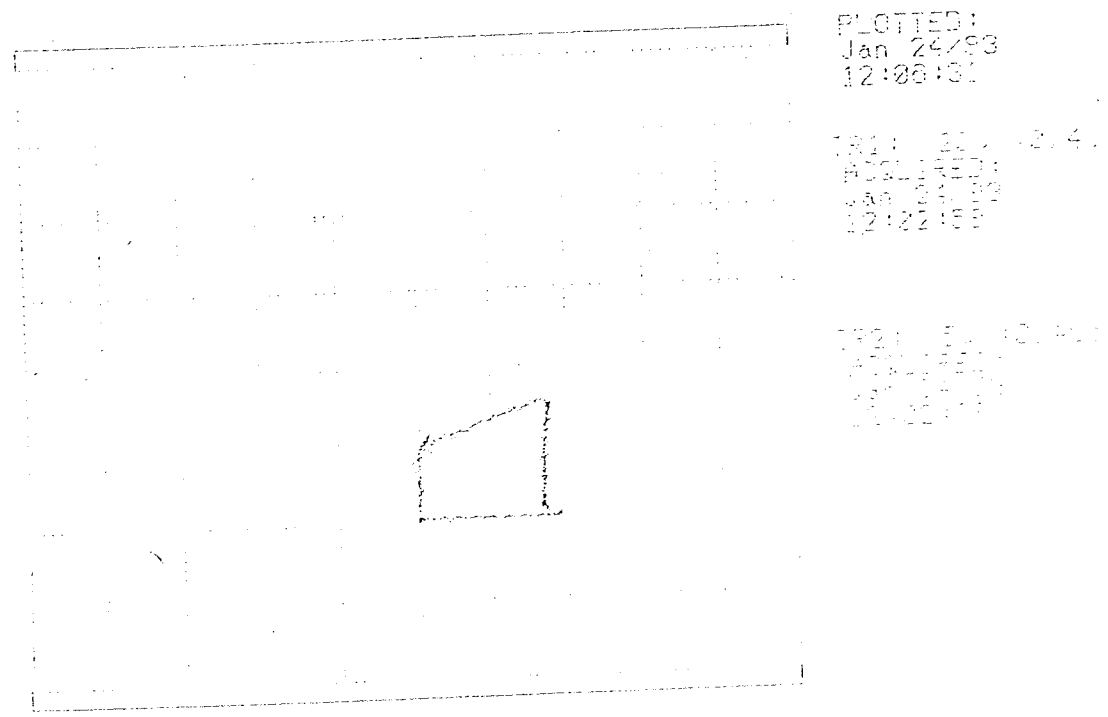

Figure 6.29. Transfer function characteristics of the current limiter

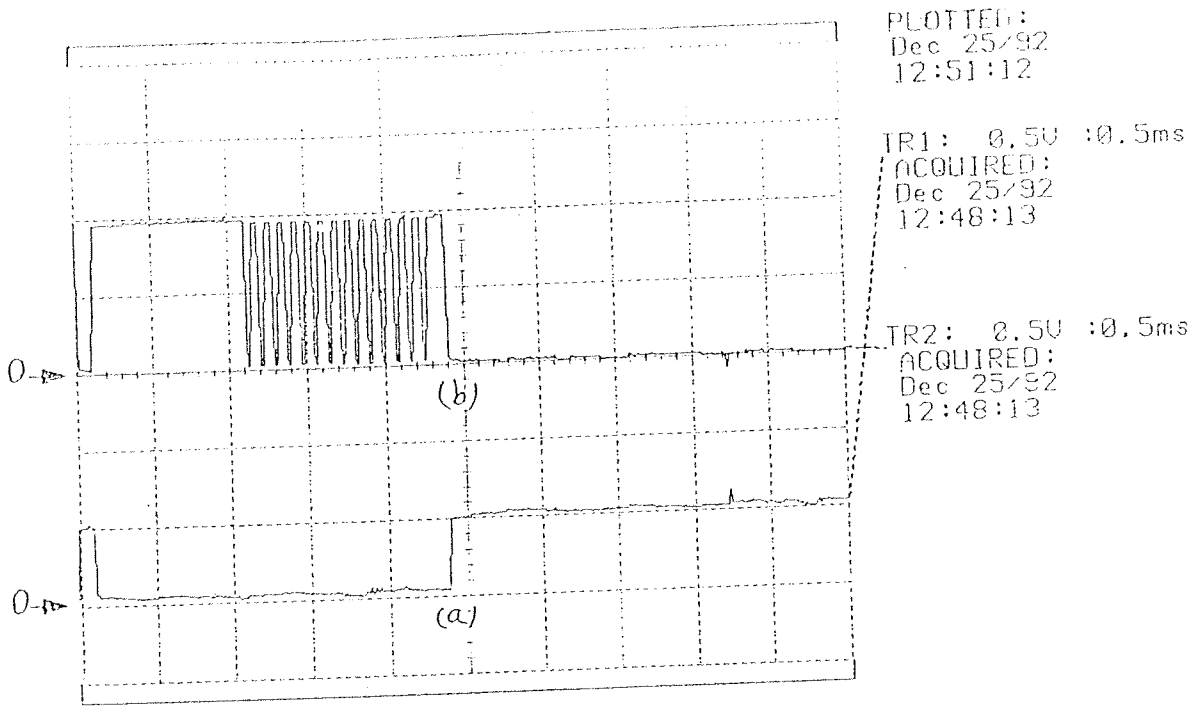

Figure 6.30. a) Microcontroller Pulses for Switching a Transistor b) Corresponding Gate Pulses Applied to the Transistor When Current Limiter Tries to Fix Current by Chopping.

circuitry. That it, it shows the microprocessor pulses and the corresponding pulses applied to the gate of the transistor when current limiter tries to fix current at a rated value by continuously turning on/off (chopping) transistor (See Fig.6.30). That is, in the region (I) although the microprocessor output to a transistor is low (which means that the transistor should be on) gate of IGT is becoming on and off i.e. this transistor is chopping because of the operation of current limiter.

in the drive given as the address of closing switches [illegible]
phase. This data is used for the current limiter. Moreover, this is an important criterion in the implementation of the waveform detection which is a future work.

Note that in this work aim was not to design a processor card, which nowadays has become a fairly standard process, but, was to develop a system which is controlled by the microprocessor. That's why, the Intel's EV80C51FB Evaluation board was used as the processor card. Although using this ready card has saved our time and has given us debugging capabilities (for the programs written), it has unfortunately put some limitations for us such as reducing number of external interrupts and available output ports for the user (as was explained in chapter V). A strongly advised future work is to design the microprocessor card suitable for our aim with a ROM containing the program.

At this stage the aim was implementing a flexible system on which any desired microprocessor based speed control may be achieved in future (which involves development of control strategy either through models or using approaches which rely on knowing input and outputs of the system).

In any microprocessor based system, software has an important role and it should be written cleverly. The software written in this work is a user programmable software. That is, user is able to communicate with the software and determine the value of different control parameters, under which motor should be rotated. Therefore one can investigate motor performance in detail, under various control parameters. Hence important results may be obtained for a sophisticated control in future.

The software written in this work is in modular form in order to be able to use its modules in future softwares. In this work, it is also explained how the microcontroller can change the three control parameters; phase current, advance angle, and conduction time. To

change the phase current by the processor a D/A is used. Although the D/A used in this work is a 10-bit one, only 6 bits of it are used. This is due to the limitation put by the usage of the Evaluation Board here (the number of output pins of the Evaluation board available to user are limited). Here since only 6 bits of the D/A are used, 2^6=64 different current values between 1 and 5 Amps can be selected. As in future, programs may be written for speed control of the motor which may require to change phase current values in smaller steps (if one can use all 10 bits of the D/A then between 1 and 5 Amps he can select 2^{10}=1024 different current values) it is advised to make the microprocessor card suitable for this aim (as a future work).

As the Evaluation Board used here has a serial port, which can be connected to a terminal, user communication is performed using a terminal. Since only few keys of the terminal's keyboard are used by the user, a future work can be to replace terminal with a small keyboard and a LCD display. Note that with terminal used here, data send and receive is performed serially. If faster communication is required, one can use a display and a keyboard with parallel connections to the processor card.

In the third chapter the logic diagram of the Enable circuitry was presented. In this work, this circuitry is made in the power drive using ICs. As a further work one can discard the Enable circuitry from the power drive and write an assembly program, using the boolean processing instructions of 8051, to perform the function of the Enable circuitry. Moreover the Gate ICs block in the Current Limiter circuitry also may be replaced by software. But, one should notice that replacing these circuits with software has the drawback of using microprocessor time, and therefore one should consider speed of the processor and its timing before replacing hardware with software.

One of the most important works that should be done in future is to develop a control technique. The type of control will be speed control of the motor. In other words, a software should be written for the processor to enable the user to enter his required speeds and then

motor accelerate in an optimum way to the desired speed. The program should be also able to get new speeds from user, while rotating, and then decelerate or accelerate in an optimum way to these new entered speeds.

One further work can be to make the power drive circuitry quite smaller using VLSI technique.

REFERENCES

[1] H.B.Ertan, O.F.Yagan, and A.Diriker, "Optimum parameters for doubly salient motors driven by a voltage source drive", 1990 Proceedings, 806 (September, 1990).

[2] H.B.Ertan, M.Tohumcu, "Prediction of performance of switched reluctance motor for design purposes", ICEM 88 (1988).

[3] P.J.Clarkson, P.P.Acarnley, "Stability limits for dynamic operation of variable reluctance stepping motor systems", IEE Proc. Part B, No.6, 135 (November, 1988).

[4] D.W.J.Pulle, "Performance of spilt coil switched reluctance drive", IEE Proc. Part B, No. 6, 135 (November, 1988).

[5] H.B.Ertan, "Analytical prediction of torque and inductance characteristics of identically slotted doubly salient reluctance motors, IEE Proc. Pt.b, No.4, 133, 230, (July, 1986).

[6] J.R.French, "Switched reluctance motor drives for rail traction: relative assessment", IEE Proc. Part B, No.5, 131 (September, 1984).

[7] W.F.Ray, R.M.Davis, P.J.Lawrenson, J.M.Stephenson, N.N.Fulton, and R.J.Blake, "Switched reluctance motor drives for rail traction: a second view", IEE Proc. Part B, No.5, 131 (September, 1984).

[8] P.J.Lawrenson, J.M.Stephenson, P.T.Blenkinsop, J.Corda, and N.N.Fulton, "Variable speed switched reluctance motors", IEE Proc. No.4, 127, 253 (1980).

[9] J.M.Stephenson, J.Corda, "Computation of torque and current in doubly salient reluctance motors from nonlinear magnetization data",

IEE Proc. No.2, 126, 393 (1979).

[10] A.J.C.Bakhuizen, "On the calculation of permeance and forces between doubly slotted structures", J.Appl.Sci.&Eng., 19 (1975).

[11] M.Tohumcu, "Optimum Design of Switching Reluctance Motors", Ph.D.Thesis, Middle East Technical University, Ankara, Turkey (1985).

[12] P.P.Acarnley, "Stepping motors: A guide to modern theory and practice" IEE control Engineering series 19, (1984).

[13] R.M.Davis, W.F.Ray, and R.J.Blake, "Inverter drive for Switched Reluctance motor: Circuits and component ratings" Proc. IEE. Pt.B. No.2, 128, 126 (March, 1981).

[14] D.A.Torrey, and J.H.Lang, "Optimal efficiency excitation of variable reluctance motor drives" IEEE Proc. Vol.138, No.1, 1 (Jan. 1991).

[15] C.Pollock, and B.W.Williams, "A unipolar converter for a switched reluctance motor" IEEE Trans. on Industry Appli. No.2, 26, 222 (March/April 1990).

[16] C.Pollock, and B.W.Williams, "Power converter circuits for Switched Reluctance motors with the minimum number of switches" IEE Proc. Pt.B. No.6, 137, 373 (November, 1990).

[17] D.A.Torrey, and J.H.Lang, "Modeling a nonlinear variable reluctance motor drive" IEE. Proc. Pt.B. No.5, 137, 314 (September, 1990).

[18] M.Ehsani, "Drive technology simplification", International AEGEAN conference on Electrical Machines and power electronics ACEMP92, 524 (1992).

[19] B.K.Bose, T.J.E.Miller, P.M.Szczesny, and W.B.Bicknell,

"Microcomputer control of switched reluctance motor", IEEE Trans. on industry appli. No.4, IA-22 (July/August 1986).

[20] P.H.Chappel, W.F.Ray, R.J.Blake, "Microprocessor control of a variable reluctance motor", IEE Proc Pt.B. No.2 ,131 (March 1984).

[21] S.Senturk, "A transistorized switched reluctance motor drive", Msc. Thesis in Electrical Engineering, Middle East Technical University, Ankara (1989).

[22] W.R.Skanadore," Methods for utilizing high speed switching transistors in high energy switching environments ", General semiconductor industries, Inc. Tempe, Arizona, pp 1-10.

[23] W.Mcmurray, "Selection of snubbers and clamps to optimize the design of transistor switching converters" IEEE Trans. on industry appli No.4, IA-16, 513 (July/August, 1980).

[24] R.E.Tarter, Principles of solid state power conversion, pp 72-75.

[25] J.R.Frus, and B.C.Kuo, "Closed loop control of step motors using waveform detection" Proceedings, International conference on stepping motors and systems, (July, 1976).

[26] J.R.Frus, and B.C.Kuo, "Closed loop control of step motors without feedback encoders" Proceedings, Fifth annual symposium on incremental motion control systems and devices, (May, 1976).

[27] B.C.Kuo, and A.Cassat, "On current detection in variable reluctance step motors" Proceedings, 6th annual symposium on incremental motion control systems and devices, (1977).

[28] P.P.Acarnley, R.J.Nill, and C.W.Hooper, "Detection of rotor position in stepping and switched motors by monitoring of current waveforms" IEEE Trans. on industrial electronics No.3, IE-32, 215 (August, 1985).

[29] M.Jufer, and S.Campiche, "Self synchronization of a one phase stepping motor by a bridge circuit of its coil" Swiss Federal Institute of technology Lausanne, Switzerland.

[30] P.Ferraris, G.Giors, L.Pecorara, and F.Piglione, "An adaptive method for stepping motor control" Polytechnic of Turin, Turin, Italy.

[31] P.H.Chappell, "Winding current in a Switched Reluctance motor" IEE Proc. Pt.B. No.5, 134, 227 (September, 1987).

[32] _____, Embedded Control Applications, Intel Co., California (1988).

[33] _____, EV80C51FB Microcontroller evaluation board, User's manual, Intel Co., California (1988).

APPENDICES

APPENDIX A

DATA SHEETS OF IGT7E20CS

Current Sensing IGT™ Transistors

Insulated Gate Bipolar Transistors

25 A, 500 V

$r_{DS}(on)$ = 0.105 Ω

Features:

- *Low $V_{CE}(sat)$ - 1.8 V typ. @ 25 A*
- *Ultra-fast turn-on - 150 ns typical*
- *Polysilicon MOS gate - voltage controlled turn on/off*
- *High current handling - 25 A @ 85°C case*
- *Current sensing pilot*

TERMINAL DIAGRAM

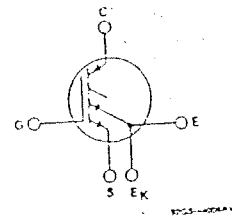

N-CHANNEL ENHANCEMENT MODE

The GSI525 and/or IGT7E20CS IGT™ Transistor (Insulated-Gate Bipolar Transistor) is a MOS-Gated power-switching device combining the best features of power MOSFETs and bipolar transistors with current sensing pilots. The result is a device that has the high input impedance of MOSFETs and the low on-state conduction losses of bipolar transistors. The gate characteristics of the IGT™ Transistor are similar to power MOSFETs but its equivalent $r_{DS}(on)$ drain resistance is ten times lower and varies only moderately between 25°C and 150°C, thus offering extended power handling capability.

The IGT™ Transistor is ideal for many high voltage switching applications up to 5 kHz where low conduction losses are essential; ac and dc motor controls, power supplies and drivers for solenoids, relays, and contactors.

TERMINAL DESIGNATION

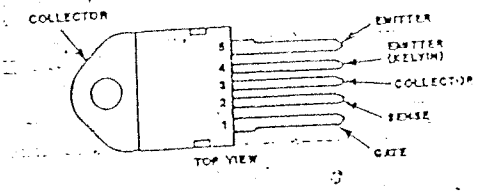

TO-218 (5 LEAD)

MAXIMUM RATINGS

COLLECTOR-EMITTER VOLTAGE (V_{GE} = 0 V)	V_{CES}	500		V
COLLECTOR-GATE VOLTAGE (R_{GE} = 1 MΩ)	V_{CGR}	500		V
CONTINUOUS DRAIN CURRENT	I_C			
At T_C = 85°C		25		A
PULSED COLLECTOR CURRENT	I_{CM}*	80		A
GATE-EMITTER VOLTAGE	V_{GE}	±20		V
TOTAL POWER DISSIPATION	P_D			
At T_C = 25°C		125		W
Derate Above 25°C		1		W/°C
OPERATING AND STORAGE JUNCTION TEMPERATURE RANGE	T_J, T_{STG}	-40 to +150		°C
THERMAL RESISTANCE, JUNCTION TO CASE	$R_{\theta JC}$	1		°C/W
MAXIMUM LEAD TEMPERATURE FOR SOLDERING PURPOSES	T_L			
1/8 inch from case for 5 seconds		260		°C

*Repetitive Rating: Pulse width limited by maximum junction temperature. Gate control turn-off not allowed above 50 amperes.

Harris Semiconductor IGBT product is covered by one or more of the following U.S. patents:

4,364,073	4,417,385	4,430,792	4,443,931	4,466,176	4,532,534	4,567,641
4,587,713	4,618,872	4,620,211	4,631,564	4,639,754	4,639,762	4,641,162
4,644,637	4,682,195	4,684,413	4,717,679	4,794,432	4,801,986	4,803,533
4,809,045	4,810,665					

ELECTRICAL CHARACTERISTICS, T_C = 25° C Unless Otherwise Specified

CHARACTERISTIC		TEST CONDITIONS	LIMITS MIN.	LIMITS TYP.	LIMITS MAX.	UNITS
OFF CHARACTERISTICS						
Collector-Emitter Breakdown Voltage	BV_{CES}	V_{GE} = 0 V, I_C = 250 μA	500	—	—	V
Collector Cut-off Current	I_{CES}	V_{CE} = Max. Rating V_{GE} = 0 V, T_C = 25° C	—	—	250	μA
		V_{CE} = Max. Rating x 0.8 V_{GE} = 0 V, T_C = 125° C(1)	—	—	4	mA
Gate-Emitter Leakage Current	I_{GES}	V_{GE} = ±20 V	—	—	±500	nA
ON CHARACTERISTICS(2)						
Gate Threshold Voltage	$V_{GE}(th)$	V_{CE} = V_{GE}, I_C = 500 μA T_C = 25° C T_C = 150° C	2 —	4 2	5.5 —	V
Collector-Emitter Saturation Voltage	$V_{CE}(sat)$	V_{GE} = 15 V, I_C = 25 A T_C = 25° C T_C = 150° C	— —	1.8 1.9	2.6 —	V
DYNAMIC CHARACTERISTICS						
Input Capacitance	C_{ies}	V_{GE} = 0 V V_{CE} = 25 V f = 1 MHz	—	2300	—	pF
Output Capacitance	C_{oes}		—	250	—	
Reverse Transfer Capacitance	C_{res}		—	35	—	
SWITCHING CHARACTERISTICS(2) (See Figs. 8 & 9)						
Turn-on Delay Time	$t_d(on)$	Resistive Load, T_J = 150° C I_C = 25 A, V_{CE} = 400 V V_{GE} = 15 V $R_G(on)$ = 50 Ω, $R_G(off)$ = 50 Ω	—	100	—	ns
Rise Time	t_r		—	150	—	
Turn-off Delay Time	$t_d(off)$		—	0.6	—	μs
Fall Time	t_f		—	3	—	
Turn-off Delay Time	$t_d(off)$	Inductive Load, T_J = 150° C L = 45 μH, I_C = 25 A $V_{CE}(clamp)$ = 400 V, V_{GE} = 15 V $R_G(on)$ = 50 Ω, $R_G(off)$ = 50 Ω	—	1.5	2.5	μs
Fall Time	t_f		—	1.2	1.6	
Turn-off Switching Losses	E_T		—	5	8	mJ
PILOT CHARACTERISTICS(2)(3)(4)						
Pilot - Emitter Kelvin Voltage	V_{PEK}	V_{GE} = 15 Vdc, R_P = 1 KΩ				V
I_C = 20 A			1	1.3	1.6	
I_C = 30 A			—	1.45	—	
I_C = 40 A			—	1.7	—	

(1) Applies for 3.3° C per watt maximum thermal resistance, case to ambient.

(2) Pulse test: Pulse widths ≤ 300 μs, duty cycle ≤ 2%.

(3) Refer to Fig. 5(a).

(4) When not in use connect P to Emitter.

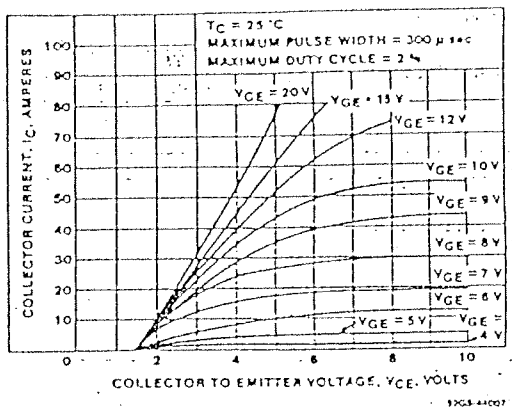

Fig. 1 - Typical output characteristics.

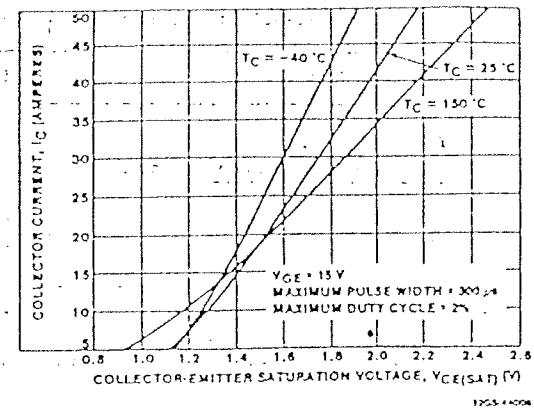

Fig. 2 - Typical collector-emitter saturation voltage

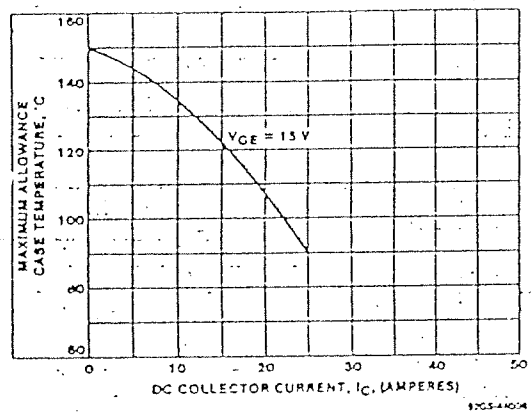

Fig. 3 - Maximum allowable dc collector current vs. case temperature.

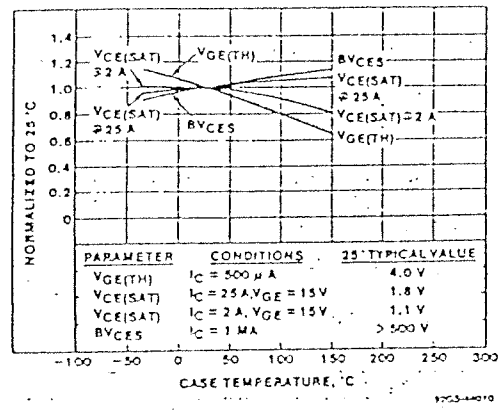

PARAMETER	CONDITIONS	25° TYPICAL VALUE
$V_{GE(TH)}$	I_C = 500 μ A	4.0 V
$V_{CE(SAT)}$	I_C = 25 A, V_{GE} = 15 V	1.8 V
$V_{CE(SAT)}$	I_C = 2 A, V_{GE} = 15 V	1.1 V
BV_{CES}	I_C = 1 MA	> 500 V

Fig. 4 - Typical temperature dependence of parameters.

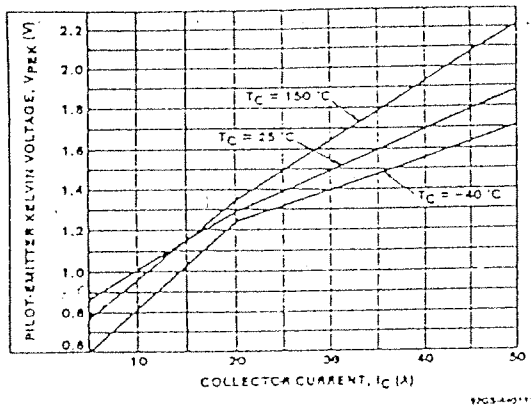

Fig. 5(a) - Typical emitter pilot characteristics - 1 KΩ pilot resistor.

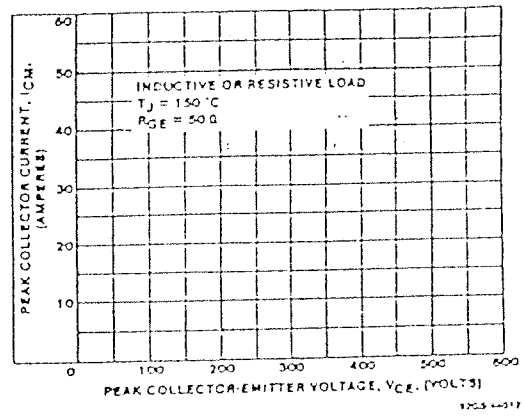

Fig. 5(b) - Turn-off safe operating area.

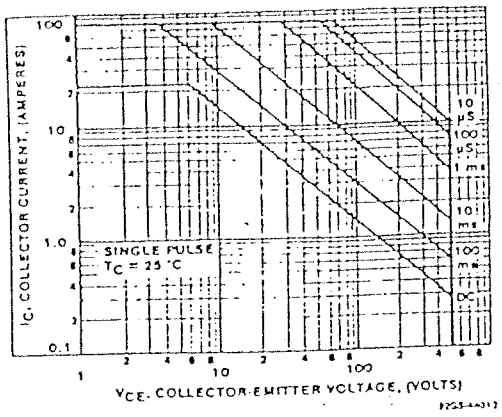

Fig. 6 - Active region safe operating area.

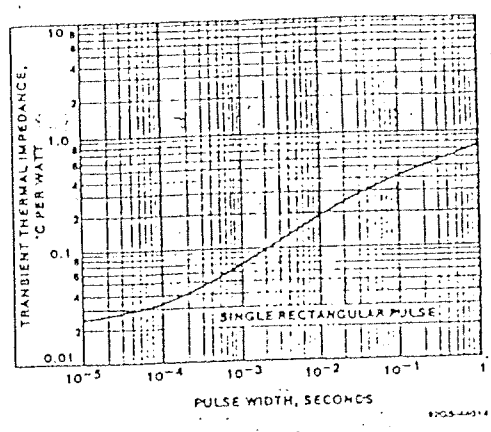

Fig. 7 - Maximum transient thermal impedance.

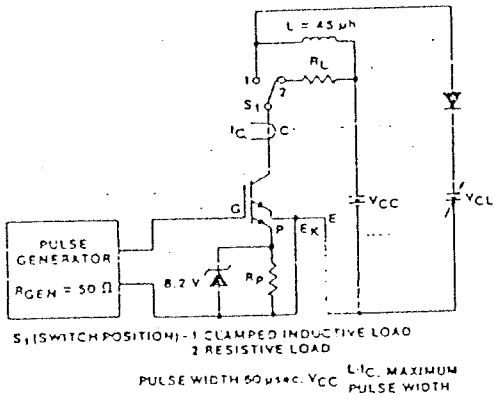

Fig. 8 - Basic switching test circuit.

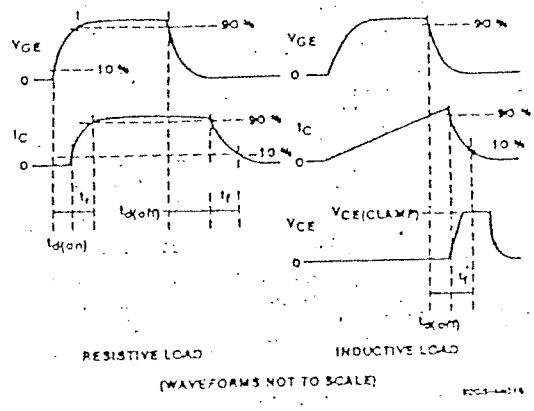

Fig. 9 - Switching waveforms.

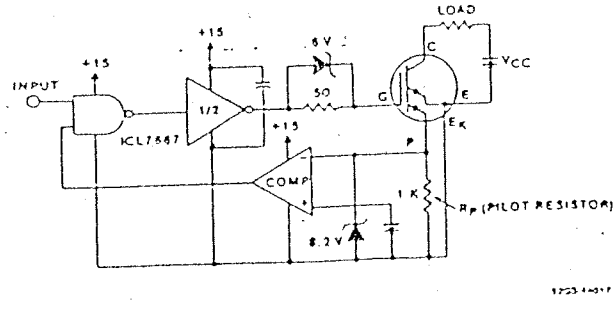

Fig. 10 - Typical circuit utilizing the pilot for overcurrent protection.

APPENDIX B

PRINTED CIRCUIT BOARDS

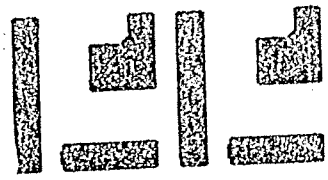

Figure B.1. PCB of Snubber Circuit (Soldering Side)

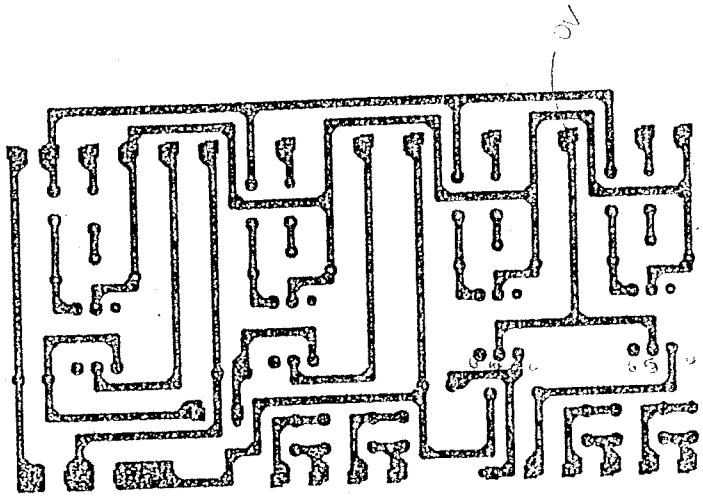

Figure B.2. PCB of Isolation and Inversion Circuit (Soldering Side)

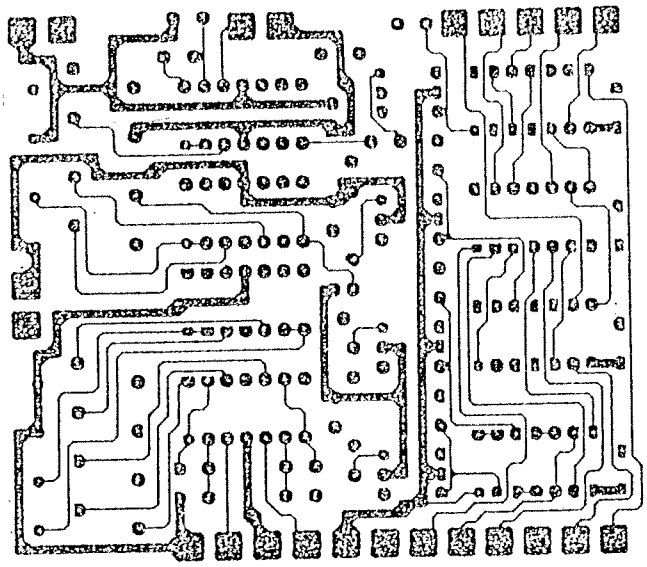

(a)

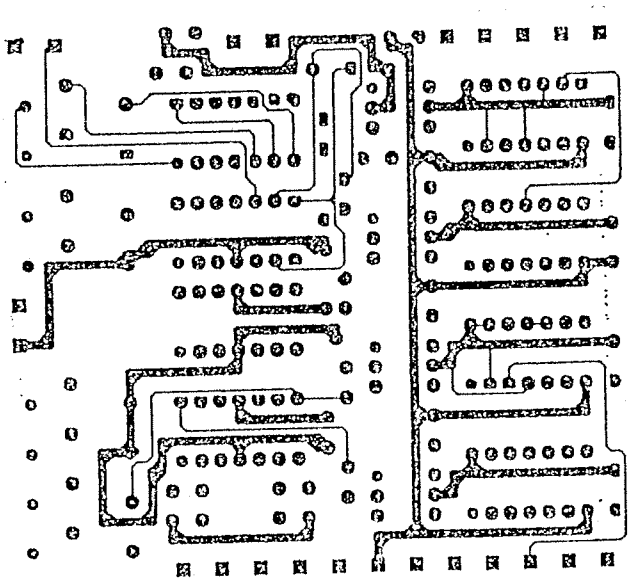

(b)

Figure B.3. PCB of Current Limiter Circuit. a) Soldering Side
b) Component Side

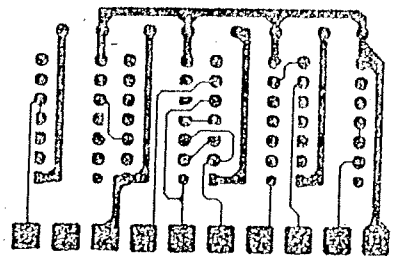

(a)

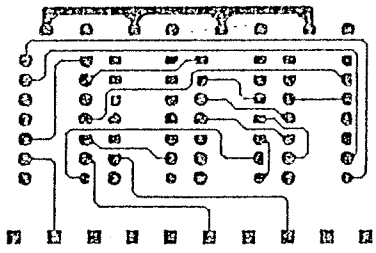

(b)

Figure B.4. PCB of Enable Circuit. a) Soldering Side
b) Component Side.

APPENDIX C

ASSEMBLY PROGRAM

```
$ep
$title(THESIS.A51) date(5.JAN.1993)
$nomod51
$nosymbols
$nolist
$include(rg51fa.pdf)
$list

;STRING DEFINITIONS, START AT ADDRESS 5000H
       ORG 5000H
DYWTECP: DB 'DO YOU WANT TO ENTER CONTROL PARAMETERS?(y/n) ',00H
EAA: DB 'ENTER ADVANCE ANGLE:(0,1/2,1/4,1/8,1/16,1/32) ',00H
EPC: DB 'ENTER PHASE CURRENT:(1.0,1.5,2.0,2.5,3.0,3.5,4.0,4.5,5.0)
',00H
EMOO: DB 'ENTER MODE OF OPERATION:(o,t,h) ',00H
DYWRBC: DB 'DO YOU WANT ROTATION BE CW?(y/n) ',00H
SR: DB'START ROTATION?(y/n) ',00H
MS: DB 'MOTOR STOPPED ',00H

;VARIABLES
CAPTURE DATA  40H    ;USED IN PCA SUBROUTINE
PERIOD  DATA  42H    ;TIME BETWEEN FEEDBACK PULSES
NEXTFIRST DATA 44H   ;USED IN PCA SUBROUTINE
RLN DATA 46H         ;REPEAT LEAD NUMBER FOR LEAD ANGLE
FCURRENT DATA 47H    ;VALUE OF CURRENT FIXED BY USER
CURRENT DATA 23H     ;DTOA VALUE FOR CURRENT
NEWCURRENT DATA 24H ;NEWCURRENT SENT TO DAC VIA PORTS
LEADNUM DATA 25H     ;REPEAT OF DIV BY 2 FOR ADV.ANGLE

BIT_CW BIT 20H.0     ;SET MEANS CLOCKWISE ROTATION
CAPNUM BIT 20H.1     ;DETERMINE CAPTURE NUMBER
FEEDBACK BIT 20H.2   ;FEEDBACK RECEIVED
T1PASSED BIT 20H.3   ;TIMER 1 HAS PASSED
ZEROLEAD BIT 20H.4   ;WHEN SET MEANS LEAD ANGLE IS ZERO
FIRSTTIME BIT 20H.5 ;FIRST TIME ENTER LOOP FOR ZERO LEAD

     ORG 4000H       ;PROGRAM STARTS FROM HERE AT RESET
     JMP INIT
```

```
        ORG 401BH       ;ADDRESS OF TIMER1 INTERRUPT VECTOR
        JMP TIMER1_INT

        ORG 4023H       ;ADDRESS OF SERIAL INTERRUPT VECTOR
        JMP SERIAL_INT

        ORG 4033H       ;ADDRESS OF PCA INTERRUPT VECTOR
        JMP PCA_INTERRUPT

        ORG 4050H
INIT:                   ;THIS PART IS INITIALIZATION
;INITIALIZE TIMER2 IN THE BAUDRATE GENERATOR MODE
        MOV T2CON,#00110000B
        MOV RCAP2L,#LOW(65328)    ;BAUD RATE=2400
        MOV RCAP2H,#HIGH(65328)
        SETB TR2                  ;START TIMER2
        MOV SCON,#01010000B ;SERIAL PORT,MODE1,8-BIT UART
;COMMUNICATION WITH USER STARTS
;THIS PART PROGRAM ASKS USER WHETHER HE WANTS
;TO ENTER CONTROL PARAMETER VALUES OR NOT
DM22:   CALL PUT_CRLF
        MOV DPTR,#DYWTECP
        CALL PUT_STRING
        CALL GET_CHAR
        CJNE A,#'n',DM1
        MOV CURRENT,#00111111B
        CLR ZEROLEAD        ;LEAD ANGLE NOT 0
        MOV RLN,#02H        ;LEAD T/4
        CALL GET_CHAR
        CALL PUT_CRLF
        JMP D2
DM1:    CJNE A,#'y',DM22
        CALL GET_CHAR
        CALL PUT_CRLF
;THIS PART IS TO GET ADVANCE ANGLE
DM9:    MOV DPTR,#EAA
        CALL PUT_STRING
        CALL GET_CHAR
        CALL GET_ADV_ANG
;THIS PART IS TO GET PHASE CURRENT
DM20:   MOV DPTR,#EPC
        CALL PUT_STRING
        CALL GET_CHAR
        CALL GET_CURRENT
;THIS PART IS TO GET MODE OF OPERATION
D2:     MOV DPTR,#EMOO
        CALL PUT_STRING
        CALL GET_CHAR
        CJNE A,#'o',TPHON   ;IF NOT O THEN GO TO TPHON
        MOV R7,#11001100B   ;STATE OF SWITCHES
        JMP D3
TPHON: CJNE A,#'t',HS     ;IF NOT T THEN GO TO HS
```

```
        MOV R7,#10001000B ;STATE OF SWITCHES
        JMP D3
HS:     CJNE A,#'h',D2 ;KEY PRESSED NOT H ASK QUESTION AGAIN
D3:     CALL GET_CHAR
        CALL PUT_CRLF
;This part is for writing IS IT CW?
D10:    MOV DPTR,#DYWRBC
        CALL PUT_STRING
        CALL GET_CHAR
        CJNE A,#'y',DNOTCW  ;is answer y?
        SETB BIT_CW       ;MAKE 1 THE BIT 20.0 FOR CW
        jmp D4
DNOTCW:CJNE A,#'n',D10 ;KEY PRESSED IS N GO TO NEXT LINE
        CLR BIT_CW
D4:     CALL GET_CHAR
        CALL PUT_CRLF
;This part is for writing START ROTATION?
D11:    MOV DPTR,#SR
        CALL PUT_STRING
        CALL GET_CHAR
        CJNE A,#'y',NOSTAR ;answer is y go to next line
        JMP D5
NOSTAR:CJNE A,#'n',D11 ;KEY PRESSED NOT N QUESTION AGAIN
        CALL GET_CHAR
        CALL PUT_CRLF
        JMP DM22    ;ASK ALL QUESTION FROM BEGINING AGAIN
D5:     CALL GET_CHAR
        CALL PUT_CRLF
;INITIALIZE BITS AND STORAGE LOCATIONS
        SETB FIRSTTIME  ;AT START FOR ZERO LEAD
        SETB ES      ;ENABLE SERIAL PORT INTERRUPT
        MOV CURRENT,#00111111B  ;DIGITAL DATA FOR 5A
        MOV NEWCURRENT,#00111111B ;5A FOR FIRST STEP
        MOV R6,#00H         ;R6 IS #OF FIRST 3 STEPS
;INITIALIZE PCA TIMER
        MOV CMOD,#00H       ;Fosc/12
        MOV CH,#00H
        MOV CL,#00H
;INITIALIZE MODULE 0 IN CAPTURE MODE
        MOV CCAPM0,#21H ;CAPTURE RISING EDGES ON P1.3
;INITIALIZE TIMER1
        MOV TMOD,#00010000B ;16 BIT TIMER
        MOV TH1,#00H
        MOV TL1,#01H
        SETB ET1
        SETB EA
        SETB T1PASSED
        CLR CAPNUM    ;NEXT CAPTURE IS FIRST CAPTURE
        CLR FEEDBACK         ;FOR NEXT INSTRUCTION
        SETB EC              ;ENABLE PCA INTERRUPT
```

```
        CALL ISSUE_STEP_COMMAND
        SETB TR1                ;START TIMER
OA2:    JNB FEEDBACK,OA1
        CLR TR1
        JMP OA4
OA1:    JB T1PASSED,OA2
OA4:    CALL ISSUE_STEP_COMMAND
        CLR FEEDBACK            ;FOR NEXT INSTRUCTION
OA3:    JNB FEEDBACK,OA3
        INC R6
        CJNE R6,#02H,OA4
S4:     CALL ISSUE_STEP_COMMAND
L4:     JNB ZEROLEAD,NZL ;LEAD ANGLE NOT ZERO GO TO NZL
        JNB FIRSTTIME,ZL1 ;CHECH WHETHER IT IS FIRST COMMING
        CLR FIRSTTIME   ;FROM NOW ON NOT FIRST COMING
        JMP FFC
NZL:    SETB T1PASSED
        SETB TR1    ;START TIMER1
L6:     JB T1PASSED,L6    ;WAIT TILL TIME IS PASSED
ZL1:    CALL ISSUE_STEP_COMMAND
FFC:    CLR FEEDBACK
L3:     JNB FEEDBACK,L3
        JMP L4
;This section is for switching transistors
ISSUE_STEP_COMMAND:
        MOV CURRENT,FCURRENT
        MOV NEWCURRENT,FCURRENT
        MOV R0,#24H    ;FOR INDIRECT ADDRESSEING
        ANL NEWCURRENT,#00000111B     ;FOR P1.0,1,2
        MOV A,R7
        XCHD A,@R0
        MOV C,CURRENT.3
        MOV P3.2,C
        MOV C,CURRENT.4
        MOV P3.4,C
        MOV C,CURRENT.5
        MOV P3.5,C
        MOV P1,A
        MOV A,R7     ;TO FIND NEXT STATE OF TRANSISTORS
        JB BIT_CW,CWISE ;IS ROTATION CW
        RL A                ;FOR CCW
        JMP L5
CWISE:  RR A
L5:     MOV R7,A      ;STORE FOR NEXT TRANSFER TO PORT1
RET
;this routine outputs the string located in code memory
;whose address is given in DPTR
PUT_STRING:
         CLR A
         MOVC A,@A+DPTR
```

```
          JZ EXIT
          CALL PUT_CHAR
          INC DPTR
          JMP PUT_STRING
     EXIT:
RET
;This routine outputs a single character
;which is given in A to console
PUT_CHAR:
          MOV SBUF,A
          JNB TI,$
          CLR TI
RET
;This routine outputs a carriage return and 2 line feed
PUT_CRLF:
          MOV R0,#02
    D6:   MOV A,#0DH        ;CARIAGE RETURN
          CALL PUT_CHAR
          MOV A,#0AH        ;LINE FEED
          CALL PUT_CHAR
          DJNZ R0,D6
RET
;This routine gets a 4 character string from console
;and stores it in memory at the address given in R0
GET_NUM:
          MOV R2,#5    ;SET UP STRING LENGTH
          MOV R1,00H ;R0 VALUE MAY BE NEEDED FOR RESTART
GET_LOOP:CALL GET_CHAR
          SUBB A,#30H ;TO CHANGE FROM ASCII TO NUMBERS
          MOV @R1,A
          INC R1
          DJNZ R2,GET_LOOP
RET
;THIS PART TO GET ADVANCE ANGLE
GET_ADV_ANG:
         CJNE A,#'0',DM2
         SETB ZEROLEAD      ;LEAD ANGLE=0
         JMP DM3
DM2:     CLR ZEROLEAD
         CJNE A,#'1',DM4
         CALL GET_CHAR
         CJNE A,#'/',DM8
         CALL GET_CHAR
         CJNE A,#'2',DM4
         MOV RLN,#01H       ;LEAD ANGLE 1/2
         JMP DM3
DM4:     CJNE A,#'4',DM5
         MOV RLN,#02H       ;LEAD ANGLE 1/4
         JMP DM3
DM5:     CJNE A,#'8',DM6
```

```
        MOV RLN,#03H        ;LEAD ANGLE 1/8
        JMP DM3
DM6:    CJNE A,#'1',DM7
        CALL GET_CHAR
        CJNE A,#'6',DM8
        MOV RLN,#04H        ;LEAD ANGLE 1/16
        JMP DM3
DM7:    CJNE A,#'3',DM8
        CALL GET_CHAR
        CJNE A,#'2',DM8
        MOV RLN,#05H        ;LEAD ANGLE 1/32
        JMP DM3
DM8:    CALL PUT_CRLF
        JMP DM9
DM3:    CALL GET_CHAR
        CALL PUT_CRLF
RET
;This routine gets a single character from
;terminal the character is returned in A
get_char:
         JNB RI,$
         CLR RI
         MOV A,SBUF
         MOV SBUF,A
RET
WRITE:
       CALL PUT_CRLF
       CALL PUT_STRING
       CALL GET_CHAR
       CALL PUT_CRLF
RET
GET_CURRENT:
       CJNE A,#'1',DM12
       CALL GET_CHAR
       CJNE A,#'.',DM
       CALL GET_CHAR
       CJNE A,#'5',SEC2
       MOV FCURRENT,#00000111B ;1.5A
       JMP DM11
 DM:   JMP DM19
 SEC2: CJNE A,#'0',DM19
       MOV FCURRENT,#00000000B ;1A
       JMP DM11
 DM12: CJNE A,#'2',DM13
       CALL GET_CHAR
       CJNE A,#'.',DM19
       CALL GET_CHAR
       CJNE A,#'5',SEC3
       MOV FCURRENT,#00010111B ;2.5A
```

```
        JMP DM11
SEC3:   CJNE A,#'0',DM19
        MOV FCURRENT,#00001111B ;2A
        JMP DM11
DM13:   CJNE A,#'3',DM15
        CALL GET_CHAR
        CJNE A,#'.',DM19
        CALL GET_CHAR
        CJNE A,#'5',SEC4
        MOV FCURRENT,#00100000B ;3.5A
        JMP DM11
SEC4:   CJNE A,#'0',DM19
        MOV FCURRENT,#00100000B ;3A
        JMP DM11
DM15:   CJNE A,#'4',DM16
        CALL GET_CHAR
        CJNE A,#'.',DM19
        CALL GET_CHAR
        CJNE A,#'5',SEC5
        MOV FCURRENT,#00111000B ;4.5A
        JMP DM11
SEC5:   CJNE A,#'0',DM19
        MOV FCURRENT,#00110000B ;4A
        JMP DM11
DM16:   CJNE A,#'5',DM19
        CALL GET_CHAR
        CJNE A,#'.',DM19
        CALL GET_CHAR
        CJNE A,#'0',DM19
        MOV FCURRENT,#00111111B ;5A
        JMP DM11
DM19:   CALL PUT_CRLF
        JMP DM20
DM11:   CALL GET_CHAR
        CALL PUT_CRLF
        JMP D2
RET
;THIS IS PCA INTERRUPT SUBROUTINE TO FIND TIME BETWEEN
;FEEDBACK PULSES AND INITIALIZE TIMER TO GIVE LEAD ANGLE
PCA_INTERRUPT:
        CLR CCF0        ;CLEAR MODULE 0'S EVENT FLAG
        SETB FEEDBACK   ;HAS RECEIVED THE FEEDBACK
        JB CAPNUM,SECOND_CAPTURE
FIRST_CAPTURE:
        MOV CAPTURE,CCAP0L
        MOV CAPTURE+1,CCAP0H
        SETB CAPNUM     ;SIGNIFY FIRST CAPTURE COMPLETE
        RETI
SECOND_CAPTURE:
        PUSH ACC
        PUSH PSW
```

```
        MOV NEXTFIRST+1,CCAPOH
        CLR C
        MOV A,CCAPOL      ;16 BIT SUBTRACTION
        SUBB A,CAPTURE
        MOV PERIOD,A
        MOV A,CCAPOH
        SUBB A,CAPTURE+1
        MOV PERIOD+1,A
        JB ZEROLEAD,NOTT1 ;DON'T FIND T1 VALUE FOR 0 LEAD
        MOV LEADNUM,RLN   ;INITIALIZE TIMER1
REP1:   CLR C
        MOV A,PERIOD+1
        RRC A
        mov period+1,a
        MOV A,PERIOD
        RRC A
        mov period,a
        DJNZ LEADNUM,REP1
        MOV A,PERIOD+1
        CPL A
        MOV TH1,A
        MOV A,PERIOD
        CPL A
        MOV TL1,A
NOTT1:  MOV CAPTURE,NEXTFIRST
        MOV CAPTURE+1,NEXTFIRST+1
        POP PSW
        POP ACC
        RETI
;TIMER1'S INTERRUPT SUBROUTINE
TIMER1_INT:
        CLR TR1
        CLR T1PASSED
RETI
;SERIAL PORT'S SUBROUTINE
SERIAL_INT:
        JB TI,GONDER
        MOV A,SBUF
        CJNE A,#'s',NOSTOP ;S IS PRESSED STOP ROTATION
        MOV P1,#00000000B;TURN ON ALL SWITCHES STOP MOTOR
        MOV P1,#11111111B ;TURN OFF ALL TRANSISTORS
        MOV DPTR,#MS
        CALL WRITE
        JMP STOPIT
NOSTOP:CLR RI
GONDER:CLR TI
D7:     RETI
        CSEG
STOPIT:CLR EC ;DISABLE FEEDBACK RECEPTION
END
```

APPENDIX D

PIN DIAGRAM OF THE EV80C51FB BOARD

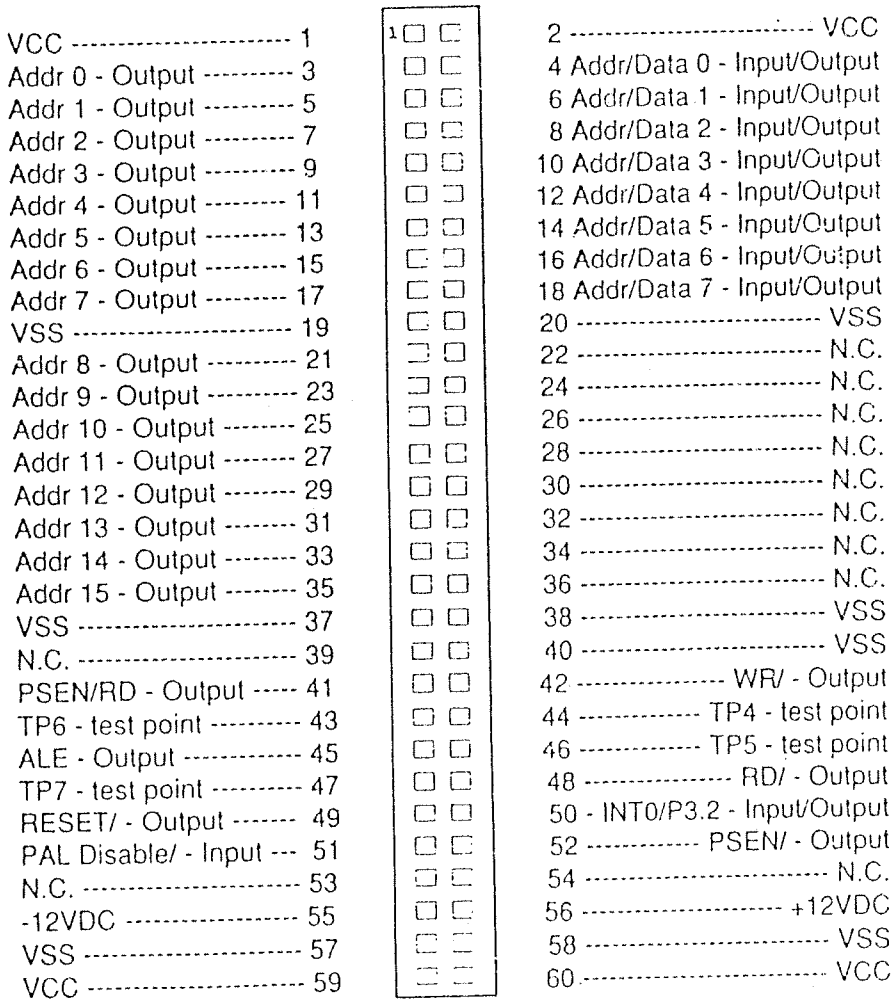

Figure D.1. JP2 Memory Expansion Connector

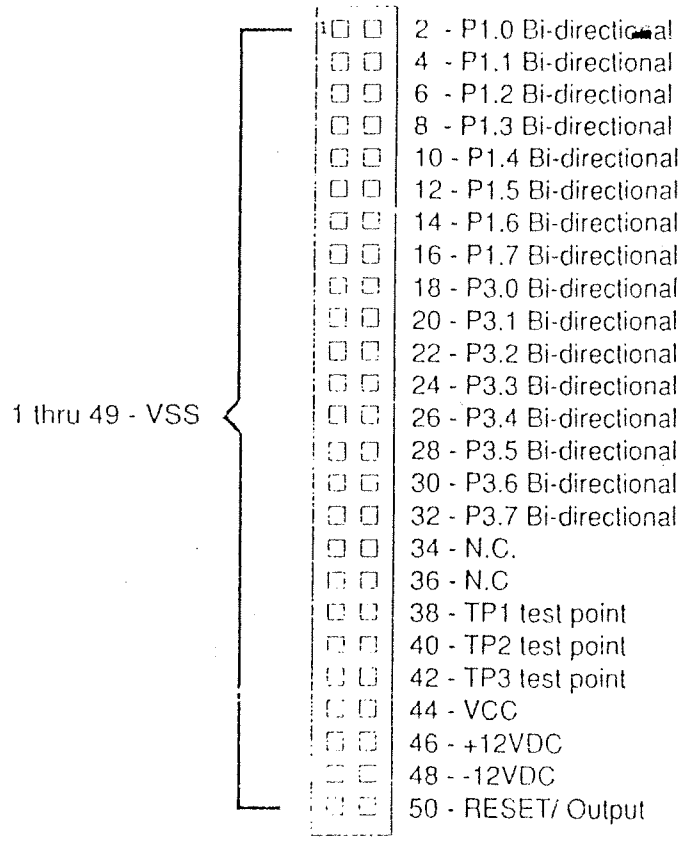

Figure D.2. JP3 I/O Expansion Connector

APPENDIX E

DRIVE PHOTOGRAPHS

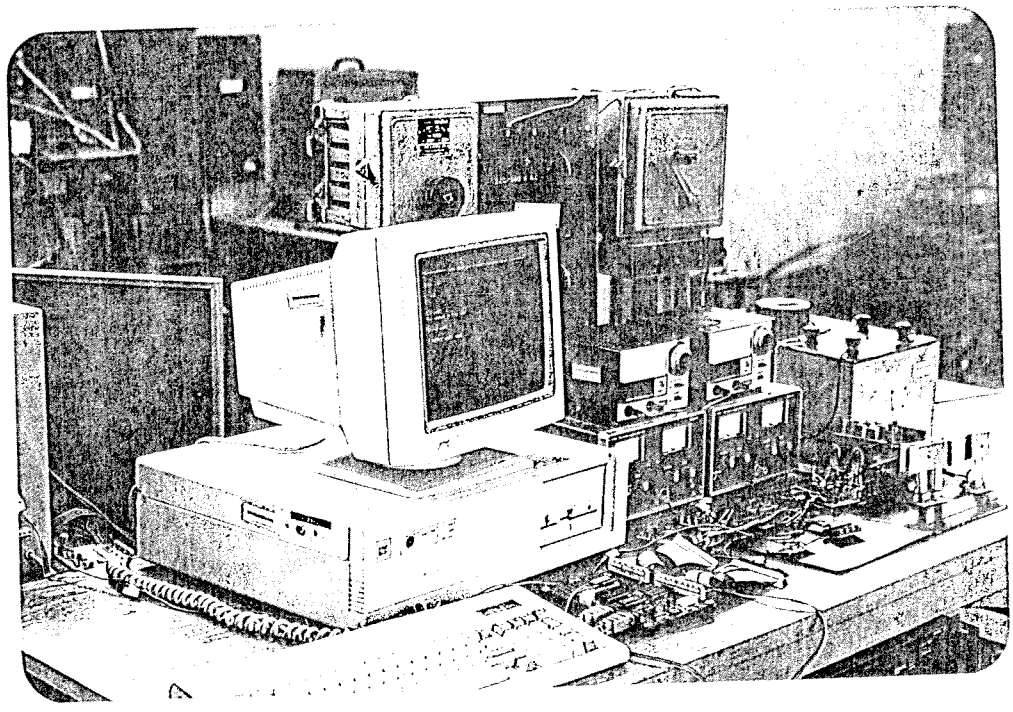

Figure E.1. General Outlook of the Drive Circuit

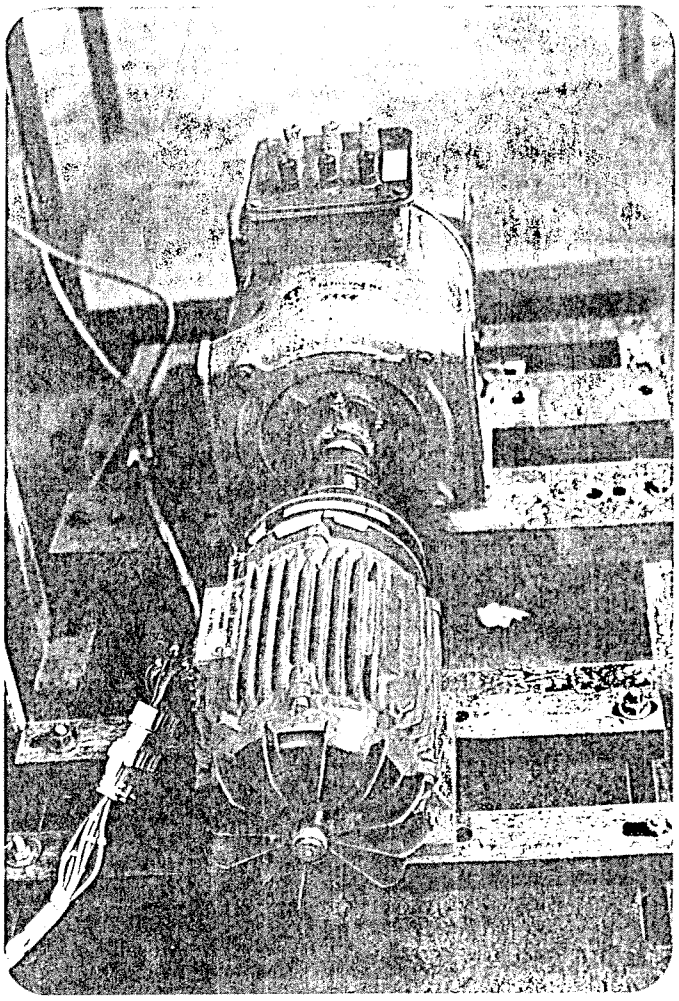

Figure E.2. The Prototype Motor and the Test System